INTERACTIVE EFFECTS OF N FERTILIZATION RATE, CULTIVARS AND PLANTING DATE UNDER CLIMATE CHANGE ON MAIZE (*Zea mays* L.) YIELD USING CROP SIMULATION AND STATISTICAL DOWNSCALING OF CLIMATE MODELS

BY

CHARLES BWALYA CHISANGA

A thesis submitted in fulfillment of the requirements for the degree of Doctor of Philosophy in Integrated Soil Fertility Management

THE UNIVERSITY OF ZAMBIA

May 2019

DECLARATION

I Charles Bwalya Chisanga hereby declare that the dissertation is my original work, and has not been submitted for a degree award in any other University.

Charles Bwalya Chisanga — Date: 29-05-2019

Supervisors:

Dr. Elijah Phiri — Date: 29. 5. 2019

Prof. Vernon R.N. Chinene — Date: 29/05/2019

COPYRIGHT

APPROVAL

This thesis of **CHARLES BWALYA CHISANGA** was approved as fulfilling the requirement for the award of the degree of Doctor of Philosophy (PhD) in **INTEGRATED SOIL FERTILITY MANAGEMENT (ISFM)** by the University of Zambia.

Examiner 1: Prof. O.I. Lungu Signature: [signature] Date: 29/05/2019

Examiner 2: Dr. K. Munyinda Signature: [signature] Date: 29/05/2019

External examiner: Dr. C. Shepande Signature: [signature] Date: 29/05/2019

Chairperson
Board of Examiner: Prof. T. Kalinda Signature: [signature] Date: 29/5/2019

Principal
Supervisor: DR E. Phiri Signature: [signature] Date: 29.5.2019

ABSTRACT

Generating new information using traditional agricultural trials which are expensive is not sufficient to meeting novel agro-technologies. Planting date (PD), low soil fertility and climate change influences maize (*Zea mays* L.) growth and yield. Local-scale impacts of future climate change (CC) and variability (CV) on PD, N fertilizer rate (N), cultivar, maize growth, and yield is not well documented in Zambia. The impact of climate change and extreme climate indices on maize yield in AERII are carried out at large spatial scales, missing out on local-scale impacts, mitigation and adaptation potentials under which farmers operate.

Statistical downscaling models such as stochastic weather generator (Long Ashton Research Station Weather Generator [LARS-WG]) and delta-based methods (Agricultural Model Intercomparison and Improvement Project (AgMIP) protocols) have not been applied locally to assess the impact of climate change. Additionally, the AgMIP protocols have not been applied to downscale climate scenarios using Representative Concentration Paths (RCP4.5 and RCP8.5). Changes in temperature and precipitation would have a significant impact on maize phenology and yield. Two field experiments were conducted at Zambia Agriculture Research Institute at Mount Makulu (Lat: 15.550^{o} S, Lon: 28.250^{o} E, altitude: 1213 m) in Zambia to assess the effect of PD, N and cultivars on yield and yield parameters and to predict the impact of climate change on maize productivity in the 2050s. The irrigated experiment was arranged in a Split-plot design with maize cultivars (ZMS606, PHB30G19and PHB30B50) and N fertilizer rates (67.20, 134.40 and 201.60 kg N ha^{-1}) as main-plots and sub-plots, respectively. These cultivars were selected as major cultivars planted by small scale farmers and their long commercial life. The rainfed experiment was a split-split plot design with PDs, cultivars, and N as the main-plots, sub-plot, and sub-subplots, respectively. Each field experiment had three replicates.

Daily weather data were obtained from the Zambia Meteorological Department and AgMERRA. Plant growth, grain, and biomass yield were observed at phenological stages. The ANOVA for grain yield and yield parameters were computed using the *sp.plot* and *ssp.plot* functions in Agricolae R package. Significant differences between means were tested using Fisher-LSD Test ($p<0.05$). Site weather data, soil data, cultivar characteristic, and management required by the crop models were also collected. The rainfed (2016/2017) and irrigated (2016) field experimental data were used for calibrating and validating the crop simulation models (CSMs), respectively.

Expert Team on Sector Specific Indices (ET-SCI) of extreme temperature and precipitation were computed after checking weather data (1963-2012) for quality, homogeneity, and trends using ClimPACT2. The APSIM-Maize v7.9 and CERES-Maize v4.7 models were calibrated using rainfed experimental site data. Days after planting (DAP) to anthesis, and maturity, grain and biomass yield, LAI and soil water content measurements were used to calibrate the CSMs. Cultivar-specific parameters (CSPs) in DSSAT CERES-Maize model were computed using the generalized likelihood uncertainty estimation (GLUE). The CSPs in APSIM-Maize were computed using a stepwise approach starting with phenology, soil water, soil N, biomass and grain yield. The models were validated using the irrigated field experimental site data. Root mean squared error (RMSE), normalized RMSE, R^2, and d-stat were used to evaluate the agreement between simulated and observed values.

Climate scenarios were generated using LARS-WG and AgMIP protocols. The suitability of LARS-WG in generating current and future climate scenarios was evaluated using CMIP3 HadCM3 and BCM2 global climate models (GCMs) for B1 and A1B scenarios. The current (1980-2010) and future (2040-2070) climate scenarios used as inputs into the CSMs were generated using 5 GCMs (E, I, K, O, R) and RCPs (RCP4.5 and RCP8.5) scenarios using the AgMIP protocols. APSIM-Maize and CERES-Maize models were used to evaluate maize yield to response to PD, N, cultivar and climate scenarios assuming constant management. Future changes in phenology and yield were estimated as the difference between future and baseline period.

Extreme precipitation (PRCPTOT, R30 mm, RX5day, R95pTOT) indices were statistically non-significant. Mount Makulu warming are due to increase in mean and maximum temperature. LARS-WG projected an increase in temperature (Observed station data [1.50^{o}C (B1: 2050), 1.84^{o}C (A1B: 2050)], AgMERRA data [1.48^{o}C (B1: 2050), 1.84^{o}C (A1B: 2050)]) and variability in precipitation. The projected ensemble mean annual temperature using the AgMIP protocols is expected to increase by 1.82°C (RCP4.5) and 2.48^{o}C (RCP8.5). However, rainfall is projected to decrease by 1.46% (RCP4.5) and 1.91% (RCP8.5). APSIM-Maize and CERES-Maize models simulated fewer DAP to anthesis and maturity relative to the baseline. Maize grain yield (-6.90 - +4.06 (RCP4.5), -10.80 - +5.00% (RCP8.5) [APSIM-Maize]; -0.59 to +25.77% (RCP4.5) and -6.52 to +20.21% (RCP8.5) [CERES-Maize]) would decrease or increase relative to the baseline. PD, N, and rainfall would affect future grain yield.

The simulated versus observed values of DAP to anthesis, and maturity, grain yield, grain size, and grain number m^{-2} and soil water content had normalized root mean square error < 20% and d-stat > 0.71. The models can be used to predict phenology and yield. Using an ensemble mean of the CSMs, DAP to anthesis (-11.28 to -9.39% [RCP4.5]; -14.28 to -12.65% [RCP8.5]) and maturity (-10.52 to -9.43% [RCP4.5]; -14.01 to -12.75% [RCP8.5]) would reduce in 2050. The % change in grain would range from 2.78 to 9.94%, -3.81 to -8.88% and -2.33 to 10.63% under N1, N, and N3, respectively. Grain yield would increase/or decrease with delay in PD (RCP4.5 [PD1 = 2.57%; PD2=3.31%; PD3=4.37%]; RCP8.5 [PD1 = -1.11%; PD2=-0.29%; PD3=1.08%]). The current PDs and cultivars with lower N (N1) would increase grain yield in future. However, grain yield would increase with higher N (N3) at PD3.

To establish credibility in CSMs for use at a local scale, they have to be adequately calibrated and validated. The calibration and validation of APSIM-Maize and CERES-Maize models were necessary for their application to new cultivars to minimize uncertainty. CSMs can be used to simulate probable outcomes in crop management strategies, N fertilizer rate, PD and impact of climate change on crop growth and yield. Earlier PDs with lower N would lead to an increase in grain yield than at higher N. Proposed improvements in the CSMs are phenological stage duration and LAI prediction under subtropical environments. The mitigation and adaptation strategies for CC includes changing PDs, N management, cultivar selection, water management, and tillage practices. Future model evaluations may be needed for new cultivars.

Key words: AgMERRA, AgMIP, APSIM-Maize, CERES-Maize, climate change, climate indices, climate variability, CSM, delta-based method, GCM, GDD, LARS-WG, nitrogen, planting date, RCPs, statistical downscaling

DEDICATION

To my wife Astridah Lombe Chisanga for her full-hearted support, love, and patience.

To my family and friends for their support and encouragement throughout my studies.

To the memory of my late father, Emmanuel Musuba Chisanga.

ACKNOWLEDGEMENTS

I would like to thank my supervisors; Dr. Elijah Phiri and Professor Vernon Chinene for their guidance, support and encouragement they provided me during the study and writing of the dissertation. I also wish to thank the following: Professor Mikhail A. Semenov, Decision Support System for Agro-technology Transfer (DSSAT), and Agricultural Production Simulator (APSIM) Teams for the provision of the Long Ashton Research Station Weather Generator (LARS-WG), DSSAT and APSIM software which were used in this study.

I recognize the financial support from the Agricultural Productivity Programme for Southern Africa (APPSA) under the Zambia Agricultural Research Institute (ZARI) Central Station for the study. I also wish to thank the Director of the Zambia Agricultural Research Institute (ZARI) Mr. Moses Mwale, APPSA Coordinator Mr. Laston Milambo, the Programme Officer, the Farm Manager and all members of staff from Zambia Agricultural Research Institute (ZARI) Central Research Station for their support. I also thank the Ministry of Agriculture (MoA) for granting me study leave and the Zambia Meteorological Department (ZMD) for providing me with the weather data. Finally, I wish to thank my wife Astridah Lombe Chisanga for her support and encouragement throughout my study.

The assistance of all other persons not mentioned by name is gratefully acknowledged.

TABLE OF CONTENTS

LIST OF FIGURES

LIST OF TABLES

LIST OF APPENDICES

ACRONYMS AND ABBREVIATIONS

AERs	Agro-ecological Regions
AGCMs	Atmospheric Global Circulation Models
AgMERRA	Agricultural Modern-Era Retrospective Analysis for Research and Applications
AgMIP	Agricultural Model Inter-comparison and Improvement Project
ANOVA	Analysis of Variance
APSIM	Agricultural Production Systems Simulator
APSRU	Agricultural Production Systems Research Unit
AR3	Third Assessment Report
AR4	Fourth Assessment Report
AR5	Fifth Assessment Report
BCCR-BCM2.0	Bergen Climate Model Version 2
BOM	Bureau of Meteorology
CCI	Commission for Climatology
CCSM4	Community Climate System Model version 4
CDFs	Cumulative Distribution Functions
CDPF	Cumulative density probability function
CERES	Crop Environmental Resource Synthesis
CGR	Crop Growth Rate
CH4	Methane
CHUs	Crop Heat Units
CMIP3	Third Coupled Model Inter-comparison Projects
CMIP5	Fifth Coupled Model Inter-comparison Projects
CO2	Carbon Dioxide
CSIRO	Climate Change in Australia
CSM	Crop Simulation Models
CSP	Cultivar Specific Parameter
DAP	Days After Planting
DSSAT	Decision Support Systems for Agrotechnology Transfer
DUL	Drained Upper Limit
ENSO	El Nino Southern Oscillation (ENSO)
ETCCDI	Expert Team on Climate Change Detection and Indices
ET CRSCI	Expert Team on Climate Risk and Sector-specific Indices
ET-SCI	Expert Team on Sector-specific Climate Indices
FAO	Food and Agriculture Organisation
GCM	General Circulation Model/Global Climate Model
GDDs	Growing Degree Days
GFDL-ESM2M	Geophysical Fluid Dynamics Laboratory-Earth System Model 2M
GHG	Greenhouse Gases
GRZ	Government of the Republic of Zambia
HadCM3	Hadley Centre Couple Model version 3
HadGEM2-ES	Hadley Centre Global Environmental Model 2 - Earth System
HUE	Heat Use Efficiency
IPCC	Intergovernmental Panel on Climate Change

IPCC-TGICA	Intergovernmental Panel on Climate Change and Task Group on Data and Scenario Support for Impact and Climate Analysis
ISI-MIP	Inter-Sectoral Impact Model Inter-comparison Project
ITCZ	Inter-Tropical Convergence Zone
JCOMM	Joint WMO-Intergovernmental Oceanographic Commission of the United National Educational, Scientific and Cultural Organization (UNESCO) Technical Commission for Oceanography and Marine Meteorology (JCOMM)
LAD	Leaf Area Duration
LAI	Leaf Area Index
LAR	Leaf Area Ratio
LARS-WG	Long Ashton Research Station Weather Generator
LL	Lower Limit
LSD	Least Significant Difference
LWR	Leaf Weight Ratio
MAE	Mean Absolute Error
MIROC5	Model for Interdisciplinary Research on Climate version 5
mLAI	Maximum Leaf Area index
MoA	Ministry of Agriculture
MPI-ESM-MR	Max Planck Institute - Earth System Model - Medium Resolution
MTENR	Ministry of Tourism, Environment and Natural Resources
N2O	Nitrous Oxide
NCA	National Climate Assessment
NAR	Net Assimilation Rate
NOAA	National Oceanic and Atmospheric Administration
NSW	New South Wales
ORS	Onset of the Rainy Season
PAR	photosynthetic active radiation
PD	Panting Date
PTI	Phenothermal Index
RCMs	Regional Climate Models
RCPs	Representative Concentration Pathways
RGR	Relative Growth Rate
RMSE	Root Mean Square Error
NRMSE	normalized RMSE
RUE	Radiation Use Efficiency
sd	Standard deviation
SE	Standard error of the mean
SED	Semi-Empirical Distribution
SSA	Sub-Saharan Africa
SWUS	South-Western U.S.
UNDP	United Nations Development Programme
USCSP	United States Country Studies Programme
USDA	United States Department of Agriculture
WCRP	World Climate Research Programme
WMO	World Meteorological Organization
ZARI	Zambia Agriculture Research Institute
ZMD	Zambia Meteorological Department

CHAPTER ONE: INTRODUCTION

1.1 Background

Maize (*Zea mays* L.) is an important cereal crop in the world after wheat and rice (New South Wales, NSW, 2009). Maize yield is being affected by climate change which is difficult to be controlled by farmers. Climate change is a statistically significant variation in either the mean state of the climate or in its variability that persists for extended periods (Yin et al., 2014). Maize is a major cereal crop in sub-Saharan Africa (Alexandratos and Bruinsma, 2012) and is Zambia's staple crop grown by small-scale (80%) and commercial farmers (20%) (Arslan et al., 2014; Mulenga and Wineman, 2014). Rainfall is the most important climatic factor that influences rainfed maize growth and yield. It is projected that drought and heat stress would intensify and become more frequent in rainfed maize growing regions of the world (Hatfield and Prueger, 2015). The extreme temperature has a drastic impact on plant productivity (Hatfield and Prueger, 2015). However, there is insufficient research to document these effects at local scale.

The global mean temperature has increased by 0.5^{o}C in the last 100 years (Suman, 2007). Similarly, the mean temperature in Africa has been rising by 0.05^{o}C per decade while rainfall shows variability. Changes in temperature and rainfall affect crop growth rates, as well as water and soil fertility. By 2050, the climate would be warmer by 1.8°C, and maize yield would decrease by 5% relative to today due to heat stress and shortening of the phenology stages (Jaggard et al., 2010). Xu et al. (2016) estimated that 60% more food would be required by 2050. Prolonged dry spells and shorter rainfall seasons in the past 20 years have reduced maize yields by 40% of the long-term average in agro-ecological regions (AER) I and II of Zambia (UNDP, 2010).

Maize growth and yield are inhibited by nitrogen application rate (Abedinpour and Sarangi, 2018; Mburu et al., 2010). Nitrogen (N) is the most limiting nutrient controlling the primary production of agricultural systems. Therefore, research on soil fertility management, planting date (PD) and weather to enhance maize growth and yield using crop simulation models (CSMs) is vital. CSMs are decision support tools used to evaluate soil processes, crop growth and yield response to climate change and variability, management, PD (Anapalli et al., 2016; Liaqat et al., 2018), N (soil

fertility) and soil water content. They can accurately simulate crop growth and yield with prior soil properties data, cultivar, and management (Abedinpour and Sarangi, 2018). CSMs have been used to determine optimal maize PD (Adnan et al., 2019; Chisanga et al., 2015), long-term N fertilizer management (Kisaka et al., 2015) and irrigation regime under diverse environmental conditions (Wolday and Hruy, 2015).

The Decision Support Systems for Agrotechnology Transfer (DSSAT) (Hoogenboom et al., 2010; Jones et al., 1986, 2003) and Agricultural Production Systems Simulator (APSIM) (Keating et al., 2003) as CSMs are widely used in climate change and variability studies (Salo et al., 2016). The APSIM and CERES-Maize models have been tested under different environments, including model performance in long-term cropping systems, climate change and variability (Keating et al., 2003; Liu et al., 2013; Lizaso et al., 2011). Their use has increased in Africa through the Agricultural Models Inter-Comparison Project (AgMIP) initiative (Rosenzweig et al., 2013). APSIM and CERES-Maize models employ simplified functions to predict the growth and yield of maize as influenced by genetics, climate, soils, and management. CSMs are used to quantify the impact of climate change and crop management on yield. Studies using CSM ensemble can give valuable information about model accuracy and uncertainty, but such studies are of recent development with limited coverage in Zambia (Martre et al., 2015; Wallach et al., 2016).

1.2 Statement of the problem

The generating of new evidence using traditional agricultural trials which are expensive is not sufficient to meeting novel agro-technologies. PD, low soil fertility and climate change influences crop growth and yield. Rainfall is an important climatic factor that influences rainfed maize growth and yield which is a function of water and nutrient availability. Limited water supply has an effect on soil fertility which becomes less significant. It is, therefore, important to evaluate the effects of PD and N on maize growth and yield and their interaction under climate change. Local scale impacts of future climate change and variability on PD, N, cultivar and yield is not well documented in Zambia. The impact of climate change and extreme climate indices are carried out at large spatial scales, aggregated over entire country or region missing out on local-scale impacts under which farmers operate. Statistical downscaling models such as stochastic weather generators and delta-based methods have not been applied

locally to assess the impact of climate change. Additionally, the AgMIP protocols have not been applied to downscale climate scenarios using Representative Concentration Pathways (RCP4.5 and RCP8.5) at the local scale.

1.3 General objectives

To assess the effect of N fertilizer rate, planting date and cultivar type on yield and yield parameters and to predict the impact of climate change on maize productivity in the 2050s.

1.3.1 Specific objectives

To achieve the general objective, the following were the specific objectives:

1. To assess the effect of nitrogen fertilizer rate on physiological traits, yield and yield components for three maize cultivars under irrigated conditions;
2. To evaluate the effect of planting date and nitrogen fertilizer rate on yield and yield components for three maize cultivars under rainfed conditions;
3. To calibrate and validate APSIM and CERES-Maize models in simulating maize growth, yield, and soil water balance;
4. To investigate the suitability of the LARS-WG in predicting climate change in the 2050s;
5. To examine the changes in selected ET-SCI climate indices on temperature and precipitation extremes at Mount Makulu; and
6. To predict the impact of climate change on maize yield using climate scenarios in the 2050s.

1.4 Null hypotheses

1. Planting date and nitrogen fertilizer rate had no significant effect on maize cultivar yield and yield parameters;
2. There are no significant differences between observed and simulated values during calibration and validation of the APSIM and CERES-Maize models;
3. There are no significant differences between observed and synthetic time series data using LARS-WG;
4. There are no significant changes in ET-SCI climate indices for Mount Makulu; and

5. There are no significant differences in maize yields simulated using RCP4.5 and RCP8.5 scenarios (2040-2069) relative to the baseline.

1.5 Rationale

Climate change, and variability and extreme climate indices affect crop nitrogen demand and materialization directly and indirectly (Salo et al., 2016). CSMs are widely applied in optimizing nitrogen in agriculture and in estimating the effects of different nitrogen fertilizer rates and timing on maize growth and yield (Salo et al., 2016). They can be used to evaluate maize growth and yield as a function of weather (climate scenarios), PD and soil fertility. They can also be used to assess maize yield potential by varying nitrogen fertilizer rates, PDs, and management across a wide range of environmental conditions. To inform policy, the evidence is needed of the possible impacts of climate change on PD, cultivar, nitrogen fertilizer rate and maize growth and yield. To simulate the impact of climate change and variability on maize growth and variability, APSIM-Maize and CERES-Maize models requires parameterization, calibration, and validation.

New cultivars could be simulated using CSMs for new areas without having to conduct expensive field experiments. APSIM-Maize and CERES-Maize models provide an accurate simulation of maize growth, yield, and N uptake in response to different N fertilizer rates and PDs (Liu et al., 2012). The application of climate scenarios and CSMs to study the potential impact of climate change and climate variability provides a direct link between models, agro-meteorology, and concerns of society.

1.6 Organization of thesis

The thesis is divided into five chapters. Chapter one is the general introduction, highlighting the effect of planting date (PD), nitrogen fertilizer application rate, cultivar and climate change on maize growth and yield. It also presents the statement of the problem, study objectives, null hypotheses and rationale. Chapter two reviews maize growth stages, effect of PD, nitrogen fertilizer application rate, cultivar, climate change and variability on maize growth and yield. It also discusses crop simulation, and statistical downscaling models, Expert Team on Sector Specific Indices (ET-SCI), Agricultural and Model-Intercomparison and Improvement Project (AgMIP), situational analysis of climate change in Zambia and implication of climate change on

maize using APSIM and DSSAT-CERES-Maize models. Furthermore, the chapter reviews downscaling of climate data, APSIM-Maize and CERES-Maize models. Chapter three, the general methodolgies applied to the field experimental sites are presented. Other relevant approaches like weather data used, soil characterization, plant materials, clibration and validation of APSIM-Maize and CERES-Maize models, stoachastic weather data generation assessment and impact of climate change on maize growth and maize using global climate models (GCMs) and two representative Concentration Pathways (RCP4.5 and 8.5) are presented. Chapter four presents and discusses the results based on specific objectives and hypotheses. The conclusions and recommendations are presented in Chapter five.

CHAPTER TWO: LITERATURE REVIEW

2.1 Introduction

Agriculture is one of the most sensitive sectors facing climate change and variability. According to IPCC 5th Assessment Report (AR5), global (land and ocean) average temperature has shown a 0.85ºC (0.65-1.06ºC) and 0.74±0.18ºC increase from 1800-2012 and 1906-2005 (IPCC, 2013a; IPCC, 2007c), respectively. By 2050, the world climate would be warmer by 1.8°C (Jaggard et al., 2010). In Zambia, the mean temperature has increased by 1.3ºC while rainfall has reduced by 2.3% per decade from 1961-1990.

Global Climate Models (GCMs) with very coarse spatial resolutions (50-400 km) are tools being used in simulating the current and future climate change due to increasing greenhouse gas (GHG [carbon dioxide (CO_2), methane (CH_4) and nitrous oxide (N_2O)]) concentrations (Figure 1). The average global concentrations of different atmospheric GHGs have continued to increase (IPCC, 2013b) (Figure 2). Figure 2 shows the radiative forcing estimates in 2011 relative to 1750 with uncertainties aggregated for climate change drivers. Therefore, the spatial-temporal scale mismatches between GCMs and crop simulation models are bridged through downscaling. Dynamic or statistical downscaling can be used to generate site-specific climate data for impact studies under different emission scenarios and GCM pairings. To date, GCMs cannot provide reliable precipitation data as inputs into crop simulation models. Using GCMs, statistical downscaling and crop models offer a direct link between climate, crop and economic models in understanding climate change impact on crop growth and yield.

Very little has been documented at the local scale how maize growth and yield would change under future climate scenarios from 2040-2069 (the 2050s). CSMs such as APSIM-Maize and CERES-Maize models could be employed in evaluating the effects of climate change on planting date (PD), N fertilizer rates, cultivar, biomass, and grain yield. Crop simulation models also offer opportunities for exploring cultivar potential for new areas without establishing expensive field trials.

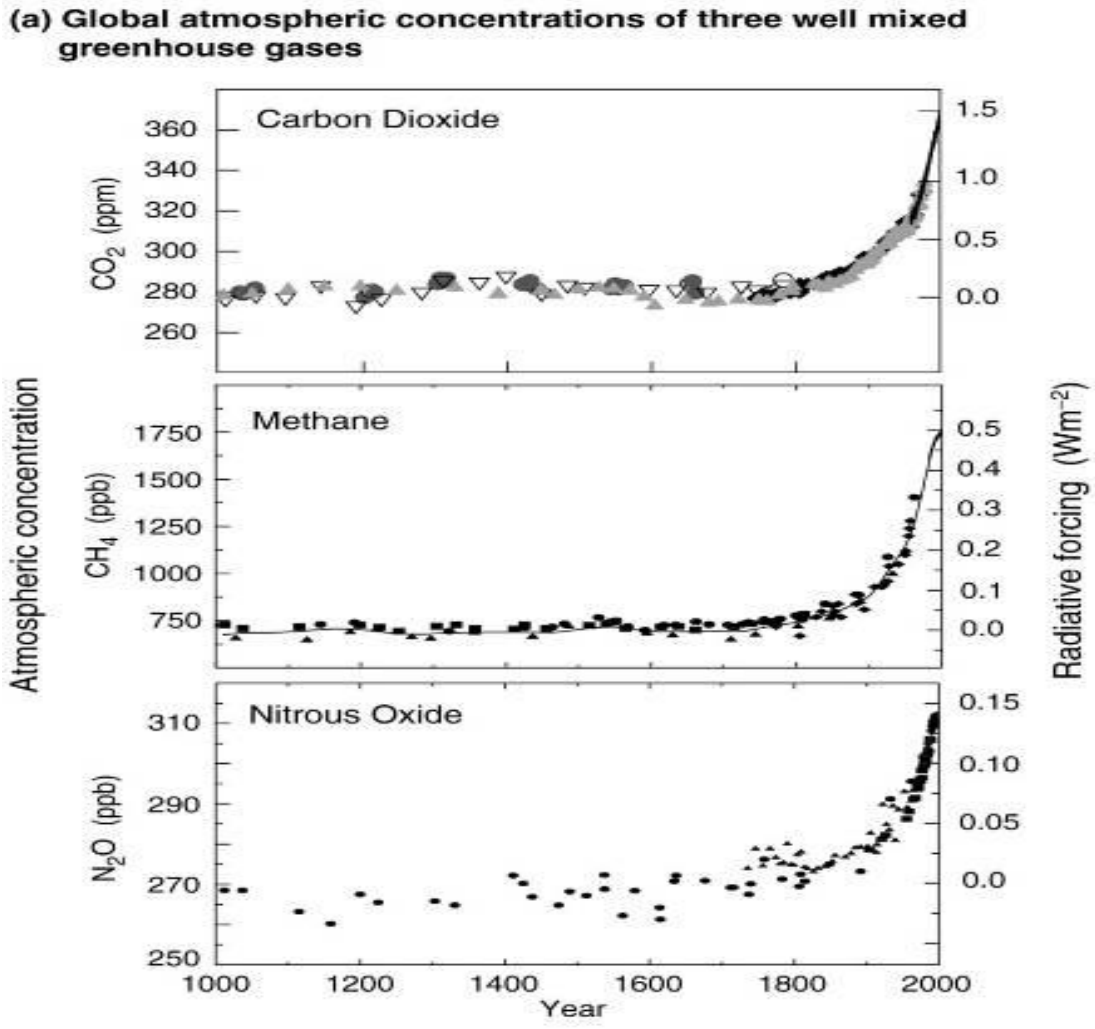

Figure 1: Predicted Atmospheric concentration of GHGs

Source: IPCC (2007b)

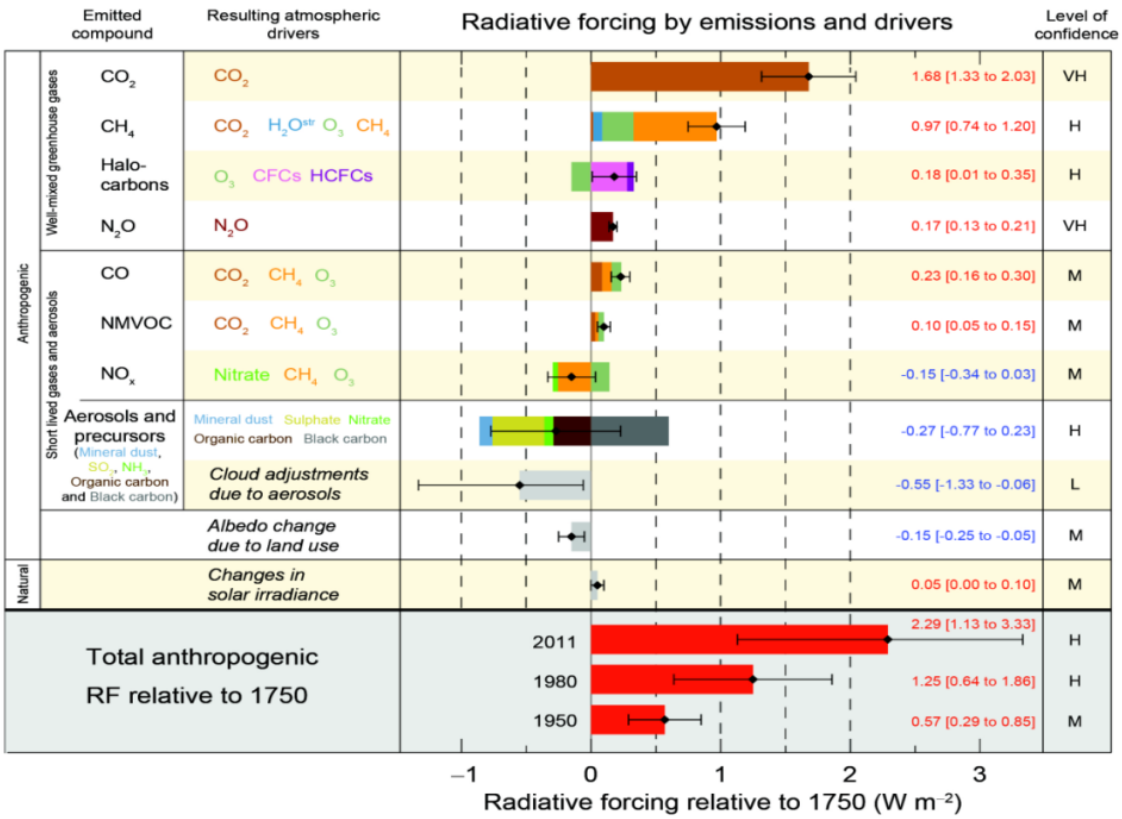

Figure 2: Observed trends in global greenhouse gas and aerosols concentrations

Source: IPCC (2013b)

2.2 Maize growth stages

Maize is the third most important cereal crop after wheat and rice (NSW, 2009). It is grown across a wide range of climates mainly in humid subtropics and warmer temperate regions. It grows well on deep, well-drained and fertile soils. The maize growth stages are divided into vegetative (V) and reproductive (R) stage as shown in Table 1. The first and last V stages are emergence (VE) and tasseling (VT). The number of leaves (n) varies depending on the cultivar and environment. The leaf stage is identified by the top leaf with a visible full collar, and they are described using the leaf collar method (Hoogenboom et al., 1999; NSW, 2009). The V or R stages are defined when 50% or more of the plants are in a specific stage. The developmental growth stages of maize vary according to cultivar and maturity. Early maturing cultivars produce fewer leaves and develop faster than late maturing. Physiological maturity is identified by when 50% of plants have a black layer at the base of the seed (Hoogenboom et al., 1999).

Table 1: Growth and development stages

Vegetative stages	Reproductive Stages
Emergence (VE)	silking (R1)
first leaf collar (V1)	blister (R2)
second leaf collar (V2)	milk (R3)
third leaf collar (V3)	dough (R4)
nth leaf collar (V(n))	dent (R5)
tasseling (VT)	maturity (R6)

Source: NSW (2009); Hoogenboom et al. (1999)

2.3 Effect of PD, N, and cultivar on maize growth and yield

Maize as a C4 crop requires water, solar radiation, carbon dioxide, and nitrogen efficiently during photosynthesis (NSW, 2009). Maize is influenced by changes in temperature (10-30^{o}C) and rainfal, and this is associated with PDs (Ali et al., 2018; NSW, 2009). Below 10^{o}C and above 30^{o}C maize growth reduces and ceases, respectively (NSW, 2009). Maize plant requires 450 - 600 mm of water per season mainly acquired from the soil moisture reserves (du Plessis, 2003). The irrigation requirement is determined by cultivar selection, soil water holding capacity, evaporation, irrigation efficiency and in-crop rainfall (du Plessis, 2003; NSW, 2009). Farmers can manipulate the environment by managing factors such as cultivar selection, tillage, fertilization, and irrigation.

The effect of PD on maize yield has been studied in Pakistan by Ali et al. (2018). Their results indicated that early planting of maize cultivars gave higher grain yield and yield traits. This also avoids heat stress that affects critical growth stages of cultivars such as anthesis and ripening (Ali et al., 2018; Sánchez et al., 2014). The optimum PD for maize and its validation is essential to sustain productivity under climate change especially during anthesis. Higher yields have been reported in the Great Plains of the US and northern China with earlier planting in warmer climatic conditions (Myoung et al., 2016). Wider deviations from the optimum PD reduce maize yield. In order to reduce future impacts of climate change, earlier PDs and new cultivar with higher thermal time should be promoted (Liu et al., 2013). It has been reported that early or too late planting of maize reduces yield (Ali et al., 2018). PD and associated growing season length are factors affecting crop growth and yield (Myoung et al., 2016).

2.4 Factors affecting maize growth and yield

Maize cultivars, optimal plant population density, soil fertility, water, and timely weeding are management factors that affect optimal maize yield. Low productivity of maize can be attributed to PD, weather (rainfall), low soil fertility (chemical fertilizer application) and management practice during the growing season. PD influences maize growth and yield (Beiragi et al., 2011). Selecting optimal PD is the most important management practice under rainfed maize production (Du Plessis, 2003) and is largely linked to the long-term climatic conditions (Nape, 2011). Small scale farmers use multiple PDs to ensure successful crop growth and yield since PD affects the duration of the vegetative and reproductive phases of maize. Late planting of maize cultivars assists during a delayed onset of the rains to avoid dry spells during the growing season. However, multiple PDs affect maize growth and yield due to changes in temperature and soil moisture (Beiragi et al., 2011). In the USA, strategies for shifting and timing of N application and reducing N rates have been formulated (Banger et al., 2018).

2.5 Crop simulation models

Crop simulation models (CSMs) are diverse in their structure, functions and parameter values (Asseng et al., 2013; Hussain et al., 2018). CSMs offer alternatives to field trials for assessing PD, N fertilizer rate and cultivar selection by running computer-based experiments. CSMs should be comprehensive taking into account the dynamics of crop-soil-weather interaction (Jing et al., 2017). Most CSMs have been developed for favorable production environments of temperate regions and require adequate data to be calibrated for application to new areas and cultivars (White and Grace, 1999).

Model calibration is the adjustment of cultivar-specific parameters (CSPs) so that simulated values compare well with observed values (Hussain et al., 2018; Jones et al., 2010). Phenological phases should be simulated accurately and be the first step when calibrating CSMs (Archontoulis et al., 2014a). Phenology varies among cultivars and needs to be estimated every time a new cultivar is introduced in CSMs. Calibrating growth and yield parameters is meaningless until phenology is well simulated. Calibration

improves with sufficient data on phenology, soil, management, and yield. The pitfall in calibrating CSMs is having insufficient data on initial soil conditions, crop growth and yield. Lack of CSPs has led some researchers to use generic cultivars in order to predict yield (Archontoulis et al., 2014a; Boote et al., 2003; Mourice et al., 2014; Yang et al., 2004).

Crop model validation is the process by which the model is run against independent data, without modifying model parameters (Hoogenboom et al., 1999). Model validation depends on it predicting independent values well. All CSMs require adequate calibration, testing, and validation against observed values (Sinclair and Seligman, 1995; Thorp et al., 2009). Limited studies exploring uncertainties introduced by CSMs have been documented (Rosenzweig et al., 2013). The APSIM and DSSAT models different in modeling incoming solar radiation and photosynthetic active radiation (PAR). APSIM uses Beer's law approach (Monsi and Saeki, 2004) while DSSAT uses the approach described by Spitters et al. (1986). APSIM-Maize and CERES-Maize calibration parameters are quite demanding.

2.5.1 Agricultural Production Systems Simulator (APSIM)

The Agricultural Production Systems Simulator (APSIM) is a dynamic soil-plant-atmosphere model (Knörzer et al., 2011). APSIM is a modular modeling framework developed by the Agricultural Production Systems Research Unit (APSRU) in Australia (Keating et al., 2003; Keating and McCown, 2001; McCown et al., 1995). It runs on a daily time-step and mimics crop growth and development, yield, soil water balance, and nitrogen dynamics either for a single crop or crop rotations in response to climatic and management (He et al., 2015; Knörzer et al., 2011). The modeling framework of APSIM is made up of the biophysical modules, management modules, various modules to facilitate data input and output and a simulation engine that drives the simulation process and facilitates communication between independent modules (Figure 3).

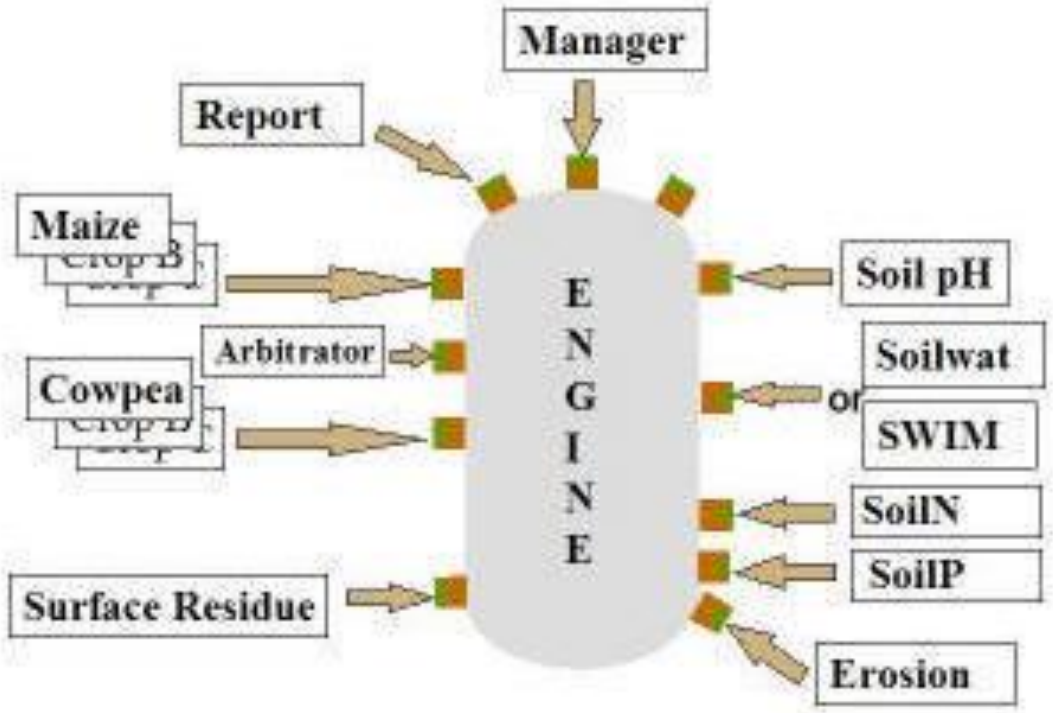

Figure 3: APSIM modelling framework

Source: (Ahmed and Hassan, 2011; Keating et al., 2003)

The crop modules for barley, canola, chickpea, cotton, cowpea, hemp, fababean, lupin, maize, millet, mucuna, mungbean, navy bean, peanut, pigeon pea, sorghum, soybean, sunflower, wheat, and sugarcane are accessible in APSIM (Keating et al., 2003). The model includes a 'climate change' module that allows temperature and rainfall data to be adjusted and includes carbon assimilation algorithms that respond to increased CO_2 concentrations. According to Archontoulis et al. (2014a), DEVEL2 and NAG are optimization programme relevant to the APSIM model and have been used to estimate phenological parameters. Other automated parameter optimization software like LHS (Latin Hypercubic Sampling) and PEST (Parameter Estimation Software) are available with limited applications (Ma et al., 2011). These tools have not been operationally made available to APSIM users and were not designed to optimize phenological parameters for the APSIM model. The development of an optimization tool in APSIM to simplify the calibration of phenology which is not available in APSIM is advantageous for people using the crop model and dealing with new cultivars.

APSIM minimum input data includes site weather data, crop phenology, soil water, soil carbon per layer, nitrogen (N), NO_3-N, soil bulk density per layer, phosphorus (P), surface residues and management (Knörzer et al., 2011; McCown et al., 1996). In this study, the same minimum data required to calibrate and validate the APSIM-Maize module were collected from the experimental sites.

2.5.1.1 APSIM-Maize model

The APSIM-Maize model consists of phenology, leaf development, biomass production, and partitioning (Archontoulis et al., 2014a; Brown et al., 2014). The crop phenology is divided into sub-phases, and the duration of each phase is determined by temperature and photoperiod and can be affected by water and N stresses. APSIM-Maize differs from the CERES-Maize in routines which kill crops in response to severe water deficit during the early-to mid-vegetative stage (Carberry and Abrecht, 1991).

New maize cultivars were introduced into APSIM-Maize by defining several variables as shown in Table 2. These variables define the accumulation of thermal time units within the individual growth stages, plant development and the switching from vegetative to reproductive phase. The APSIM-maize model simulates the maize developmental stage in terms of accumulated thermal time (growing degree days [GDDs]). The GDDs is estimated using a linear relationship calculated with 3h temperatures interpolated from daily maximum and minimum temperature. The GDDs durations for the subsequent phases are dependent on CSPs.

Table 2: CSPs used in APSIM-Maize

Phenology	Coefficients	Explanation	Units
Phylochron	Leaf_app_rate1		
Thermal time units	tt_emerg_to_endjuv	tt from emergence to end of the juvenile stage	°Cd
	tt_flower_to_maturity	tt from silking to physiological maturity	°Cd
	tt_flag_to_flower	tt from flag leaf to silking	°Cd
	tt_emerg_to_endjuv	tt from emergence to end of the juvenile stage	°Cd
	tt_endjuv_to_init	tt from the end of juvenile to floral initiation	°Cd
	tt_flower_to_start_grain	tt from silking to start effective grain fill period	°Cd
Grain growth	grain_gth_rate units	grain growth rate	*
Grain No.	head_grain_no_max	potential kernel number per ear	°Cd

Note: tt: thermal time; *grain growth rate = unit is in mg grain^{-1} day^{-1}
Source: Knörzer et al. (2011)

In APSIM-Maize model, a trial and error method (Ahmed et al., 2016a; Archontoulis et al., 2014a; Mthandi et al., 2014) has been used to calibrate new cultivars and this is a stepwise approach (starting with crop phenology, soil water, soil nitrogen, biomass production, partitioning, and yield). The accuracy in a stepwise approach depends on the type and quality of measured data and experience of the user. Archontoulis et al. (2014) reported that calibrating the APSIM phenology is robust whether it is done manually or automatically. Many CSMs are calibrated manually, and the procedure is not transferable to another model; neither is the automatic methods (Ma et al., 2011).

2.5.2.1 DSSAT-Cropping System Model (CSM)

The Decision Support System for Agrotechnology Transfer (DSSAT) version 4.7 comprises 42 crop simulation models. It is supported by database management programmes for soil, weather, and crop management and experimental data, and by utilities and application programmes to be functional. The crop simulation models simulate growth, development, and yield as a function of the soil-plant-atmosphere dynamics, soil, and plant water, nitrogen, phosphorus and carbon dynamics (Hoogenboom et al., 2010; Jones et al., 2010, 2003). One of the crop simulation models is the CERES-Maize model that has been calibrated and validated under local conditions in this study.

2.5.2.1.1 CERES-Maize model

The DSSAT CERES (Crop Environmental Resource Synthesis) maize model is a process-oriented, management-level model that simulates crop growth and development, soil water balance and nitrogen balance (Jones et al., 1986; Kiniry et al., 1997; Liu et al., 2012; Yang et al., 2004). Central to the model are routines that estimate phenology and growth without limiting root soil water and fertility. It is widely used and recognized reference for comparing new developments in maize simulation (Lizaso et al., 2011). The model has evolved over the past years into a widely used model and has been tested under a wide range of environments (Deb et al., 2015b; Xiong et al., 2007). It accurately predict yield variability, N uptake and maize growth response to nitrogen (Pang et al., 1997) and has been used to explore new cultivars for new areas (Bationo et al., 2012) and to determine the optimum PDs (Chisanga et al., 2015; Soler et al., 2005) under future climate scenarios (RCP4.5 and RCP8.5). APSIM is a modular modeling framework that runs at a daily time-step and simulates crop growth and development, yield, soil water, and nitrogen dynamics either for a single crop or crop rotations in response to climatic and management (Keating et al., 2003).

The CERES-Maize model requires daily weather data, crop management, cultivar characteristics, cultivar genetic information, soil profile characteristics, crop phenology, leaf area index, initial soil condition, biomass and grain yield as input data (Ahmed et al., 2017; Lin et al., 2017). The soil input file (fileS) in DSSATCERES-Maize model does not offer automated procedure during calibration and validation. The soil water balance is based on Ritchie's model where the concept of drained upper limit (DUL) and drained lower limit (LL) of the soil is used as the basis of the available soil water (Boote et al., 2008; Garrison et al., 1999; Ritchie et al., 2009; Valeriano et al., 1993).

The CERES-Maize model requires six cultivar-specific parameters (CSPs) (genotype specific coefficients) (P1, P2, P5, G2, G5, and PHINT) shown in Table 3 for its calibration. The "P" CSPs (P1, P2, and P5) are computed using observed anthesis and physiological maturity dates. The "P" CSPs are used to determine the timing of the phenological phases (dates of anthesis and maturity). The G2 and G5 control grain size, grain number m^{-2},

grain and biomass yield (Hoogenboom et al., 2010; Jones et al., 2010). The PHINT defines leaf tip appearances.

Table 3: CSPs used in CERES-Maize model

Coefficients	Development Aspects	Units
P1	GDDs (based on 8°C) from emergence to end of the juvenile phase	°Cd
P2	Photoperiod sensitivity coefficient (01.0)	
P5	GDDs(based on 8°C) from silking to maturity	°Cd
	Growth Aspects	
G2	Maximum possible number of kernels per plant	
G3	Potential kernel growth rate (mg day^{1})	mg day^{1}
PHINT	GDDs required for a leaf tip to appear(based on 8°C)	°Cd

Source: Hoogenboom et al. (2010)

In the CERES-Maize model, the plant life cycle is divided into several phases (Hoogenboom et al., 2010). The rate of development is governed by growing degree-days (GDD) or thermal time whose computation is based on daily maximum and minimum temperatures. The GDD required to progress from one growth stage to another is either defined as user input or are computed internally based on user inputs and assumptions about the duration of intermediate stages.

New cultivars can be calibrated using sensitivity analysis, generalized likelihood uncertainty estimation (GLUE) or genetic coefficient calculator (GENCALC) (Hoogenboom et al., 1999). GENCALC and the GLUE embedded within DSSAT software are two software used to estimate CSPs for the DSSAT crop models using the measured crop phenology, biomass and grain yield data. The GENCALC and GLUE programmes include anthesis date and biomass at maturity as input data, traits not routinely measured by plant breeders (Hoogenboom et al., 1999). The GLUE and GENCALC only optimize crop parameters. GENCALC software was developed by L. A. Hunt (Hoogenboom et al., 1999) and is available in DSSAT v3.5, v4.5-4.7. The GLUE programme has been integrated into DSSAT versions 4.5-4.7 using the R language, a free software environment for statistical computing (Hoogenboom et al., 2010). More details on how the CSPs are computed in DSSAT are provided by Jones et al. (2010).

2.5.3 Validation of crop simulation models

APSIM-Maize and CERES-Maize models have been validated over a wide range of environments and has also been used to study the potential impact of climate change and variability on crop productivity (Adnan et al., 2017; Archontoulis et al., 2014a; Asseng et al., 2013; Dokoohaki et al., 2016; Keating et al., 2003; Knörzer et al., 2011; Mourice et al., 2014; Pang et al., 1997). Crop model evaluation is accomplished by inputting minimum dataset, running the model, and comparing simulated versus observed values.

2.5.4 Model evaluation

Crop simulation models have been evaluated by comparing simulated versus observed values (days to flowering, and maturity, grain and biomass yield) (Lin et al., 2017). Accuracy of the models is usually evaluated using d-index, modeling efficiency (ME); root mean square error (RMSE), normalized RMSE (NRMSE) and predicted deviation (PD) (Jones et al., 2010; Jones and Thornton, 2003; Willmott, 1982; Willmott et al., 1985). The simulation was considered excellent with NRMSE <10%, good if 10-20%, acceptable or fair if 20-30%, and poor >30% (Jamieson et al., 1995; Zhang et al., 2012).

2.6 Crop simulation model ensembles

Working with ensembles of CSMs is a recent development (Wallach et al., 2016). A lot can be drawn and learned from the field of climate modeling and to make ensemble modeling with CSMs more informative and rigorous (Wallach et al., 2016). In modeling, there are uncertainties in simulated values, and these can be evaluated by using an ensemble of CSMs. The variability among the models in the ensemble measures the uncertainty instead of a point prediction (Harris et al., 2010). It has been observed that ensemble means or medians provide robust estimates of growth and yield than an individual model (Martre et al., 2015; Salo et al., 2016). The number of CSMs in an ensemble is important as it affects the mean, median and variability of the ensemble output (Wallach et al., 2016). It is difficult to organize and carry out studies with multiple CSMs. However, it is much easier to conduct studies with fewer CSMs. The effect of ensemble composition has not been properly appraised as observed by (Rodríguez et al., 2019).

2.7 Effect of climate change on PD, N, cultivar, and yield

In the past three decades, historical maize yields in China has increased under cultivar selection, crop management and changes in climate (Liu et al., 2013). Butler et al. (2018) also reported similar results. Maize yield has increased due to warmer conditions and earlier planting of maize cultivars (Butler et al., 2018). Maize is influenced by changes in temperature and rainfall associated with PDs and growing season length (Ali et al., 2018; Myoung et al., 2016). The effect of PD on maize yield has been studied in Pakistan by (Ali et al., 2018). Their results indicated that early planting of maize cultivars gave higher yield and yield traits. This also avoids heat stress affects critical growth stages of cultivars (Ali et al., 2018). The optimum PD for maize and its validation is essential to sustain productivity under climate change especially during anthesis. Higher yields have been reported in the Great Plains of the US and northern China with earlier planting in warmer climatic conditions (Myoung et al., 2016). Wider deviations from the optimum PD reduce maize yield. In order to reduce future impacts of climate change, earlier PDs and new cultivar with higher thermal time should be promoted (Ali et al., 2018; Liu et al., 2013).

2.7.1 Effect of planting date on maize growth and yield

Maize cultivars, optimal PD, soil fertility, water, and timely weeding are management factors that affect optimal maize yield. Low productivity of maize can be attributed to PD, weather (rainfall), low soil fertility and management practice during the growing season. PD influences maize growth and yield (Beiragi et al., 2011). Selecting optimal PD is the most important management practice under rainfed maize production (du Plessis, 2003). PD is largely linked to long-term climatic conditions (Nape, 2011). Small scale farmers use multiple PDs to ensure successful crop growth and yield since PD affects the duration of the vegetative and reproductive phases of maize. Multiple PDs, N fertilizer application rates, cultivar selection and management practices affect maize growth and yield due to changes in temperature and soil moisture (Beiragi et al., 2011). PD is a critical factor for capturing higher solar radiation without nutrient and soil moisture deficiency.

2.7.2 Effect of nitrogen fertilizer rate on maize growth and yield

Nitrogen (N) is the most important nutrient that affects maize growth and yield, and its availability in the soil varies with place and time. Nitrogen deficiency affects photosynthesis by reducing leaf area and accelerates leaf senescence. Its deficiency is the second biggest limiting parameter after drought in tropical maize production since maize responds positively to adequate nitrogen application (Lafitte et al., 1997). The soil N varies between season and location (Nape, 2011). Soil N influences soil N status and availability of soil water content. Soil temperature and root soil water content affect N fertilizer application rate. Early PDs usually have adequate N, and this exceeds crop demand. As the season progresses soil N is depleted causing N stress (Sangoi, 2001).

In Zambia, important factors determining the PD of maize is soil fertility, soil moisture and soil temperature (Chinene, 1985). The recommended PD in Zambia is normally November, at the beginning of the rains and it is influenced by cultivars. Nitrogen is a limiting factor in growing maize followed by phosphorus and potassium. The N application rate is influenced by initial soil fertility and rainfall. Lower application of N would perform better in lower rainfall. Maize requires between 450 and 600 mm of rainfall per season mainly acquired from root soil moisture (Du Plessis, 2003). Rainfed maize growth and yield are severely inhibited by soil water stress and high temperatures.

2.8 Simulated impacts of climate change on planting date, N, cultivar, and yield

Simulated maize yield in Himalayan foothills of India using the CERES-Maize model and A2 and B2 climate scenarios showed reduced maize yield from 10.7-18.2% (Deb et al., 2015). Future climate simulations by Masanganise et al. (2012) in Zimbabwe showed that temperature would increase between 1 and 2^{o}C relative to the baseline (1971-2000). A study by Araya et al. (2017) using CERES-Maize, climate scenarios (RCP4.5 and RCP8.5), two irrigation regimes and three PDs in Kansas revealed that grain yield would decline due to shortening of the growing season and higher temperatures. Simulation of maize phenology and yield using APSIM-Maize showed an increase in yield by 4% at Himalayan foothills of India with earlier PDs (Araya et al., 2017; Deb et al., 2015a). The use of traditional PDs in the 2050s would result in reduced maize yield while adopting

dynamic planting strategies would increase maize yield. To maintain crop yields, farmers require a suite of adaptation strategies (Kucharik, 2008). Adjusting planting dates and introduction of new cultivars with improved traits have been recommended as adaptations to climate change (Fodor et al., 2017; Wang et al., 2016). The choice of this strategy would largely depend on how the local and regional climate changes.

2.9 Temperature and precipitation climate indices

The World Meteorological Organization (WMO) define climate extremes as rare meteorological and climatological phenomena that surpass a defined threshold (Das et al., 2003). Changes in extreme weather and climate events such as droughts, floods, frosts, and heat waves have significant impacts on society. It is, therefore, important to analyze extreme weather indices (Peterson, 2005). Changes in the frequency of temperature extremes may result in changes of the mean, the variance, and or both. Variability in precipitation changes distribution mean and spread (Soltani et al., 2016). Climate change also alters precipitation frequency, and this can change the length of dry/wet spells.

Observations and understanding the mechanisms associated with extreme events could provide useful insights for resource planners and policy makers to formulate mitigation and adaptation strategies (Alexander, 2016; Soltani et al., 2016). Comprehensive local and regional studies are important in assessing the impacts of extreme indices and events. The Intergovernmental Panel on Climate Change (IPCC) in its Third Assessment Report (AR3) of 2001 undertook a global assessment of long-term changes in temperature and precipitation (Alexander, 2016). The report highlights increased precipitation events, decreased and increased the frequency of extreme low and high temperature, respectively.

The monitoring, detection, and attribution of changes in climate extremes require daily time series data (Peterson, 2005). The IPCC AR4 (2007) observed that climate change is affecting precipitation across the world as reflected in the mean and variability estimates (Hashmi et al., 2009; Osman et al., 2014). The Zambian climate, however, has a history of droughts and floods (MTENR et al., 2007). Many studies have investigated climate

change and extreme weather events at the global and regional scale (Dos Santos et al., 2011) but a few of these have been undertaken ata local scale in Zambia.

The Expert Team on Climate Change Detection and Indices (ETCCDI) has developed 27 climate indices (Alexander and Herold, 2016; Alexander et al., 2006; Huang et al., 2011). These indices are based on daily temperature and precipitation to document the change in climate extremes over poorly studied areas to enhance global analysis (Alexander et al., 2013, 2006; Alexander and Herold, 2016). The indices were developed with the detection and attribution of the research community in mind (Alexander and Herold, 2016). To detect changes in climate extremes, the set of indices should be statistically robust and possess a high signal-to-noise ratio (Alexander et al., 2013). Conversely, the Expert Team on Climate Risk and Sector-specific Indices (ET CRSCI) (Table 4 and Table 5) spearheaded the development of ClimPACT software for calculating climatic indices (Alexander et al., 2013).

The ClimPACT2 is an R software package that was written in r-code to calculate Sector-specific Climate Indices (ET-SCI) and other additional climate extreme indices from data stored in text and netCDF files. ET-SCI indices represent a set of over 60 climate extremes indices together with ETCCDI indices. ClimPACT2 provides useful indices for application in Health, Agriculture and Food Security, and Water Resources and Hydrology Sectors. ClimPACT2 is based on the computations in RClimDEX software developed by the World Meteorological Organization (WMO) Commission for Climatology (CCl)/World Climate Research Programme (WCRP) on Climate Variability and Predictability (CLIVAR)/JCOMM. It also directly incorporates the R packages climdex.pcic and climdex.pcic.ncdf developed by the Pacific Climate Impacts Consortium (PCIC). Three methods can be used to compute climate indices using a station text file (Alexander and Herold, 2016). The development and analysis of ET-SCI have made a significant contribution to climate change discussions in the IPCC ARs (Alexander, 2016).

The ETCCDI recommends the use of the RHTest software to check for quality and homogeneities in daily time series data (Dos Santos et al., 2011; Wang et al., 2010). The

literature reviewed indicated that there is insufficient information on trends in climate extremes especially in developing countries at local-scale due to insufficient resources and limited access to data, Zambia is no exception. The ET-SCI climate indices on temperature and precipitation extremes at Mount Makulu have been analyzed in this study.

Table 4: Core ET-SCI extreme temperature and precipitation indices

	Indices	Definition	Units	Time scale	Sector(s)
1	SU	No. of days when TX > 25 °C	days	Mon/A	H
2	TR	No. of days when TN > 20 °C	days	M/A	H, AFS
3	GSL	Annual No. of days between the first occurrence of 6 consecutive days with TM > 5 °C and the first occurrence of 6 consecutive days with TM < 5 °C	days	A	AFS
4	TXx	Warmest daily TX	°C	M/A	AFS
5	TNn	Coldest daily TN	°C	M/A	AFS
6	WSDI	Annual No. of days contributing to events where 6 or more consecutive days experience TX > 90th percentile	days	A	H, AFS, WRH
7	CSDI	Annual No. of days contributing to events where 6 or more consecutive days experience TN < 10th percentile	days	A	H, AFS
8	CSDId	Annual No. of days contributing to events where d or more consecutive days experience TN < 10th percentile	days	A	H, AFS, WRH
9	TXgt50p	Percentage of days where TX > 50th percentile	%	M/A	H, AFS, WRH
10	TX95t	Value of 95th percentile of TX	°C	Daily	H, AFS
11	TXge30	No. of days when TX >= 30 °C	days	M/A	H, AFS
12	TXge35	No. of days when TX >= 35 °C	days	M/A	H, AFS
13	CDDcoldn	The annual sum of TM - n (where n is a user-defined location-specific base temperature and TM > n)	degree-days	A	H
14	GDDgrown	The annual sum of TM - n (where n is a user-defined location-specific base temperature and TM > n)	degree-days	A	H, AFS
15	CDD	Maximum No. of consecutive dry days (when PR < 1.0 mm)	days	M/A	H, AFS, WRH
16	R20mm	No. of days when PR >= 20 mm	days	M/A	AFS, WRH
17	PRCPTOT	Sum of daily PR >= 1.0 mm	mm	M/A	AFS, WRH
18	R95pTOT	100*r95p / PRCPTOT	%	A	AFS, WRH
19	R99pTOT	100*r99p / PRCPTOT	%	A	AFS, WRH
20	RXdday	Maximum d-day PR total	mm	M/A	H, AFS, WRH
21	SPEI	A measure of "drought" using the Standardized Precipitation Evapotranspiration Index on time scales of 3, 6 and 12 months	unit less	Custom	H, AFS, WRH

Note: H = Health, AFS = Agriculture and Food security; and WRH = Water Resources and Hydrology; A = Annual; M = Monthly
Source: Alexander (2014); Alexander and Herold (2016)

Table 5: Non-core ET-SCI extreme temperature and precipitation indices

	Short name	Definition	Units	Time	Sector(s)
1	DTR	Mean difference between daily TX and daily TN	°C	M/A	
2	TNx	Warmest daily TN	°C	M/A	
3	TXn	Coldest daily TX	°C	M/A	
4	TMm	Mean daily mean temperature	°C	M/A	
5	TXm	Mean daily maximum temperature	°C	M/A	
6	TNm	Mean daily minimum temperature	°C	M/A	
7	TX10p	Percentage of days when TX < 10th percentile	%	A	
8	TX90p	Percentage of days when TX > 90th percentile	%	A	
9	TN10p	Percentage of days when TN < 10th percentile	%	A	
10	TN90p	Percentage of days when TN > 90th percentile	%	A	
11	CWD	Maximum annual number of consecutive wet days (when PR >= 1.0 mm)	days	A	
12	R10mm	Number of days when PR >= 10 mm	days	M/A	
13	Rnnmm	Number of days when PR >=nn	days	M/A	
14	SDII	Annual total PR divided by the number of wet days (when total PR >= 1.0 mm)	mm/day	A	
15	R95p	The annual sum of daily PR > 95th percentile	mm	A	
16	R99p	The annual sum of daily PR > 99th percentile	mm	A	
17	Rx1day	Maximum 1-day PR total	mm	M/A	
18	Rx5day	Maximum 5-day PR total	mm	M/A	
19	HWN(EHF/Tx90/Tn90)	The number of individual heat waves that occur each summer. A heat wave is defined as 3 or more days where either the EHF is positive, TX > 90th percentile of TX or where TN > 90th percentile of TN.	events	A	H, AFS, WRH
20	HWF(EHF/Tx90/Tn90)	The number of days that contribute to heatwaves as identified by HWN.	days	A	H, AFS, WRH
21	HWD(EHF/Tx90/Tn90)	The length of the most prolonged heat wave identified by HWN.	days	A	H, AFS, WRH
22	HWM(EHF/Tx90/Tn90)	The mean temperature of all heat waves identified by HWN.	°C (C2 for EHF)	A	H, AFS, WRH
23	HWA(EHF/Tx90/Tn90)	The peak daily value in the hottest heat wave (defined as the heat wave with the highest HWM).	°C (°C2 for EHF)	A	H, AFS, WRH
24	CWN_ECF	The number of individual 'cold waves' that occur each year.	events	A	H, AFS, WRH
25	CWA_ECF	The minimum daily value in the coldest 'cold wave' (defined as the cold wave with the lowest ECF_HWM).	C2	A	H, AFS, WRH
26	CWF_ECF	The number of days that contribute to 'cold waves' as identified by ECF_HWN.	days	A	H, AFS, WRH

Note: H =: Health, AFS =: Agriculture and Food security and WRH = Water Resources and Hydrology; A = Annual; M = Monthly

Source: Alexander (2014); Alexander and Herold (2016)

2.10 Downscaling of climate data

Two downscaling techniques are used in generating climate scenarios: dynamical (10-50 km) and statistical. Dynamical downscaling techniques use numerical equations governing the atmosphere on a finer grid (Chen et al., 2012; Devak and Dhanya, 2014). It is based on Regional Climate Models (RCMs) which are nested within the GCM and generate finer spatial resolution output.

There are three statistical downscaling techniques: (i) synoptic weather typing; (ii) stochastic weather generators; and (iii) regression methods or transfer-functions (CSIRO and BOM, 2015; Semenov and Barrow, 2002; Wilby and Dawson, 2007). The weather generators are computer models used to produce synthetic time series of daily weather data at a single site based on the statistics of the baseline climate (IPCC-TGCIA, 2007). Statistical downscaling techniques try to establish empirical relationships between the predictors and predictands (Chen et al., 2012; Devak and Dhanya, 2014). An example of a stochastic weather generator is the Long Ashton Research Station Weather Generator (LARS-WG) (Semenov and Barrow, 2002, 1997; Semenov and Brooks, 1999). It is used to generate synthetic weather data at a single site based on observed statistical characteristics of weather at a single site for the current and future climate conditions.

The synthetic weather data can be used in areas with insufficient daily observed time series to estimate the probability of extreme events (Semenov et al., 1998; Wang, 2015; Zanchetta et al., 2009). Daily observed weather data of 20-35 year is recommended to determine robust statistical parameters (Mckague et al., 2005; Semenov and Barrow, 2002; Stockle et al., 2003). The suitability of LARS-WG in generating synthetic weather data has not been evaluated in Zambia. The relative strengths and weaknesses of statistical downscaling techniques are shown in Table 6.

Table 6: Relative strengths and weaknesses of statistical downscaling methods

Method	Strengths	Weaknesses
Weather typing/weather classification (e.g., analog method, hybrid approaches, fuzzy classification, self-organizing maps, Monte Carlo methods, recursive partitioning)	1. Yields physically interpretable linkages to surface climate 2. Versatile (e.g., can be applied to surface climate, air quality, flooding, erosion, etc.) 3. Compositing of extreme events 4. Yields physically interpretable linkage to surface climate 5. Versatile can be applied to surface climate quality, air quality, flooding, erosion, etc. 6. Compositing of extreme events	1. Require a classification scheme 2. Circulation can be insensitive to future climate forcing 3. May not capture intra-type variation in surface climate 4. Precipitation changes produced by changes in the frequency of weather patterns are rarely consistent with the changes produced by the host GCM unless additional predictors such as atmospheric humidity are employed
Weather generators (e.g., Markov chains, stochastic model (**LARS-WG**), spell length methods, storm arrival times, mixture modelling)	1. Simultaneous weather generation at multiple sites 2. Multivariate outputs 3. Spatial interpolation of model parameters using landscape 4. Captures variability across a range of space-time scales	1. Arbitrary adjustment of parameters for future climate 2. Unanticipated effects on secondary variables of changing precipitation parameters
Regression methods/Transfer functions (e.g., Linear [**Delta method]** and non-linear regression, multi-linear regression, artificial neural networks, principal canonical correlation analysis, kriging, gene expression programming)	1. Relatively straight forward to apply 2. Employs a full range of available predictor variables 3. Transparency of relationships 4. Most commonly used statistical downscaling techniques due to their simplicity and effectiveness 5. Regularly used because of their ease of implementation and their low computation requirements	1. Poor representation of observed variance 2. May assume linearity and normality of data 3. Poor representation of extreme events 4. They under predict daily precipitation variance 5. Have relatively low predictability of local amounts by large-scale forcing alone

Source: Lapp et al. (2008); Masoud et al. (2005); Wang (2015); Wilby et al. (2004); Wilby and Dawson (2004)

2.11 Agricultural Model Inter-comparison and Improvement Project

Quantifying the impacts of climate change and variability in sub-Saharan Africa (SSA) has been explored under the Agricultural Model Intercomparison and Improvement Project (AgMIP) (www.agmip.org) (Kassie et al., 2014). The AgMIP aims to improve the description of climate-crop-and-economic interactions in models and to foster the application of multiple crop simulation models in climate impact assessments (Asseng et al., 2013; Kassie et al., 2014). The AgMIP launched in October 2010 is an international research programme that focuses on climate, crop, and economic modeling in coordinated global and regional assessments of the future impact of climate change on world food security. The goals of AgMIP (Rosenzweig et al., 2013) are to advance the characterization of world food security substantially under climate change and to improve adaptive capacity in developing and developed nations.

The AgMIP manages inter-comparison studies on global biophysical and economic modeling, and this brings together key international modeling groups to test the observational and future impact of climate change under the Inter-Sectoral Impact Model Intercomparison Project (ISI-MIP) (Rosenzweig et al., 2013). Crop models operate at a regional and global scale. At the global scale, crop models can be simulated using gridded, point or aggregated data. Analysing impacts of climate change and variability in the agricultural sector requires multi-disciplinary efforts to link current and future climate scenarios to crop and economic models (Rosenzweig et al., 2015). CSMs outputs are used as inputs into the global and regional economic models to evaluate global and regional vulnerabilities, price effects, changes in comparative advantage and potential mitigation, and adaptation strategies.

The AgMIP uses 1980-2010 as the baseline and three future time periods (2010-2039, 2040-2069 and 2070-2099) as shown in Table 7. The 2010-2039 period is used to understand climate variability and to develop effective adaptation and mitigation strategies. The 2040-2069 and 2070-2099 periods are used to assess the impact of climate change and variability (Rosenzweig et al., 2015). The AgMIP Protocols define the processes and tasks required to undertake inter-comparisons and multiple-model assessments proficiently and systematically (Rosenzweig et al., 2015, 2013). The protocols are designed to guide climate modeling, crop simulation modeling, and economic modeling. The Protocols have been implemented in South Asia (Sri Lanka)

and Eastern and South Africa (Ethiopia, Kenya, Tanzania, Ugand, and South Africa) (Rosenzweig et al., 2013). However, the protocols have not been applied in Zambia at either regional or local scale to evaluate the impacts of climate change on agricultural productivity. Under AgMIP protocols, future scenarios are produced using the delta-based method, and these can be applied to most adaptation activities.

Table 7: Carbon dioxide concentrations for AgMIP climate scenarios and time periods

Scenario and Period	Planting year coverage	Mid-year	ppm CO_2
Current (Historical)	1980-2009	1995	360
RCP4.5 Near-term	2010-2039	2025	423
RCP8.5 Near-term	2010-2039	2025	423
RCP4.5 Mid-Century	2040-2069	2055	499
RCP8.5 Mid-Century	2040-2069	2055	571
RCP4.5 End-of-Century	2070-2099	2085	532
RCP8.5 End-of-Century	2070-2099	2085	801

Source: Rosenzweig et al. (2014c)

Climate scenarios under AgMIP can be generated based on 20 GCMs at the best-calibrated site in the region of interest (Rosenzweig et al., 2014). Moreover, farm survey sites can only use a subset of 5 GCMs (**Error! Reference source not found.**) to generate climate scenarios for crop simulation that focuses on the primary climate change impact questions. This GCM subset has been used in South-east Asia, Europe, and Africa due to their long history of development, assessment, higher spatial resolution, established performance and suitability (McSweeney et al., 2012; Msongaleli et al., 2015). The Agricultural Modern-Era Retrospective Analysis for Research and Applications (AgMERRA) weather data have been used as alternatives in regions where quality observational time series data are unavailable (Zare et al., 2016). The 5 GCMs and AgMERRA weather data have been used in this study to assess the impact of climate change and variability on maize growth and yield in the 2050s.

2.11.1 Delta-based method or change factor Downscaling Approach

The direct method of generating higher spatial resolution climate scenarios is to apply coarse resolution GCM outputs to a high quality observed climate using the delta method (Wilby et al., 2004). The GCM outputs are scenarios of climate change rather than actual values (Qian et al., 2005). In the delta method, the differences between

GCM future and baseline time series data are added to historical monthly or daily observations (Ruiter, 2012). The delta-based method is a robust, easily understood and accurate statistical downscaling technique. Unfortunately, its weakness is that the number of rain-days per month in the future does not change. Additionally, future solar radiation is assumed to be the same as that of the baseline. The delta-based method has been applied in this study to downscale the GCMs. The outputs from the delta-based method have been used in crop simulation studies.

2.12 Situational analysis of climate change in Zambia

2.12.1 Temperature and precipitation

Zambia is characterized by a dry and wet climate (Palijah, 2015; Sichingabula, 1998). The annual rainfall is strongly influenced by the shifting of the Pacific Ocean's El Nino Southern Oscillation (ENSO), the Inter-Tropical Convergence Zone (ITCZ) and the Congo Air Boundary. The mean annual temperature has increased since 1960 by 1.3ºC (MTENR, 2010; Muchanga, 2012; UN, 2012). Warming rates per decade of 0.48ºC, 0.34ºC, and 0.26ºC have been observed across the country for Agricultural Ecological Regions (AERs) I, II, and III (Figure 4) based on 1970-2000. The AERs differ on the amount of precipitation: Region I is a low rainfall (<800 mm/year) area which covers the country's major valleys; Region II, the medium rainfall (800-1000 mm/year) area, covers Sandveld plateau of Central, Eastern, Lusaka, and Southern provinces; and Region III has the highest rainfall (1000-1500 mm/year). There has been a decrease in annual rainfall of 2.3% per decade since 1960 (MTENR, 2010; UN, 2012).

In Zambia, the threat of climate change is characterized by floods and droughts (Fumpa-Makano, 2011). In the last 20 years, maize yield has reduced by 40% in AERs I and II as a result of shortening rain season and persistent dry spell (UNDP, 2010). Zambia experienced droughts (1916/17, 1924/25, 1949/50, 1983/84, 1987/88, 1991/92, 1994/95 and 1997/98) and high intensity of floods (2006/2007, 2007/08, 2009/2010) (Sichingabula, 1998). The worst of these was the 1991/92 droughts, and 2006/07 floods (Fumpa-Makano, 2011). There has been a tendency for late-onset and early withdrawal of rains in Zambia (Fumpa-Makano, 2011). The strong dependence on maize as the staple food in Zambia is a serious concern and requires much useful adaptation options to reduce adverse impacts of climate change since much of the maize is grown by small-scale farmers and is rainfed.

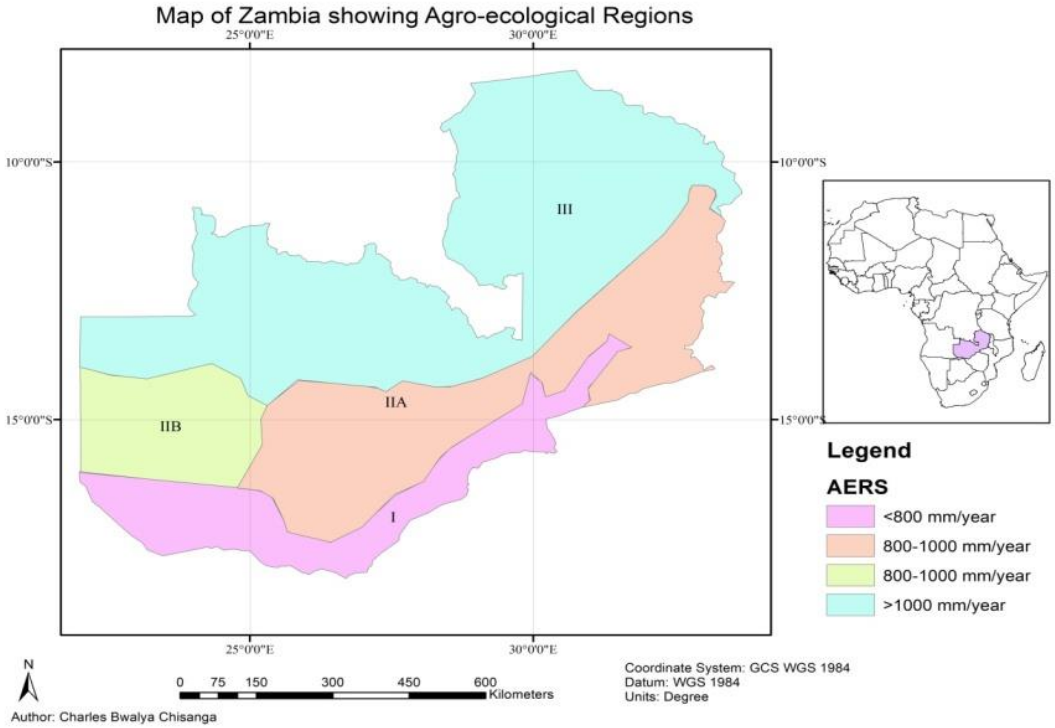

Figure 4: Agro-ecological Regions of Zambia
Source: JAICAF (2008); Veldkamp et al. (1984)

Temperature projections from GCMs suggest an increase in temperature by the end of the century ranging from 2.4 to 4.3°C relative to 1961-1990 (GIZ, 2014). GCMs predictions over Zambia indicated that rainfall in AER I, IIa and IIb has decreased with significant warming detected in AER I while rainfall in AER III has increased (Arslan et al., 2015). The estimated maize yield decline in Zambia is concentrated in Southern and Eastern provinces, highlighting the importance of how climate change impacts on crop yields. The ability of the agricultural sector in Zambia to cope with projected changes in rainfall and temperatures is limited due to low levels of investment, land degradation and limited access to agricultural inputs (Arslan et al., 2015).

2.12.2 Impact of climate change on maize yield using APSIM and DSSAT models in Zambia

Many studies on climate change impacts on agriculture are performed at large spatial scales, and it is difficult to identify useful on-farm mitigation and adaptive measures (Zinyengere et al., 2014). There are also fewer studies that have used CSMs to simulate

the effect of climate change on PD, N fertilizer rate and cultivar and yield at the local scale. The APSIM and CERES-Maize model have been used in Zambia in simulating maize growth and yield (Chinene, 1985; Chisanga et al., 2015; GRZ and UNDP, 2007; Mwansa, 2016). An evaluation of the effect of water and nitrogen on maize grain yield indicated that nitrogen and water availability limited grain yield (Chinene (1985). Studies using DSSAT v3 and climate scenarios predicted a reduction in rainy days and shortening of the growing season and these would inhibit maize attaining maturity in AER I and II of Zambia (GRZ and UNDP, 2007; MTENR et al., 2007; UNDP, 2010). The suggested adaptation strategies were planting drought resistant and open-pollinated cultivars (GRZ and UNDP, 2007). A study by Mwansa (2016), revealed that maize yield in conservation farming would be affected by temperature rise rather than variability in precipitation.

2.13 Implication of climate change and climate indices on soils in AERII

Climate change and extreme temperature indices (heat stress and heat wave) affects the biodiversity of soil directly (heat stress alters soil temperature and moisture) and directly (vegetation communities and organic matter decomposition rates are altered). Heat stress is an important parameter that limits plant growth and development especially during pollination (phenological phase).

Maize and other crops such as soybean are susceptible to extreme heat and water stress especially during early vegetative and reproductive stages. Extreme heat stress leads to a reduction of photosynthesis, plant stomata conductance and transpiration and this affects root development and crop yield. Rising soil temperature due to heat stress above the optimal thresholds impedes root soil water and nutrient uptake by plants. Extreme air and soil temperature can damage different plant parts. Therefore, it is important to have sufficient root soil water during heat wave and heat stress periods as a mitigation strategy.

A close relationship between air temperature and soil temperature exists. An increase in air temperature would certainly lead to an increase in soil temperature. The increasing soil temperature accelerates the decomposition of organic matter, soil nutrient release, soil processes, microbe’s activity, nitrification rate and accentuates chemical weathering of minerals. The reduction in organic matter as a result of rapid

decomposition leads to decreased water infiltration rates, soil aggregate stability, soil water holding capacity, susceptibility to soil erosion, nutrient availability and compaction. It is estimated that constant inputs of carbon to soil from vegetation under climate change (changes in temperature, rainfall, and evapotranspiration) would cause a significant change in CO_2 dynamics and organic matter (Karmakar et al., 2016). The type of vegetation cover also affects soil temperature due to climate change or adaptation strategy.

2.14 Conclusion

A proper understanding of the impact of climate change on crop yield is appropriate as it relates to aspects of cultivar selection, PDs, and nitrogen fertilizer application rates. Parameterization, calibration and validation are required by both statistical downscaling, and CSMs to be used efficiently in conducting research that would conserve resources and contribute to developing mitigation and adaptation strategies that meet the world's needs for food. Calibration input data for CSMs consists of soil, weather, phenology, LAI, yield and yield parameters. The CSMs are validated using independent data not used in the calibration process and is necessary for their application to new cultivars and environments. An accurately calibrated and validated CSM enables end-users, planners, and policy-makers to have confidence in their predictive abilities.

CHAPTER THREE: MATERIALS AND METHODS

3.1 Description of the study site and soils

The study was conducted at the Zambia Agricultural Research Institute (ZARI) Central Research Station at Mount Makulu, in Chilanga, Zambia (latitude: 15.550^{o} S, longitude: 28.250^{o} E, altitude: 1213 m). The study site is located in Agro-ecological Region II (AER II) of Zambia as shown in Figure 5. Mount Makulu was selected based on availability of land, equipment (Diviner Probe for measuring profile soil water content), irrigation water from the dam, weather data from the Mount Makulu weather station, hired labour and security.

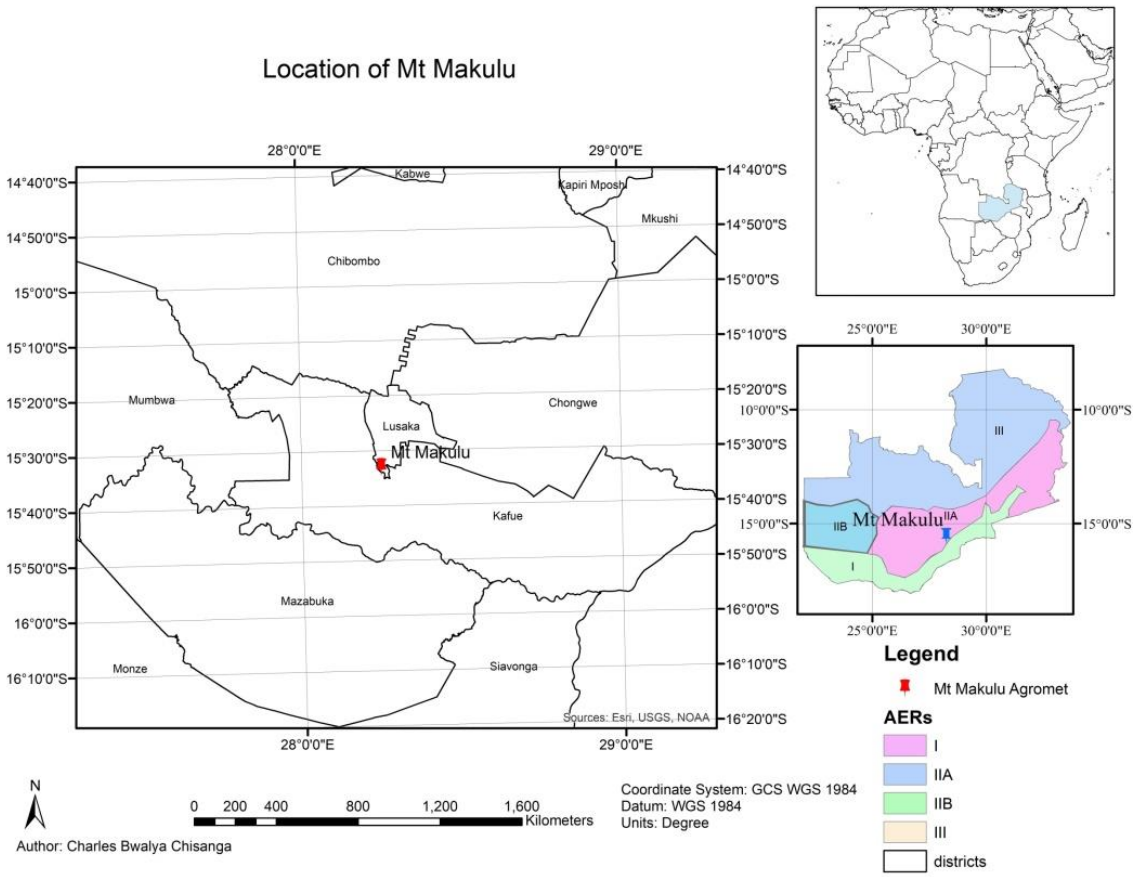

Figure 5: Location of Mount Makulu
Source: (Chisanga et al., 2017)

The soil at the study site is classified in USAD Soil Taxonomy (Soil Survey Staff, 2014) as Clayey, Mixed, Hyperthermic, Typic Paleustalf in Soil Taxonomy and as a Eutric Nitisol (WRB, 2015). The physiography of the Makeni series forms a long straight slope (1%) at the edge of a plateau the Lusaka plain. It is well drained, yellowish red to red (2.55YR), deep to very deep, clayey soil with high activity clayey, medium base saturation and clayey topsoil.

3.2 Weather data

3.2.1 Observed weather data

The daily weather data (latitude and longitude of the weather station, rainfall (precip), maximum (Tmax), and minimum (Tmin) temperature, solar radiation (Srad) [1st May 2016 - 30th June 2017]) used as input into the CSMs were obtained from the Zambia Meteorological Department (ZMD) (Figure 6). CSMs require accurate solar radiation data to drive the simulation of photosynthesis and the carbon balances that govern plant growth. The weather data used for the irrigated field experimental site was from 1st May 2016 to 30th November 2016, and the Tmin, Tmax, Tmean, and rainfall were 13.76^{o}C, 28.64^{o}C, 21.21^{o}C and 71.70 mm for the whole period, respectively. The mean temperature ranged from 13.20^{o}C - 31.05^{o}C. Conversely, the rainfall, solar radiation, mean, maximum and minimum temperature under rainfed conditions during the 2016/2017 season were 930.17 mm, 18.93 MJ m^{-2} day^{-1}, 21.83^{o}C, 15.36^{o}C and 28.29^{o}C, respectively.

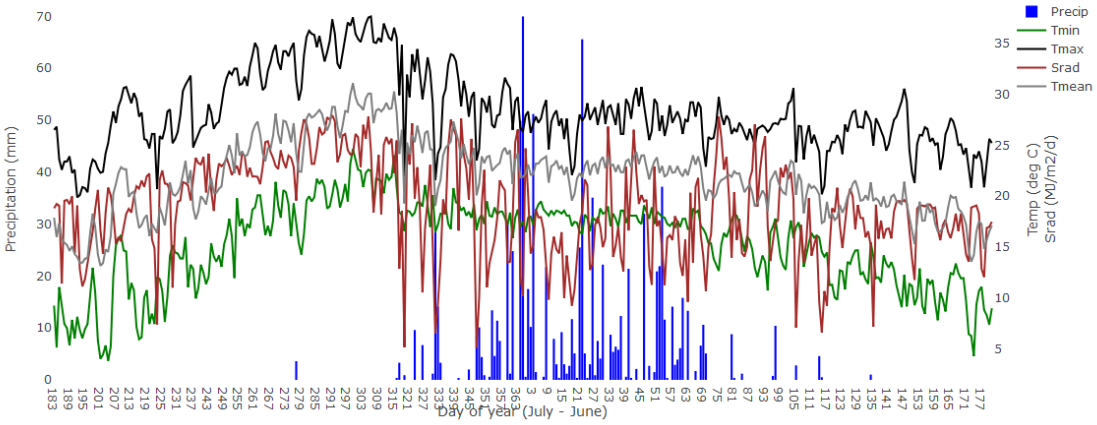

Figure 6: Daily weather data for Mount Makulu

3.2.2 Historical observed station and AgMERRA weather data

Historical daily climate data were obtained from the Zambia Meteorological Department (ZMD) and Agricultural Modern-Era Retrospective Analysis for Research and Applications (AgMERRA) for the period 1963-2012 and 1980-2010, respectively (Figure 7). The AgMERRA climate forcing datasets were created as an element of the Agricultural Model Intercomparison and Improvement Project (AgMIP) to provide consistent, daily time series data over the 1980-2010 period with global coverage of climate variables required for agricultural models (Ruane et al., 2015). The 1980-2010 time slice is of particular importance for agricultural modeling efforts due to the necessity to calibrate models for improved inter-comparison as well as for acting as a baseline upon which future climate scenarios can be statistically and dynamically constructed. The AgMERRA datasets are stored at 0.25°×0.25° horizontal resolution (~25km). Using 30 years to define climatology is a common practice and this period has become a key to perform model calibration, and evaluations, climate sensitivity studies and climate analysis (Semenov and Stratonovitch, 2015).

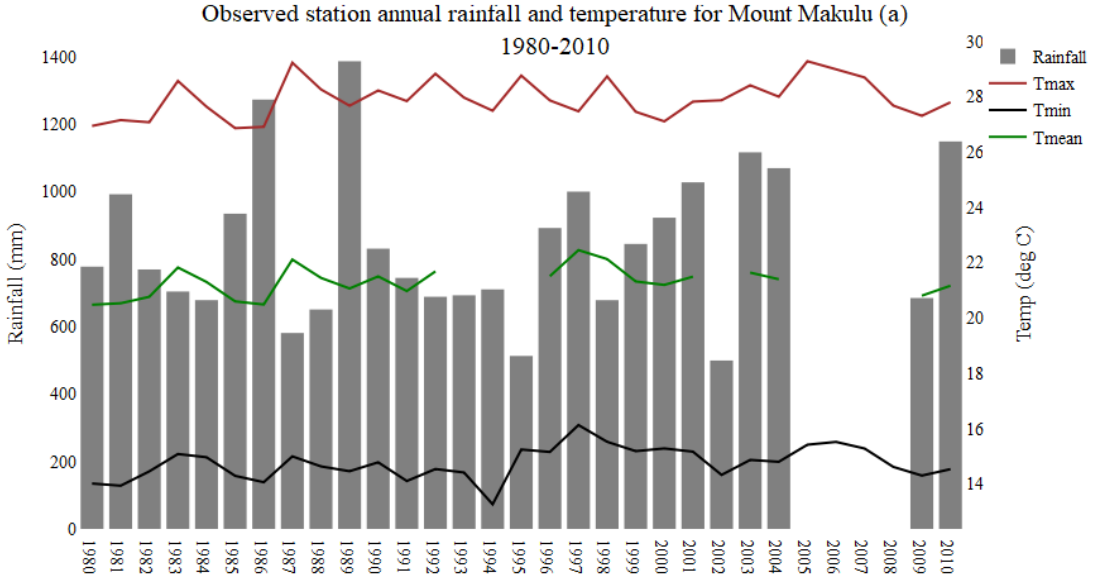

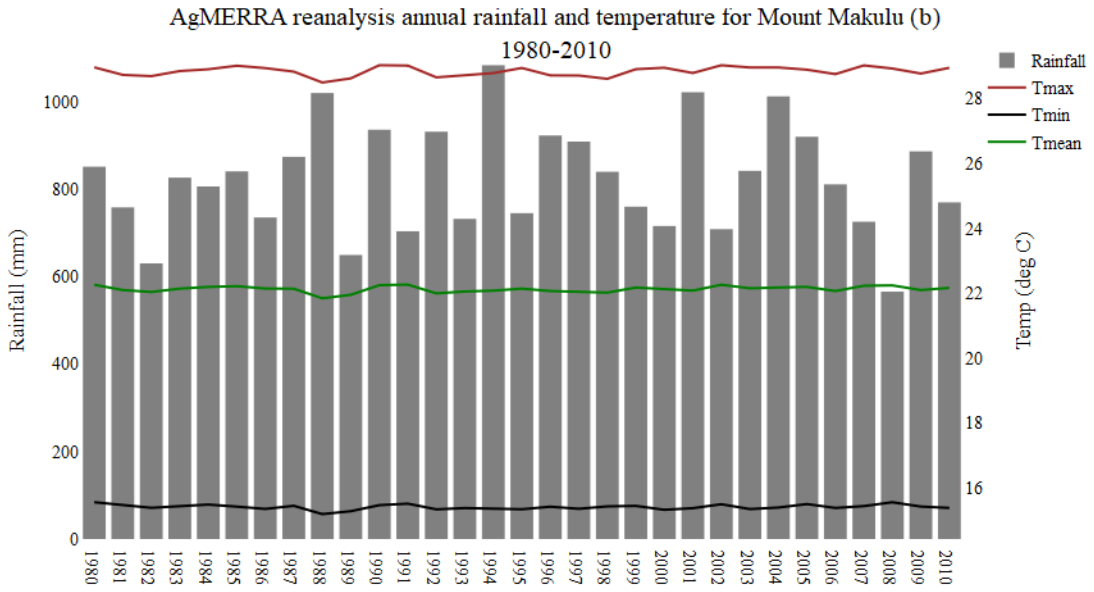

Figure 7: Observed station (a) and AgMERRA reanalysis (b) data for rainfall and temperature

3.3 Soil characterization

Soil samples were collected before land preparation and planting (Table 10 and Table 11). Ten auger soil samples were collected from five depths (0-20, 20-40, 40-60, 60-80, 80-100 cm) before planting at the irrigated and rainfed field experimental site (Table 8 and Table 9). The soil samples were thoroughly mixed, and a composite sample was put in one bag for each layer. A duplicate set of sub-samples from the composite were collected for soil chemical analysis. Field moist soil samples for NO_3-N and NH_4-N determinations were stored in a cooler, refrigerated and analyzed within a week. To determine gravimetric and volumetric soil water, the sub-samples were weighed and oven dried at 105°C for 24 hours. The remaining sub-Samples were air-dried and passed through a 2 mm sieve and used for physical properties analysis.

The soil samples from the irrigated and rainfed field experimental sites were analyzed for texture, pH, exchange potassium (K), extractable phosphorus (P), organic carbon, ammonium (NH_4^+) and nitrate (NO_3^-) at Zambia Agriculture Research Station (ZARI) using standard methods (Table 8 and Table 9) (Hoogenboom et al., 1999; Saxton and Rawls, 2006; Soil Survey Staff, 2014). The pedotransfer functions in DSSAT and SPAW

(Soil-Plant-Air-Water) model (Saxton and Rawls, 2006; Saxton and Willey, 2006) were used to determine the values for bulk density, wilting point or Lower Limit of soil water content (LL15), Drained Upper Limit of soil water content (DUL), saturated soil water content (SAT) and hydraulic conductivity. More detailed on how the soil chemical and physical characterization was done is provided in Appendix 1. A summary of the physical and chemical soil characteristics from the field experimental sites are shown in Table 8 and Table 9.

Table 8: Soil physical characteristics at experimental sites

Depth (cm)	0-20	20-40	40-60	60-80	80-100	Analysis method
Soil texture	clay	clay	clay	clay	clay	SPAW
Silt (%)	12.80	16.80	12.80	18.80	2.80	Hydrometer method
Sand (%)	39.60	35.60	37.60	41.60	37.60	
Clay (%)	47.60	47.60	49.60	39.60	59.60	
Bulk density (g cm^{-3})	1.43	1.41	1.41	1.46	1.36	SPAW
LL (cm^3 cm^{-3})	0.287	0.287	0.299	0.244	0.350	
DUL (cm^3 cm^{-3})	0.407	0.409	0.419	0.363	0.470	
SAT (cm^3 cm^{-3})	0.459	0.467	0.468	0.447	0.487	
SHC (mm h^{-1})	0.350	0.500	0.290	1.480	0.010	

Note: LL = lower limit (Wilting point); DUL = drained upper limit (Field Capacity); SAT = saturation; SHC = Saturated hydraulic conductivity; SPAW =Soil-Plant-Air-Water

Table 9: Soil chemical characteristics at experimental sites

Depth (cm)	0-20	20-40	40-60	60-80	80-100	Analysis method
Total N (%)	0.031	0.042	0.054	0.061	0.036	Modified Kjeldahl
NO_3N (ppm)	29.90	48.70	56.40	70.10	42.80	
NH_4N (ppm)	18.00	29.20	33.90	42.10	25.70	
P (mg kg^{-1})	10.00	11.00	10.00	18.00	12.00	Bray 1
K (mg kg^{-1})	1.05	0.99	1.12	0.59	0.89	Ammonium acetate
Ca (cmol(+) kg^{-1})	11.00	9.30	3.40	2.90	3.20	Ammonium acetate
Mg (cmol(+) kg^{-1})	3.50	2.70	2.30	1.00	1.30	Ammonium acetate
OC (%)	0.35	0.57	0.66	0.82	0.50	Walkley& Black
CEC (cmol(+) kg^{-1})	15.57	13.02	6.85	4.52	5.42	Ammonium acetate

Note: P = Phosphorus; P = Potassium; Mg = Magnesium; OC = organic carbon

3.4 Maize cultivars used

The maize cultivars, PHB 30G19, PHB 30B50 and ZMS 606 are medium maturity with the comparative relative maturity of 120-130 days. PHB30B50 is recommended to be grown under irrigation while PHB30G19 and ZMS 606 can be grown under irrigated and

rainfed conditions in Zambia, respectively. PHB30G19 and PHB30B50 are white and yellow cultivars, respectively produced by Pioneer. The ZMS 606 is exceptionally good drought tolerance. The selected cultivars have a long commercial life, and they can be applied in different locations locally using CSMs. These cultivars were selected based on the major cultivars planted by the small scale farmers.

3.5 Field experimental designs

Two field experiments (irrigated and rainfed) were established at ZARI to evaluate PD, N and cultivar effect on maize growth and yield components. The experiments were conducted at the same site differing in initial soil, and weather conditions and time the field trial was established. The experimental field sites were also used to generate dataset required to calibrate and validate the APSIM-Maize and CERES-Maize models.

3.5.1 Irrigated field experimental site

Two days before planting, the site was disced to a depth of about 30 cm and harrowed. Individual plot sizes were 6 meters (12 rows) by 5 meters. The plots were separated from each other by a2-meter distance to prevent cross-contamination of treatments. Seeds were sown by hand at 5 cm depth in a flat seedbed in 0.50-meter row spacing and 0.30 meter spacing between plants. Weeds were controlled using herbicides and hand hoes during the growing period. The experiment design under irrigated field experimental site was a Split-plot design consisting of three maize cultivars (ZMS 606, Pioneer hybrids PHB 30G19, and PHB 30B50) and three nitrogen fertilizer rates (N1, N2, and N3) with three replicates. Cultivar and N were the main plot and subplots, respectively. 120 (N1), 240 (N2) and 360 (N3) kg/ha NPK 10-20-10 (N, P_2O_5, K_2O) was applied as a basal dressing at the date of planting. 120 (N1), 240 (N2) and 360 (N3) kg urea (46% N) were applied as a top dressing. All field observations for the irrigated experimental site are shown in Table 10.

Table 10: Summary of data collected from the irrigated field experiment site

Cultivars	ZMS 606			30G19			30B50		
N (kg N ha^{-1})	N1	N2	N3	N1	N2	N3	N1	N2	N3
Pre-plant sampling	26th May 2016			26th May 2016			26th May 2016		
Land preparation	26th May 2016								
Basal dressing and planting	5th June 2016								
Seeding rate	80,000 seeds ha^{-1}								
Thinning date	12th July 2016								
Top dressing	29th Aug 2016								
Herbicide	7th July 2016 (Stellar star and Nicosulfuron 750 WDG)								
Pesticide	1st Sept 2016 (AVI-Monocrotophos)								
Termidan	24th Oct 2016								
Phenological stage									
Emergence (VE)	19th June 2016			19th June 2016			18th June 2016		
V6	24th July 2016			22nd July 2016			22nd July 2016		
V8	6th Sept 2016			5th Sept 2016			2nd Sept 2016		
R1	17th Sept 2016			18th Sept 2016			13th Sept 2016		
R4	10th Oct 2016			10th Oct 2016			6th Oct 2016		
R6	5th Nov 2016			5th Nov 2016			3rd Nov 2016		
Biomass sampling									
V6	26th Jul 2016			26th Jul 2016			26th Jul 2016		
V8	8th Aug 2016			8th Aug 2016			8th Aug 2016		
R1 (Anthesis)	19th Sept 2016			19th Sept 2016			19th Sept 2016		
R4	12th Oct 2016			12th Oct 2016			7th Oct 2016		
Final harvest	10th Nov 2016								

3.5.1.1 Application of irrigation water

FAO CropWAT was used to design the irrigation schedule for the field experiments. Only 738 mm of irrigation water was applied to the maize crop instead of the scheduled total gross irrigation of 1,074.7 mm. This was as a result of insufficient rainfall being harvested during the previous season in the off-shore dam.

3.5.2 Rainfed field experimental site

The rainfed field experiment was a Split-split plot design with PDs (3 planting dates [PD1, PD2, PD3]) at 14 day intervals, cultivar (ZMS 606, PHB 30G19, PHB 30B50) and N fertilizer rate (N1, N2, N3) being the main plot, subplo, and sub-subplots, respectively. Individual plot sizes were 6 meters (7 rows) by 5 meters. The plots were separated from each other by a 2-meter distance. Three seeds were sown by hand at 5 cm depth in a flat seedbed in 0.75-meter row spacing by 0.50 meter spacing between plants per station and later thinned to two plants. Field observations for the rainfed experimental site are shown in Table 11. Weeding and fertilizer application was as explained in section 3.5.1 Irrigated field experimental site.

Table 11: Summary of data collected from the rainfed experiment site

	PD1									PD2									PD3								
Cultivars	ZMS 606			30G19			PHB 30B50			ZMS 606			PHB 30G19			PHB 30B50			ZMS 606			PHB 30G19			PHB 30B50		
N rate	1	2	3	1	2	3	1	2	3	1	2	3	1	2	3	1	2	3	1	2	3	1	2	3	1	2	3
Land preparation	29-Nov-16																										
Basal dressing/planting				12-Dec-16									26-Dec-16									09-Jan-17					
Top dressing				30-Jan-17									17-Feb-17									03-Mar-17					
Herbicides	14-Dec-16																										
Herbicides	23-Dec-2016 & 18-Jan-2017																										
Weeding	17-Jan-17																										
Pesticides	29-Dec-16																										
Phenological stages																											
Emergence	19-Dec-16			19-Dec-16			18-Dec-16			04-Jan-17			04-Jan-17			03-Jan-17			17-Jan-17			16-Jan-17			17-Jan-17		
V6	06-Jan-17			06-Jan-17			06-Jan-17			20-Jan-17			20-Jan-17			19-Jan-17			06-Feb-17			06-Feb-17			05-Feb-17		
R1	15-Feb-17			15-Feb-17			13-Feb-17			04-Mar-17			2-Mar-17			04-Mar-17			19-Mar-17			19-Mar-17			17-Mar-17		
R4	14-Mar-17			14-Mar-17			12-Mar-17			28-Mar-17			28-Mar-17			26-Mar-17			12-Apr-17			12-Apr-17			10-Apr-17		
R6	14-Apr-17			15-Apr-17			13-Apr-17			28-Apr-17			27-Apr-17			27-Apr-17			18-May-17			18-May-17			19-May-17		
Biomass sampling																											
V6	06-Jan-17			06-Jan-17			06-Jan-17			20-Jan-17			20-Jan-17			20-Jan-17			06-Feb-17			06-Feb-17			06-Feb-17		
R1	15-Feb-17			15-Feb-17			13-Feb-17			04-Mar-17			04-Mar-17			2-Mar-17			21-Mar-17			21-Mar-17			21-Mar-17		
R4	16-Mar-17			16-Mar-17			16-Mar-17			30-Mar-17			30-Mar-17			28-Mar-17			13-Apr-17			13-Apr-17			13-Apr-17		
Final harvest				03-May-17									15-May-17									01-Jun-17					

Note: 1 = N1; 2 = N2; 3 = N3; Pesticide = Monocrotophos, Fustac; Herbicide = Nicosulfuron; Termites: Terminator (Imidacloprid 30.5% SC) 350g of Imidacloprid litre^{-1}

3.5.3 Evaluation of plant growth

3.5.3.1 Field observation and measurements

Field observation and biomass sampling (destructive sampling) were done at vegetative (VE, V6) and reproductive (R1, R4, and R6) stages for both field experiments (Hoogenboom et al., 1999). The maize leaf area index (LAI) was computed by multiplying the manually measured length and maximum width and multiplied by 0.75, the maize calibration factor (Karuma et al., 2016). All observed agronomic practices are presented in Table 10 and Table 11. Biomass was oven dried at 70^{o}C for 72 hours after being sorted.

3.5.4 Measurement of soil water content

Access tubes were installed in each experimental plot, and soil water content measurements were taken two to three times per week at 10 cm interval to a depth of 100 cm using Diviner 2000 series II probe. A series of readings taken by the Diviner 2000 series II assisted in showing trends of crop water use in the soil profile. The measured soil water content with the Diviner probe was used as part of the minimum dataset required by APSIM-Maize and CERES-Maize models.

3.5.5 Growing Degree Days and Crop Heat Units

Plants require a specific amount of heat units to develop from one growth stage to another, such as from emergence to V6 stage and this heat is called Growing Degree Days (GDD) or heat units and are calculated for each day starting the day after planting. GDDs and crop heat units (CHUs) were calculated from the minimum and maximum temperatures (Bartholomew, 2014) using Equation 1 and Equation 2 below. Maize has a base temperature of 8°C, and each maize hybrid has a certain GDD requirement to reach maturity (Neild et al., 1978). The equation below is commonly used to calculate GDD for maize and other crops as well (McMaster and Wilhelm, 1997).

The plant growth rate and biomass yield depends on the amount of solar radiation (Srad) intercepted and converted into dry matter (Behling et al., 2015). Maize yield and yield components are closely related to the intercepted photosynthetically active radiation (PAR) and the rate of its conversion into the dry matter also known as radiation use

efficiency (RUE) (MacCarthy et al., 2009; Mburu et al., 2010). Equation 3 and Equation 4 below were used to compute the phenothermal (PTI) and heat use efficiency, respectively.

$$GDD = \sum \left(\left(\frac{T_{max} + T_{min}}{2} \right) - T_{base} \right) \quad \text{Equation 1}$$

$$Daily\ CHU = \frac{1.8(T_{min} - 4.4) + 3.33(T_{max} - 10) - 0.084(T_{max} - 10)^2}{2} \quad \text{Equation 2}$$

$$Phenothermal\ (PTI) = \frac{GDD}{Growth\ duration} \quad \text{Equation 3}$$

$$Heat\ use\ efficiency\ (HUE) = \frac{Grain\ yield\ (kg/ha)}{GDD} \quad \text{Equation 4}$$

Where: GDD is the growing degree-days, Tmax and Tmin are the daily maximum and minimum temperatures, respectively, and T_{base} is the minimum temperature threshold.

3.5.6 Data analysis

The effect of nitrogen fertilizer rate and cultivar on crop growth indices (leaf area index [LAI], leaf area [LA], Crop Growth Rate [CGR], Relative Growth Rate [RGR], Leaf Area Ratio [LAR], Net Assimilation Rate [NAR] and Leaf Area Duration [LAD]), yield and yield components observed at the irrigated experimental site was evaluated by split-plot analysis of variance using the ***sp.plot*** function in Agricolae package (de Mendiburu, 2016) in R Programming software.

Crop growth rate (CGR), net assimilation rate (NAR), leaf area ratio (LAR) and leaf weight ratio (LWR) were computed according to the equations below:

Leaf area index (LAI): The Leaf area index was calculated using Equation 5 (McKee, 1964):

$$\text{Leaf area(LA)} \Big/ \text{Plant (cm}^2\text{)} = \text{Leaf}_\text{L} * \text{Leaf}_\text{W} * 0.75 \qquad \text{Equation 5}$$

Leaf area duration (LAD) was determined by Equation 6 by Ahmad et al. (2010):

$$\text{LAD} = (\text{LAI}_1 + \text{LAI}_2) * (\text{T}_2 - \text{T}_1) * 0.5 \qquad \text{Equation 6}$$

Crop growth rate (CGR): It was calculated in terms of g cm^{-2} day^{-1} using Equation 7 by (Ahmadi et al., 2014):

$$\text{CGR} = \frac{\text{W}_2 - \text{W}_1}{(\text{T}_2 - \text{T}_1)} \qquad \text{Equation 7}$$

Net assimilation rate (NAR): Net assimilation rate is defined as the increase of plant material per unit of leaf area per unit of time(Saberi and Aishah, 2013). NAR can be described by yield (g cm^{-2} day^{-1}) and leaf area per unit land area at several time intervals. It wascalculated in terms of g cm^{-2} leaf area day^{-1} using Equation 8 below:

$$\text{NAR} = \frac{\text{W}_2 - \text{W}_1}{\text{T}_2 - \text{T}_1} \text{x} \frac{\text{lnLA}_2 - \text{lnLA}_1}{\text{LA}_2 - \text{LA}_1} \qquad \text{Equation 8}$$

Relative growth rate (RGR): The RGR of a plant is the product of leaf area ratio (LAR; leaf area per unit total plant biomass) and net assimilation rate (NAR; dry matter gain per unit leaf area per unit time). RGR was calculated in terms of g g^{-1} day^{-1} (or mg g^{-1} day^{-1} [g is the existing mass of the plant]) using Equation 9 below:

$$\text{RGR} = \frac{\text{lnW}_2 - \text{lnW}_1}{\text{T}_2 - \text{T}_1} \qquad \text{Equation 9}$$

Leaf area ratio (LAR): It was calculated in terms of $cm^2\ g^{-1}$ using Equation 10 below:

$$LAR = \frac{\frac{LA_1}{W_1} + \frac{LA_2}{W_2}}{2} \qquad \text{Equation 10}$$

Where: W_1: total biomass measured at the first sampling, LA_1: leaf area measured at the first sampling, W_2: total biomass measured at the second sampling, LA_2: leaf area measured at the second sampling, T_1: first sampling time, LW_1: leaf biomass measured at the first sampling, T_2: second sampling time, LW_2: leaf biomass measured at the second sampling, GA: ground area, *ln*: Natural logarithm.

The effect of PD, N, and cultivar on yield and yield components, LAI, cob width, and length observed at the rainfed experimental site were subjected to Split-split plot analysis of variance using the ***ssp.plot*** function in Agricolae package. Means were separated using Fisher-LSD (Least Significant Difference) Test at $p<0.05$. The ANOVA tables for the irrigated and rainfed experimental sites are in Appendix 2 and Appendix 3.

3.6 Calibration and validation of the APSIM and CERES-Maize models

The APSIM-Maize and CERES-Maize models were calibrated and validated using rainfed and irrigated field experimental site data during 2016/2017 and 2016 season, respectively. Calibration of the CSMs was necessary for their application to new cultivars. The CSMs require input parameters for weather data, soil, phenology, LAI, dry matter accumulation, biomass and grain yield and these were calibrated using experimental site data from 2016/2017 which included three PDs, N and maize cultivars. The rainfed experimental site data with least-stressed treatments for each cultivar was used to calibrate the APSIM-Maize and CERES-Maize models to ensure accurate fitted values for maize growth and yield. The irrigated field experiment experienced water stress and was used as independent data for validation.

3.6.1 Description of the crop simulation models

3.6.1.1 APSIM-Maize module

The APSIM v7.9 used in this study includes APSIM-Maize, SoilWater, SoilN, Fertilizer and Surface SOM modules (Mthandi et al., 2014). Important parameters for SoilWater and SoilN are presented in Table 8 and Table 9. The APSIM-maize module[1] simulates maize growth on a daily time-step which responds to climate (temperature, rainfal, and radiation from the input module), soil water supply (from the soilwat module) and soil N (from the soiln module). The APSIM-Maize returns information on its soil water and N uptake to the soilwat and soiln modules daily for reset. Information on crop cover is also provided to the soilwat module for calculating evaporation rates and runoff. Maize stover and root residues are 'passed' from maize to the residue and soiln module respectively at harvest of the maize crop.

In APSIM, U and CONA parameters similar to the CERES-Maize model are used to determine first and second evaporation stages. Parameterization of the APSIM-Maize and CERES-Maize were based on rainfed field experimental site data for the parameters shown in Table 8 and Table 9. The U and CONA were set at 6 mm, and 3.5 mm day^{1}, respectively and these parameters are crop specific and determine the rate of root extension and lower limit of crop water extraction. The Air-dry (mm mm^{1}) soil moisture limit at which soil dry by evaporation was calculated as 0.5 × LL15 (015 cm soil layer), 0.9 × LL15 (1530 cm soil layer) and at deeper depths same as LL15 (Dalgliesh et al., 2016). Crop lower limit (CLL in mm mm^{-1}) was taken as equal to LL15.

Simulation runs with default maize cultivars in APSIM-Maize showed that these were not able to cope with Zambian soil, weather and input variables; therefore, crop growing stages were not simulated adequately. The growth and development module of APSIM-Maize uses a set of different coefficients as presented in Table 12 to define the phenology, crop growth and yield (Famba, 2011; Fosu-mensah, 2012; Knörzer et al., 2011; Mesfin et

[1] https://www.apsim.info/Documentation/Model,CropandSoil/CropModuleDocumentation/Maize.aspx, accessed on 21st March 2019

al., 2015; Wang et al., 2009). In APSIM-Maize model, the A_130 cultivar was used as the starting point for calibrating the ZMS 606, PHB 30G19 and PHB 30B50 cultivars. The CSPs were obtained step by step based on observed phenological stages (anthesis and maturity days after planting [dap]), leaf area index (LAI), biomass and grain yield (grain growth rate and grain number) using the manual trial and error method until the simulated values were within 9-20% of the observed values (Ahmed and Hassan, 2011).

3.6.1.2 DSSAT CERES-Maize model

Six parameters (P1, P2, P5, G2, G3, and PHINT) (Table 13) that describe phenology, biomass and grain yield were calibrated using GLUE (Dokoohaki et al., 2017; Jones et al., 2003; Jones and Thornton, 2003) for each of the maize cultivars. The model parameters were optimized using the GLUE rather than the GENCALC programme. This provided better calibration of the cultivars and simulation of maize growth, and yield and N uptake in response to different N and PDs. More detailed on DASST CERES-Maize model are provided in section 2.5.2.1 DSSAT-Cropping System Model (CSM).

3.6.2 Model input data

The datasets used as inputs into APSIM-Maize and CERES-Maize are shown in Table 8, Table 9, Table 10, Table 11, Table 12 and Table 13.

3.6.3 Model evaluation

3.6.3.1 Crop simulation model calibration

APSIM-Maize and CERES-Maize models were evaluated for simulating days after planting (DAP) to anthesis, and maturity, the percent difference between simulated and observed values (%PD), LAI, soil water content (SWC), grain size, grain number m^{-2}, biomass and grain yield. Several statistical indicators were used to evaluate their performance. The use of an ensemble of different indicators was necessary to sufficiently evaluate their performance (Willmott, 1984; Willmott et al., 1985). Model efficiency (EF, the higher the value the better), root mean square error (RMSE) and normalized RMSE (NRMSE), d-stat ($0 \leq d \leq 1$) and mean absolute error (MAE) were used to evaluate the CSMs (Harrison, 1990; Jones et al., 1986; Willmott, 1982). The simulation was excellent

with NRMSE <10%, good if 10-20%, acceptable or fair if 20-30%, and poor >30% (Jamieson et al., 1995; Zhang et al., 2012). In an adequately calibrated CSM, the EF and R^2 should be above 0.70 and 0.80, respectively (Archontoulis et al., 2014a). $d \geq 0.70$ and $EF \geq 0$ are considered acceptable in evaluation (Jing et al., 2017). CSM under or over-estimating the observed values was checked using the coefficient of residual mass (CRM) (Ahmed et al., 2016b). The evaluation statistics were computed using the equations below.

$$R^2 = \left(\frac{n(\sum xy) - (\sum x)(\sum y)}{\sqrt{[n\sum x^2 - (\sum x)^2]\left[n\sum y^2 - (\sum y)^2\right]}} \right)^2 \quad \text{Equation 11}$$

$$EF = 1 - \left(\frac{\sum (P_i - O_i)^2}{\sum (O_i - \bar{O}\ )^2} \right) \quad \text{Equation 12}$$

$$RMSE = [N^{-1} \sum_{i=1}^{n} (P_i - O_i)^2]^{0.5} \quad \text{Equation 13}$$

$$RMSEn = \frac{RMSE}{O} * 100\% \quad \text{Equation 14}$$

$$d = 1 - \left[\frac{\sum \left(P_i - O_i\right)^2}{\sum \left(|P_i^{`}| - |O_i^{`}|\right)^2} \right] \quad \text{Equation 15}$$

$$MAE = N^{-1} \sum_{i=1}^{n} |P_i - O_i| \quad \text{Equation 16}$$

Where: P_i, O_i, $\bar{O}$ and n are the simulated, observed, average observed values and the number of observations for studied variables, respectively.

3.6.3.2 Crop simulation model validation

The models were validated using irrigated experimental site data. The main focus of the validation was simulation of DAP to anthesis, and maturity, LAI, biomass, and grain yield. CSPs derived from the calibration were used in the validation to confirm the robustness of the CSMs at the local scale. The performance of the CSMs was validated using metrics of d-stat, R^2, RMSE, NRMSE, %PD and CRM.

Table 12: CSPs used in APSIM-Maize

Phenology	Coefficients	Explanation	Units	Default	ZMS 606	PHB 30G19	PHB 30B50
	tt_emerg_to_endjuv	tt from emergence to end of juvenile stage	°Cd	244	240	238.5	242
	tt_flower_to_maturity	tt from silking to physiological maturity	°Cd	1078	820	817	805
	tt_flag_to_flower	tt from flag leaf to silking	°Cd	1	1	1	1
	tt_emerg_to_endjuv	tt from emergence to end of juvenile stage	°Cd	244	240	238.5	242
	tt_endjuv_to_init	tt from end of juvenile to floral initiation	°Cd	0	0	0	0
	tt_flower_to_start_grain	tt from silking to start effective grain fill period	°Cd	150	150	190	192
Grain growth	grain_gth_rate units	grain growth rate	mg grain^{-1} day^{-1}	9.17	9.00	9.17	9.17
Grain number	head_grain_no_max	potential kernel number per ear	°Cd	800	640	655	520

Note: tt: thermal time

Table 13: CSPs used in CERES-Maize model

Coefficients	Development Aspects	Units	ZMS 606	PHB 30G19	PHB 30B50
P1	GDDs (based on 8^{o}C) from emergence to end of the juvenile phase	°Cd	159.00	209.90	155.10
P2	Photoperiod sensitivity coefficient (01.0)		1.8500	0.4410	1.7630
P5	GDDs(based on 8^{o}C) from silking to maturity	°Cd	810.20	815.90	800.40
	Growth Aspects				
G2	Maximum possible number of kernels per plant		945.00	840.80	795.60
G3	Potential kernel growth rate (mg day^{1})	mg day^{-1}	8.559	8.840	15.340
PHINT	GDDs required for a leaf tip to appear(based on 8^{o}C)	°Cd	59.700	56.00	59.730

3.7 Assessment of LARS-WG in predicting climate change in 2020, 2050 and 2080 based on HadCM3 and BCM2 GCMs

3.7.1 Description of the Long Ashton Research Station Weather Generator

The Long Ashton Research Station Weather Generator (LARS-WG) is a stochastic weather generator used for the simulation of weather data at a single site for current and future climate scenarios (Semenov and Barrow, 2002; Semenov and Stratonovitch, 2010). It can simulate daily weather data based on observed statistical characteristics of weather at a single site. The LARS-WG v5.5 used in this study incorporates climate scenarios based on 15 GCMs used in the IPCC 4th Assessment Report (2007) to better deal with uncertainties in GCMs. The model also improves the simulation of extreme weather events such as extreme daily precipitation, duration of wet/dry spells and heat waves (Semenov and Stratonovitch, 2010).

3.7.2 Generation of climate scenarios with LARS-WG

The process of generating local-scale daily climate scenario data in LARS-WG is divided into two steps: Site Analysis; and Generator (Semenov and Barrow, 2002; Semenov and Stratonovitch, 2010). The baseline data (observed station data [1981-2010] and AgMERRA reanalysis [1981-2010]) were used to perform site analysis and to generate synthetic time series data using the Hadley Centre Couple Model version 3 (HadCM3) and Bergen Climate Model version 2 (BCCR-BCM2) (Otterå et al., 2009) GCMs under B1 (Low GHG emission scenario) and A1B (medium GHG emission scenario). The HadCM3 and BCCR-BCM2 were used in the IPCC Third and Fourth Assessment Reports and also contributed to the Fifth Assessment Reports (Mohamed and Lahcen, 2015).

The model was used to generate 30 years of synthetic daily precipitation, minimum and maximum temperature for Mount Makulu for the time slice 2011-2030 (near future [2020]) and 2046-2065 (medium future [2055]) based on the SRB1 and SRA1B from HadCM3 and BCR2 GCMs (Table 14). In LARS-WG model, the GCMs variables are not directly applied, but the model applies proportionally local station climate variables, which are adjusted to the current climate change (Hassan and Harun, 2013). The extreme

properties of rainfall were analyzed using LARS-WG v5.5 using baseline data (Observed station data: 1981-2010 and AGMERRA data: 1981-2010) for Mount Makulu.

3.7.3 Testing the performance of LARS-WG

Statistical tests for calibrating and validating LARS-WG were the Kolmogorov-Simirnov (K-S), T-test and F-test (Qian et al., 2005). These statistical tests are based on the assumption that the observed/AgMERRA and synthetic weather data are both random samples from existing distributions and test the null hypothesis (Semenov et al., 1998). The precipitation and temperature annual means were computed using a multi-model ensemble under SRA1B and SRB1 scenarios as shown in Table 14. The statistics were accurately for Mount Makulu if the computed mean annual temperature (^{o}C) and precipitation (mm year^{-1}) amounts were within the 95% confidence interval (CI95) for the synthetic data.

The performance was also checked by using the coefficient of correlation (R) and the coefficient of the determinant (R^2). The coefficient of determination of a linear regression model is the quotient of the variances of the generated (Gen) and observed (Obs) values. The coefficient of determination was computed using Equation 17 below.

$$R^2 = \frac{\sum(\widehat{G}_\iota - \bar{G})^2}{\sum(O_i - \bar{O})^2} \qquad \text{Equation 17}$$

Where $O_i$are the observed values, $\bar{O}$ and $\bar{G}$are the means, and $\widehat{G}_\iota$is the generated value.

Table 14: CO_2 concentrations (ppm) for selected climate scenarios specified in the Special Report on Emissions Scenarios (SRES) (Nakicenovic et al., 2000; Shamsnia and Pirmoradian, 2013)

Scenario	Key assumption	CO_2 concentration (ppm) 2011-2030	2046-2065	2081-2100
B1 ("low" GHG emission scenario")	Population convergence throughout the world, changes in economic structure (pollutant reduction and introduction to clean technology resources).	410	492	538
A1B ("medium" GHG emission scenario)	Rapid economic growth, maximum population growth during the half century and after that decreasing trend, rapid modern and effective technology growth.	418	541	674
A2 ("high" GHG emission scenario)	Rapid world population growth, heterogeneous economics in the direction of regional conditions throughout the world.	414	545	754

Note: CO_2 concentration for the baseline scenario, 1960-1990, is 334 ppm

3.8 Evaluating ET-SCI climate indices of temperature and precipitation extremes for Mount Makulu

3.8.1 Climate indices

The Expert Team on Sector-specific Climate Indices (ET-SCI) related to daily temperature and precipitation characteristics were analyzed. A full descriptive list of the indices is found in Alexander et al. (2013) and Alexander (2016). ET-SCI extreme temperature and precipitation indices were used to answer questions concerning aspects of the climate system that affect many human and natural systems with particular emphasis on extremes. The temperature indices describe cold and warm weather extremes while the precipitation indices describe wet weather extremes. The studied indices were divided into five categories (Appendix 4) as adapted from Alexander et al. (2006) and Fonseca et al. (2016) and are presented in Table 4 and Table 5.

3.8.2 Quality control and homogenization

The RHTests (RHtestsV4 and RHtests_dlyPrcp) software packages by ETCCDI (Alexander et al., 2013, 2006; Panda et al., 2016) were used to check for data quality and homogeneity. The RHtestsV4 and RHtests_dlyPrcp provided a free option for checking in-homogeneities in temperature and precipitation, respectively. Details on quality control and data homogenization are well documented by Wang (2008) and Wang and Feng (2015b, 2013a, 2013b). The penalized maximal T-test and penalized maximal F-test were used to check for homogeneity of the historical data series (Costa and Soares, 2009; Wang, 2008; Wang et al., 2010).

3.8.3 Computation and analysis of climate indices

ClimPACT2 (Alexander et al., 2013; Alexander and Herold, 2016) was used to calculate the core and non-core ET-SCI indices shown Table 4 and Table 5, respectively. It directly incorporates the R packages climdex.pcic and climdex.pcic.ncdf developed by the Pacific Climate Impacts Consortium (PCIC). Time-series of daily minimum temperature (TN), daily maximum temperature (TX) and daily precipitation (PR) were used as inputs into the ClimPACT2. Many of the climate indices were calculated at both annual and monthly time scales.

The heat wave (HW) computations used in ClimPACT2 are based on (Perkins and Alexander, 2013) with some slight modifications to the Excess Heat Factor (EHF). Three HW definitions are used in ClimPACT2, and these definitions are based on the 90th percentile of TN (minimum daily temperature) designated Tn90, the 90th percentile of TX (maximum daily temperature) designated Tx90 and the EHF. The EHF combines a measure of the temperature of a particular day relative to the baseline period, with a measure of the potential acclimatization that occurred in the preceding 30 days. The two measures are represented by excess heat indices (EHI) of significance (sig) and acclimatization (acc), respectively as expressed in Equation 18 and Equation 19 below.

$$EHI_{sig} = \frac{(T_i + T_{i-1} + T_{i-2})}{3} - T_{95} \qquad \text{Equation 18}$$

$$EHI_{acc} = (T_i + T_{i-1} + T_{i-2}) - (T_{i-1} + \cdots + T_{i-30})/30 \qquad \text{Equation 19}$$

where Ti represents the mean daily temperature, (TXi + TNi)/2, of the day i and T95 represent the 90th percentile of T over the baseline period 1963 - 2012.

The EHF is a combination of the above two excess heat indices and expressed as in Equation 20 below.

$$EHF = EHI_{sig} x\ max(1, EHI_{acc}) \qquad \text{Equation 20}$$

All HW definitions in ClimPACT2 are calculated over the extended summer period with the exceptions of the EHF and Excess Cold Factor (ECF) (Nairn and Fawcett, 2014, 2013). In the southern hemisphere, the extended summer season includes November to March (Alexander, 2016). More details on computing indices using ClimPACT2 software package are provided in Alexander et al. (2013), Alexander and Herold (2016), Alexander (2016) and Perkins and Alexander (2013). The core and non-core ET-SCI sector-specific indices were statistically tested for significance at a 95% level ($p<0.05$). Each slope

(positive or negative) was categorized into four classes indicating highly significant, significant, negative non-significant or positive non-significant.

3.8.4 Trends in time series data

The Mann-Kendall test is a commonly-used nonparametric test for time series trend (Akinbile et al., 2015; Butler, 2015; Mcleod, 2011). The annual time series data for Mount Makulu was tested for trends and slopes using the Mann-Kendall test in the R Programming software. More details on testing for trends in precipitation and temperature are provided by Akinbile et al. (2015), Butler (2015) and Mcleod (2011). The Mann-Kendall test statistic was calculated according to Equation 21 below:

$$s = \sum_{k-1}^{n-1} \sum_{k=k+1}^{n} sgn(x_j - x_k) \qquad \text{Equation 21}$$

Where n is the length of the time series $x_i...x_n$, and sgn (.) is a sign function, x_j and x_k are values in years j and k, respectively. The expected value of S equals zero for series without trend, and the variance was computed using Equation 22 below:

$$\sigma^2(S) = \frac{1}{18}\left[n(n-1)(2n-4) - \sum_{p=1}^{q} t_p(t_p-1)(2t_p+5)\right] \qquad \text{Equation 22}$$

moreover, q is the number of tied groups; t_p is the number of data values in the P*th* group.

The Z statistic was used to test the null hypothesis, H_0, that the data are randomly ordered in time, against the alternative hypothesis, H_1, where there is an increasing or decreasing monotonic trend (Akinbile et al., 2015; Butler, 2015; Mcleod, 2011). The Z-test statistic is then given in Equation 23 below:

$$Z = \begin{cases} \frac{s-1}{\sqrt{\sigma^2(s)}} \; if \; S > 0 \\ 0 \quad if \; S = 0 \\ \frac{s+1}{\sqrt{\sigma^2(s)}} \; if \; S < 0 \end{cases}$$ Equation 23

3.9 Evaluating the impact of climate change on maize yield based on 5 CMIP5 GCMs under RCPs for the 2050s

3.9.1 Baseline and future climate

The climate scenarios for the baseline and future climate were generated from the AgMERRA data set, following the AgMIP protocols (Jones and Thornton, 2013; Rosenzweig et al., 2013). The AgMIP approach involves the use of multiple climates, crop and socio-economic models to simulate future crop yields. The present analysis is based on 5 CMIP5 GCMs (E, I, K, O, R) (Table 15), RCP4.5 and RCP8.5. Future climate scenarios were generated by perturbing the daily baseline (1980-2010) with a delta-based method (Hudson and Ruane, 2015; Rosenzweig et al., 2014; Ruane et al., 2013).

Table 15: Coupled Model Inter-comparison Project Phase 5 (CMIP5) subset GCMs considered under AgMIP

Model and ID	Modeling Centre	Country	Lat	Lon
CCSM4 (E)	Community Climate System Model, Climate and Global Dynamics Division/National Centre for Atmospheric Research	USA		
GFDL-ESM2M (I)	Geophysical Fluid Dynamics Laboratory	US-NJ	2.5	2.5
HadGEM2-ES (K)	Met Office Hadley Centre	UK-Exeter	1.75	1.25
MIROC5 (O)	Atmosphere and Ocean Research Institute (University of Tokyo), National Institute for Environmental Studies and Japan Agency for Marine-Earth Science and Technology	Japan	1.42	1.41
MPI-ESM-MR (R)	Max Planck Institute for Meteorology (MPI-M)	Germany	1.87	1.87

The delta-based method is an ordinary bias correction method, which is often used to reduce the bias between the GCMs outputs and observations (Fowler et al., 2007). The main goal of this method was to modify the daily time series in future years by adding monthly mean changes of GCM outputs. Five deltas were computed as the changes from 5 GCMs control to future projections, then monthly applied on baseline climate to produce 5 future daily sets (Rosenzweig et al., 2013; Trzaska and Schnarr, 2014). The deltas were computed using RCP scenarios from 2040-2069. For temperature, the same delta was applied to a minimum and maximum temperatures. Changes in temperature and rainfall in 2050 relative to the baseline were estimated based on GCM outputs. The adjusted formula for modified daily precipitation is expressed in Equation 24, and the modified daily temperature (Abera et al., 2018) is expressed in Equation 25.

$$P_{adj.fur,d} = P_{obs,d} * \sum_{i=1}^{k} P_i \left(\frac{\overline{P}_{GCM.fur,m}}{\overline{P}_{GCM.ref.m}} \right) \quad \text{Equation 24}$$

where $P_{adj.fur,d}$ is the adjusted daily rainfall for the future years, $P_{obs,d}$ is the observed daily rainfall for the base years, $\overline{P}_{GCM.fur,m}$ is the monthly mean rainfall of the GCM outputs for the future years, $\overline{P}_{GCM.ref.m}$ is the monthly mean rainfall of the GCM outputs for the base years, pi is the weight of each grid cell, and k is the number of the grid cells.

Whereas, the adjusted daily temperature $T_{adj.fur,d}$ is given by:

$$T_{adj.fur,d} = T_{obs,d} * \sum_{i=1}^{k} P_i \left(\overline{T}_{GCM.fur,m} - \overline{T}_{GCM,ref,m} \right) \quad \text{Equation 25}$$

where $T_{adj.fur,d}$ is the adjusted daily temperature (maximum and minimum temperatures) for the future years, $T_{obs,d}$ is the observed daily temperature for the base years, $\overline{T}_{GCM.fur,m}$ is the monthly mean temperature of the GCM outputs for the future years, $\overline{T}_{GCM,ref.m}$ is

the monthly mean temperature of the GCM outputs for the baseline, P_i is the weight of each grid cell, and k is the number of the grid cells.

The AgMIP Quick and Dirty User Interface (QUADUI) tool (http://www.agmip.org/tools) was used to translate weather files from AgMIP format to APSIM, and DSSAT met/weather file. The multi-model GCM ensembles were used as they reduce errors and reproduce a more realistic plausible future climate (Araya et al., 2015; Hao et al., 2013).

3.9.2 Yield changes under future climate scenarios

The impact of climate change on PD, N, cultivar, maize growth, and yield were simulated for 30 years (1980-2010, 2040-2070) using APSIM-Maize and CERES-Maize models. The results focused on percent change in DAP to anthesis, and maturity, biomass and grain yield relative to the baseline. The grain yield was analyzed using ensembles, probability density functions (PDFs), cumulative distribution functions (CDF), cumulative probability distribution functions (CPDFs), tables, and graphs, coefficient of variation (CV = sd/mean), standard deviation (sd) and mean. The standard deviation is a measure of variability that indicates how spread the data is around the mean.

CHAPTER FOUR: RESULTS AND DISCUSSION

4.1 Effect of cultivar and N rate on maize growth indices and yield

4.1.1 Crop growth indices

The effect of N and cultivar treatment on crop growth indices are presented in Table 16 and Figure 8. Crop growth indices varied in response to cultivar and N. The treatment effect of N significantly affected Relative Growth Rate (RGR) (R4-R6) and Net Assimilation Rate (NAR) (V6-R4) (Table 16). The maize cultivars exhibited significant differences in RGR (V6-R1) and LAR (V6-R4). PHB 30G19 had the highest NAR followed by PHB 30B50 and ZMS 606. Using pooled data, NAR value was highest at N1 followed by N2 and N3. Soil moisture stress after silking notably decreased the NAR among the maize cultivars during their growth period. NAR represents the plant's net photosynthetic effectiveness in capturing light and assimilating CO_2 (Saberi and Aishah, 2013).

The RGR and leaf Area Ratio (LAR) were significantly affected by cultivar treatment effect (Table 16 and Figure 8). ZMS 606 with higher LAR value from V6 to dough stage gave higher grain, and biomass yield, grain number $m^{-2,}$ and grain number cob^{-1} followed by PHB 30B50 and PHB 30G19. LAR indicated variation in the growth parameters and biomass accumulation among the cultivars and as a consequence led to variation in yield parameters. Similar results have been reported by Adebo and Olaoye (2010) and Daur et al. (2010). Pooled data for LAR showed that N2 had the highest value followed by N3 and N2.

Crop Growth Rate (CGR), leaf area duration (LAD) and leaf area index (LAI) were non-significant at all treatment levels. The findings of Ahmad et al. (2010) who observed variation in CGRs for different maize cultivars do not agree with this study. Although LAI is a factor that plays a vital role in plant production for both quantitative and qualitative traits as reported by Lukeba et al. (2013), it was non-significantly. The results of this study are not in agreement with Valadabadi and Farahani (2010) who reported that leaf area is influenced by genotype, climate, and soil fertility.

Table 16: Treatment effects of cultivar and N on plant growth indices

Treatment/cultivar	LAD	CGR (V6-R1)	CGR (R1-R4)	CGR (R4-R6)	RGR (V6-R1)	RGR (R1-R4)	RGR (R4-R6)	LAR (V6-R4)	NAR (V6-R4)
ZMS 606	130.43[a]	2.24[b]	4.46[a]	-4.16[a]	4.79[b]	5.19[a]	4.59[a]	46.21[a]	0.002[a]
PHB 30B19	157.02[a]	3.15[ab]	3.32[ab]	-5.93[a]	5.18[a]	5.33[a]	4.44[a]	32.05[b]	0.002[a]
PHB 30B50	143.77[a]	3.25[a]	3.13[b]	-4.76[a]	5.12[a]	5.29[a]	4.55[a]	41.27[ab]	0.001[a]
Significance	ns	ns	ns	ns	*	ns	ns	*	ns
LSD 5%	42.31	0.97	1.16	1.83	0.32	0.20	0.31	9.48	0.0006
CV %	22.49	25.69	24.35	-28.32	4.81	2.89	5.18	18.19	21.65
Nitrogen (N) rate									
N1	130.08[a]	3.09[a]	3.97[a]	-6.23[a]	5.127[a]	5.35[a]	4.39[a]	37.22[a]	0.0023[a]
N2	155.41[a]	2.72[a]	3.55[a]	-4.31[a]	4.984[a]	5.22[a]	4.59[a]	43.98[a]	0.0018[b]
N3	145.74[a]	2.82[a]	3.39[a]	-4.30[a]	4.982[a]	5.24[a]	4.60[a]	38.33[a]	0.0019[ab]
Significance	ns	ns	ns	ns	ns	ns	*	ns	*
LSD 5%	42.31	0.71	2.34	2.12	0.32	0.20	0.31	13.57	0.0005
CV %	22.49	24.10	62.52	-41.69	4.81	2.89	5.18	33.16	20.55
Interaction (V*N)									
Significance		ns	ns	ns	ns	ns	ns	ns	ns

Note: Means sharing the same letter in the table do not differ statistically at $p < 0.05$; LSD = Least Mean Differences; * = Significant at 5% level; ** = Highly significant at 5%; NS = Non significant; wt = weight; CGR, RGR and NAR are in g cm^{-2} d^{-1}; LAR is in cm^2 g^{-1}

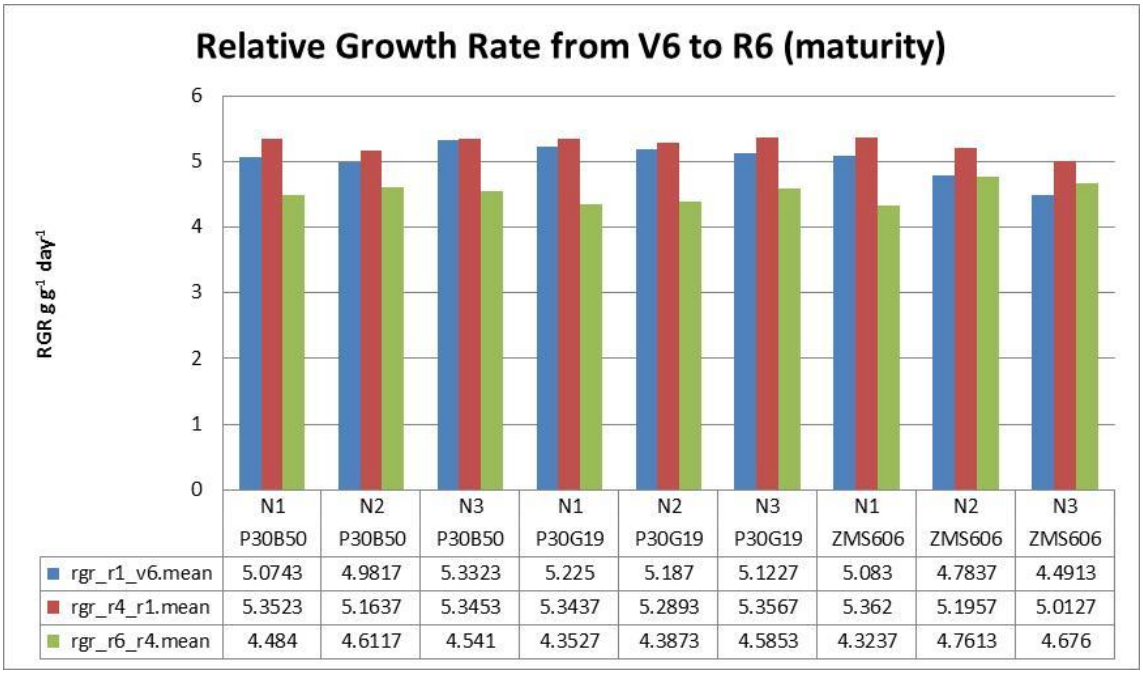

	N1 P30B50	N2 P30B50	N3 P30B50	N1 P30G19	N2 P30G19	N3 P30G19	N1 ZMS606	N2 ZMS606	N3 ZMS606
rgr_r1_v6.mean	5.0743	4.9817	5.3323	5.225	5.187	5.1227	5.083	4.7837	4.4913
rgr_r4_r1.mean	5.3523	5.1637	5.3453	5.3437	5.2893	5.3567	5.362	5.1957	5.0127
rgr_r6_r4.mean	4.484	4.6117	4.541	4.3527	4.3873	4.5853	4.3237	4.7613	4.676

Figure 8: Relative growth rate from V6 to R6

4.1.2 Total dry matter (TDM)

4.1.2.1 Grain yield, biomass, cob, husk and ear weight

The relationship between nitrogen fertilizer rate and yield and yield components were evaluated under irrigated conditions for 2016 as shown in Table 17, Table 18 and Table 19. Grain yield is the main target of maize production. The grain and husk yield were significantly affected by N fertilizer rate and cultivar treatment effect. The highest husk yield was observed from ZMS 606 (383.94 kg ha^{-1}) followed by PHB 30G19 (301.56 kg ha^{-1}) and PHB 30B50 (267.27 kg ha^{-1}). Pooled data for husk yield showed that N1 (375.48 kg ha^{-1}) had the highest followed by N2 (289.70 kg ha^{-1}) and N3 (287.59 kg ha^{-1}), respectively. Grain, biomass (R6), cob, ear, and biomass (V6) yield and seed number m^{-2} were significantly affected by the treatment effect of N fertilizer rate. The ZMS 606 had higher grain yield than the Pioneer cultivars. The planting of ZMS 606 may be suitable under irrigated condition even though grain yields are not significantly different from the Pioneer cultivars. The vegetative growth stage (V6) was influenced by the treatment effect of cultivar and N fertilizer rate. The response to N treatment effect is variable depending on the amount and distribution of moisture, soil fertility, and cultivar. Arif et al. (2010)

and Bashir et al. (2012) reported that yield and yield component of maize was increased by increasing the application of nitrogen fertilizer rate and their results agree with the findings of this study.

The N influenced the accumulation of yield and yield components, and this is consistent with the findings of Fetahu et al. (2014). The variations in the rate of nitrogen application can strongly influence yield and yield components as observed by Sangoi (2001). The study results are in agreement with the findings of Singh and Hadda (2014) and Inamullah et al. (2011) who reported that increased grain yield was affected by higher rates of nitrogen application. An increase in grain yield of maize with an increase in N has been reported by Muchow et al. (1990) and Zeidan et al. (2006).

4.1.2.2 Grain number cob^{-1}, seed number m^{-2} and 100 seed weight

Grain number cob^{-1} and seed number m^{-2} were highly significantly affected by the N fertilizer rate (Table 17). The seed number m^{-2} increased with higher N fertilizer rate. The maximum and a minimum number of grains per ear were recorded at N3 and N2, respectively. ZMS 606 recorded the highest mean grain number of 349.8 followed by PHB 30G19 (292.6) and PHB 30B50 (281.9). This is also in agreement with Zeidan et al. (2006) who concluded that grain number per ear was maximum at the highest nitrogen level.

Table 17: Treatment effects of cultivar and N rate on yield and yield components

Treatment/ cultivar	**Grain yield** kg ha^{-1}	**Grain No.**	**Stover** kg ha^{-1}	**Biomass** kg ha^{-1}	**Seed m^{-2}** number	**Cob wt.** kg ha^{-1}	**Ear wt.** kg ha^{-1}	**Husk** kg ha^{-1}	**Stem** kg ha^{-1}	**Veg** kg ha^{-1}
ZMS 606	7171.57^{a}	349.83^{a}	2668.23^{a}	9839.80^{a}	2798.67^{a}	1172.06^{a}	8343.64^{a}	383.94^{a}	476.83^{a}	847.94^{a}
PHB 30B19	6117.01^{b}	292.64^{a}	2590.51^{a}	8707.53^{a}	2341.10^{b}	1224.87^{a}	7884.22^{a}	301.56^{ab}	430.00^{a}	808.44^{a}
PHB 30B50	6620.01^{b}	281.87^{a}	2723.91^{a}	9344.00^{a}	2254.94^{b}	1264.13^{a}	7884.22^{a}	267.27^{a}	498.47^{a}	915.44^{a}
Significance	ns	ns	ns	ns	ns	ns	ns	*	ns	ns
LSD 5%	1043.9	42.67	421.91	1277.9	341.36	177.29	1212.80	108.19	127.70	235.32
CV %	15.31	23.00	18.70	21.8	23.00	24.3	23.70	14.50	19.00	23.2
N rate										
N1	5656.87^{b}	266.57^{b}	2509.77^{a}	8166.65^{b}	2132.55^{b}	1050.60^{b}	6707.48^{b}	375.48^{a}	440.01^{a}	815.25^{a}
N2	7114.69^{a}	320.35^{b}	2740.85^{a}	9855.54^{a}	2562.81^{a}	1290.29^{a}	8404.86^{a}	289.70^{a}	498.00^{a}	897.48^{a}
N3	7137.11^{a}	337.42^{a}	2732.03^{a}	9869.14^{a}	2699.35^{a}	1320.29^{a}	8457.41^{a}	287.59^{a}	467.29^{a}	859.09^{a}
Significance	**	**	ns	*	**	*	*	ns	ns	ns
LSD 5%	1043.90	42.67	421.91	1277.90	341.36	177.29	1212.80	108.19	129.70	235.32
CV %	15.30	13.50	15.44	13.40	13.50	14.14	15.00	33.17	27.00	26.73
Interaction (V*N)										
Significance	ns	ns	ns	ns	ns	ns	ns	ns	ns	ns

Note: Means sharing the same letter in the table do not differ statistically at $p < 0.05$; LSD = Least Mean Differences; * = Significant at 5% level; ** = Highly significant at 5%; NS = Non significant; sqm=square meter; wt = weight

The R^2 (0.82) values between the grain number cob^{-1} and N for the pooled data were 281.87 (PHB 30B50), 292.64 (PHB 30G19), and 349.83 (ZMS 606), respectively. The number of grain number cob^{-1} increased with higher N application rate. Kandil (2013) also reported that the differences in grain weight could be due to differences in N fertilizer rates. This was attributed to variation in the response of maize cultivars' nutrition.

The seed number m^{-2} was significantly influenced by N at $p<0.05$. Pooled data indicated that the highest seed number m^{-2} was observed at the highest N application rate. The highest seed number m^{-2} was observed under ZMS 606. The 100-grain weight varied significantly ($p<0.05$) among the maize cultivars. The maximum 100-grain weight was recorded under PHB 30B50 (31.39 g), PHB 30G19 (29.3 g) and lastly ZMS 606 (27.53 g). Differences in the 100-grain weight have also been reported by Ahmad et al. (2010). The differences in 100-grain weight may have resulted from differences in the initial size of the spikelets, in growth rates during the exponential and linear phases of grain filling period. Soil moisture stress after silking notably decreased pooled values for 100-grain weight with increasing N rate. Ahmad et al. (2010) observed that initial grain weight after pollination was a critical factor in the early growth of the kernels.

4.1.2.3 Harvest index, stover, stem, vegetative, and leaf at vegetative and reproductive stage

The harvest index (HI), stover weight, stem weight, vegetative weight, leaf weight, biomass at anthesis (silking) and dough stage, leaf area index at vegetative (V6) and reproductive (anthesis and dough) stages of the three maize cultivars were not significantly affected by N treatment effect at $p<0.05$ and there was no interaction between treatments at all levels as shown in Table 18. The HI is defined as the physiological efficiency and ability of a crop to convert the total dry matter into economic yield. Nitrogen rates showed no significant difference for HI of the three maize cultivars. The results of this study are in agreement with Arif et al. (2010) who also observed that the N rate did not affect HI.

Table 18: Treatment effects of cultivar and N rate on yield and yield components

Treatment/ cultivar	**Leaf** kg ha^{-1}	**HI**	**100-grain wt.** g	**LAI at V6** m^2 m^{-2}	**V6 biomass** kg ha^{-1}	**LAI at R4**	**R1 biomass** kg ha^{-1}	**R4 biomass** kg ha^{-1}
ZMS 606	371.11^{a}	0.72^{a}	27.53^{c}	0.30^{ab}	415.11^{b}	3.04^{a}	10270.00^{b}	18483.56^{a}
PHB 30B19	378.44^{a}	0.80^{a}	29.33^{b}	0.26^{a}	572.44^{a}	3.66^{a}	15197.33^{a}	21042.37^{a}
PHB 30B50	416.96^{a}	0.71^{a}	31.39^{a}	0.37^{a}	467.56^{b}	3.41^{a}	14244.44^{ab}	20003.56^{a}
Significance	ns	ns	**	ns	*	ns	ns	ns
LSD 5%	118.53	0.04	1.72	0.10	79.92	0.80	3257.20	4095.10
CV %	33.5	2.70	4.47	33.00	14.60	22.80	25.00	16.00
Nitrogen (N) rate								
N1	375.23^{a}	0.69^{a}	29.04^{a}	0.30^{a}	496.00^{ab}	3.05^{a}	14198.22^{a}	21424.00^{a}
N2	399.48^{a}	0.72^{a}	30.26^{a}	0.29^{a}	426.67^{b}	3.70^{a}	12544.89^{a}	19004.44^{c}
N3	391.81^{a}	0.72^{a}	28.96^{a}	0.35^{a}	532.44^{a}	3.38^{a}	12968.89^{a}	19101.33^{b}
Significance	ns	ns	ns	ns	*	ns	ns	ns
LSD 5%	118.53	0.04	1.72	0.10	79.92	0.80	3257.20	4095.10
CV %	29.68	5.12	4.47	31.24	16.04	22.84	24.00	20.10
Interaction (V*N)								
Significance	ns	ns	ns	ns	ns	ns	ns	ns

Note: Means sharing the same letter in the table do not differ statistically at $p < 0.05$; LSD = Least Mean Differences; * = Significant at 5% level; ** = Highly significant at 5%; NS = Non significant; sqm=square meter; wt = weight

4.1.2.4 Effect of SWC on the total dry matter and grain yield

The cultivar biomass and grain yield varied from 7.49 - 11.51 ton ha^{-1} and 5.27 - 7.73 ton ha^{-1}, respectively. As the season progressed, less irrigation water was being applied from three times to once per week. Water stress in maize increased with reducing irrigation water, and this contributed to biomass and grain yield reduction as the season progressed. This result is supported by similar observations by Rudnick and Irmak (2013) who reported that adequate soil water availability led to both a better uptake and use of N thus increasing crop biomass and yield. Stress as a result of water deficiency from silking to maturity stage affected the ultimate size and yield of ears, and this assentation is also supported by du Plessis (2003). Adverse conditions such as water stress and nitrogen deficiency reduce plant growth and silk development (Sangoi, 2001; Singh and Hadda, 2014). Nitrogen is the most yield-limiting nutrient, and application plays a significant role in improving soil fertility (Singh and Hadda, 2014).

4.2 Effect of PD, cultivar, and N on yield and yield parameters under rainfed conditions

4.2.1 Growing degree days, crop heat units, phenothermal index and heat use efficiency of maize

Computed cumulative growing degree days (GDD), crop heat units (CHU), solar radiation (Srad), and precipitation at vegetative and reproductive stages, grain yield, growth duration, PTI and HUE for the 2016/2017 season are shown in Table 19 and Table 20. The precipitation, Srad, mean, maximum and minimum temperature during the 2016/2017 season were 930.17 mm, 18.93 MJ m^{-2} day^{-1}, 21.83ºC, 15.36ºC and 28.29ºC, respectively. As the season progressed, precipitation, Srad, maximum and minimum temperatures reduced. PD1 recorded higher meteorological parameters compared to PD2 and PD3. Maize planted during PD2 experienced less cumulative GDDs compared to PD1 and PD3 during the grain filling period. PD1 had more GDDs, CHU, Srad, higher seasonal temperature and precipitation than PD2 and this increased biomass and grain yield. The PD3 had higher cumulative Srad and CHUs than PD1 and PD2. However, the cumulative precipitation amount received during PD3 was lower compared to PD1 and PD2, and this could have contributed to low grain yield.

The GDDs decreased with delay in P, and this study agrees with Dahmardeh (2012). Consequently, phenothermal index (PTI) and heat use efficiency (HUE) reduced with delay in PDs as shown in Table 20. The number of days during grain filling reduced with delay in PD. Delay in PD also reduced the PTI and heat use efficiency (HUE) due to decreasing GDDs and grain yield, respectively. PD1 with longer grain filling period, higher PTI and HUE was associated with higher grain yield at all treatment levels (Table 20). The number of days from silking to physiological maturity for PD1 was more than at PD2. The maize crop at PD1 had higher grain yield and biomass than at PD2 and PD3 due to sufficient amount of cumulative precipitation, PTI and HUE. Temperature affects the duration of crop growth and grain filling and also the time incident radiation can be intercepted (Muchow et al., 1990). The number of days to anthesis and maturity decreases with increasing temperature and reducing soil water, and this reduces grain and biomass yield.

Table 19: Computed cumulative GDD, CHU, Srad and precip at vegetative and reproductive stages of maize

Growth Stages	Planting date 1											
	ZMS 606				PHB 30G19				PHB 30B50			
	Precip	Srad	GDDs	CHUs	Precip	Srad	GDDs	CHUs	Precip	Srad	GDDs	CHUs
Emergency	61.30	151.32	147.85	569.00	61.30	151.32	569.00	569.00	53.80	129.77	132.60	510.90
V6	318.90	441.06	389.80	1,478.13	318.90	441.06	389.80	1,478.13	318.90	441.06	389.80	1,478.13
Silking (R1)	649.90	1,105.69	982.25	3,749.83	649.90	1,105.69	982.25	3,749.83	617.90	1,066.07	950.25	3,632.28
Dough stage (R4)	826.10	1,537.91	1,367.60	5,246.80	826.10	1,537.91	1,367.60	5,246.80	826.10	1,500.74	1,343.30	5,146.80
Maturity (R6)	847.58	2,169.10	1,776.88	6,852.76	850.37	2,176.23	1,789.03	6,904.86	847.58	2,149.40	1,761.62	6,799.04
	Planting date 2											
Growth Stages	ZMS 606				PHB 30G19				PHB 30B50			
	Precip	Srad	GDDs	CHUs	Precip	Srad	GDDs	CHUs	Precip	Srad	GDDs	CHUs
Emergency	225.70	185.17	145.50	560.80	225.70	185.17	145.50	560.80	224.20	166.44	130.30	502.89
V6	292.40	406.95	376.25	1,469.43	292.40	406.95	376.25	1,469.43	292.10	393.09	362.50	1,414.19
Silking (R1)	708.90	1,148.00	1,015.85	3,906.82	695.60	1,122.56	985.15	3,795.36	708.90	1,148.00	1,015.85	3,906.82
Dough stage (R4)	743.20	1,594.73	1,343.25	5,192.30	743.20	1,594.73	1,343.25	5,192.30	743.20	1,558.06	1,317.30	5,087.33
Maturity (R6)	762.25	2,108.68	1,708.39	6,659.43	757.17	2,065.51	1,664.64	6,468.36	762.25	2,097.97	1,698.85	6,615.54
	Planting date 3											
Growth Stages	ZMS 606				PHB 30G19				PHB 30B50			
	Precip	Srad	GDDs	CHUs	Precip	Srad	GDDs	CHUs	Precip	Srad	GDDs	CHUs
Emergency	27.30	121.75	130.85	514.32	24.60	110.23	117.50	458.95	27.30	121.75	130.85	514.32
V6	252.30	453.14	421.25	1,636.73	252.30	453.14	421.25	1,636.73	240.00	439.09	406.90	1,579.33
Silking (R1)	484.90	1,190.58	1,012.85	3,907.97	484.90	1,190.58	1,012.85	3,907.97	484.90	1,144.12	985.20	3,800.46
Dough stage (R4)	506.37	1,655.87	1,324.74	5,147.29	506.37	1,655.87	1,324.74	5,147.29	506.38	1,611.09	1,298.04	5,045.86
Maturity (R6)	515.27	2,228.83	1,754.32	6,890.01	515.27	2,244.70	1,766.29	6,939.26	515.27	2,228.83	1,754.32	6,890.01

Note: Precip in mm; srad in Mj m^{-2} d^{-1}; GDD in ^{o}Cd; CHU in ^{o}Cd

Table 20: Computed grain yield, growth duration, NUE, PTI and HUE

					PD1				
	ZMS 606			PHB 30G19			PHB 30B50		
N rate	N1	N2	N3	N1	N2	N3	N1	N2	N3
Grain yield kg ha^{-1}	9,182.80	8,731.40	7,896.10	8,369.40	7,931.60	9,733.60	9,489.80	9,560.90	10,791.70
Growth duration (days)	123.00	123.00	123.00	124.00	124.00	124.00	122.00	122.00	122.00
PTI	14.45	14.45	14.45	14.43	14.43	14.43	14.44	14.44	14.44
HUE (^{o}Cd)	5.17	4.91	4.44	4.68	4.43	5.44	5.39	5.43	6.13
					PD2				
	ZMS 606			PHB 30G19			PHB 30B50		
N rate	N1	N2	N3	N1	N2	N3	N1	N2	N3
Grain yield kg ha^{-1}	6,854.00	8,174.00	6,536.20	7,336.90	6,496.80	7,909.50	7,901.70	5,273.70	7,987.40
Growth duration (days)	121.00	121.00	121.00	117.00	117.00	117.00	120.00	120.00	120.00
PTI	14.12	14.12	14.12	14.23	14.23	14.23	14.16	14.16	14.16
HUE (^{o}Cd)	4.01	4.78	3.83	4.41	3.90	4.75	4.65	3.10	4.70
					PD3				
	ZMS 606			PHB 30G19			PHB 30B50		
N rate	N1	N2	N3	N1	N2	N3	N1	N2	N3
Grain yield kg ha^{-1}	5,962.40	6,511.80	6,083.10	6,142.60	6,061.80	6,065.80	5,567.30	6,883.90	6,315.40
Growth duration (days)	129.00	129.00	129.00	130.00	130.00	130.00	129.00	129.00	129.00
PTI	13.60	13.60	13.60	13.59	13.59	13.59	13.60	13.60	13.60
HUE (^{o}Cd)	3.40	3.71	3.47	3.48	3.43	3.43	3.17	3.92	3.60

4.2.2 Biomass at V6, anthesis and dough stage

The cultivar treatment effect was very highly significant at leaf blade (R1, R4) and leaf sheath (R6). The vegetative growth stage (V6) and leaf blade (R1) was influenced by the interaction between PD and cultivar as shown in Table 21a. The interaction effect between the PD and cultivar at V6 and leaf blade (R1) was highly significant at $p<0.05$. All the other treatment effects were non-significant. The mean biomass of pooled data for PD1, PD2, and PD3 at V6 was 11.38 g, 8.49 g and 8.31 g, respectively. Pooled data for the N treatment effect indicated that application of N1, N2, and N3 were 9.28 g, 9.66 g and 9.24 g, respectively. Application of N2 had higher biomass followed by N1 and N3. PHB 30G19 had the highest mean biomass (9.45) followed by PHB 30B50 (9.37) and ZMS 606 (9.36). Maize cultivars respond differently to N fertilizer application rate.

4.2.3 Total dry matter (TDM) at V6, and the final harvest

Planting date (PD) treatment effect at maturity on stem weight (R6), grain yield (R6), biomass (R6) and cob length was significant (Figure 9, Table 21a, Table 22b, and Table 23c). Across the cultivars, PD1 resulted in higher biomass and grain yield than at PD3. PD effect on cob width was highly significant ($p<0.05$) while PD effect on 100-grain weight and harvest index (HI) were very highly significant ($p<0.05$). A study by Amjadian et al. (2015) showed that delay in planting reduces kernel number and grain yield in maize. In cases where planting is delayed, knowledge on how the maize cultivar maturity interacts with the environmental parameters is key to developing mitigating strategies that lead to optimizing and stabilizing grain yield (Tsimba et al., 2013). PD effect on pooled grain yield was significant. Results indicated that the PD effect influenced grain yield. Maize grain yield increased at higher nitrogen fertilizer application rate. Similar results have been reported by Arif et al. (2010) and Bashir et al. (2012).

Cultivar treatment effect significantly influenced cob weight (R6), husk (R6), stover (R6), biomass (R1, R4, R6), leaf sheath (R6) and leaf blade (R1, R4) (Table 21a, Table 22, and Table 23c). This showed that maize cultivars responded differently to environmental conditions. The coefficient of variation for grain yield (PD=28.8%, N=22.0%, V=15.0%) and biomass (PD=25.2%, N=20.4%, V=14.1%) was higher than 12% at all treatment

levels and considered inefficient by Gomez and Gomez (1984). Across the cultivars, delay in PD reduced biomass and grain yield. The results show that the cultivars were statistically different and each performed differently as influenced by PD and N treatment effect. The treatment effect of N did not statistically affect the yield and yield component. The effect of PD on biomass and grain yield has also been observed by Malekabadi et al. (2014). The maize cultivars varied significantly in biomass and grain yield, and such findings are comparable to those by Beiragi et al. (2011) who observed that both PD and cultivar significantly influenced total grain yield and yield components.

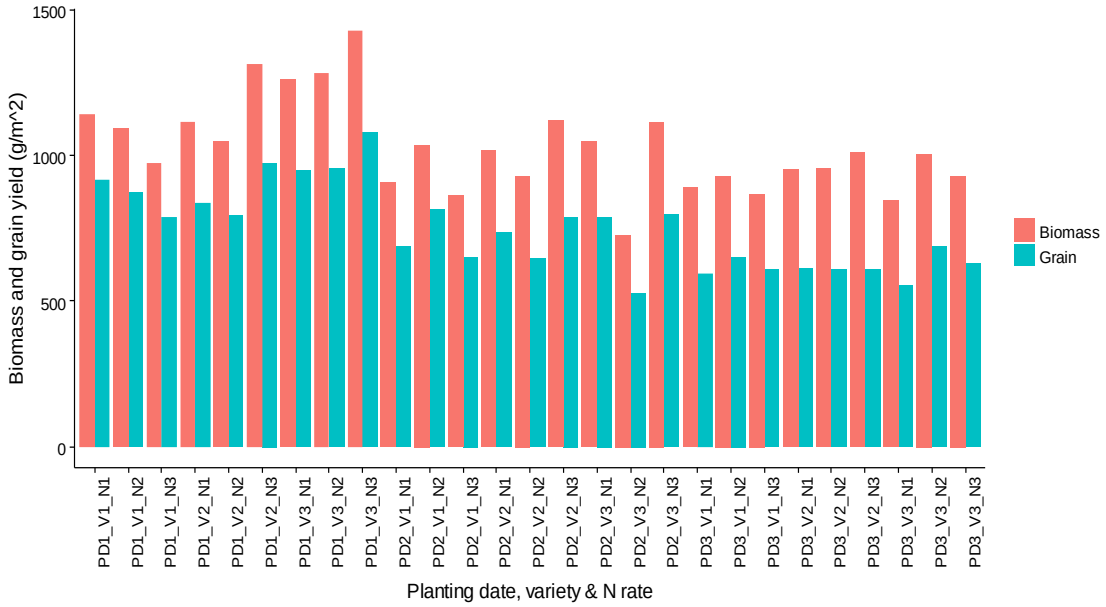

Figure 9: PD, cultivar and N effect on biomass and grain yield

4.2.4 Seed No m^{-2}, HI, cob length, cob width, 100-grain weight, and LAI

Cultivar treatment effect significantly influenced seed number m^{-2},100-grain weight, cob weight, cob length, harvest index (HI) and LAI (V6, R1, R4) at $p<0.05$. The PD and cultivar treatment effects were very highly significant on 100-grain weight and HI. The 100-grain weight reduced with the delay in PD. The 100-grain weights were 33.62 g, 34.52 g and 40.34 g for the ZMS 606, PHB 30G19 and PHB 30B50 cultivars, respectively. Results showed that cultivar PHB 30B50 had a higher weight of 100 grains. Pooled data showed an increase in seed number m^{-2} at higher N rate (N3). PD, cultivar and the interaction between cultivar and PD significantly influenced the100-grain weight.

The treatment effects of PD and cultivar were highly significant and significant for cob width and length, respectively. Higher N fertilizer rate increased cob width and length. The PD and cultivar treatment effect on cob length, and width for ZMS 606, PHB 30G19 and PHB 30B50 were significant ($p<0.05$). The cultivar cob length and width responded differently to the PD treatment effect. PD effect was significant on 100-grain weight and (Peykarestan and Seify, 2012) has reported similar results. Mousavi et al. (2012) have also reported a significant effect of PD on HI of maize. Higher nitrogen fertilizer application rate increased seed number m^{-2} (Nemati and Sharifi, 2012; Sharifi and Namvar, 2016; Zeidan et al., 2006). PD and cultivar interaction had a very highly significant effect on cob length, and this has also been reported by Mousavi et al. (2012).

The cultivar and N rate treatment effect on LAI (R1 and R4) and LAI (V6) was very highly significant at $p<0.05$, respectively as shown in Table 23c. Results indicated that LAI for each cultivar (PHB 30G50=3.85 m^2 m^{-2}; PHB 30G19=3.61 m^2 m^{-2}; ZMS 606=3.15 m^2 m^{-2}) was different at silking and dough stages. The interaction effect of cultivar and N fertilizer rate effect on LAI (R1) was highly significant. They were variations in LAI among the cultivars at silking as a result of N fertilizer application rate. The largest LAI (3.65 m^2 m^{-2}) was recorded at the highest N fertilizer application rate (N3).

Table 21a: Treatment effect of PD, cultivar, and N on yield and yield components

Treatment/ cultivar	**V6** g m^{-2}	**R1 biomass** g m^{-2}	**R4 biomass** g m^{-2}	**R1 leaf blade** g m^{-2}	**R4 leaf blade** g m^{-2}	**R6 leaf blade(g m^{-2})** g m^{-2}	**R6 leaf sheath(g m^{-2})** g m^{-2}
PD1	11.38[a]	256.7[a]	449.40[a]	100.36[a]	93.67[a]	271.9[ab]	232.2[a]
PD2	8.49[a]	212.6[a]	501.67[a]	80.77[b]	97.91[a]	325.9[a]	214.1[a]
PD3	8.31[a]	263.2[a]	534.41a	91.17[ab]	89.00[a]	262.7[b]	208.9[a]
Significance	ns	ns	ns	ns	ns	ns	ns
LSD 5%	4.21	59.10	130.69	18.03	24.14	54.93	45.03
CV %	59.3	32	34.9	26.3	34.2	25.3	27.3
ZMS 606	9.36[a]	229.9[b]	461.04[a]	77.56[c]	80.98[c]	215.8[b]	187.6[b]
PHB 30B19	9.45[a]	270.0[a]	504.88[a]	104.46[a]	105.7[a]	334.2[a]	231.8[a]
PHB 30B50	9.37[a]	232.7[b]	519.56[a]	90.27[b]	93.90[b]	310.5[a]	235.8[a]
Significance	ns	*	ns	***	***	ns	***
LSD 5%	1.14	33.23	62.74	7.90	9.95		26.07
CV %	19.5	24.7	19.5	15.8	19.3	26.1	21.6
Nitrogen (N) rate							
N1	9.28[a]	246.2[a]	506.10[a]	88.66[a]	94.33[a]	271.2[a]	231.7[a]
N2	9.66[a]	248.9[a]	461.42[a]	88.67[a]	91.77[a]	279.1[a]	206.3[a]
N3	9.24[a]	237.7[a]	517.96[a]	94.96[a]	94.48[a]	310.3[a]	217.1[a]
Significance	ns	ns	ns	ns	ns	ns	ns
LSD 5%	1.09	59.1	57.18	10.53	10.94	54.34	35.54
CV %	21.9	24.9	23.0	19.6	19.7	31.9	27.4
Interaction (PD* V)							
Significance	**	ns	ns	**	ns	ns	ns
Interaction (V*N)							
Significance	ns	ns	ns	ns	*	*	ns
Interaction (V*PD*N)							
Significance	ns	ns	ns	ns	ns	ns	ns

Note: Means sharing the same letter in the table do not differ statistically at $p < 0.05$; LSD = Least Mean Differences; * = significant at 5% level; ** = highly significant at 5% level; *** = very highly significant at 5% level; ns = Non significant; At R6 weight=g m^{-2} (g m^{-2}* 10=ton ha^{-1}); wt. = weight; two plants were analyzed at V6, R1 and R4

Table 22b: Treatment effect of PD, cultivar and N on yield and yield components

Treatment/ cultivar	**R6 stem (g m^{-2})**	**R6 cob (g m^{-2})**	**R6 husk (g m^{-2})**	**R6 stover (g m^{-2})**	**R6 grain (g m^{-2})**	**R6 biomass (g m^{-2})**
PD1	376.6[b]	158.0a	408.8[a]	277.5ab	907.6[a]	1185.0a
PD2	450.2[a]	140.8a[b]	356.1[a]	258.0b	716.3[b]	974.3[b]
PD3	425.6[a]	128.4[b]	384.8[a]	314.5a	617.7[b]	932.2[b]
Significance	*	ns	ns	ns	*	*
LSD 5%	39.7	24.95	68.21	21.1	162.5	196.2
CV %	12.6	23.2	23.6	21.1	28.8	25.2
ZMS 606	413.1[b]	109.10[b]	381.6[b]	234.5b	732.6[a]	967.1[b]
PHB 30G19	445.4[a]	157.8[a]	420.5[a]	318.0a	733.9[a]	1052.0[a]
PHB 30B50	394.0[b]	160.3[a]	347.5[b]	297.4a	775.2[a]	1073.0[a]
Significance	ns	***	**	***	ns	*
LSD 5%	31.56	11.88	37.77	24.20	61.78	80.01
CV %	13.7	15.1	17.9	15.5	15	14.1
Nitrogen (N) rate						
N1	408.9[a]	137.37[a]	372.1[a]	278.2a	742.3[a]	1020.0[a]
N2	422.0[a]	137.74[a]	382.5[a]	272.6a	729.2[a]	1002.0[a]
N3	421.5[a]	152.07[a]	392.1[a]	299.2a	770.2[a]	1069.0[a]
Significance	ns	ns	ns	ns	ns	ns
LSD 5%	37.93	16.18	61.86	31.88	97.59	124.6
CV %	15.3	19.2	27.2	19.0	22.0	20.4
Interaction (PD*V)						
Significance	ns	***	ns	**	ns	ns
Interaction (V*N)						
Significance	ns	*	ns	*	ns	*
Interaction (V*PD*N)						
Significance	ns	ns	ns	ns	ns	ns

Note: Means sharing the same letter in the table do not differ statistically at $p < 0.05$; LSD = Least Mean Differences; * = significant at 5% level; ** = highly significant at 5% level; *** = very highly significant at 5% level; ns = Non significant; At R6 weight=g m^{-2}square meter (g m^{-2} * 10=ton ha^{-1}); wt. = weight; two plants were analyzed at V6, R1 and R4

Table 23c: Treatment effect of PD, cultivar, and N on yield and yield components

	100 grain wt (g)	Seed no m^{-2}	Cob width	Cob length	HI	V6 lai	R1 lai	R4 lai
Treatment/cultivar								
PD1	42.35[a]	2153a	5.49[a]	21.43[a]	0.77[a]	0.34[a]	3.81[a]	3.39[a]
PD2	34.27[b]	2064a	5.29[b]	21.3[a]	0.73[b]	0.34[a]	3.48[a]	3.34[a]
PD3	31.86[c]	2014a	5.04[c]	18.43[b]	0.66[c]	0.32[a]	3.31[a]	2.94[a]
Significance	***	ns	**	*	***	ns	ns	ns
LSD 5%	1.25	17.90	0.20	1.70	0.02	0.04	0.84	0.89
CV %	4.6	57.8	5.10	11.1	4.6	22.3	31.5	36.6
ZMS 606	33.62[b]	2258[a]	5.17[b]	19.48[a]	0.75[a]	0.34[a]	3.15[b]	2.79[b]
PHB 30G19	34.52[b]	2210[a]	5.51[a]	20.78[a]	0.69[c]	0.32[a]	3.61[a]	3.49[a]
PHB 30B50	40.34[a]	1763[b]	5.14[b]	20.91[a]	0.72[b]	0.34[a]	3.85[a]	3.38[a]
Significance	***	***	***	*	***	ns	***	***
LSD 5%	2.80	167.6	0.16	1.85	0.02	0.04	0.30	0.37
CV %	14	56.5	3.30	7.8	3.8	20.5	15.5	20.8
Nitrogen (N) rate								
N1	36.70[a]	2061[a]	5.27[a]	20.33[a]	0.72[a]	0.29[b]	3.44[a]	3.23[a]
N2	35.91[a]	2054[a]	5.24[a]	20.33[a]	0.73[a]	0.32[b]	3.51[a]	3.12[a]
N3	35.87[a]	2116[a]	5.31[a]	20.51[a]	0.72[a]	0.40[a]	3.65[a]	3.31[a]
Significance	ns	ns	ns	ns	ns	***	ns	ns
LSD 5%	3.43	13.74	0.10	0.94	0.02	0.04	0.48	0.39
CV %	16	44.2	5.60	16.5	4.1	18.3	23.1	20.5
Interaction (V*PD)								
Significance	**	ns	ns	***	ns	ns	**	ns
Interaction (V*N)								
Significance	ns	ns	ns	ns	ns	ns	ns	ns
Interaction (V*PD*N)								
Significance	ns	ns	ns	ns	ns	ns	ns	ns

Note: Means sharing the same letter in the table do not differ statistically at $p < 0.05$; LSD = Least Mean Differences; * = significant at 5% level; ** = highly significant at 5% level; *** = very highly significant at 5% level; ns = Non significant; At R6 weight=g m^{-2} (g m^{-2} * 10=ton ha^{-1}); wt. = weight; two plants were analyzed at V6, R1 and R4

4.3 Calibration and validation of APSIM and CERES-Maize models

4.3.1 Evaluation of APSIM-Maize and CERES-Maize models

Cultivar-specific parameters (CSPs) computed for maize cultivars are shown in Table 12 and Table 13. ZMS606 had been calibrated for the CERES-Maize under rainfed conditions in 2013/2014 by Chisanga et al. (2015). CSMs simulate dry matter production as a function of climate, soil properties, and management practices. The model outputs included DAP to anthesis, and maturity, root-zone soil water content, LAI, grain size, unit grain weight, harvest index, biomass, and grain yield among others. The simulation outputs for all treatments in both experimental sites are presented in Table 24, Table 25, Table 26, Table 27, Table 28, Table 29, Table 30, Table 31, Table 32, Table 33, Table 34, Table 35, Table 36, Table 37, Table 38, Table 39, Table 40, Table 40 and Table 41. Measured and simulated values were compared graphically and analyzed statistically as shown in Appendix 5 and Appendix 6. Overall results and statistical evaluation and deviations between the observed and simulated values are discussed in this section.

4.3.2 Performance of APSIM-Maize and CERES-Maize models in simulating growth and yield for three maize cultivars

4.3.2.1 Days after planting to anthesis and maturity

The calibration results are presented in Table 24, Table 25, Table 26, Table 27, Table 28, Table 29, Appendix 5 and Appendix 6. A comparison of the simulated and measured DAP to anthesis and maturity showed very small differences. The %PD values for anthesis and maturity at PD1 (CERES-Maize) were close to or equal to zero and this indicted excellent agreement between simulated and observed values. The %PD for anthesis and maturity were <20% of the observed values. Simulated DAP to anthesis and maturity were excellent (NRMSE < 10%) for both models. Pooled values in CERES-Maize model for the RMSE for anthesis and maturity were 2.89 and 3.13 days, respectively. In APSIM-Maize, pooled values for the RMSE for anthesis and maturity were 1.91 and 3.35 days, respectively. ZMS 606 (0.58 days) and PHB 30G19 (0.82 days) cultivars in APSIM-Maize and CERES-Maize models at anthesis had the lowest RMSE, respectively. The CSMs provided acceptable results on observed versus simulated values of DAP to anthesis and maturity.

4.3.2.2 Biomass and grain yields

APSIM-Maize and CERES-Maize models were parameterized to simulate grain size, grain number m^{-2}, biomass, and grain yield under three N fertilizer application rates for the three maize cultivars (Table 24, Table 25, Table 30, Table 31, Table 32, Table 33, Table 34, Table 35, Table 36 and Table 37, Appendix 5 and Appendix 6). The %PD for grain yield at some treatment levels (PDs) was <20%. The PD analysis showed that delayed PD from December 12, 2016, to December 26, 2016, and January 9, 2017, caused a decrease in yield for all cultivars.

Observed and simulated values for grain yield, grain size, and grain number m^{-2} for APSIM-Maize and CERES-Maize had NRMSE between 20-30% and considered acceptable in CSM evaluation. Biomass RMSE for APSIM-Maize and CERES-Maize were 3.19 ton ha^{-1} and 2.87 ton ha^{-1}, respectively and was poorly simulated (NRMSE > 30%). RMSE between observed and predicted value by APSIM-Maize for grain yield for ZMS 606, PHB 30G19 and PHP 30B50 were 1.28, 1.27, 1.56 ton ha^{-1}, respectively as compared to CERES-Maize with RMSE 0.67 ton ha^{-1} (ZMS 606), 0.68 ton ha^{-1} (PHB 30G19) and 1.11 ton ha^{-1} (PHB 30B50). The grain yield for ZMS 606 and PHB 30G19 was simulated accurately by both models.

The simulated grain size and grain number m^{-2} in APSIM-Maize were considered good (NRMSE = 10-20%) (Table 34 and Table 36) for all the cultivars. In CERES-Maize, the simulated grain size were considered good (ZMS 606 and PHB 30B50 [NRMSE = 10-20%]) and acceptable (PHB 30G19 [NRMSE = 22.10%]) (Table 35 and Table 37). The simulated grain number m^{-2} was good (ZMS 606 and PHB 30G19 [NRMSE = 10-20%]) and acceptable (PHB 30B50 [NRMSE = 24.84%]) (Table 35 and Table 37). The CERES-Maize model explained 63%, 86% and 72% of the variation in observed grain size, biomass and grain yield, respectively. In APSIM-Maize, 85% of biomass yield was explained by the model. In this study, the APSIM-Maize performed better in simulation grain size and grain number m^{-2}. Similarly, the CERES-Maize performed better in

simulation grain yield. APSIM-Maize and CERES-Maize models can be used to simulate grain yield, grain siz, and grain number m^{-2} under local conditions in Zambia.

4.3.2.3 Leaf area index

The NRMSE for the mLAI in APSIM-Maize and CERES-Maize were poor (NRMSE > 30%) and good (NRMSE = 18.68%), respectively (Table 38, Table 39, Appendix 5 and Appendix 6). Inaccurate simulation of mLAI in CERES-Maize can also be seen in %PD which was >36%. The mLAI in the models was under-predicted at all treatment levels. Similar results using the CERES-Maize model have been reported by Chisanga et al. (2015). The APSIM-Maize and CERES-Maize models simulate LAI, but in this situation, the functions performed poorly. APSIM by default underestimates early season LAI (Jin et al., 2016). To overcome this proble, APSIM-Maize calibration was done for the whole season to reduce the underestimation of LAI in the early season. Simulated mLAI ranged from 3.02-3.35 m^2 m^{-2} (APSIM-Maize) and 1.44-2.18 m^2 m^{-2} (CERES-Maize). Typical LAI values for maize cultivars in dry-land areas under rainfed are 2.50-2.90 (Kisaka et al., 2016) and this is in agreement with the results from APSIM-Maize model. LAI provides an index of maize plant growth and is an essential input data (Hoogenboom et al., 1999).

4.3.2.4 Simulation of root soil water content in the soil layers

The simulated soil water content statistics for pooled data are shown in Table 40 and Table 41 below. The predictive ability of the CERES-Maize model was excellent (NRMSE = <10%, soil layers: 40 cm), good (NRMSE = 10-20%, soil layers: 20-30 cm, 50-70 cm) and acceptable (NRMSE = 20-30%, soil layer: 10 cm, 80 cm). In APSIM-Maize model, the predictive ability of the model was excellent (NRMSE = <10%, soil layers: 30-50 cm) and good (NRMSE =10-20%, soil layers: 10 cm, 60-80 cm). The computed NRMSE for the CSMs are considered acceptable (Jing et al., 2017). APSIM soilwat module requires that LL and DUL are determined under field conditions (Archontoulis et al., 2014b). PD analysis showed that the amount of root-zone soil water available for plant growth and rainfall decreased during each maize growing period and this affected biomass and grain yield. Root soil water profile layers of 5-15, 15-30 and 30-45 cm thickness are important for simulating correct root soil water balance and plant water uptake (Nangia et al., 2010).

Table 24: Comparison between observed and simulated phenology, mLAI, biomass, grain, and grain size in CERES-Maize model

	Anthesis			Maturity			mLAI			Biomass			Grain			Unit wt			grain no		
Planting Date 1																					
Trt	Obs	Sim	%PD	Obs	Sim	%PD	Obs	Sim	%PD	Obs	Sim	%PD	Obs	Sim	%PD	Obs	Sim	%PD	Obs	Sim	%PD
V1N1	65	64	-1.54	123	123	0.00	3.70	1.54	-58.38	11.40	13.70	20.18	9.20	8.80	-4.35	0.37	0.38	2.15	2401	2322	6.91
V1N2	65	64	-1.54	123	123	0.00	3.29	1.55	-52.89	10.90	13.70	25.69	8.70	8.70	0.00	0.38	0.38	0.53	2276	2328	2.28
V1N3	65	64	-1.54	123	123	0.00	3.15	1.56	-50.48	9.80	13.80	40.82	7.90	8.80	11.39	0.37	0.37	0.00	2128	2341	10.01
V2N1	65	65	0.00	124	124	0.00	3.79	1.96	-48.28	11.20	14.80	32.14	8.40	8.80	4.76	0.37	0.38	2.70	2251	2297	2.04
V2N2	65	65	0.00	124	124	0.00	3.68	1.97	-46.47	10.50	14.70	40.00	7.90	8.80	11.39	0.41	0.38	-7.32	1922	2299	19.61
V2N3	65	65	0.00	124	124	0.00	4.45	1.98	-55.51	13.10	14.80	12.98	9.70	8.80	-9.28	0.38	0.38	0.00	2519	2305	-8.50
V3N1	63	64	1.59	122	122	0.00	4.22	1.54	-63.51	12.50	14.40	15.20	9.50	10.10	6.32	0.51	0.51	0.00	1867	1996	6.91
V3N2	63	64	1.59	122	122	0.00	4.56	1.55	-66.01	12.70	14.50	14.17	9.60	10.20	6.25	0.50	0.51	2.00	1952	2001	2.51
V3N3	63	64	1.59	122	122	0.00	5.00	1.56	-68.80	14.20	14.50	2.11	10.80	10.20	-5.56	0.52	0.51	-1.92	2063	2012	-2.47
Planting Date 2																					
V1N1	67	64	-4.48	123	127	3.25	3.57	1.56	-56.30	9.10	12.00	31.87	6.90	7.60	10.14	0.32	0.36	12.50	2113	2195	3.88
V1N2	67	64	-4.48	123	127	3.25	3.45	1.56	-54.78	10.40	11.90	14.42	8.20	7.50	-8.54	0.34	0.34	0.00	2421	2194	-9.38
V1N3	67	64	-4.48	123	127	3.25	3.26	1.60	-50.92	8.60	12.00	39.53	6.50	7.60	16.92	0.30	0.34	13.33	2190	2218	1.28
V2N1	66	65	-1.52	122	128	4.92	3.75	1.91	-49.07	10.20	12.80	25.49	7.30	7.60	4.11	0.34	0.36	5.88	2146	2146	0.00
V2N2	66	65	-1.52	122	128	4.92	3.58	1.93	-46.09	9.30	12.70	36.56	6.50	7.50	15.38	0.30	0.35	16.67	2125	2154	1.36
V2N3	66	65	-1.52	122	128	4.92	4.08	1.94	-52.45	11.20	12.90	15.18	7.90	7.70	-2.53	0.34	0.36	5.88	2311	2158	-6.62
V3N1	68	62	-8.82	122	123	0.82	3.64	1.47	-59.62	10.50	12.10	15.24	7.90	7.90	0.00	0.43	0.42	-2.33	1861	1908	2.53
V3N2	68	62	-8.82	122	123	0.82	3.20	1.47	-54.06	7.30	12.00	64.38	5.30	7.90	49.06	0.35	0.41	17.14	1497	1907	27.39
V3N3	68	62	-8.82	122	123	0.82	3.18	1.50	-52.83	11.00	12.30	11.82	8.00	8.10	1.25	0.37	0.42	13.51	1908	1929	1.10
Planting Date 3																					
V1N1	66	65	-1.52	129	130	0.78	3.18	1.60	-49.69	10.10	10.80	6.93	6.00	5.80	-3.33	0.32	0.21	-34.38	2300	2793	21.43
V1N2	66	65	-1.52	129	130	0.78	3.34	1.59	-52.40	8.90	10.70	20.22	6.50	5.80	-10.77	0.31	0.21	-32.26	2425	2755	13.61
V1N3	66	65	-1.52	129	130	0.78	3.34	1.59	-52.40	8.70	10.60	21.84	6.10	5.60	-8.20	0.32	0.20	-37.50	2068	2789	34.86
V2N1	69	68	-1.45	129	134	3.88	3.61	2.18	-39.61	9.50	11.70	23.16	6.10	5.30	-13.11	0.31	0.19	-38.71	2043	2768	35.49
V2N2	69	68	-1.45	129	134	3.88	4.02	2.18	-45.77	9.60	11.80	22.92	6.10	5.50	-9.84	0.33	0.20	-39.39	2243	2765	23.27
V2N3	69	68	-1.45	129	134	3.88	3.40	2.17	-36.18	10.10	11.90	17.82	6.10	5.60	-8.20	0.33	0.20	-39.55	2331	2745	17.76
V3N1	67	62	-7.46	130	127	-2.31	3.55	1.45	-59.15	8.40	10.30	22.62	5.60	5.50	-1.79	0.35	0.24	-31.43	1568	2291	46.11
V3N2	67	62	-7.46	130	127	-2.31	3.59	1.44	-59.89	10.00	10.10	1.00	6.90	5.40	-21.74	0.33	0.24	-27.27	1628	2266	39.19
V3N3	67	62	-7.46	130	127	-2.31	3.72	1.44	-61.29	9.30	10.10	8.60	6.30	5.30	-15.87	0.29	0.23	-20.69	1521	2298	51.08

Note: DAP = Days after planting (anthesis, physiological maturity); mLAI (m^2 m^{-2}) = maximum leaf area index, biomass (t ha^{-1}), unity weight (g); Negative deviations indicate under prediction while positive deviations indicate over prediction; %PD = percentage prediction deviation, Sim = Simulated; Obs = observed; DAP = Days after planting; mLAI = maximum leaf area index; V1 = ZMS 606; V2 = PHB 30G19; V3 = PHB 30B50; Trt = Treatment

Table 25: Comparison between observed and simulated phenology, mLAI, biomass, grain, and grain size in APSIM-Maize model

	Anthesis			Maturity			mLAI			Biomass			Grain			Unit wt			grain no		
Planting Date 1																					
Trt	Obs	Sim	%PD	Obs	Sim	%PD	Obs	Sim	%PD	Obs	Sim	%PD	Obs	Sim	%PD	Obs	Sim	%PD	Obs	Sim	%PD
V1N1	65	65	0.00	123	124	0.81	3.70	3.18	-14.05	11.40	15.40	35.09	9.20	8.90	-3.26	0.37	0.39	4.84	2401	2261	-0.86
V1N2	65	65	0.00	123	124	0.81	3.29	3.19	-3.04	10.90	15.40	41.28	8.70	8.90	2.30	0.38	0.39	3.17	2276	2262	-0.62
V1N3	65	65	0.00	123	124	0.81	3.15	3.19	1.27	9.80	15.40	57.14	7.90	8.90	12.66	0.37	0.39	5.41	2128	2262	6.30
V2N1	65	65	0.00	124	124	0.00	3.79	3.19	-15.83	11.20	15.50	38.39	8.40	8.90	5.95	0.37	0.38	2.70	2251	2324	3.24
V2N2	65	65	0.00	124	124	0.00	3.68	3.19	-13.32	10.50	15.50	47.62	7.90	8.90	12.66	0.41	0.38	-7.32	1922	2324	20.92
V2N3	65	65	0.00	124	124	0.00	4.45	3.19	-28.31	13.10	15.50	18.32	9.70	8.90	-8.25	0.38	0.38	0.00	2519	2324	-7.74
V3N1	63	65	3.17	122	123	0.82	4.22	3.14	-25.59	12.50	15.30	22.40	9.50	8.00	-15.79	0.51	0.43	-15.69	1867	1851	-0.86
V3N2	63	65	3.17	122	123	0.82	4.56	3.14	-31.14	12.70	15.30	20.47	9.60	8.00	-16.67	0.50	0.43	-14.00	1952	1852	-5.12
V3N3	63	65	3.17	122	123	0.82	5.00	3.14	-37.20	14.20	15.30	7.75	10.80	8.00	-25.93	0.52	0.43	-17.31	2063	1852	-10.23
Planting Date 2																					
V1N1	67	67	0.00	123	130	5.69	3.57	3.34	-6.44	9.10	15.40	69.23	6.90	8.70	26.09	0.32	0.40	25.00	2113	2175	2.93
V1N2	67	67	0.00	123	130	5.69	3.45	3.34	-3.19	10.40	15.80	51.92	8.20	8.70	6.10	0.34	0.40	17.65	2421	2175	-10.16
V1N3	67	67	0.00	123	130	5.69	3.26	3.34	2.45	8.60	15.80	83.72	6.50	8.70	33.85	0.30	0.40	33.33	2190	2175	-0.68
V2N1	66	67	1.52	122	128	4.92	3.75	3.34	-10.93	10.20	15.80	54.90	7.30	8.80	20.55	0.34	0.38	11.76	2146	2290	6.71
V2N2	66	67	1.52	122	128	4.92	3.58	3.34	-6.70	9.30	15.80	69.89	6.50	8.80	35.38	0.30	0.38	26.67	2125	2290	7.76
V2N3	66	67	1.52	122	128	4.92	4.08	3.35	-17.89	11.20	15.80	41.07	7.90	8.80	11.39	0.34	0.38	11.76	2311	2290	-0.91
V3N1	68	65	-4.41	122	125	2.46	3.64	3.29	-9.62	10.50	15.60	48.57	7.90	7.70	-2.53	0.43	0.43	0.00	1861	1790	-3.82
V3N2	68	65	-4.41	122	125	2.46	3.20	3.29	2.81	7.30	15.60	113.70	5.30	7.70	45.28	0.35	0.43	22.86	1497	1790	19.57
V3N3	68	65	-4.41	122	125	2.46	3.18	3.29	3.46	11.00	15.60	41.82	8.00	7.70	-3.75	0.37	0.43	16.22	1908	1790	-6.18
Planting Date 3																					
V1N1	66	65	-1.52	129	130	0.78	3.18	3.05	-4.09	10.10	13.50	33.66	6.00	7.50	25.00	0.32	0.29	-9.38	2300	2586	12.43
V1N2	66	65	-1.52	129	130	0.78	3.34	3.05	-8.68	8.90	13.50	51.69	6.50	7.50	15.38	0.31	0.29	-6.45	2425	2586	6.64
V1N3	66	65	-1.52	129	130	0.78	3.34	3.05	-8.68	8.70	13.50	55.17	6.10	7.50	22.95	0.32	0.29	-9.38	2068	2586	25.05
V2N1	69	66	-4.35	129	129	0.00	3.61	3.05	-15.51	9.50	13.50	42.11	6.10	7.30	19.67	0.31	0.28	-9.68	2043	2582	26.38
V2N2	69	66	-4.35	129	129	0.00	4.02	3.05	-24.13	9.60	13.50	40.63	6.10	7.30	19.67	0.33	0.28	-15.15	2243	2582	15.11
V2N3	69	66	-4.35	129	129	0.00	3.40	3.05	-10.29	10.10	13.50	33.66	6.10	7.30	19.67	0.33	0.28	-15.15	2331	2582	10.77
V3N1	67	64	-4.48	130	128	-1.54	3.55	3.02	-14.93	8.40	13.60	61.90	5.60	7.20	28.57	0.35	0.35	0.00	1568	2053	30.93
V3N2	67	64	-4.48	130	128	-1.54	3.59	3.02	-15.88	10.00	13.60	36.00	6.90	7.20	4.35	0.33	0.35	6.06	1628	2053	26.11
V3N3	67	64	-4.48	130	128	-1.54	3.72	3.02	-18.82	9.30	13.60	46.24	6.30	7.20	14.29	0.29	0.35	20.69	1521	2053	34.98

Note: DAP = Days after planting (anthesis, physiological maturity); mLAI (m^2 m^{-2}) = maximum leaf area index, biomass (t ha^{-1}), unity weight (g); Negative deviations indicate under prediction while positive deviations indicate over prediction; %PD = percentage prediction deviation, Sim = Simulated; Obs = observed; DAP = Days after planting; mLAI = maximum leaf area index; V1 = ZMS 606; V2 = PHB 30G19; V3 = PHB 30B50; Trt = Treatment

Table 26: APSIM-Maize model calibration statistics for anthesis (DAP)

	APSIM-Maize							
Cultivar	NRMSE	EF	d	RMSE	ME	MAE	CRM	R^2
V1	0.87	0.50	0.89	0.58	-0.33	0.33	0.87	0.75
V2	2.74	-0.15	0.53	1.83	-0.67	1.33	0.01	0.06
V3	4.10	-0.57	0.35	2.71	-1.33	2.67	0.02	0.11

Note: V1 = ZMS 606; V2 =: PHB 30G19; V3 = PHB 30B50

Table 27: CERES-Maize model calibration statistics for anthesis (DAP)

	CERES-Maize							
Cultivar	NRMSE	EF	d	RMSE	ME	MAE	CRM	R^2
V1	2.90	-4.50	0.42	1.91	-1.67	1.67	0.03	0.00
V2	1.22	0.77	0.93	0.82	-0.67	0.67	0.01	0.94
V3	6.89	-3.43	0.28	4.55	-3.33	4.00	0.05	0.96

Table 28: APSIM-Maize model calibration statistics for maturity (dap)

	APSIM-Maize							
Cultivar	NRMSE	EF	d	RMSE	ME	MAE	CRM	R^2
V1	3.30	-1.13	0.63	4.12	3.00	3.00	-0.02	0.25
V2	2.77	-0.38	0.65	3.46	2.00	2.00	-0.02	0.18
V3	1.73	0.67	0.86	2.16	0.67	2.00	-0.01	0.84

Note: V1: ZMS 606; V2: PHB 30G19; V3: PHB 30B50

Table 29: CERES-Maize model calibration statistics for maturity (dap)

	CERES-Maize							
Cultivar	NRMSE	EF	d	RMSE	ME	MAE	CRM	R^2
V1	2.32	-1.34	0.73	2.89	2.33	2.33	-0.02	0.82
V2	3.61	-1.35	0.71	4.51	3.67	3.67	-0.03	0.60
V3	1.46	0.77	0.91	1.83	-0.67	1.33	0.01	0.96

Note: V1: ZMS 606; V2: PHB 30G19; V3: PHB 30B50

Table 30: APSIM-Maize model calibration statistics for biomass

	APSIM-Maize							
Cultivar	NRMSE	EF	d	RMSE	ME	MAE	CRM	R^2
V1	53.31	28.91	0.25	5.21	5.09	5.09	-0.52	0.12
V2	43.30	15.62	0.30	4.56	4.41	4.41	-0.42	0.19
V3	43.16	-3.89	0.43	4.60	4.18	4.18	-0.39	0.15

Note: V1 = ZMS 606; V2 = PHB 30G19; V3 = PHB 30B50

Table 31: CERES-Maize model calibration statistics for biomass

	CERES-Maize							
Cultivar	NRMSE	EF	d	RMSE	ME	MAE	CRM	R^2
V1	68.08	0.39	0.89	2.86	2.22	2.23	-0.53	0.87
V2	63.74	0.42	0.89	3.03	2.40	2.41	-0.51	0.89
V3	55.31	0.61	0.92	2.65	1.90	1.92	-0.40	0.87

Note: V1 = ZMS 606; V2 = PHB 30G19; V3 = PHB 30B50

Table 32: APSIM-Maize model calibration statistics for grain yield

	APSIM-Maize							
Cultivar	NRMSE	EF	d	RMSE	ME	MAE	CRM	R^2
V1	17.41	-0.30	0.66	1.28	1.03	1.10	-0.14	0.60
V2	17.34	-0.15	0.66	1.27	1.00	1.18	-0.14	0.58
V3	20.13	0.25	0.44	1.56	-0.13	1.29	0.02	0.62

Note: V1 = ZMS 606; V2 = PHB 30G19; V3 = PHB 30B50

Table 33: CERES-Maize model calibration statistics for grain yield

	CERES-Maize							
Cultivar	NRMSE	EF	d	RMSE	ME	MAE	CRM	R^2
V1	9.16	0.64	0.91	0.67	0.13	0.56	-0.02	0.84
V2	9.27	0.67	0.93	0.68	-0.04	0.62	0.01	0.76
V3	14.31	0.62	0.91	1.11	0.08	0.79	-0.01	0.69

Note: V1 = ZMS 606; V2 = PHB 30G19; V3 = PHB 30B50

Table 34 APSIM-Maize model statistics for grain size

	APSIM-Maize							
Cultivar	NRMSE	EF	d	RMSE	ME	MAE	CRM	R^2
V1	15.05	-2.30	0.61	0.05	0.02	0.04	-0.07	0.19
V2	12.39	-0.68	0.68	0.04	0.00	0.04	0.00	0.22
V3	15.02	0.44	0.72	0.06	0.00	0.05	0.01	0.51

Note: V1 = ZMS 606; V2 = PHB 30G19; V3 = PHB 30B50

Table 35: CERES-Maize model calibration statistics for grain size

	CERES-Maize							
Cultivar	NRMSE	EF	d	RMSE	ME	MAE	CRM	R^2
V1	19.25	-4.40	0.55	0.06	-0.02	0.05	0.07	0.57
V2	22.10	-4.35	0.52	0.08	-0.03	0.06	0.10	0.33
V3	14.28	0.50	0.91	0.06	-0.02	0.04	0.04	0.79

Note: V1 = ZMS 606; V2 = PHB 30G19; V3 = PHB 30B50

Table 36: APSIM-Maize model calibration statistics for grain number m^{-2}

	APSIM-Maize							
Cultivar	NRMSE	EF	d	RMSE	ME	MAE	CRM	R^2
V1	10.21	-2.07	0.42	230.55	82.89	175.11	-0.04	0.00
V2	12.81	-1.94	0.37	283.20	188.56	236.56	-0.09	0.00
V3	17.52	-1.43	0.22	308.84	135.44	250.11	-0.08	0.32

Note: V1 = ZMS 606; V2 = PHB 30G19; V3 = PHB 30B50

Table 37: CERES-Maize model calibration statistics for grain number m^{-2}

	CERES-Maize							
Cultivar	NRMSE	EF	d	RMSE	ME	MAE	CRM	R^2
V1	14.66	-5.33	0.35	330.92	176.89	246.67	-0.08	0.00
V2	16.41	-3.83	0.30	362.67	194.00	275.56	-0.09	0.00
V3	24.84	-3.89	0.30	437.91	304.78	316.11	-0.17	0.31

Note: V1 = ZMS 606; V2 = PHB 30G19; V3 = PHB 30B50

Table 38: APSIM-Maize model calibration statistics for mLAI

	APSIM-Maize							
Cultivar	NRMSE	EF	d	RMSE	ME	MAE	CRM	R^2
V1	7.27	-1.07	0.48	0.24	-0.17	0.20	0.05	0.10
V2	18.15	-4.35	0.40	0.69	-0.62	0.62	0.16	0.03
V3	24.30	-1.58	0.42	0.94	-0.70	0.75	0.18	0.06

Note: V1 = ZMS 606; V2 = PHB 30G19; V3 = PHB 30B50

Table 39: CERES-Maize model calibration statistics for mLAI

	CERES-Maize							
Cultivar	NRMSE	EF	d	RMSE	ME	MAE	CRM	R^2
V1	51.54	-103.17	0.14	1.73	-1.73	1.73	0.51	0.15
V2	47.83	-36.14	0.20	1.83	-1.84	1.82	0.47	0.06
V3	62.91	-16.30	0.29	2.42	-2.37	2.36	0.61	0.60

Note: V1 = ZMS 606; V2 = PHB 30G19; V3 = PHB 30B50

Table 40: APSIM-Maize model calibration statistics for root soil water content

	APSIM-Maize		
soil layer depth (cm)	NRMSE	RMSE	R^2
10	16.08	0.04	0.72
20	8.37	0.03	0.69
30	7.69	0.03	0.70
40	7.34	0.03	0.63
50	9.56	0.04	0.50
60	11.74	0.05	0.36
70	11.69	0.05	0.30
80	14.12	0.06	0.21

Table 41: CERES-Maize model calibration statistics for root soil water content

	CERES-Maize				
soil layer depth (cm)	NRMSE	EF	d	RMSE	ME
10	28.95	0.40	0.75	0.09	-0.01
20	19.53	0.48	0.75	0.07	0.00
30	10.25	0.62	0.84	0.04	0.00
40	9.79	0.51	0.81	0.04	-0.01
50	11.95	0.21	0.73	0.05	-0.02
60	11.74	0.06	0.67	0.05	-0.02
70	11.69	-0.15	0.66	0.05	-0.02
80	21.18	-3.66	0.47	0.09	-0.08

4.3.3 Validation of APSIM-Maize and CERES-Maize models

4.3.3.1 Phenology (anthesis and maturity days after planting)

The observed and simulated phenological stages are presented in Table 42, Table 44, Table 46 and Table 47. Validation statistics have been used to evaluate the predictive ability, usefulness, and robustness of the models. In APSIM-Maize, DAP to anthesis

and maturity ranged from 87-88 and 135-137 under irrigated conditions, respectively. The evaluation of anthesis and maturity were good (NRMSE=10-20%) with RMSE being 16.69 and 17.36 days, respectively. DAP to anthesis and maturity of the maize cultivars in CERES-Maize ranged from 80-86 and 130-137 days, respectively. Both models under-predicted the DAP to anthesis and maturity. The RMSE for anthesis (NRMSE=19.94%) and maturity (NRMSE=12.77%) using the CERES-Maize model were 20.67 and 19.54 days. DAP to anthesis and maturity increased due to reduced solar radiation and cooler air temperature at the experimental field site. The APSIM-Maize and CERES-Maize models simulate DAP to anthesis and maturity, but in this situation, the functions performed poorly. White and Grace (1999) stated that maize CSMs reliably predict the effects of temperature on crop duration, a major determinant of yield. However, they ignore other effects such as extreme high/or low temperatures, nutrient deficiencies on duration and drought stress.

4.3.3.2 Leaf area index, biomass and grain yield

The calibrated models were evaluated against the end of season mLAI, grain size, grain number m^{-2}, grain, and biomass yield (Table 42, Table 43, Table 44, Table 45, Table 46 and Table 47). The mLAI in APSIM-Maize and CERES-Maize ranged from 3.26-3.37 m^2 m^{-2} and 1.61-2.11 m^2 m^{-2} under irrigated conditions. The RMSE for mLAI in APSIM-Maize (NRMSE=16.75%) and CERES-Maize (NRMSE=49.56%) were 0.57 m^2 m^{-2} and 1.67 m^2 m^{-2} and considered to be good and poor, respectively.

The simulated grain size (RMSE=0.02 g, NRMSE=6.25%, R^2=0.80, d-stat=0.75), grain number m^{-2} (RMSE=456.21 grain m^{-2}, NRMSE=18.51%), grain (RMSE=1.34 t ha^{-1}, NRMSE=20.18%) and biomass (RMSE=3.96 t ha^{-1}, R^2=0.72, EF=0.71, d-stat=0.92) using APSIM-Maize were excellent and good, respectively. The simulated grain size (NRMSE=21.14%, R^2=0.72, EF=-6.15, d=0.55) and grain number m^{-2} (NRMSE=26.91%, R^2=0.10, EF=-1.79, d=0.52) using CERES-Maze were good. The simulated grain (NRMSE=45.08%) and biomass (NRMSE=71.64%) yield were poor. The APSIM-Maize performed better in evaluating grain yield, grain size, and grain number m^{-2} compared to CERES-Maize. The accuracy of the simulated outcome in CSMs using new cultivars depends on rigorous calibration to minimize uncertainties.

Table 42a: Results of the validation of APSIM-Maize model

	Anthesis			Maturity			mLAI			Biomass		
Trt	Obs	Sim	%PD	Obs	Sim	%PD	Obs	Sim	%PD	Obs	Sim	%PD
V1N1	104	88	-15.38	153	137	-10.46	2.93	3.36	14.71	7.20	16.10	123.61
V1N2	104	88	-15.38	153	137	-10.46	2.96	3.37	13.85	11.20	16.10	43.75
V1N3	104	88	-15.38	153	137	-10.46	3.25	3.37	3.69	10.50	16.10	53.33
V2N1	105	87	-17.14	153	135	-11.76	2.69	3.26	21.19	8.30	16.00	92.77
V2N2	105	87	-17.14	153	135	-11.76	4.23	3.27	-22.70	8.40	16.10	91.67
V2N3	105	87	-17.14	153	135	-11.76	4.07	3.27	-19.63	10.20	16.10	57.84
V3N1	104	88	-15.38	153	135	-11.76	3.52	3.36	-4.55	8.50	16.00	88.24
V3N2	104	88	-15.38	153	135	-11.76	3.90	3.37	-13.59	9.90	16.00	61.62
V3N3	104	88	-15.38	153	135	-11.76	2.81	3.37	19.93	9.40	16.00	70.21

Table 43b: Results of the validation of APSIM-Maize model

	Grain yield (ton ha^{-1})			Grain size (g)			Grain #		
Trt	Obs	Sim	%PD	Obs	Sim	%PD	Obs	Sim	%PD
V1N1	5.30	7.70	45.28	0.24	0.27	12.50	2206	2833	28.42
V1N2	8.50	7.70	-9.41	0.26	0.27	3.85	3263	2835	-13.12
V1N3	7.70	7.70	0.00	0.26	0.27	3.85	2926	2837	-3.04
V2N1	5.50	7.70	40.00	0.25	0.27	8.00	2053	2901	41.31
V2N2	5.70	7.70	35.09	0.26	0.27	3.85	2195	2902	32.21
V2N3	7.10	7.70	8.45	0.25	0.27	8.00	2775	2904	4.65
V3N1	6.20	6.80	9.68	0.29	0.29	0.00	2139	2335	9.16
V3N2	7.10	6.70	-5.63	0.31	0.29	-6.45	2230	2337	4.80
V3N3	6.60	6.70	1.52	0.28	0.29	3.57	2397	2338	-2.46

Note: DAP: Days after planting (anthesis, physiological maturity); mLAI (m^2 m^{-2}): maximum leaf area index, biomass (t ha^{-1}), unity weight (g); Negative deviations indicate under prediction while positive deviations indicate over prediction; %PD: percentage prediction deviation, Sim: Simulated; Obs: observed; DAP: Days after planting; mLAI: maximum leaf area index; V1: ZMS 606; V2: PHB 30G19; V3: PHB 30B50; Trt: Treatment

Table 44a: Results of the validation of CERES-Maize model

	Anthesis			Maturity			mLAI			Biomass		
Trt	Obs	Sim	%PD	Obs	Sim	%PD	Obs	Sim	%PD	Obs	Sim	%PD
V1N1	104	88	-15.38	153	137	-10.46	2.93	3.36	14.71	7.20	16.10	123.61
V1N2	104	88	-15.38	153	137	-10.46	2.96	3.37	13.85	11.20	16.10	43.75
V1N3	104	88	-15.38	153	137	-10.46	3.25	3.37	3.69	10.50	16.10	53.33
V2N1	105	87	-17.14	153	135	-11.76	2.69	3.26	21.19	8.30	16.00	92.77
V2N2	105	87	-17.14	153	135	-11.76	4.23	3.27	-22.70	8.40	16.10	91.67
V2N3	105	87	-17.14	153	135	-11.76	4.07	3.27	-19.63	10.20	16.10	57.84
V3N1	104	88	-15.38	153	135	-11.76	3.52	3.36	-4.55	8.50	16.00	88.24
V3N2	104	88	-15.38	153	135	-11.76	3.90	3.37	-13.59	9.90	16.00	61.62
V3N3	104	88	-15.38	153	135	-11.76	2.81	3.37	19.93	9.40	16.00	70.21

Table 45b: Results of the validation of CERES-Maize model

	Grain			Grain size			grain no		
Trt	Obs	Sim	%PD	Obs	Sim	%PD	Obs	Sim	%PD
V1N1	5.30	7.70	45.28	0.24	0.27	12.50	2206	2833	28.42
V1N2	8.50	7.70	-9.41	0.26	0.27	3.85	3263	2835	-13.12
V1N3	7.70	7.70	0.00	0.26	0.27	3.85	2926	2837	-3.04
V2N1	5.50	7.70	40.00	0.25	0.27	8.00	2053	2901	41.31
V2N2	5.70	7.70	35.09	0.26	0.27	3.85	2195	2902	32.21
V2N3	7.10	7.70	8.45	0.25	0.27	8.00	2775	2904	4.65
V3N1	6.20	6.80	9.68	0.29	0.29	0.00	2139	2335	9.16
V3N2	7.10	6.70	-5.63	0.31	0.29	-6.45	2230	2337	4.80
V3N3	6.60	6.70	1.52	0.28	0.29	3.57	2397	2338	-2.46

DAP: Days after planting (anthesis, physiological maturity); mLAI (m^2 m^{-2}): maximum leaf area index, biomass (t ha^{-1}), unity weight (g)

Table 46: Results of the validation statistics for APSIM-Maize model

	Anthesis	Maturity	Grain yield	Biomass yield	Grain size	Grain No m^{-2}	mLAI
NRMSE	16.00	12.77	20.18	73.98	6.25	18.51	16.75
RMSE	16.69	19.54	1.34	6.87	0.02	456.21	0.57
R^2	1.00	0.00	0.00	0.04	0.80	0.10	0.11
EF	-1946.00		-0.76	-31.47	0.38	-0.32	-0.07
MAE	20.67	17.33	1.01	6.77	0.01	354.44	0.50
CRM	0.20	0.11	-0.11	-0.73	-0.04	-0.09	0.01
Pearson	0.63	NA	-0.01	0.20	0.89	0.32	-0.33
d	0.04		0.48	0.23	0.75	0.59	0.11

Table 47: Results of the validation statistics for the CERES-Maize model

	Anthesis	Maturity	Grain yield	Biomass yield	Grain size	Grain No m^{-2}	mLAI
NRMSE	19.94	11.34	45.08	71.64	21.14	26.91	49.56
RMSE	20.80	17.36	2.99	6.65	0.06	663.29	1.67
R^2	0.40	0.00	0.05	0.07	0.72	0.10	0.14
EF	-1946.00		-7.77	-29.45	-6.15	-1.79	-8.37
MAE	20.67	19.33	2.79	6.51	0.05	568.89	1.59
CRM	0.20	0.13	-0.42	-0.70	-0.18	-0.22	0.47
Pearson	0.63	NA	0.21	0.27	0.85	0.32	0.38
d	0.04	NA	0.35	0.24	0.55	0.52	0.36

4.4 Suitability of the LARS-WG in predicting climate change for the 2050s based on HadCMS3 and BCM2 GCMs

4.4.1 Calibration and validation of LARS-WG

Statistical test for evaluating the suitability of LARS-WG in simulating precipitation for Mount Makulu is presented in Table 48, Table 49, Table 50, Table 51 and Table 52. It can be observed from the K-S-test that the model performed very well in fitting the DJF (wet/dry), MAM (wet/dry), JJA (wet) and SON (dry) seasons for the two datasets. The LARS-WG was more capable in simulating the seasonal distributions of the wet/dry spells and daily precipitation distributions for each month. Similar results have been reported by Hassan, (2014) and Qian et al. (2004). The ratios of mean length of wet and dry spells in LARS-WG of a future climate to those of the current climate are used to adjust wet and dry spells scenarios for the future (Qian et al., 2005; Semenov and Barrow, 2002). The model performed poorly in fitting the JJA (dry) season. The reason for the poor performance is attributed to the lack of precipitation recorded in JJA (dry). Table 48, Table 49, Table 50 and Table 51 present the KS-test for daily rain distribution. The assessment results show that LARS-WG performance in simulating daily rainfall distributions for the JFMAOND was perfect except for the months of MJJAS (Observed) and MJJAS (AgMERRA reanalysis). The poor performance was due to lack of precipitation during the period under consideration.

The simulation of Tmax and Tmin for both data sets was perfect (Table 52, Table 53, Table 54 and Table 55). The synthetic weather data generated using stochastic weather generators can be used as inputs into crop and hydrological models. Weather generators generate synthetic weather time series which have statistical properties similar to the observed data (Qian et al., 2004).

Table 48: Results of K-S-test for seasonal wet/dry SERIES distribution for AgMERRA

Season	Wet/dry	N	K-S	p-value	Assessment
DJF	wet	12	0.049	1.0000	Perfect fit
DJF	dry	12	0.045	1.0000	Perfect fit
MAM	wet	12	0.077	1.0000	Perfect fit
MAM	dry	12	0.075	1.0000	Perfect fit
JJA	wet	12	0.000	1.0000	Perfect fit
JJA	dry	12	0.131	0.9824	Very good fit
SON	wet	12	0.079	1.0000	Very good fit
SON	dry	12	0.098	0.9997	Perfect fit

Table 49: Results of K-S-test for seasonal wet/dry SERIES distribution for observed data

Season	Wet/dry	N	K-S	p-value	Assessment
DJF	wet	12	0.030	1.0000	Perfect fit
DJF	dry	12	0.193	0.7751	Perfect fit
MAM	wet	12	0.034	1.0000	Perfect fit
MAM	dry	12	0.175	0.8366	Perfect fit
JJA	wet	12	0.000	1.0000	Perfect fit
JJA	dry	12	1.000	0.0000	Very poor fit
SON	wet	12	0.070	1.0000	Very good fit
SON	dry	12	0.135	0.9761	Perfect fit

Table 50: Results of KS-test for daily RAIN distributions for AgMERRA data

Month	N	K-S	p-value	Assessment
J	12	0.073	1.0000	Perfect fit
F	12	0.068	1.0000	Perfect fit
M	12	0.121	0.9929	Perfect fit
A	12	0.099	0.9997	Perfect fit
M	12	0.206	0.6609	Good fit
J	12	0.261	0.3593	Very poor fit
J	12	0.566	0.0006	Very poor fit
A	12	0.348	0.0955	Very poor fit
S	12	0.305	0.1932	Very poor fit
O	12	0.092	1.0000	Perfect fit
N	12	0.170	0.8611	Perfect fit
D	12	0.068	1.0000	Perfect fit

Table 51: Results of KS-test for daily RAIN distributions for station observed data

Month	N	K-S	p-value	Assessment
J	12	0.132	0.9809	Perfect fit
F	12	0.052	1.0000	Perfect fit
M	12	0.055	1.0000	Perfect fit
A	12	0.098	0.9997	Perfect fit
M	12	0.348	0.0955	Very poor fit
J	12	0.000	1.0000	Perfect fit
J			ND	
A			ND	
S	12	0.217	0.5954	Good fit
O	12	0.523	0.3975	Perfect fit
N	12	0.040	1.0000	Perfect fit
D	12	0.055	1.0000	Perfect fit

ND: Not determined

Table 52: Results of KS-test for daily Tmin distributions for AgMERRA data

Month	N	K-S	p-value	Assessment
J	12	0.053	1.0000	Perfect fit
F	12	0.106	0.9989	Perfect fit
M	12	0.106	0.9989	Perfect fit
A	12	0.053	1.0000	Perfect fit
M	12	0.106	0.9989	Perfect fit
J	12	0.106	0.9989	Perfect fit
J	12	0.053	1.0000	Perfect fit
A	12	0.053	1.0000	Perfect fit
S	12	0.106	0.9989	Perfect fit
O	12	0.106	0.9989	Perfect fit
N	12	0.053	1.0000	Perfect fit
D	12	0.106	0.9989	Perfect fit

Table 53: Results of KS-test for daily Tmax distributions for AgMERRA data

Month	N	K-S	p-value	Assessment
J	12	0.053	1.0000	Perfect fit
F	12	0.053	1.0000	Perfect fit
M	12	0.053	1.0000	Perfect fit
A	12	0.106	0.9989	Perfect fit
M	12	0.158	0.9125	Perfect fit
J	12	0.158	0.9125	Perfect fit
J	12	0.106	0.9989	Perfect fit
A	12	0.106	0.9989	Perfect fit
S	12	0.106	0.9989	Perfect fit
O	12	0.106	0.9989	Perfect fit
N	12	0.053	1.0000	Perfect fit
D	12	0.106	0.9989	Perfect fit

Table 54: Results of KS-test for daily Tmin distributions for station observed data

Month	N	K-S	p-value	Assessment
J	12	0.053	1.0000	Perfect fit
F	12	0.053	1.0000	Perfect fit
M	12	0.105	0.9991	Perfect fit
A	12	0.106	0.9989	Perfect fit
M	12	0.106	0.9989	Perfect fit
J	12	0.106	0.9989	Perfect fit
J	12	0.053	1.0000	Perfect fit
A	12	0.106	0.9989	Perfect fit
S	12	0.106	0.9989	Perfect fit
O	12	0.106	0.9125	Perfect fit
N	12	0.106	0.9989	Perfect fit
D	12	0.053	1.0000	Perfect fit

Table 55: Results of KS-test for daily Tmax distributions for station observed data

Month	N	K-S	p-value	Assessment
J	12	0.053	1.0000	Perfect fit
F	12	0.053	1.0000	Perfect fit
M	12	0.106	0.9989	Perfect fit
A	12	0.053	1.0000	Perfect fit
M	12	0.106	0.9989	Perfect fit
J	12	0.106	0.9991	Perfect fit
J	12	0.106	1.0000	Perfect fit
A	12	0.106	0.9125	Perfect fit
S	12	0.106	0.9989	Perfect fit
O	12	0.106	0.9989	Perfect fit
N	12	0.106	09989	Perfect fit
D	12	0.105	0.9991	Perfect fit

4.4.2 KS-test for seasonal frost and heat spells distributions: Effective N, KS statistic, and p-value at Mount Makulu

The seasonal frost and heat spells distributions and the statistical values are presented in Table 56. As shown in Table 56, Mount Makulu did not experience any seasonal frost. However, the site experienced heat stress during DJF, MAM, JJ, and SON with probabilities of 0.0110, 0.0786, 0.2522, and 0.9995 for AgMERRA reanalysis and 0.7833, 0.0010, 0.0596 and 0.9761 for Observed, respectively at $p<0.05$. The results indicate that there were a much higher heat spell events during DJF and SON at Mount Makulu. The warming of the climate can have consequences corresponding to percentage changes in the occurrence of climate extremes that include increased probability of observed heat extremes (Lewis and King, 2017).

Table 56: Results of KS-test for seasonal frost and heat spells distributions at Mount Makulu

AgMERRA Reanalysis data				
Months	Frost/heat spells	Degree of freedom	KS-value	p-value
DJF	No frost spells	-	-	-
DJF	heat	12	0.455	0.0110
MAM	No frost spells	-	-	-
MAM	heat	12	0.359	0.0786
JJA	No frost spells	-	-	-
JJA	heat	12	0.287	0.2522
SON	No frost spells	-	-	-
SON	heat	12	0.101	0.9995
Observed station data				
Months	Frost/heat spells	Degree of freedom	KS-value	p-value
DJF	No frost spells	-	-	-
DJF	heat	12	0.185	0.7833
MAM	No frost spells	-	-	-
MAM	heat	12	0.550	0.0010
JJA	No frost spells	-	-	-
JJA	heat	12	0.374	0.0596
SON	No frost spells	-	-	-
SON	heat	12	0.135	0.9761

4.4.3 Monthly means and standard deviations for precipitation, maximum and minimum temperature

Comparison between the monthly mean and standard deviation of precipitation and temperature for the two data sets used in the analysis are presented in Figures 22 and 23. The results showed the very good performance of LARS-WG in fitting the monthly means of precipitation, maximum (Tmax) and minimum (Tmin) temperature statistics. LARS-WG well modeled the mean monthly totals of precipitation, minimum and maximum temperature. This shows that the LARS-WG was highly capable of reproducing precipitation, maximum and minimum temperature values from daily time series for Mount Makulu. In a similar study where LARS-WG was used, Semenov et al. (1998) were able to reproduce the monthly means of maximum and minimum temperature accurately.

Results from statistical tests indicate that there was no significant difference in simulated monthly precipitation compared to the observations. Researchers such as Hassan et al. (2014) and Hassan and Harun (2013) indicated that downscaling of precipitation was more complicated and challenging to obtain a good agreement

between observed and generated values compared to downscaling of temperature. This was due to the conditional process which depended on intermediate processes within the rainfall process such as an occurrence of humidity, cloud cover, and wet-days. One of the challenges weather generators face was how well to simulate interannual variability (Qian et al., 2004). The monthly means of precipitation and minimum and maximum temperature values were generated accurately by LARS-WG, giving correlation coefficients and coefficient of determinants equal to the unit, respectively (Figure 10). The R^2 for the mean monthly precipitation, minimum, and maximum temperature had a strong linear relationship between observed/AgMERRA and synthetic data as presented in Figure 10.

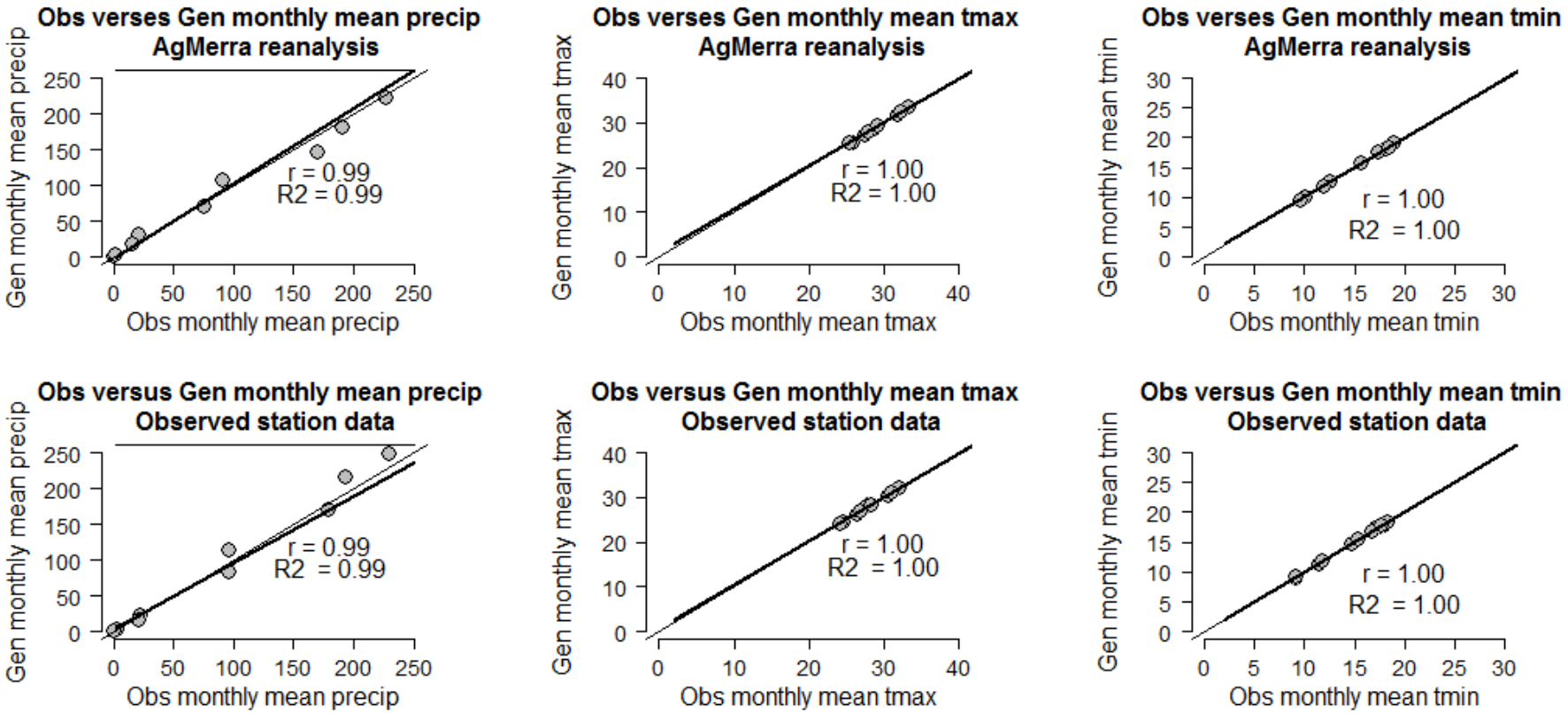

Figure 10: Results of monthly mean observed versus precipitation, maximum and minimum temperature (AgMERRA reanalysis and Observed station data)

Regarding standard deviation, LARS-WG showed excellent performance for precipitation for all the months except February (over-estimated the standard deviation) and November (under-estimated the standard deviation). Qian et al. (2004) observed that the means and variances of daily synthetic weather data are supposed to be non-significantly different from those calculated from the observed time series. It is also important that synthetic weather series follows a probability distribution which is not statistically different from the observed time series. The temperature monthly standard deviations of the generated values were under-estimated for both data sets (Observed station and AgMERRA reanalysis data) by the model, and this is its shortcoming (Figure 11). Similar results have been reported by Semenov et al. (1998) and Semenov and Brooks (1999).

A study by Semenov et al. (1998) testing LARS-WG using 18 sites worldwide under-estimated the generated monthly standard deviation of the temperature compared to the observed values. The means and standard deviation of the normal vary daily, and these parameters are obtained by fitting Fourier series to the means and standard deviations of the observed values throughout the year. The daily maximum and minimum temperatures are stochastic processes with standard deviations and daily means conditioned on the wet/dry status of the day (Semenov et al., 1998). The LARS-WG should be evaluated to ensure that the data that it produces is satisfactory for the purposes for which its output is to be used. The required accuracy depends on the application of the generated current, and future scenarios and its performance would vary considerably under diverse climatic conditions.

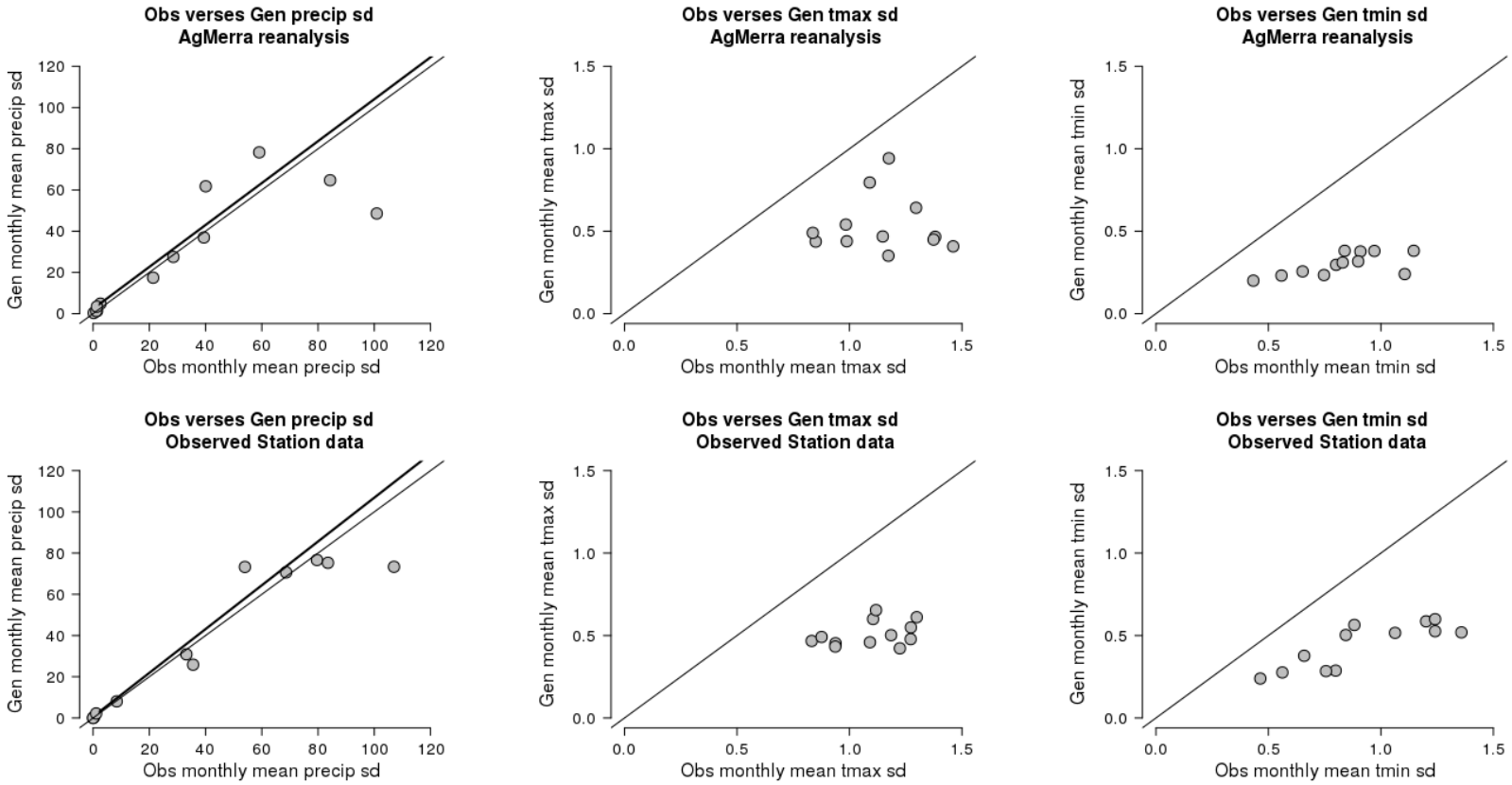

Figure 11: Results of Obs versus Gen precipitation sd, Tmax sd and Tmin sd (AgMERRA reanalysis and Observed station data)

4.4.4 Future climate scenarios for precipitation and temperature

The HadCM3 and BCCR-BCM2 GCMs under B1 and A1B scenarios in LARS-WG v5.5 were used in this study to generate future climate scenarios to better deal with uncertainties. Results for the observed station (1981-2010) and AgMERRA reanalysis (1981-2010) data indicated that the baseline had total annual precipitation of 841.2 mm/year in 64.5 days and total precipitation of 748.1 mm/year in 81.5 days, respectively. Computed mean ensemble outputs for SRB1 and SRA1B indicates that in 2020 and 2055, the number of days with precipitation would increase by 0.5-1.5 and 4-4.5 days under the observed station and AgMERRA data, respectively. The difference in the number of days and precipitation amounts is due to missing data in the observed station data. The outputs from observed station data indicated that the number of days with precipitation and the amount of precipitation per year would reduce relative to the baseline. The mean amounts of precipitation would increase by 1.67%, 0.31% under SRB1 (2020), SRB1 (2055), respectively. Under the AgMERRA reanalysis data, results showed an increase in the mean amount of precipitation by 5.28%, 3.28%, 4.9% and 1.78% under SRA1B (2020), SRB1 (2020), SRA1B (2055) and SRB1 (2055), respectively. In the future, Mount Makulu would experience longer annual rainfall days, and this finding is not in agreement with the findings by Phiri et al. (2013) and UNDP (2010). Declining rainfall pattern has been observed largely in western parts of AERII of Zambia which has experienced a higher frequency of climate extreme events such as flash floods and droughts. This has negatively affected the growing season. Furthermore, Jaggard et al. (2010) projected that rainfall change over sub-Saharan Africa in the mid-century would be uncertain.

Using the observed station data, simulation indicated that temperature would increase in 2020 (0.57^{o}C [SRB1], 0.61^{o}C [SRA1B]) and 2055 (1.50^{o}C [SRB1], 1.84^{o}C [SRA1B]) relative to the baseline. Similarly, the simulated temperatures using AgMERRA data indicated that temperature would increase in 2020 (0.54^{o}C [SRB1], 0.59^{o}C [SRA1B]) and 2055 (1.48^{o}C [SRB1], 1.84^{o}C [SRA1B]). The projected temperature changes under A1B and B1 for Mount Makulu are within the threshold projected by IPCC (1.4-6.4^{o}C [A1B] and 1.1-2.9^{o}C [B1]) (Nakicenovic et al., 2000; Shamsnia and Pirmoradian, 2013).

The multi-model ensemble for the HadCM3 and BCM2 GCMs indicated that climate

signal for precipitation amount in 2020 and 2055 would increase under observed station data (SRB1) and AgMERRA reanalysis data (SRB1, SRA1B). According to the National Climate Assessment (NCA, 2010), multi-model ensembles and model inter-comparison projects (MIP) are used to assess uncertainties in future climate and climate impacts. Uncertainty in GCM outputs determines the range of possible generated future scenarios (Table 57). The multi-ensembles approach using different climate models and emission scenarios enables a move towards a complete assessment of uncertainty in future climate projections (UNFCCC, 2012).

The CI95 of the future climate scenarios for precipitation and temperature were computed for the two data sets. The CI95 shows values at the upper and lower end. The CI95 and time series for precipitation and temperature are presented in Table 57, Figure 12 and Figure 13, respectively. Semenov et al. (1998) indicated that it was vital for the synthetic data to be similar to the observed data on average and the distribution of the whole data set to be similar across their whole range. It is worth mentioning that the means of future synthetic precipitation computed under both scenarios (SRA1B and SRB1) lay within the CI95 of the observed/AgMERRA values. It canbe concluded that the statistics were simulated successfully for Mount Makulu. On the other hand, the means of synthetic annual temperature under the 2020s (SRA1B, SRB1) and 2055s (SRA1B, SRB1) scenarios lay outside the CI95 of the baseline. This means that the climate would be warmer in 2020 and 2055 relative to the baseline.

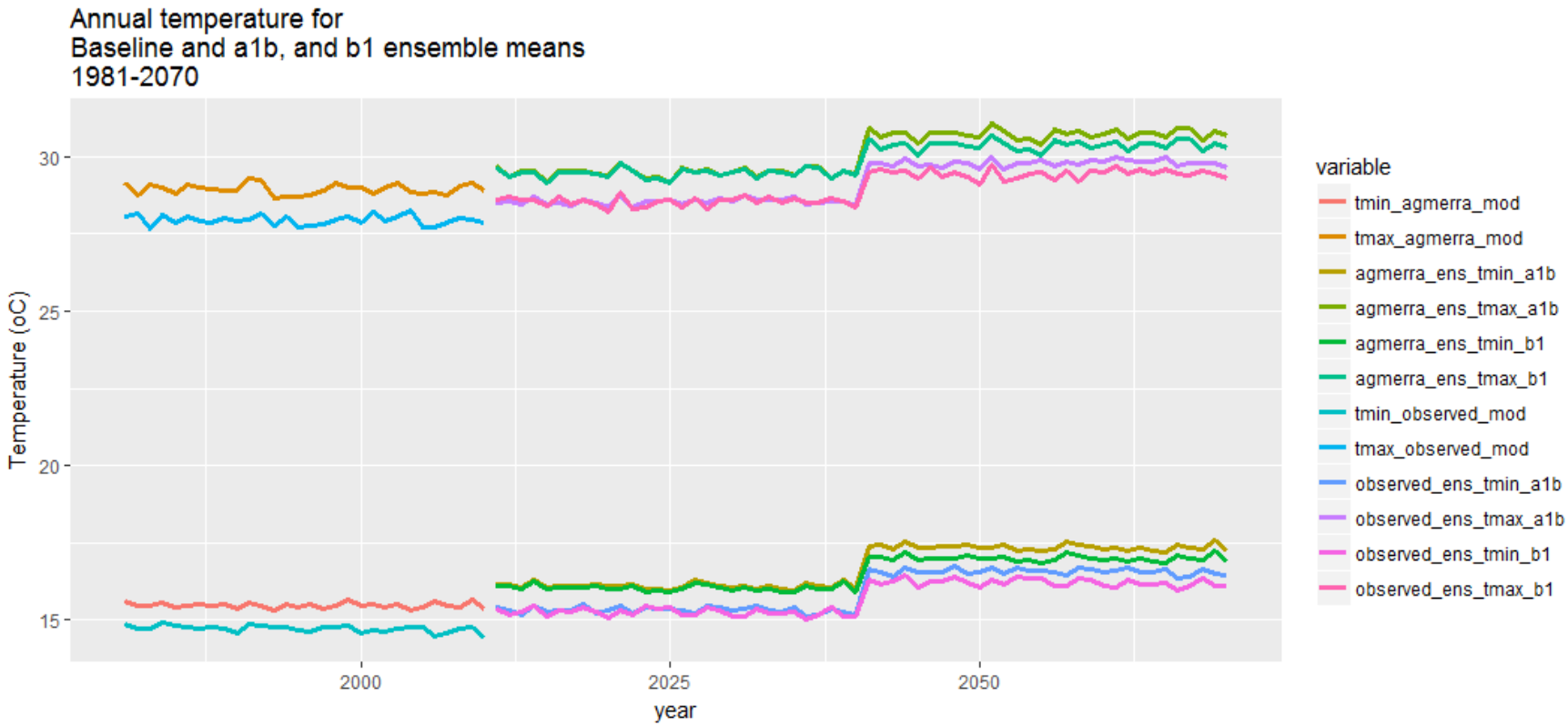

Figure 12: Simulated baseline and future annual temperature (ºC)

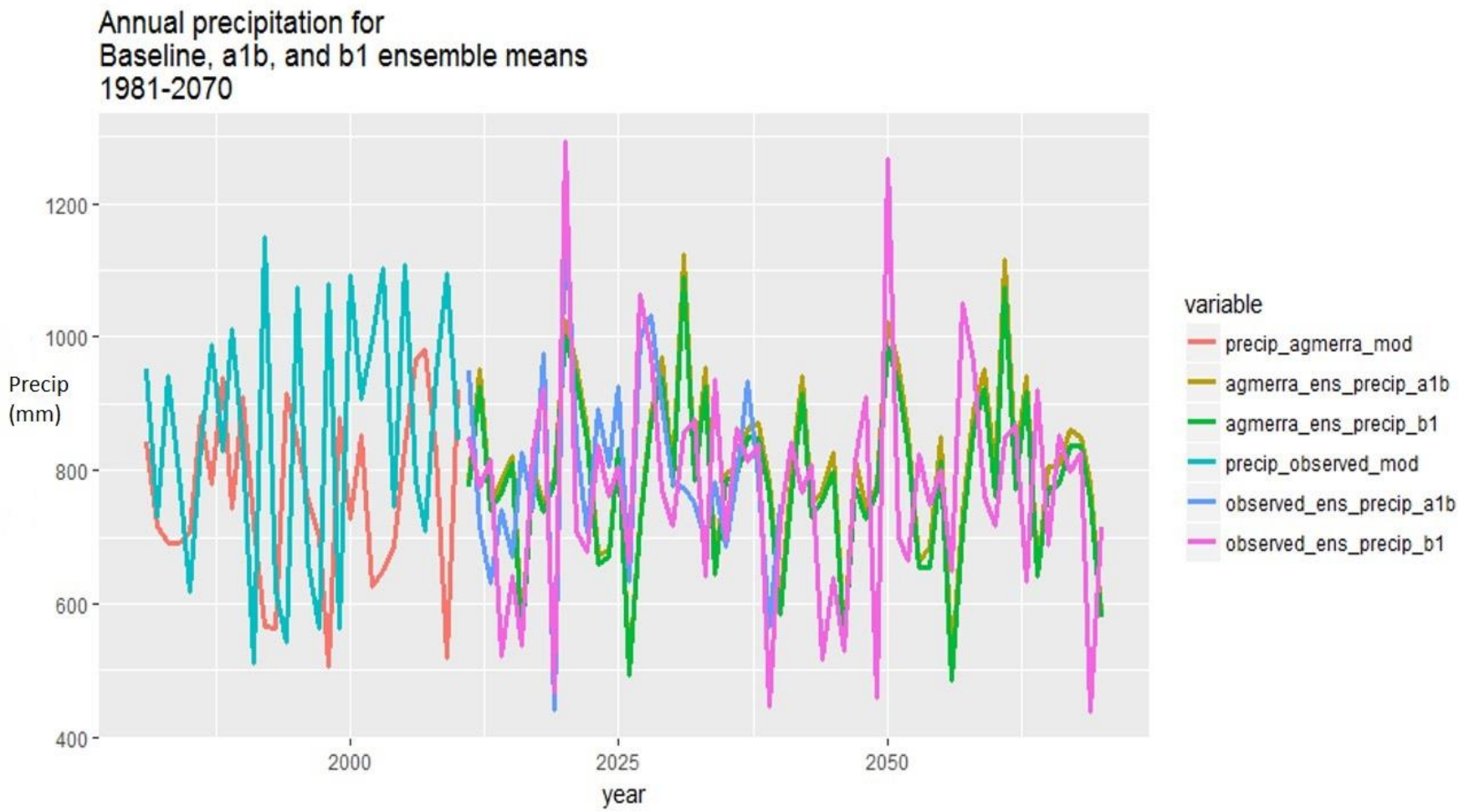

Figure 13: Simulated baseline and future precipitation (mm)

Table 57: Confidence interval for simulated precipitation (mm) and temperature (°C) for the observed and AgMERRA baseline and future scenarios (SRA1B and SRB1)

Baseline scenario						
	Observed			AgMERRA		
	mean	lower	upper	mean	lower	upper
1981-2010						
Tmin	14.72	14.68	14.76	15.47	15.44	15.51
Tmax	27.94	27.88	27.99	28.94	28.88	29.01
Tmean	21.33	21.28	21.38	22.21	22.16	22.26
Precip	854.50	781.60	927.50	764.60	715.00	814.30
Observed scenario						
	a1b ensemble			b1 ensemble		
	mean	lower	upper	mean	lower	upper
2011-2040						
Tmin	15.33	15.29	15.36	15.26	15.21	15.30
Tmax	28.54	28.50	28.58	28.53	28.48	28.59
Tmean	21.94	21.90	21.97	21.90	21.85	21.95
Precip	797.70	741.00	854.40	777.40	712.30	842.50
2041-2070						
Tmin	16.57	16.54	16.61	16.21	16.17	16.26
Tmax	29.79	29.75	29.75	29.44	29.39	29.50
Tmean	23.18	23.15	23.18	22.83	22.78	22.88
Precip	801.60	744.20	859.00	767.00	703.00	831.00
AgMERRA scenario						
	a1b ensemble			b1 ensemble		
	mean	lower	upper	mean	lower	upper
2011-2040						
Tmin	16.10	16.07	16.14	16.04	16.00	16.07
Tmax	29.49	29.43	29.54	29.46	29.40	29.51
Tmean	22.80	22.75	22.84	22.75	22.70	22.79
Precip	805.00	754.90	855.20	789.70	741.10	838.20
2041-2070						
Tmin	17.36	17.32	17.39	17.00	16.97	17.04
Tmax	30.73	30.67	30.78	30.37	30.31	30.42
Tmean	24.05	24.00	24.09	23.69	23.64	23.73
Precip	802.30	752.40	852.20	778.20	730.50	825.90

4.5 Changes in selected ET-SCI climate indices on temperature and precipitation extremes for Mount Makulu, Zambia

4.5.1 Precipitation and temperature anomalies and trends

The annual time series and trends for precipitation and temperature are presented in Figure 14 and Figure 15. The annual Tmin, Tmax, Tmean and precipitation for Mount Makulu were 14.65^{o}C, 27.53^{o}C, 21.10^{o}C and 828.53 mm from 1963-2012, respectively. The tau and p-value associated with the Mann-Kendall test for precipitation (tau = 0.0743, 2-sided p-value = 0.45155, Sen's Slope = 1.25) and minimum temperature (tau = 0.128, 2-sided p-value =0.19192, Sen's slope = 0.01) were statistically non-significant (Figure 15 a and b). This indicated that the minimum temperature had not increased significantly. In contrast, the p-value associated with the Mann-Kendall test was statistically significant for annual mean (tau = 0.402, 2-sided p-value =3.8624e-05) and maximum (tau = 0.504, 2-sided p-value =2.3842e-07) temperature, respectively. This suggested that the mean and maximum temperature exhibited the presence of a statistically significant upward trend (Figure 15 c and d) with Sen's slopes of 0.025 and 0.037, respectively. The mean temperature anomaly also shows an increasing trend and is statistically significant (tau = 0.402, 2-sided p-value =3.8624e-05, Sen's slope = 0.03) at $p<0.05$.

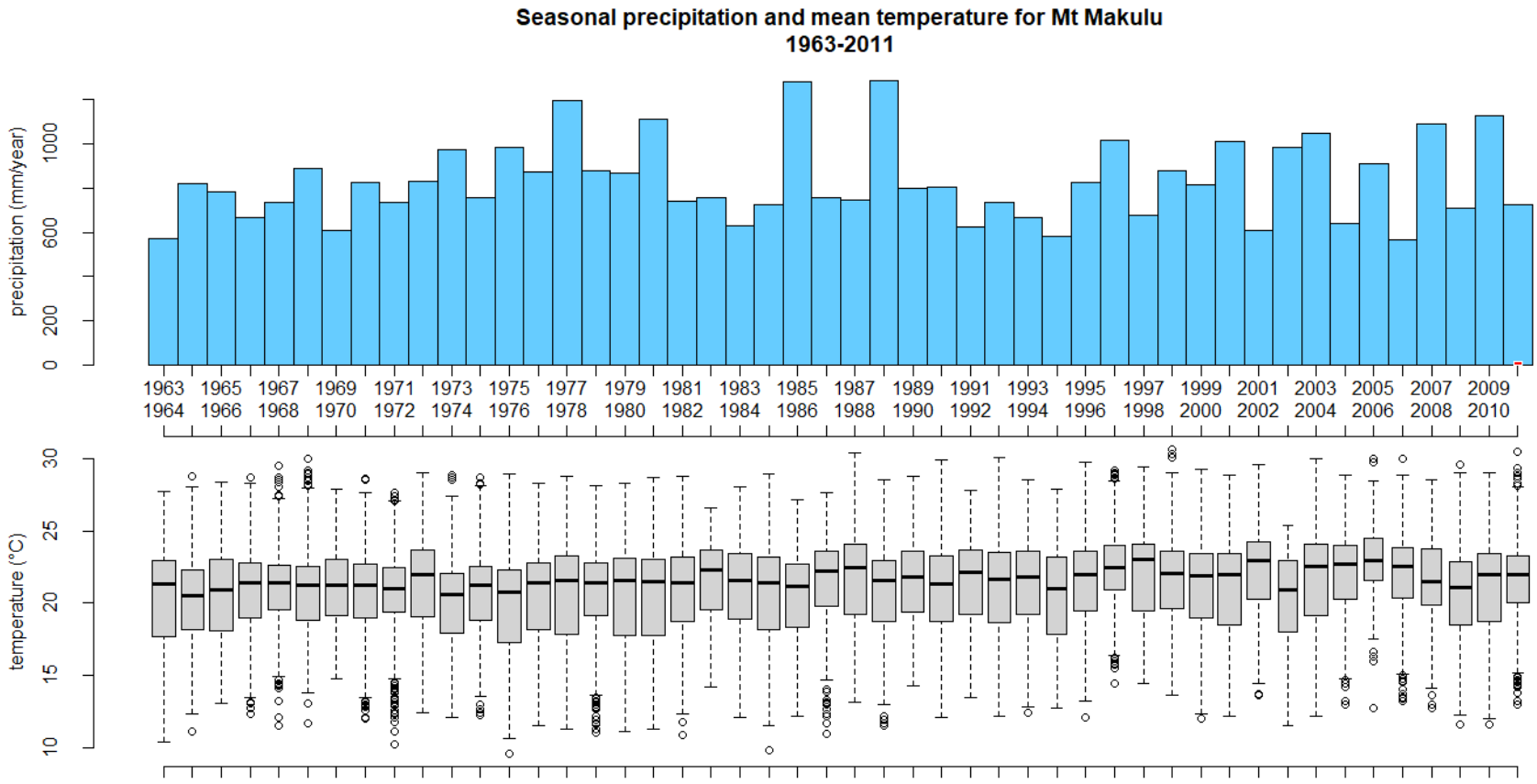

Figure 14: Seasonal precipitation and mean temperature for Mount Makulu

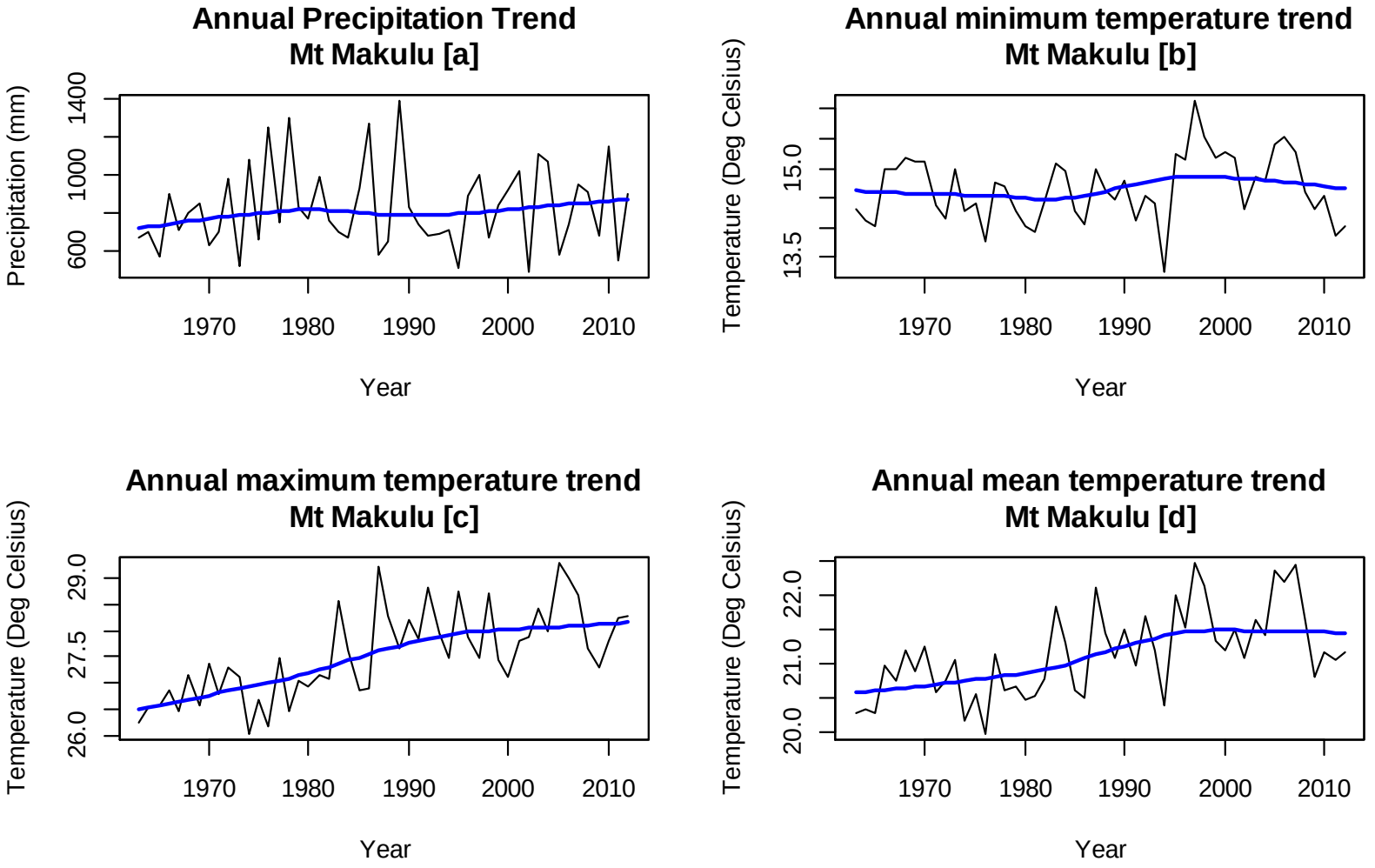

Figure 15: Observed annual precipitation (mm) and temperature (^{o}C) trends for Mount Makulu

4.5.2 Trend analysis of temperature and precipitation

The results of the trend analysis of temperature and precipitation using the ClimPACT2 software are presented in Table 58 and Table 59. The results on Agriculture and Food Security, Water Resources, and Hydrology and Health sector indices showed significant trends and exhibited significant changes on percentile based indices, absolute indices of annual maximum and minimum values, duration indices and Standardized Precipitation-Evapotranspiration Index (SPEI). The SPI index was non-significant witha slope of 0.000. The SPI value is the number of standard deviations by which the observed anomaly deviates from the long-term mean (Guenang and Kamga, 2014). Negative and positive SPI values represent rainfall deficit and surplus, respectively. Drought monitoring indices are usually applied at seasonal (6 months), annual (12 months) or even inter-annual (24 or 48 months) time-scales (Meza, 2013). The lack of high-quality analyses and credible data has been a significant obstacle to assessing changes in extreme weather events (Zhang et al., 2011).

4.5.3 Percentile-based indices

Percentile-based climate extreme indices were calculated using the baseline reference period of 1963-2012 to make results easily comparable with those from other studie, and the results are presented in Table 58 and Table 59. The fraction of days with above average temperature (TXGT50p) or the percentage of days where TX > 50th percentile significantly increased for both annual and monthly analysis from 1963-2012. The monthly and annual TX10p (amount of cool days) had been decreasing significantly with a negative trend. On the other hand, the monthly and annual TX90p (amount of hot days) and TN90p (amount of warm nights [annual]) had increased at the 90th percentile. The daily very warm days (TX95t) had also increased significantly. The analysis indicated that TX10p, TX90p, TN90p, and TX95t had increased in magnitude. In contrast, the TN10p (annual and monthly) was non-significant.

The R95pTOT (monthly and annual) and R99pTOT (monthly and annual) were non-significant with a positive trend. The lack of trend in precipitation time series data does not support the conclusion that annual rainfall in Zambia has decreased by 1.9 mm per month (2.3% per decade) since 1960 mainly in December, January and February (MTENR, 2010; UN, 2012). The authors did not state the statistical significance level

they used when making this conclusion. Akinbile et al. (2015) also found a non-significant trend in several rainfall indices derived from daily precipitation using meteorological stations in Zimbabwe.

Heatwave amplitude (HWA) as defined by either the EHF, 90th percentile of TX or the 90th percentile of TN increased significantly ($p = 0.035$). This signified that the peak daily value in the hottest heatwave (defined as the heatwave with highest HWM) increased from 1963 to 2012. Heatwave number (HWN) as defined by the Excess Heat Factor (EHF), the 90th percentile of TX or the 90th percentile of TN also increased, the mean annual temperature being 17.30^{o}C. This indicated that the number of individual heatwaves that occurred at Mount Makulu during summer (November – March in the southern hemisphere) increased. Heatwave frequency (HWF-EHF) defined by Excess Heat Factor (EHF) and heatwave frequency (HWF-Tx90) defined by the 90th percentile of TX had increased significantly at $p<0.05$. This meant that the number of days contributing to heatwave events had increased significantly. The results showed that the number of days (frequency) that contributed to heatwaves as identified by HWN had also increased. Heatwave number (HWN-Tx90) defined by the number of discrete heatwave events had increased significantly at $p<0.05$. The cold-wave number (CWN-ECF) and cold-wave frequency (CWF-ECF) had reduced significantly with negative trends.

Heat stress is the leading weather-related killer in the United States of America (NCA, 2014). Evidence-based studies indicate that the human-induced climate change had already doubled the probability of extreme heat events (NCA, 2014) and these agree with the findings of this study. Steffen et al. (2014) acknowledged that heatwave impacts are widespread and severe, human damage health, infrastructure, and natural ecosystems and decrease workplace performance and agricultural productivity. Additionally, the direct effect of excessive heat is through damaging the reproductive parts of crops responsible for producing grain and thus, reducing grain yield.

4.5.4 Absolute indices represented by temperature values

The monthly and annual maximum warmest daily temperature (TXx) had increased by 0.004^{o}C and 0.053^{o}C at Mount Makulu (Table 58 and Table 59), respectively. The annual warmest daily TN (TNx) and coldest daily TX (TXn) had increased by 0.016^{o}C

and 0.030°C, respectively. The annual number of days when the maximum temperature was at least 30°C or 35°C also increased by 1.041 and 0.266 days, respectively. The mean annual and monthly difference between daily TX and daily TN (DTR) significantly increased by 0.003°C and 0.031°C, respectively. This result is indicative that the monthly mean difference between the maximum and the minimum temperature had increased at Mount Makulu. Similarly, the mean daily temperature (TMm) and mean daily maximum temperature (TXm) had increased by 0.025°C and 0.037°C, respectively. The warming tendencies are the result of Tmax and Tmean increase. The annual and monthly minimum coldest daily temperature (TNn) was non-significant with slopes of 0.013 and 0.001, respectively. An increase in maximum (Phiri et al., 2013) and mean (Suman, 2007) temperature have been observed in AERII from 1950-2008. NCA (2014) agree with the findings of this study that extreme heat is becoming more common.

Extreme temperatures increase plant water stress, which, if not addressed, results in cessation of photosynthesis and possibly death (Steffen et al., 2014). Furthermore, there is a negative response to global maize yields due to increased temperatures. Changes in extreme weather events are the primary means by which most people experience climate change. Human-induced climate change has already increased the number and strength of some of these extreme events (NCA, 2014). The past, present and future climate impacts as reported by Mahlstein et al. (2015) could be documented and adaptation and mitigation options adopted by policy-and-decision makers.

4.5.5 Threshold indices

The number of days when TX > 25°C (SU) for both annual and monthly trend had increased significantly at $p<0.05$ with a slope of 0.009 and 1.204, respectively (Table 58 and Table 59). This result indicated an increase in the month and an annual number of days when the maximum air temperature was higher than 25°C. The annual occurrence of tropical nights (TR) was non-significant with positive trends. This means TR in which temperatures do not fall below 20°C are not on the rise at Mount Makulu as the climate changes. Mount Makulu did not experience any seasonal frost (FD) and ice days (ID) from 1963-2012. The R20mm was non-significant with positive trends. Climate extreme indices assist in describing the past, present, and future climate change scenarios (Mahlstein et al., 2015). They have been used for a long time

by assessing days with temperature or precipitation observations are above or below specific physically-based thresholds (Zhang et al., 2011). They are closely related to possible impacts and are, therefore, more illustrative to planners, researchers and policy-makers than climate means. Climate indices are widely used across sectors, and have become important impact parameters in climate change studies and impact assessment.

4.5.6 Duration indices

Duration indices define periods of excessive warmth, cold, wetness/dryness, and growing season length. Annual GSL, WSDI, CDD, and CWD were not significant with slopes of 0.003, 0.113, 0.403 and -0.01 at $p<0.05$ (Table 58 and Table 59). The GDDgrow and CDDcold22 had increased by 3.789 degree-days from 1963-2012.

4.5.7 Other indices

Meteorological, agricultural, and hydrological drought incidences are often presented as drought indices. Drought occurrence as measured by the SPEI on time scales of 3, 6 and 12 months are presented in Table 58 and Table 59. There is little differences between SPEI and SPI (Stagge et al., 2014; Vicente-Serrano et al., 2010). The SPEI is designed to take into account both precipitation and potential evapotranspiration (PET) in determining drought. The computed SPEI results indicated significant ($p<0.05$) changes in annual trends with linear slopes of -0.002, -0.001 and -0.001 for time-scales of 3, 6 and 12 months, respectively. Mount Makulu had experienced a near normal drought condition (Abdullah, 2014).

Table 58: Computed annual trends of the extreme indices of daily temperature and precipitation for Mount Makulu

	Indices	StartYr	EndYr	Slope	slope STD	P	Sign		Indices	StartYr	EndYr	Slope	slope STD	P	Sign
1	cdd (A)	1963	2012	0.403	0.302	0.188	+	46	rx5day (A)	1963	2012	-0.256	0.447	0.570	+
2	cdd (M)	1963	2012	0.007	0.18	0.7	+	47	rx5day (M)	1963	2012	0.005	0.044	0.665	+
3	cddcold22 (A)	1963	2012	3.789	0.931	0.000	***	48	sdii (A)	1963	2012	0.036	0.024	0.135	+
4	csdi (A)	1963	2012	-0.029	0.041	0.478	-	49	spei.12.month	1963	2012	-0.001	0.000	0.000	***
5	csdi5	1963	2012	-0.01	0.049	0.833	-	50	spei.3.month	1963	2012	-0.002	0.000	0.000	***
6	CWA-ECF	1963	2012	0.082	0.049	0.104	+	51	spei.6.month	1963	2012	-0.001	0.000	0.000	***
7	cwd (A)	1963	2012	-0.01	0.03	0.73	-	52	spi.12.month	1963	2012	0.001	0.000	0.048	+
8	CWF-ECF	1963	2012	-0.205	0.093	0.032	**	53	spi.3.month	1963	2012	0.000	0.000	0.826	+
9	CWM-ECF	1963	2012	0.005	0.019	0.802	+	54	spi.6.month	1963	2012	0.000	0.000	0.262	+
10	CWN-ECF	1963	2012	-0.031	0.014	0.037	**	55	su (A)	1963	2012	0.009	0.002	0.000	***
11	dtr (A)	1963	2012	0.03	0.007	0.000	***	56	su (M)	1963	2012	1.141	0.246	0.000	***
12	dtr (M)	1963	2012	0.003	0.001	0.000	***	57	tmm (A)	1963	2012	0.023	0.005	0.000	***
13	gddgrow22 (A)	1963	2012	3.789	0.931	0.000	***	58	tmm (M)	1963	2012	0.002	0.001	0.003	***
14	gsl (A)	1963	2012	0.003	0.006	0.646	+	59	tn10p (A)	1963	2012	-0.049	0.051	0.336	-
15	hddheat15	1963	2012	-0.453	0.207	0.036	-	60	tn10p (M)	1963	2012	-0.001	0.002	0.583	-
16	HWA-EHF	1963	2012	0.127	0.081	0.127	+	61	tn90p (A)	1963	2012	0.150	0.56	0.011	***
17	HWA-Tn90	1963	2012	0.044	0.028	0.133	+	62	tn90p (M)	1963	2012	0.010	0.002	0.000	***
18	HWA-Tn90	1963	2012	0.008	0.018	0.676	+	63	tnm (A)	1963	2012	0.008	0.005	0.165	+
19	HWA-Tx90	1963	2012	0.066	0.03	0.037	**	64	tnm (M)	1963	2012	0.001	0.001	0.470	+
20	HWD-EHF	1963	2012	0.072	0.041	0.087	+	65	tnn (A)	1963	2012	0.013	0.017	0.440	+
21	HWD-Tx90	1963	2012	0.036	0.024	0.144	+	66	tnn (M)	1963	2012	0.001	0.001	0.635	+
22	HWD-Tn90	1963	2012	0.008	0.018	0.676	+	67	tnx (A)	1963	2012	0.016	0.01.	0.128	+
23	HWF-EHF	1963	2012	0.164	0.071	0.025	**	68	tnx (M)	1963	2012	0.001	0.001	0.026	**
24	HWF-Tn90	1963	2012	-0.002	0.049	0.970	-	69	tr (A)	1963	2012	0.000	0.001	0.620	+
25	HWF-Tx90	1963	2012	0.245	0.07	0.001	***	70	tr (M)	1963	2012	0.052	0.066	0.430	+
26	HWM-EHF	1963	2012	0.029	0.028	0.319	+	71	tx10p (A)	1963	2012	-0.236	0.045	0.000	***
27	HWM-Tn90	1963	2012	0.014	0.019	0.465	+	72	tx10p (M)	1963	2012	-0.020	0.002	0.000	***
28	HWM-Tx90	1963	2012	0.032	0.021	0.144	+	73	tx90p (A)	1963	2012	0.210	0.079	0.012	***

Note: A: annual; M: monthly; P: p-value; sign: significant; indices in bold were significant

Table 59: Computed annual trends of the extreme indices of daily temperature and precipitation for Mount Makulu

	Indices	StartYr	EndYr	Slope	slope STD	P	Sign		Indices	StartYr	EndYr	Slope	slope STD	P	Sign
29	HWN-EHF	1963	2012	0.025	0.012	0.052	+	74	tx90p (M)	1963	2012	0.022	0.003	0.003	***
30	HWN-Tn90	1963	2012	-0.002	0.012	0.882	-	75	tx95t	1963	2012	0.011	0.001	0.000	***
31	HWN-Tx90	1963	2012	0.056	0.016	0.001	***	76	txge30 (A)	1963	2012	1.041	0.273	0.000	***
32	prcptot (A)	1963	2012	1.706	2.362	0.474	+	77	txge30 (M)	1963	2012	0.009	0.002	0.000	***
33	prcptot (M)	1963	2012	0.013	0.023	0.555	+	78	txge35 (A)	1963	2012	0.266	0.056	0.000	***
34	r10mm (A)	1963	2012	0.000	0.001	0.695	+	79	txge35 (M)	1963	2012	0.002	0.000	0.000	***
35	r10mm (M)	1963	2012	0.049	0.07	0.494	+	80	txgt50p (A)	1963	2012	0.652	0.126	0.000	***
36	r20mm (A)	1963	2012	0.000	0	0.491	+	81	txgt50p (M)	1963	2012	0.054	0.004	0.000	***
37	r20mm (M)	1963	2012	0.036	0.048	0.455	+	82	txm (A)	1963	2012	0.037	0.007	0.000	***
38	r30mm (A)	1963	2012	0.000	0	0.129	+	83	txm (M)	1963	2012	0.003	0.001	0.000	***
39	r30mm (M)	1963	2012	0.042	0.033	0.207	+	84	txn (A)	1963	2012	0.030	0.019	0.111	+
40	r95p (M)	1963	2012	1.928	1.398	0.175	+	85	txn (M)	1963	2012	0.003	0.001	0.000	***
41	r95ptot (M)	1963	2012	0.178	0.118	0.138	+	86	txx (A)	1963	2012	0.053	0.014	0.001	***
42	r99p (A)	1963	2012	0.106	0.898	0.907	+	87	txx (M)	1963	2012	0.004	0.001	0.000	***
43	r99ptot	1963	2012	0.010	0.083	0.900	+	88	wsdi (A)	1963	2012	0.113	0.110	0.309	+
44	rx1day (A)	1963	2012	-0.102	0.423	0.844	-	89	wsdi7 (A)	1963	2012	0.102	0.083	0.227	+
45	rx1day (M)	1963	2012	0.004	0.006	0.513	+								

Note: A: annual; M: monthly; P: p-value; sign: significant; indices in bold were significant

4.6 Impact of changes in precipitation and temperature on maize yield based on 5 CMIP5 GCMs under RCP4.5 and RCP8.5 for the 2050s

4.6.1 Climate change scenarios for temperature and precipitation

The baseline precipitation, solar radiation, maximum and minimum temperature are 797.96 mm, 20.80 MJ m^{-1} d^{-1}, 28.89ºC and 15.45ºC, respectively. Climate change is projected to increase temperatures and shift precipitation patterns. The simulated changes in annual precipitation, temperature and solar radiation using ensemblemean at Mount Makulu during the mid-century are presented in Table 60. Multi-model GCM ensemble projections have been recommended for climate change impact studies to take care of uncertainties embedded within GCMs (Araya et al., 2015). All GCMs show warming, while precipitation response is decidedly more variable and uncertain. Using the ensemble GCM mean, precipitation would reduce by 1.46% (RCP4.5) and 15.24% (RCP8.5). There is a large decrease in precipitation under the RCP8.5 scenario compared to RCP4.5 as shown in Figure 16. While all temperature changes are significant, the GCMs show non-significant precipitation changes, although three (CCSM4, HadGEM2-ES, MPI-ESM-LR) of the five selected GCMs show a strongly negative or positive change.

The simulated temperature ranges at the study site are suitable for growing maize as documented by Araya et al. (2015) and Cairns et al. (2013). Maize grows well at conditions between the mean temperature of 15 and 35ºC (Araya et al., 2015). Other studies reviewed (Crafts-Brandner and Salvucci, 2002) showed that maize net photosynthesis decreases at temperatures above 38ºC.

The PDF shapes for temperature follow the shapes of observed PDFs under both RCP4.5 and RCP8.5 (Figure 17) and agree with the findings of Boberg et al. (2009) and Masanganise et al. (2014). These researchers noted that the shapes of the model PDFs were in agreement with that of the observed PDFs. The PDFs for temperature shows a horizontal shifting relative to the baseline. This shows that the temperature would increase in 2050. The precipitation PDFs shows a vertical shift indicating a reduction in precipitation.

Table 60: Simulated annual climatic changes for precipitation (precip), maximum (Tmax) and minimum (Tmin) temperature, solar radiation (Srad) for the mid-century under RCP4.5 and RCP8.5 relative to the baseline data

	RCP4.5					RCP8.5				
GCM	precip		Tmax	Tmin	Srad	precip		Tmax	Tmin	Srad
	mm	%	^{o}C	^{o}C	MJ m^{-2} d^{-1}	mm	%	^{o}C	^{o}C	MJ m^{-2} d^{-1}
CCSM4	-46.70	-5.85	1.76	1.51	0.02	-56.98	-7.14	2.37	2.36	0.03
GFDL-ESM2M	0.26	0.03	1.73	1.66	0.00	-8.45	-1.06	2.14	2.06	0.03
HadGEM2-ES	48.27	6.04	2.36	2.28	0.03	68.53	8.59	3.09	3.01	0.03
MIROC5	-12.49	-1.56	1.99	1.58	0.02	-21.03	-2.63	2.56	2.41	0.03
MPI-ESM-LR	-47.56	-5.96	1.76	1.51	0.00	-58.27	-7.30	2.37	2.35	0.00
Ensemble mean	-11.63	-1.46	1.92	1.71	0.01	-15.24	-1.91	2.51	2.44	0.02

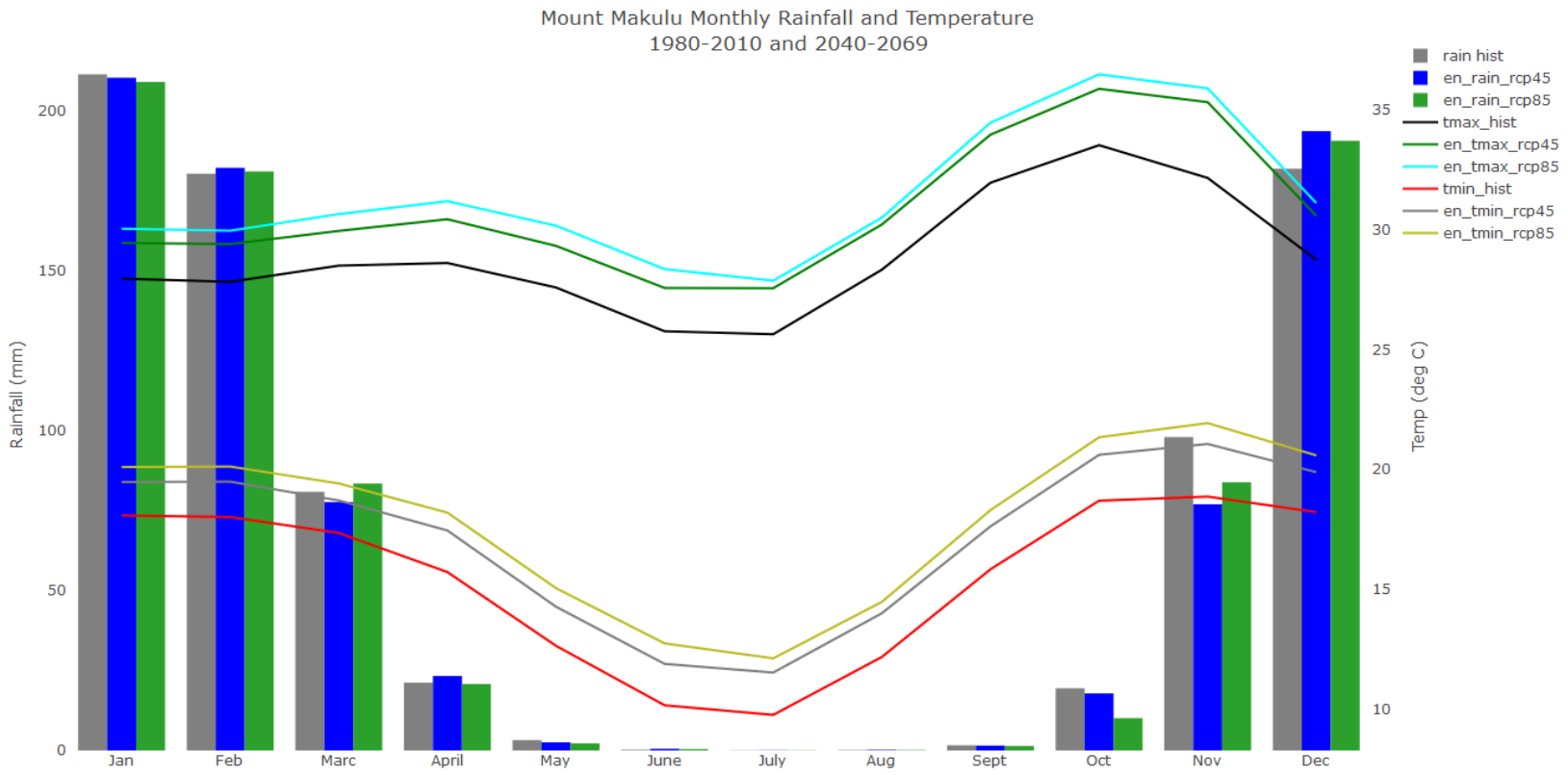

Figure 16: Monthly rainfall and temperature from 1980-2010 and 2040-2069 at Mount Makulu

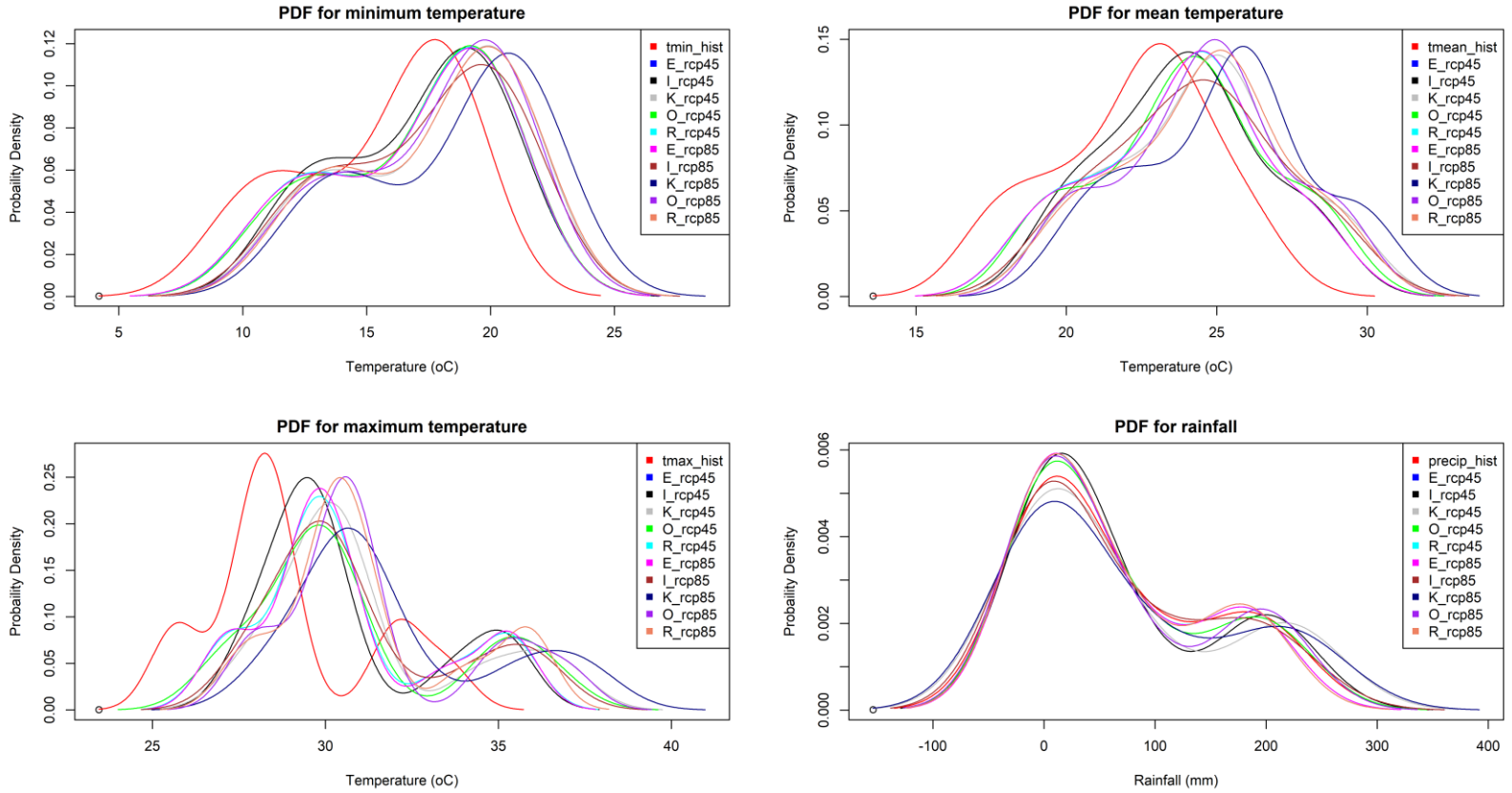

Figure 17: Comparison of observed and model PDFs for temperature (°C) and precipitation (mm) under RCP4.5 and RCP8.5

4.6.2 Projected impact of climate change on anthesis and maturity

The baseline simulated DAP at anthesis, and maturity using APSIM-Maize and CERES-Maize models were 63.57 - 65.77 days (anthesis), and 118.13 - 122.73 days (maturity) and 43.83 - 46.87 days (anthesis), and 99.17 - 104.50 days (maturity), respectively (Appendix 7 and Appendix 8). Using an ensemble mean of CSMs relative to the baseline, the percent DAP to anthesis (-11.28 to -9.39% [RCP4.5]; -14.28 to -12.65% [RCP8.5]) and maturity (-10.52 to -9.43% [RCP4.5]; -14.01 to -12.75% [RCP8.5]) would reduce in 2050. The CSMs simulated a reduced DAP to anthesis and maturity at all treatment levels which is attributed to climate change. As noted in this study, warmer climate speeds up crop development and thereby decreases DAP to anthesis and maturity. Results show that there are the higher percent change in the simulated DAP to anthesis, and maturity using CERES-Maize compared to APSIM-Maize model. PD affects the duration and timing of the vegetative and reproductive stages (Nape, 2011). As a result of this, small-holder farmers use different PDs to ensure crop yield success. Similarly, researchers like Adnan et al. (2017), Chen and Liu (2014), Lin et al. (2015) and Zhang et al. (2015) have reported a reduction in DAP to anthesis and maturity under future climate scenarios.

4.6.3 Projected impact of climate change on maize yield

4.6.3.1 Projected biomass and grain yield in 2050 relative to the baseline

The mean, standard deviation and coefficient of variation of the simulated grain yields for the baseline and future scenarios are presented in Table 61, Table 62, Table 63, Appendix 9, Appendix 10, Appendix 11, Appendix 12 and Appendix 13. Simulated percent changes in biomass and grain yield relative to the baseline using APSIM-Maize and CERES-Maize models for each GCM and RCP is provided in Appendix 14, Appendix 15, Appendix 16 and Appendix 17. The ensemble average results in lower inter-annual standard deviation than individual ensemble members. APSIM-Maize has higher standard deviations and CVs compared to CERES-Maize. Results of standard deviations show similar trends as the grain yield, and this suggests that variability normally scales with the means. Simulated future grain yield using CERES-Maize model was significant (PD[1-3]V1N1, PD[1-3]V3N1 [RCP4.5]) and very significant (PD[1-3]V3N1 [RCP4.5]), PD[1-3]V3N1 [RCP8.5]) as shown in Table 61. The grain yield reduced with delay in PD due to cooler

air temperature, lower solar radiation, and reduced precipitation. APSIM-Maize however, exhibited an increased risk of yield variability, and Guan et al. (2017) agree with the finding of this study. Adnan et al. (2017) reported reduced grain and biomass yield with delayed PD in northern Nigeria.

Table 61: Mean, median, sd and cv of grain yield (t/ha) for baseline, RCP4., and RCP8.5 at N1

	CERES-Maize				APSIM-Maize			
variable	Mean (t/ha)	sd	cv	Sign	Mean (t/ha)	sd	cv	Sign
pd1_v1n1_bs	5.40	0.52	9.71		5.69	0.91	16.03	
pd2_v1n1_bs	5.38	0.51	9.43		5.22	1.32	25.23	
pd3_v1n1_bs	5.38	0.51	9.43		4.61	1.61	34.99	
pd1_v2n1_bs	5.62	0.41	7.38		5.61	0.90	16.04	
pd2_v2n1_bs	5.62	0.41	7.38		5.10	1.34	26.29	
pd3_v2n1_bs	5.62	0.41	7.38		4.46	1.58	35.33	
pd1_v3n1_bs	5.19	0.29	5.66		5.57	0.93	16.62	
pd2_v3n1_bs	5.19	0.29	5.66		5.07	1.41	27.79	
pd3_v3n1_bs	5.19	0.29	5.66		4.47	1.58	35.27	
pd1_v1n1_rcp45	**6.00**	**0.42**	**7.03**	*****	**5.92**	**0.93**	**15.72**	**ns**
pd2_v1n1_rcp45	**6.00**	**0.42**	**7.03**	*****	**5.26**	**1.53**	**29.10**	**ns**
pd3_v1n1_rcp45	**6.00**	**0.42**	**7.03**	*****	**4.54**	**1.70**	**37.47**	**ns**
pd1_v2n1_rcp45	5.98	0.52	8.68	ns	5.78	0.96	16.57	ns
pd2_v2n1_rcp45	5.98	0.52	8.68	ns	5.10	1.54	30.14	ns
pd3_v2n1_rcp45	5.98	0.52	8.68	ns	4.38	1.68	38.23	ns
pd1_v3n1_rcp45	**6.41**	**0.28**	**4.32**	*****	**5.76**	**0.93**	**16.08**	**ns**
pd2_v3n1_rcp45	**6.41**	**0.28**	**4.32**	*****	**5.11**	**1.54**	**30.24**	**ns**
pd3_v3n1_rcp45	**6.41**	**0.28**	**4.32**	*****	**4.42**	**1.65**	**37.39**	**ns**
pd1_v1n1_rcp85	5.63	0.50	8.87	ns	5.98	0.97	16.18	ns
pd2_v1n1_rcp85	5.63	0.50	8.88	ns	5.28	1.52	28.83	ns
pd3_v1n1_rcp85	5.63	0.50	8.88	ns	4.55	1.72	37.91	ns
pd1_v2n1_rcp85	5.73	0.45	7.84	ns	5.84	0.97	16.58	ns
pd2_v2n1_rcp85	5.73	0.45	7.84	ns	5.13	1.54	30.03	ns
pd3_v2n1_rcp85	5.73	0.45	7.84	ns	4.38	1.70	38.72	ns
pd1_v3n1_rcp85	**6.06**	**0.32**	**5.31**	*****	**5.77**	**0.95**	**16.49**	**ns**
pd2_v3n1_rcp85	**6.06**	**0.32**	**5.31**	*****	**5.03**	**1.49**	**29.55**	**ns**
pd3_v3n1_rcp85	**6.06**	**0.32**	**5.31**	*****	**4.36**	**1.66**	**38.14**	**ns**

Note: sd = standard deviation; cv = coefficient of variation; sign = significant; * = significant; *** = very significant

Table 62: Mean, median, sd and cv of grain yield (t/ha) for baseline, RCP4.5 and RCP8.5 at N2

	CERES-Maize				APSIM-Maize			
variable	Mean (t/ha)	sd	cv	Sign	Mean (t/ha)	sd	cv	Sign
pd1_v1n2_bs	5.69	1.01	17.72		7.56	1.52	20.10	
pd2_v1n2_bs	5.69	1.01	17.72		6.38	2.22	34.80	
pd3_v1n2_bs	5.69	1.01	17.72		4.66	1.94	41.65	
pd1_v2n2_bs	5.49	1.01	18.44		7.36	1.50	20.36	
pd2_v2n2_bs	5.49	1.01	18.44		6.08	2.14	35.15	
pd3_v2n2_bs	5.49	1.01	18.44		4.44	1.88	42.38	
pd1_v3n2_bs	6.95	0.73	10.57		7.06	1.35	19.11	
pd2_v3n2_bs	6.95	0.73	10.57		5.84	1.98	33.83	
pd3_v3n2_bs	6.95	0.73	10.57		4.40	1.80	41.01	
pd1_v1n2_rcp45	5.90	0.51	8.61	ns	7.23	1.35	18.69	ns
pd2_v1n2_rcp45	5.90	0.51	8.61	ns	6.12	2.03	33.21	ns
pd3_v1n2_rcp45	5.90	0.51	8.61	ns	4.66	2.01	43.14	ns
pd1_v2n2_rcp45	5.43	0.61	11.20	ns	6.93	1.32	19.11	ns
pd2_v2n2_rcp45	5.43	0.61	11.20	ns	5.85	1.99	34.02	ns
pd3_v2n2_rcp45	5.43	0.61	11.20	ns	4.43	1.91	43.08	ns
pd1_v3n2_rcp45	7.27	0.44	6.06	ns	6.62	1.25	18.94	ns
pd2_v3n2_rcp45	7.27	0.44	6.06	ns	5.69	1.84	32.26	ns
pd3_v3n2_rcp45	7.27	0.44	6.06	ns	4.43	1.84	41.51	ns
pd1_v1n2_rcp85	5.37	0.56	10.37	ns	6.96	1.40	20.15	ns
pd2_v1n2_rcp85	5.37	0.56	10.37	ns	5.99	1.94	32.39	ns
pd3_v1n2_rcp85	5.37	0.56	10.37	ns	4.66	2.01	43.07	ns
pd1_v2n2_rcp85	5.11	0.59	11.60	ns	6.68	1.32	19.73	ns
pd2_v2n2_rcp85	5.11	0.59	11.60	ns	5.72	1.91	33.44	ns
pd3_v2n2_rcp85	5.11	0.59	11.60	ns	4.44	1.92	43.27	ns
pd1_v3n2_rcp85	6.81	0.60	8.79	ns	6.38	1.25	19.57	ns
pd2_v3n2_rcp85	6.81	0.60	8.79	ns	5.55	1.78	32.10	ns
pd3_v3n2_rcp85	6.81	0.60	8.79	ns	4.44	1.87	42.05	ns

Note: sd = standard deviation; cv = coefficient of variation; sign = significant; * = significant; *** = very significant

Table 63: Mean, median, sd and cv of grain yield (t/ha) for baseline, RCP4.5 and RCP8.5 at N3

	CERES-Maize				APSIM-Maize			
variable	Mean (t/ha)	sd	cv	Sign	Mean (t/ha)	sd	cv	Sign
pd1_v1n3_bs	5.97	0.94	15.70		7.77	1.74	22.38	
pd2_v1n3_bs	5.97	0.94	15.70		6.35	2.31	36.35	
pd3_v1n3_bs	5.97	0.94	15.70		4.64	1.97	42.55	
pd1_v2n3_bs	4.80	0.70	14.54		7.50	1.66	22.18	
pd2_v2n3_bs	4.80	0.70	14.54		6.06	2.21	36.54	
pd3_v2n3_bs	4.80	0.70	14.54		4.42	1.91	43.19	
pd1_v3n3_bs	7.07	0.84	11.86		7.09	1.46	20.58	
pd2_v3n3_bs	7.07	0.84	11.86		5.83	2.03	34.83	
pd3_v3n3_bs	7.07	0.84	11.86		4.38	1.83	41.86	
pd1_v1n3_rcp45	6.25	0.54	8.67	ns	7.30	1.48	20.30	ns
pd2_v1n3_rcp45	6.25	0.54	8.67	ns	6.13	2.07	33.76	ns
pd3_v1n3_rcp45	6.25	0.54	8.67	ns	4.63	2.04	44.04	ns
pd1_v2n3_rcp45	6.03	0.68	11.35	ns	6.98	1.42	20.41	ns
pd2_v2n3_rcp45	6.03	0.68	11.35	ns	5.87	2.02	34.47	ns
pd3_v2n3_rcp45	6.03	0.68	11.35	ns	4.40	1.94	44.01	ns
pd1_v3n3_rcp45	7.19	0.46	6.45	ns	6.64	1.34	20.16	ns
pd2_v3n3_rcp45	7.19	0.46	6.45	ns	5.70	1.86	32.59	ns
pd3_v3n3_rcp45	7.19	0.46	6.45	ns	4.42	1.86	42.07	ns
pd1_v1n3_rcp85	5.83	0.55	9.39	ns	6.97	1.51	21.70	ns
pd2_v1n3_rcp85	5.83	0.55	9.39	ns	6.01	1.97	32.73	ns
pd3_v1n3_rcp85	5.83	0.55	9.39	ns	4.65	2.02	43.58	ns
pd1_v2n3_rcp85	5.77	0.55	9.52	ns	6.69	1.39	20.80	ns
pd2_v2n3_rcp85	5.77	0.55	9.52	ns	5.73	1.93	33.73	ns
pd3_v2n3_rcp85	5.77	0.55	9.52	ns	4.43	1.93	43.71	ns
pd1_v3n3_rcp85	6.66	0.56	8.39	ns	6.38	1.30	20.31	ns
pd2_v3n3_rcp85	6.66	0.56	8.39	ns	5.57	1.80	32.35	ns
pd3_v3n3_rcp85	6.66	0.56	8.39	ns	4.43	1.88	42.46	ns

Note: sd = standard deviation; cv = coefficient of variation; sign = significant; * = significant; *** = very significant

4.6.3.2 Percent change in grain yield under PD, N, and cultivar

The percent change in grain yield is shown in Figure 18. Using the APSIM-Maize, the mean percent change in maize grain yield in 2050 would range from -2.88 to +4.37% (N1), -5.83 to +0.20% (N2), -6.21 to +0.58% (N3) (RCP4.5) and -3.86 to +5.42% (N1), -9.10 to +0.03% (N2), -9.99 to +0.69% (N3) (RCP8.5). The mean percent change in grain yield simulated using CERES-Maize in 2050 would range from 6.85 to 23.86% (N1), 2.00 to 6.96% (N2), 2.99 to 27.96% (N3) (RCP4.5) and 2.55 to 17.04% (N1), -

3.99 to -0.83% (N2), -4.61 to +22.80% (N3) (RCP8.5). Results show that the simulated changes in grain yield would be lower under RCP8.5 than at RCP4.5 scenario.

According to the analysis, maize cultivars would perform differently under different nitrogen fertilizer application rates and PDs. Low N fertilizer rate would be better with low maintenance at PD1. Grain yield variation caused by weather was much greater under N3 than at N1 at PD1 and PD2 for both CSMs (Figure 18). Delayed PD (PD3) at higher N fertilizer rate would increase grain and biomass yield (Appendix 7) than at PD1. Lower N fertilizer rate (N1) in the future would give a higher increase in grain yield at PD1 than at PD3. Zhang et al. (2015) agree with the findings of this study that maize yield would reduce in the future due to climate change. Simulated percent change in grain yield would reduce in 2050 due to reduced duration of the phenological stages. Shorter crop growth duration entails that less solar radiation and root soil water would be utilized by the crop. The management of PD and N fertilizer rate could be beneficial mitigation and adaptation of maize to climate change at Mount Makulu. Projected changes in temperature and precipitation would decrease maize yield in Africa as a result of the shortening DAP to anthesis and maturity (Adhikari et al., 2015).

Inadequate use of CSMs is attributed to a lack of application in policy formulation and low capacity (MacCarthy et al., 2017). Using CSMs as decision support tools by both end-users, researchers, planners, and policy-makers could lead to efficient use of nutrients in agricultural productivity. The observed differences between APSIM-Maize and CERES-Maize model projections are due to differences in sensitivity to temperature and CO_2 increases (Waha et al., 2015). Araya et al. (2015) reported an increase in maize yield for the mid-century using DSSAT and 20 GCMs and his findings to agree with this study. A prediction of 3 to 19% reduction in maize yield by 2050 was observed by Jones and Thornton (2003) using the CERES-Maize model. Challinor et al. (2016) also observed that the increase in air temperature shortens the number of days to anthesis and physiological maturity and hence, reduces grain and biomass yield. They agree with the findings of this study.

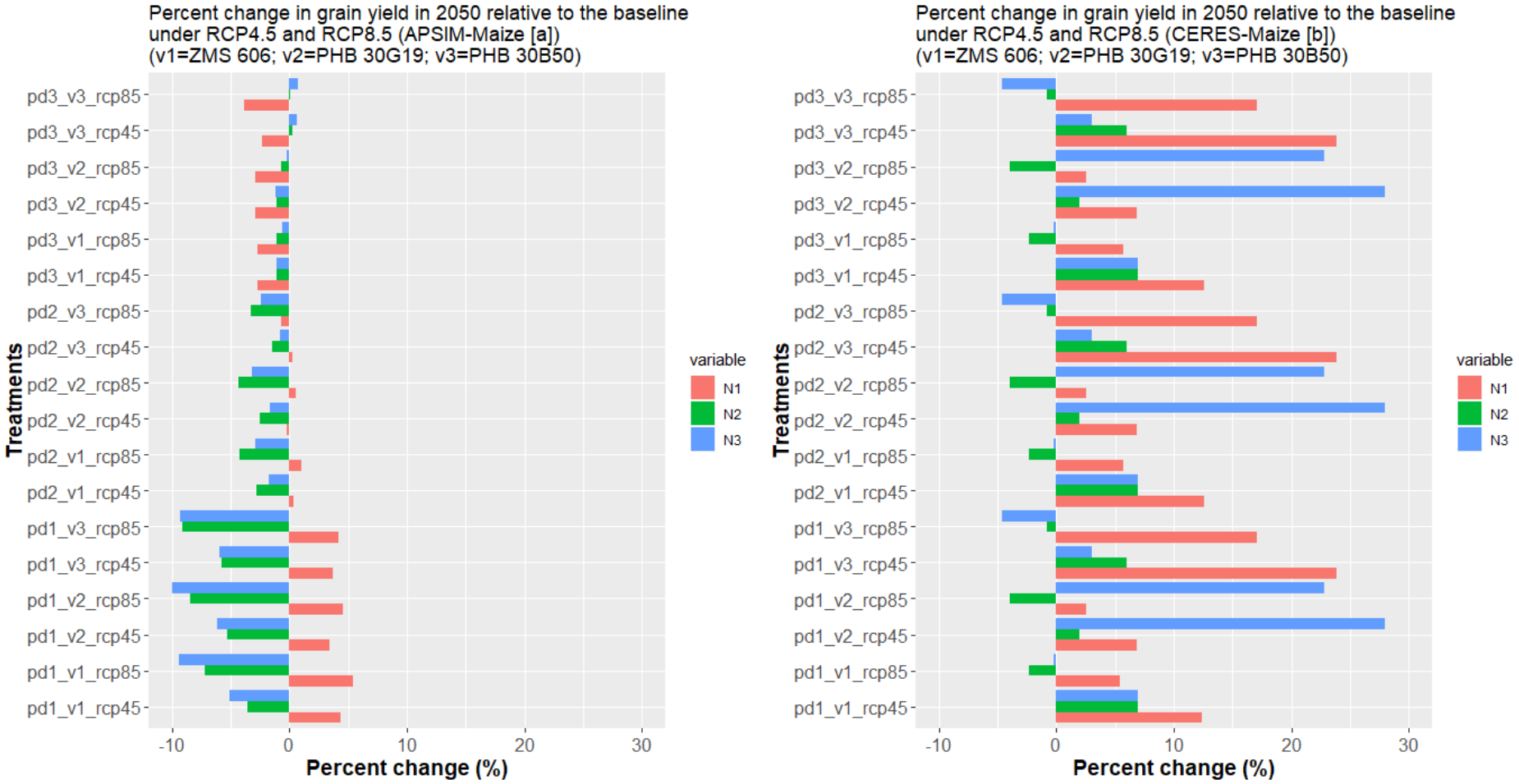

Figure 18: Percent change in grain yield under PD, and cultivar in 2050 relative to the baseline under RCP4.5 and RCP8.5 (APSIM-Maize [a]; CERES-Maize [b])

4.6.3.3 Ensemble mean of the crop simulation models

Using an ensemble of APSIM-Maize and CERES-Maize, the impact of climate change and management has been quantified for Mount Makulu. The change in grain yield for PHB 30B50 (PD1V3N1) was significant. All the other treatments were non-significant. The percent change in grain would be range from 2.78 to 9.94%, -3.81 to -8.88% and -2.33 to 10.63% under N1, N2, and N3, respectively. The percent change in grain yield would increase with delay in PD (RCP4.5 [PD1 = 2.57%; PD2=3.31%; PD3=4.37%]; RCP8.5 [PD1 = -1.11%; PD2=-0.29%; PD3=1.08%]).

The percent grain yield in the future would increase for the cultivars at all PDs with the application of N1 under both scenarios (Table 67). Grain yield for cultivar PHB 30B50 would increase at all PDs with the application of N1 and N2 illustrating the strong interaction of N and precipitation in determining grain yields in 2050. At all PDs with the application of N3, grain yield for PHB 30G19 would increase. Grain yield would increase for ZMS 606 (PD3) and PHB 30G19 (PD2, PD3) with the application of N2. Cultivar PHB 30B50 would perform better than ZMS 606 and PHB 30G19 with the application of N1 at all PDs. Less soil water content has an effect on soil fertility which becomes less significant. Earlier PD (PD1) with lower N application rate (N1) is an effective adaptation strategy in dealing with the adverse effects of future climate change. If smallholder farmers maintain N1 at all PDs, climate change would be inconsequential due to the over-riding constraint of fertility on crop yield.

Adaptation and mitigation strategies that should be used by farmers are planting drought, heat resistant and open pollinating cultivars, N management and varying PDs. Other strategies include earlier and late PDs with lower and higher N fertilizer rate, respectively. Other management strategies such as tillage, soil water conservation measures (conservation agriculture, climate-smart agriculture) and improved irrigation technologies were not considered in this study. Their effectiveness in counteracting projected negative climate change impacts needs to be quantified in the future.

An increase in temperature and precipitation variability is the main mechanism by which climate change would have a significant impact on crop growth and yield through reduced crop duration. The most effective approach in assessing the impact of

climate change on crop yield and in formulating mitigation and adaptation strategies is the use of a multi-model ensemble of CSMs and GCMs. CSMs can also be used in plant breeding targeted at specific mitigation and adaptation strategies. Martre et al. (2015) noted that studies using an ensemble of CSMs provide valuable information about model accuracy and uncertainty.

Table 64: Ensemble of baseline, and future grain yield and % change under PD and N

Treatments	Baseline grain yield (t/ha)	Future (RCP4.5) grain yield (t/ha)	Future (RCP8.5) grain yield (t/ha)	Future % change in grain yield RCP4.5	Future % change in grain yield RCP4.5
pd1_v1n1	5.55	5.96	5.81	7.48	4.69
pd2_v1n1	5.30	5.63	5.46	6.23	2.92
pd3_v1n1	5.00	5.27	5.09	5.51	1.90
pd1_v2n1	5.62	5.88	5.79	4.72	3.03
pd2_v2n1	5.36	5.54	5.43	3.36	1.31
pd3_v2n1	5.04	5.18	5.06	2.78	0.30
pd1_v3n1	**5.38**	**6.09**	**5.92**	**13.10***	**9.94**
pd2_v3n1	**5.13**	**5.76**	**5.55**	**12.28**	**8.09**
pd3_v3n1	**4.83**	**5.42**	**5.21**	**12.11**	**7.87**
pd1_v1n2	6.63	6.57	6.17	-0.91	-6.94
pd2_v1n2	6.04	6.01	5.68	-0.41	-5.88
pd3_v1n2	5.18	5.28	5.02	2.03	-3.09
pd1_v2n2	**6.43**	**6.18**	**5.90**	**-3.81**	**-8.25**
pd2_v2n2	5.79	5.64	5.42	-2.51	-6.40
pd3_v2n2	4.97	4.93	4.78	-0.70	-3.83
pd1_v3n2	7.01	6.95	6.60	-0.86	-5.85
pd2_v3n2	6.40	6.48	6.18	1.33	-3.36
pd3_v3n2	5.68	5.85	5.63	3.08	-0.88
pd1_v1n3	**6.87**	**6.78**	**6.40**	**-1.38**	**-6.84**
pd2_v1n3	6.16	6.19	5.92	0.49	-3.90
pd3_v1n3	5.31	5.44	5.24	2.54	-1.23
pd1_v2n3	6.15	6.51	6.23	5.77	1.30
pd2_v2n3	5.43	5.95	5.75	9.58	5.89
pd3_v2n3	**4.61**	**5.22**	**5.10**	**13.12**	**10.63**
pd1_v3n3	**7.08**	**6.92**	**6.52**	**-2.33**	**-7.91**
pd2_v3n3	6.45	6.45	6.12	-0.08	-5.19
pd3_v3n3	5.73	5.81	5.55	1.40	-3.14

4.6.4 Probability, and cumulative distribution functions and effect of weather on maize yield

The PDFs and CPDFs of the simulated percent change in grain yield are shown in Figure 19, Figure 20, Figure 21 and Figure 22. The PDFs display a Gaussian distribution form. The peaks of the PDF graphs are shifting leftward, and this indicates possibilities of grain yield reduction. Zhang et al. (2015) reported similar results as this study. There are uncertainties in the PDFs as to the extent N rate would affect percent change in mean grain yield under RCP4.5 and RCP8.5. There is also a negative shift in higher N as opposed to lower rates. The CDFs at all treatment levels showed that the probability of maize yield would decrease more under RCP4.5 than at RCP8.5 scenarios.

Considering the uncertainties derived from crop and climate models, the CDFs of simulated yield were used to analyze changes in maize yield in 2050s relative to the baseline. The variation in simulated grain yield would be attributed to rainfall variability and uncertainty and temperature increase under RCP4.5 and RCP8.5 during 2040-2069. The factors that caused variation in grain yield are PDs, N fertilizer rate, temperature, and rainfall. Under rainfed conditions, air temperatures of 30^{o}C reduce maize yield up to 6% (Schauberger et al., 2017). The optimal maize growing temperature has been reported to be 25°C (Adhikari et al., 2015; Lobell et al., 2011). However, an increase of temperature by one degree above 30°C reduces maize yield by 1-10% under optimal conditions. The increase in air temperature enables the crop to progress rapidly to anthesis and maturity. This shortens the life cycle of the crop leading to lower yield due to the shorter grain filling period. Overall, maize grain yield would decrease under future climate scenarios using 5 GCMs, although the % change differs among the cultivars. The effect of PDs and N fertilizer rate would affect maize cultivar grain yield differently due to changes in temperature, precipitation and root soil water content in the 2050s.

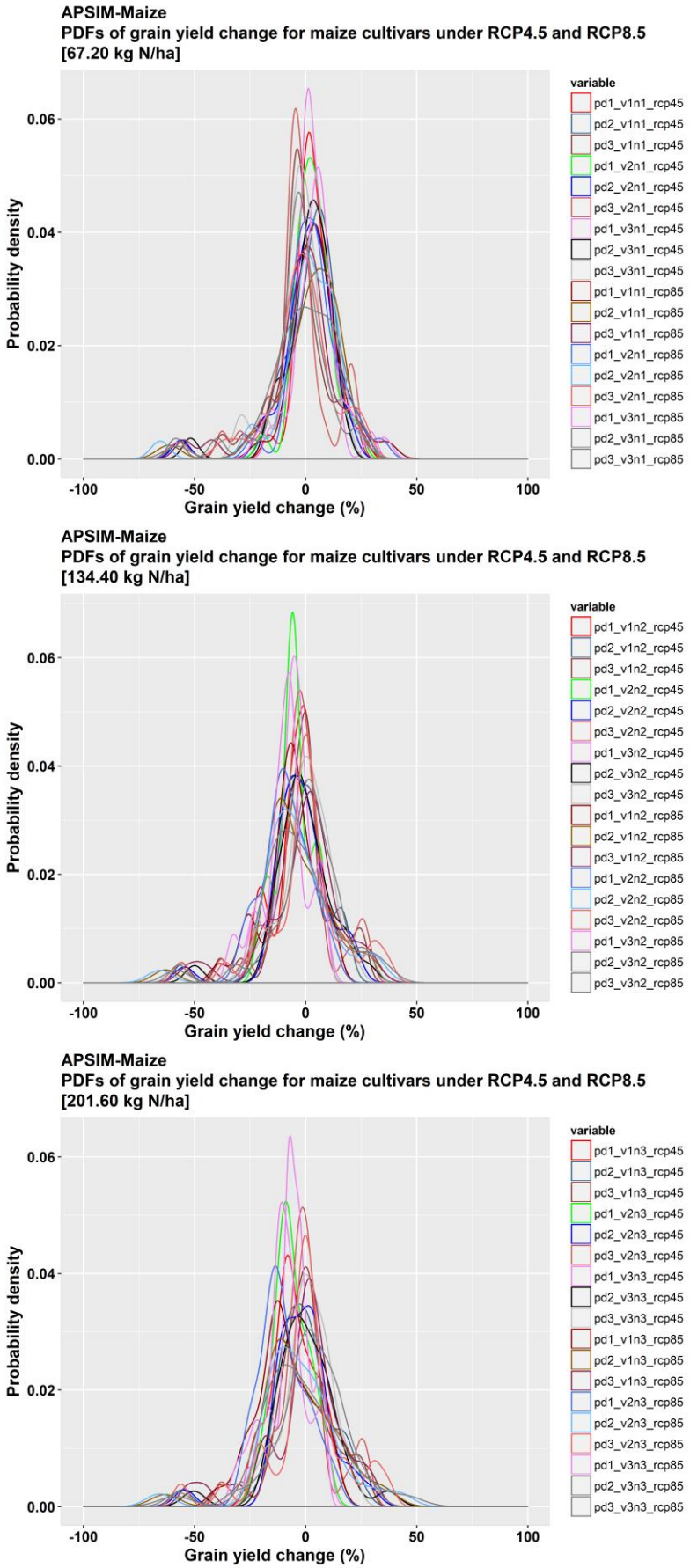

Figure 19: PDFs of % change in grain yield under PDs and N rate (APSIM-Maize)

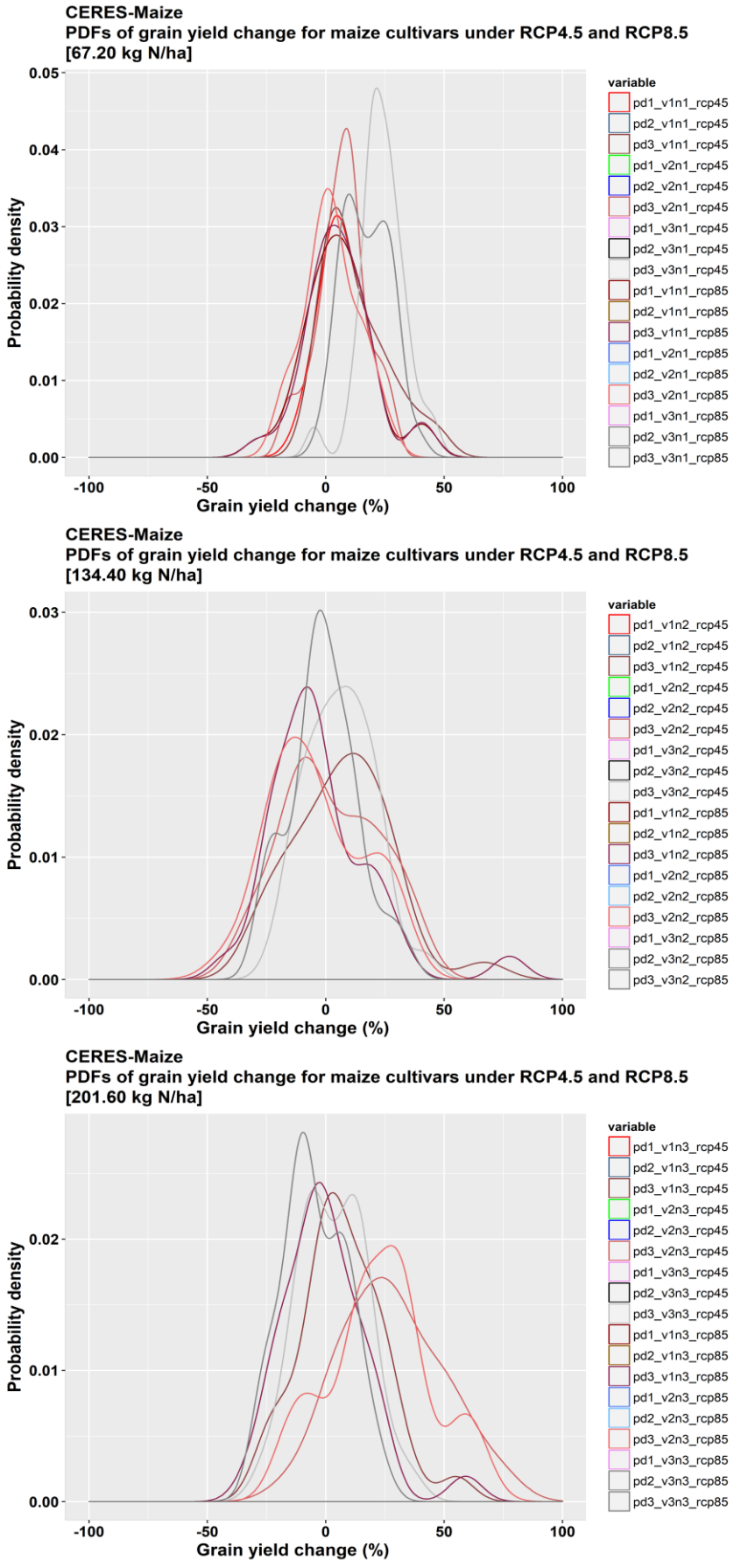

Figure 20: PDFs of % change in grain yield under PDs and N rate (CERES-Maize)

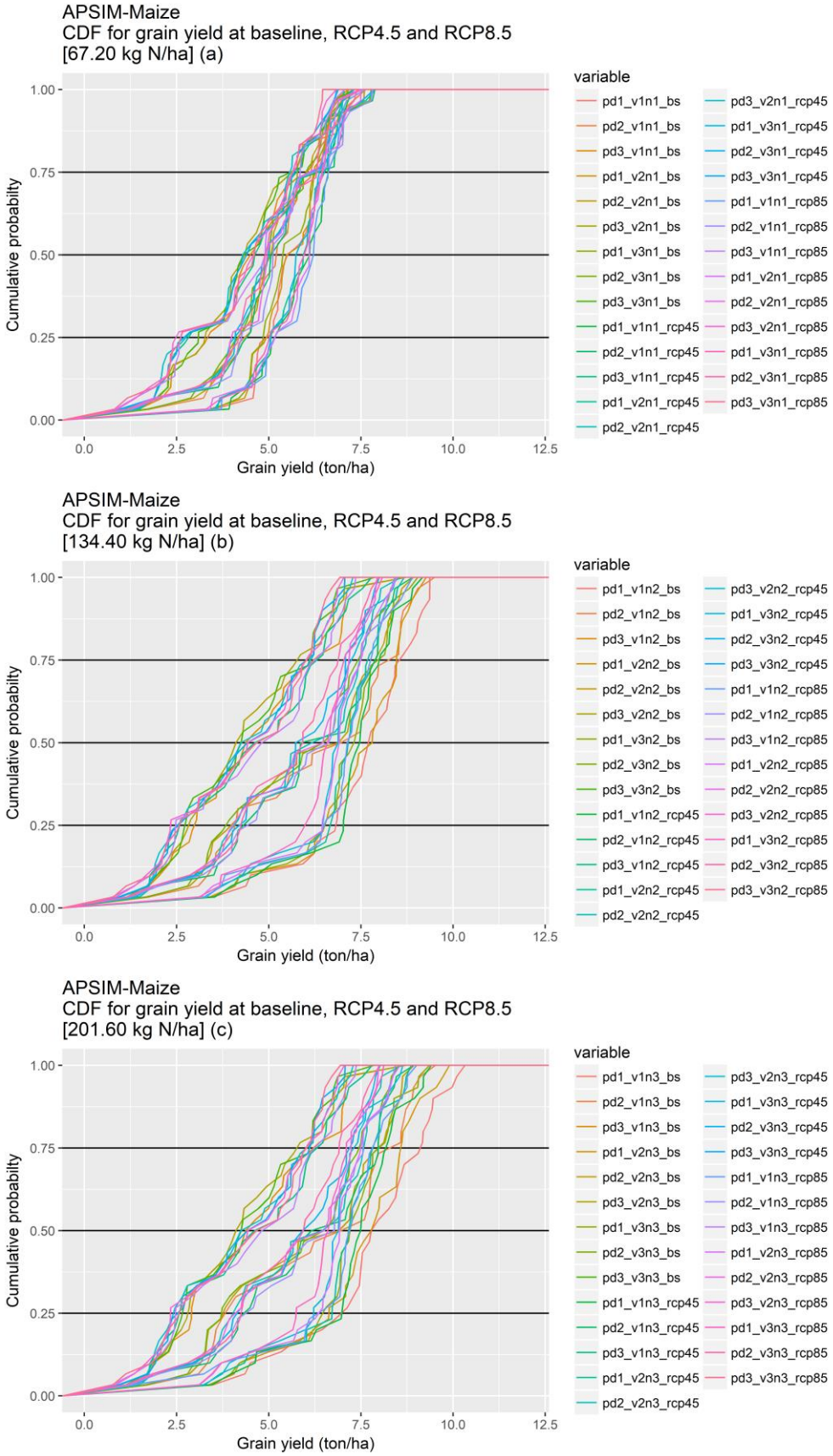

Figure 21: Effects of climate change on grain yield under PDs, N1, N2 and N3 (APSIM-Maize)

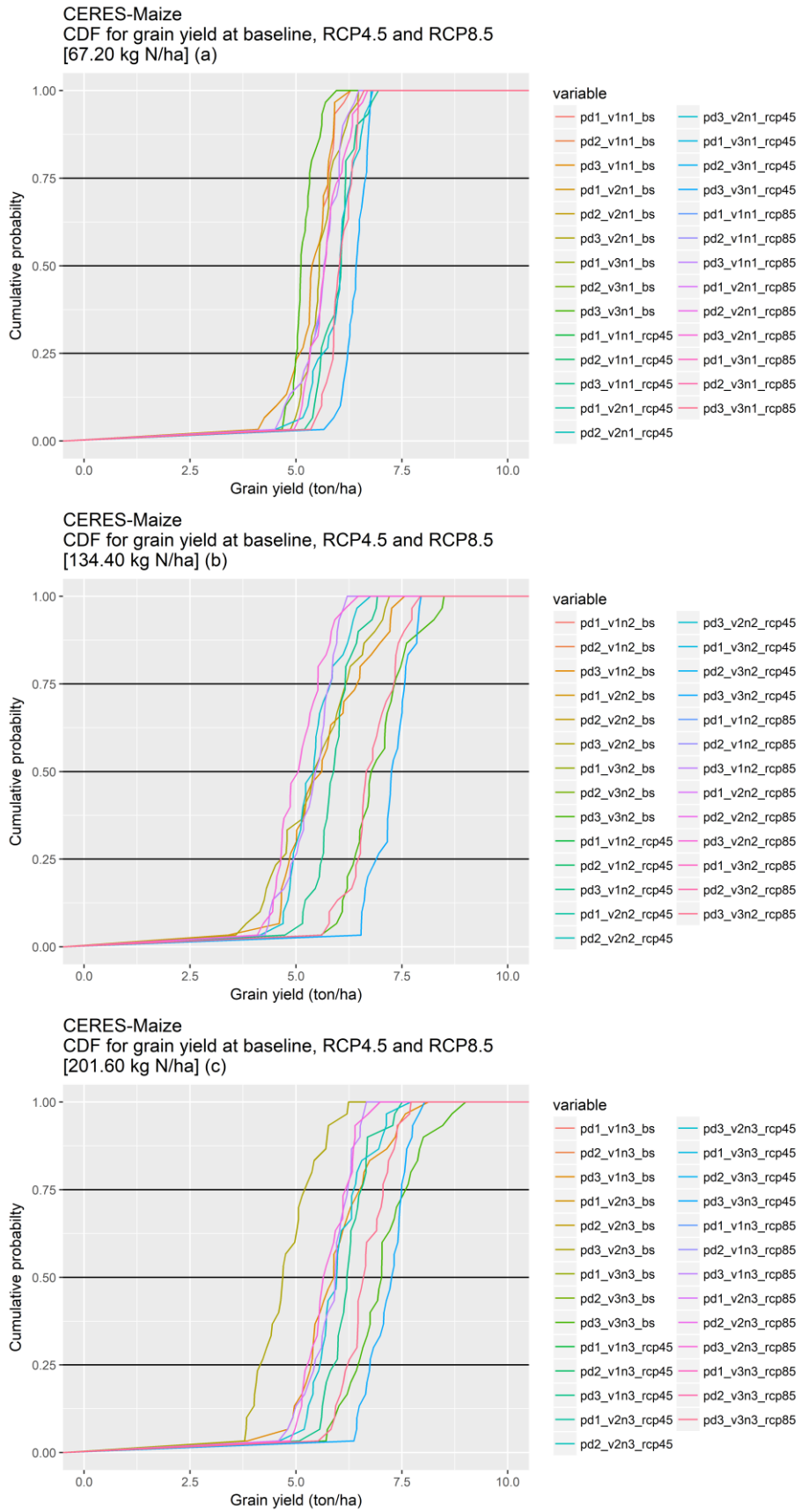

Figure 22: Effects of climate change on grain yield under PDs, N1, N2 and N3 (CERES-Maize)

CHAPTER FIVE: CONCLUSION AND RECOMMENDATIONS

5.1 Conclusion

This study has demonstrated that crop yield is influenced by PD, N, cultivar, and management. PD is a critical factor for capturing higher solar radiation without nutrient and soil moisture deficiency. Biomass and grain yield reduces with delay in PD and low soil fertility (N). PD and N effect significantly influenced maize yield.

Calibration and validation of CSMs are essential to bridge the gap between reality and simulation while identifying areas requiring improvements. Minor differences exist between simulated and observed values. For the calibration period, RMSE between simulated and observed DAP to anthesis, and maturity, grain size, grain yield, biomass yield, and mLAI were 1.91 days, 3.35 days, 0.05 g, 3.19 ton ha^{-1}, 1.38 ton ha^{-1} and 0.69 m^2 m^{-2}, respectively for the APSIM-Maize. The RMSE for DAP to anthesis, maturity, grain size, grain yield, biomass yield, and mLAI were 2.89 days, 3.13 days, 0.07 g, 2.87 ton ha^{-1}, 0.84 ton ha^{-1} and 2.04 m^2 m^{-2}, respectively for the CERES-Maize. Simulated SWC for both CSMs was acceptable (NRMSE < 30%). Future model evaluations may be needed for new cultivars released by breeders.

During validation, the simulated DAP to anthesis, and maturity for both CSMs was good (NRMSE = 20-30%). The simulated values for grain number m^{-2} and mLAI were good (NRMSE = 20-30%) for APSIM-Maize. The CERES-Maize model failed to accurately reproduce grain yield and mLAI (NRMSE > 30%). The CSMs improvement includes prediction of phenology duration and LAI. CSMs can be used to rapidly appraise new cultivars, PDs, N fertilizer rates and agro-technologies for adoption, inform policy and as decision support tools.

The weather data required by CSMs are daily precipitation, minimum and maximum air temperature, relative humidity (%), wind speed and solar radiation. Some sources for Climate data are ZMD, NOAA, AgMERRA, WorldClim, TERRACLIMATE, KNMI Climate Explorer, Climate Information Tool Kit (CLIK), CLIMGEN, MARKSIM, Climate Change Knowledge Portal, Climate Change Agriculture and Food Security, PRISM Climate Group and CAIT Climate Data Explorer. The weather data could also be generated using statistical and dynamical downscaling tools. The

quantitative effects of climate change on maize yield can be studied using statistical downscaling tools and CSMs. Multi-model ensemble simulations are necessary for providing insights into GCMs and CSMs uncertainties as well as to develop alternative adaptation and mitigation strategies. The simulated future climate using LARS-WG (1.50^{o}C [B1 scenario], 1.84^{o}C [A1B scenario]) and delta method (AgMIP protocols) (1.82^{o}C [RCP4.5], 2.48^{o}C [RCP8.5]) showed that temperature would increase while rainfall would reduce (1.46% [RCP4.5]), 1.91% [RCP8.5]).

Precipitation extreme weather indices had not taken place at Mount Makulu. Significant changes have been observed in extreme temperature indices. Tmean, Tmax and DTR had increased by 0.025^{o}C, 0.037^{o}C and 0.031^{o}C, respectively. The increase in Tmean and Tmax has resulted in heat stress and heatwaves. Additionally, Mount Makulu had experienced a near normal drought condition (1963-2012). ClimPACT2 can be used to compute extreme climate indices at both local and regional scale. Computed extreme climate indices could be used as a means of communicating climate change impact information to end-users, planners, policy makers, and scientists.

The APSIM-Maize and CERES-Maize models simulated reduced DAP to anthesis and maturity. The projected changes in temperature and rainfall would adversely reduce simulated maize yield (-6.90 - +4.06 (RCP4.5), -10.80 - +5.00% (RCP8.5) [APSIM-Maize]; -0.59 to +25.77% (RCP4.5) and -6.52 to +20.21% (RCP8.5) [CERES-Maize]) depending on PD in 2050. Therefore, new cultivars are needed that are drought resistant and efficient at utilizing N.

Using multi-model ensembles of CSMs provides robust estimates of growth and yield. Significant changes in DAP to anthesis and maturity, biomass, and grain yield were observed under RCP4.5 and RCP8.5 scenarios. The DAP to anthesis (-11.28 to -9.39% [RCP4.5]; -14.28 to -12.65% [RCP8.5]) and maturity (-10.52 to -9.43% [RCP4.5]; -14.01 to -12.75% [RCP8.5]) would reduce in 2050. The % change in grain would range from 2.78 to 9.94%, -3.81 to -8.88% and -2.33 to 10.63% under N1, N2, and N3, respectively. The percent change in grain yield would increase with delay in PD (RCP4.5 [PD1 = 2.57%; PD2=3.31%; PD3=4.37%]; RCP8.5 [PD1 = -1.11%; PD2=-0.29%; PD3=1.08%]). The current PDs and cultivars with lower N (N1) would

increase grain yield in the future. However, grain yield would increase at PD3 with N3.

5.2 Recommendations

Based on the findings of this study, the following are the recommendations:

i. In Zambia, plant breeders (Universities, Zambia Agriculture Research Institut, and seed companies) should focus on producing cultivars that would thrive under future climate scenarios and low nitrogen;
ii. Ministry of Agriculture, Health and Zambia Meteorological Department should collaborate in computing extreme climate indices using ClimPACT2 at both local (using agromet station point data) and regional level using gridded (netCDF) datasets covering the AERs of Zambia to inform policy in formulating appropriate mitigation and adaptation strategies against climate change;
iii. Plant breeders in Zambia should integrate statistical downscaling and crop simulation models in their breeding programmes in the face of climate change and variability;
iv. Statistical downscaling models (LARS-WG and delta-based methods) should be used in conjunction with hydrological and crop simulation models to study the impact of climate change and variability at the watershed level to ascertain its effects on erosion, runoff and crop yield by MoA, Livestock and Fisheries, Energy and Water Development, and Zambia Meteorological Department and Universities;
v. The ZARI should incorporate crop simulation models in their research to complement field experiments which are costly and labour intensive. CSMs may play an essential role in fostering and understanding a combination of different management options in agriculture research; and
vi. The calibrate and validated APSIM-Maize and CERES-Maize models could be used by researchers and farmers to test conservation agriculture technologies, economic risks associated with different management practices, determine the appropriate PDs, irrigation water requirement or scheduling and the nutrient requirement for optimum yield.

REFERENCES

Abdullah, H.M., 2014. Standardized precipitation evapotranspiration index (SPEI) based drought assessment in Bangladesh, in: Proceedings of 5th International Conference on Environmental Aspects of Bangladesh [ICEAB 2014]. Bangabandhu Sheikh Mujibur Rahman Agricultural University, Gazipur-1706, Bangladesh, pp. 40–42. https://doi.org/10.1080/13504509.2011.562002

Abedinpour, M., Sarangi, A., 2018. Evaluation of DSSAT- Ceres Model for Maize under Different Water and Nitrogen Levels. Sci. Technol. 26, 1605–1618.

Abera, K., Crespo, O., Seid, J., Mequanent, F., 2018. Simulating the impact of climate change on maize production in Ethiopia, East Africa. Environ. Syst. Res. 7, 1–12. https://doi.org/10.1186/s40068-018-0107-z

Adebo, F.A., Olaoye, G., 2010. Growth Indices and Grain Yield Attributes in Six Maize Cultivars Representing Two Era of Maize Breeding in Nigeria. J. Agric. Sci. 2, 218–228.

Adhikari, U., Nejadhashemi, A.P., Woznicki, S.A., 2015. Climate change and eastern Africa : a review of impact on major crops. Food Energy Secur. 110–132. https://doi.org/10.1002/fes3.61

Adnan, A.A., Diels, J., Jibrin, J.M., Kamara, A.Y., Craufurd, P., Shaibu, A.S., Mohammed, I.B., Tonnang, Z.E.H., 2019. Options for calibrating CERES-maize genotype specific parameters under data-scarce environments. PLoS One 1–20. https://doi.org/10.1101/353045

Adnan, A.A., Jibrin, J.M., Kamara, A.Y., Abdulrahman, B.L., Shaibu, A.S., 2017. Using CERES-Maize model to determine the nitrogen fertilization requirements of early maturing maize in the Sudan Savanna of Nigeria. J. Plant Nutr. 40, 1066–1082. https://doi.org/10.1080/01904167.2016.1263330

Ahmad, M., Khaliq, A., Ahmad, R., Ranjha, A.M., 2010. Allometery and Productivity of Autumn Planted Maize Hybrids under Narrow Row Spacing. Int. J. Agric. Biol. 12, 661–667.

Ahmadi, B., Hosein, A., Rad, S., Delkhosh, B., 2014. Evaluation of plant densities on analysis of growth indices in two canola forage (Brassica napus L.). Eur. J. Exp. Biol. 4, 286–294.

Ahmed, F., Choudhury, A.K., Akhter, S., Aziz, M.A., Biswas, J.C., Maniruzzaman, M., Miah, M.M.U., Rahman, M.M., Jahan, M.A.H.S., Ahmed, I.M., Sen, R., Ishtiaque, S., Islam, A.F.M.T., Haque, M.M., Hossain, M.B., Kalra, N., Rahman, M.H., 2017. Calibration and Validation of Decision Support System for Agro-Technology Transfer Model for Simulating Growth and Yield of Maize in Bangladesh. Am. J. Plant Sci. 8, 1632–1645. https://doi.org/10.4236/ajps.2017.87113

Ahmed, M., Akram, M.N., Asim, M., Aslam, M., Hassan, F., Higgins, S., Stöckle, C.O., Hoogenboom, G., 2016a. Calibration and validation of APSIM-Wheat and CERES-Wheat for spring wheat under rainfed conditions: Models evaluation and application. Comput. Electron. Agric. 123, 384–401. https://doi.org/10.1016/j.compag.2016.03.015

Ahmed, M., Akram, M.N., Asim, M., Aslam, M., Hassan, F. ul, Higgins, S., Stöckle, C.O., Hoogenboom, G., 2016b. Calibration and validation of APSIM-Wheat and CERES-Wheat for spring wheat under rainfed conditions: Models evaluation and application. Comput. Electron. Agric. 123, 384–401. https://doi.org/10.1016/j.compag.2016.03.015

Ahmed, M., Hassan, F., 2011. APSIM and DSSAT models as decision support tools, in: 19th International Congress on Modelling and Simulation, Perth, Australia,

12–16 December 2011 . Perth.
Akinbile, C.O., Akinlade, G.M., Abolude, A.T., 2015. Trend analysis in climatic variables and impacts on rice yield in Nigeria. J. Water Clim. Chang. 06.3, 534–543. https://doi.org/10.2166/wcc.2015.044
Alexander, L., 2014. The Expert Team on Climate Risk and Sector-specific Climate Indices (ET-CRSCI): Pilot workshop Western South America.
Alexander, L., Herold, N., 2016. ClimPACT2. Indices and software. A document prepared on behalf of The Commission for Climatology (CCl) Expert Team on Sector-Specific Climate Indices (ET-SCI).
Alexander, L., Yang, H., Perkins, S., 2013. ClimPACT. Indices and software. A document prepared on behalf of The Commission for Climatology (CCl) Expert Team on Climate Risk and Sector-Specific Climate Indices (ET CRSCI).
Alexander, L. V., 2016. Global observed long-term changes in temperature and precipitation extremes: A review of progress and limitations in IPCC assessments and beyond. Weather Clim. Extrem. 11, 4–16. https://doi.org/10.1016/j.wace.2015.10.007
Alexander, L. V., Zhang, X., Peterson, T.C., Caesar, J., Gleason, B., Tank, A.M.G.K., Haylock, M., Collins, D., Trewin, B., Rahimzadeh, F., Tagipour, A., Kumar, K.R., Revadekar, J., Griffiths, G., Vincent, L., Stephenson, D.B., Burn, J., Aguilar, E., Brunet, M., Taylor, M., New, M., Zhai, P., Rusticucci, M., Vazquez-Aguirre, J.L., 2006. Global observed changes in daily climate extremes of temperature and precipitation. J. Geophys. Res. Atmos. 111, 1–22. https://doi.org/10.1029/2005JD006290
Alexandratos, N., Bruinsma, J., 2012. World Agriculture towards 2030/2050: the 2012 revision (No. 12– 03), World agriculture towards 2030/2050. The 2012 Revision, ESA Working.
Ali, W., Ali, M., Ahmad, Z., Igbal, J., Anwar, S., 2018. Influence of Sowing Dates on Varying Maize (Zea Mays I.) Varieties Grown Under Agro-Climatic Condition of Peshawar. Eur. J. Exp. Biol. 8, 36. https://doi.org/10.21767/2248-9215.100077
Amjadian, M., Farshadfar, M., Gholipoor, M., Shirvani, H., 2015. The effects of planting date on the yield and yield components of corn (Zea mays L.) cultivar, single cross 704. Agric. Sci. Dev. 4, 1–3.
Anapalli, S.S., Ahuja, L.R., Gowda, P.H., Ma, L., Marek, G., Evett, S.R., Howell, T.A., 2016. Simulation of crop evapotranspiration and crop coefficients with data in weighing lysimeters. Agric. Water Manag. 177, 274–283. https://doi.org/10.1016/j.agwat.2016.08.009
Araya, A., Hoogenboom, G., Luedeling, E., Hadgu, K.M., Kisekka, I., Martorano, L.G., 2015. Assessment of maize growth and yield using crop models under present and future climate in southwestern Ethiopia. Agric. For. Meteorol. 214, 252–265. https://doi.org/http://dx.doi.org/10.1016/j.agrformet.2015.08.259
Araya, A., Kisekka, I., Lin, X., Vara Prasad, P.V., Gowda, P.H., Rice, C., Andales, A., 2017. Evaluating the impact of future climate change on irrigated maize production in Kansas. Clim. Risk Manag. 17, 139–154. https://doi.org/10.1016/J.CRM.2017.08.001
Archontoulis, S. V., Miguez, F.E., Moore, K.J., 2014a. A methodology and an optimization tool to calibrate phenology of short-day species included in the APSIM PLANT model: Application to soybean. Environ. Model. Softw. 1–13. https://doi.org/http://dx.doi.org/10.1016/ j.envsoft.2014.04.009
Archontoulis, S. V., Miguez, F.E., Moore, K.J., 2014b. Evaluating APSIM Maize,

Soil Water, Soil Nitrogen, Manure, and Soil Temperature Modules in the Midwestern United States. Agron. J. 106, 1025–1040. https://doi.org/10.2134/agronj2013.0421

Arif, M., Jan, M.T., Khan, N.U., Akbar, H., Khan, S.A., Khan, M.J., Khan, A., Munir, I., Saeed, M., Iqbal, A., 2010. Impact of Plant Populations and Nitrogen Levels on Maize 42, 3907–3913.

Arslan, A., Mccarthy, N., Lipper, L., Asfaw, S., Cattaneo, A., Kokwe, M., 2015. Climate Smart Agriculture: Assessing the Adaptation Implications in Zambia. J. Agric. Econ. 66, 753–780.

Arslan, A., McCarthy, N., Lipper, L., Asfaw, S., Cattaneo, A., Kokwe, M., 2014. Food security and adaptation impacts of potential climate smart agricultural practices in Zambia (No. 14–13), ESA Working Paper.

Asseng, S., Ewert, F., Rosenzweig, C., Jones, J.W., Hatfield, J.L., Ruane, A.C., Boote, K.J., Thorburn, P.J., Rötter, R.P., Cammarano, D., Brisson, N., Basso, B., Martre, P., Aggarwal, P.K., Angulo, C., Bertuzzi, P., Biernath, C., Challinor, A.J., Doltra, J., Gayler, S., Goldberg, R., Grant, R., Heng, L., Hooker, J., Hunt, L.A., Ingwersen, J., Izaurralde, R.C., Kersebaum, K.C., Müller, C., Naresh Kumar, S., Nendel, C., O'Leary, G., Olesen, J.E., Osborne, T.M., Palosuo, T., Priesack, E., Ripoche, D., Semenov, M.A., Shcherbak, I., Steduto, P., Stöckle, C., Stratonovitch, P., Streck, T., Supit, I., Tao, F., Travasso, M., Waha, K., Wallach, D., White, J.W., Williams, J.R., Wolf, J., 2013. Uncertainty in simulating wheat yields under climate change. Nat. Clim. Chang. 3, 627–632. https://doi.org/http://dx.doi.org/10.1038/ncliamte1916

Banger, K., Nafziger, E.D., Wang, J., Muhammad, U., Id, M.P., 2018. Simulating nitrogen management impacts on maize production in the U.S. Midwest. PLoS One 1–22.

Bartholomew, P.W., 2014. Effect of varying temperature regime on phyllochron in four warm-season pasture grasses. Agric. Sci. 5, 1000–1006.

Bashir, N., Malik, S.A., Mahmood, S., 2012. Influence of urea application on growth , yield and mineral uptake in two corn (Zea mays L.) cultivars. African J. Biotechnol. 11, 10494–10503. https://doi.org/10.5897/AJB10.2357

Bationo, A., Kihara, J., Adesina, A., 2012. Beyond Biophysical Recommendations: Towards a New Paradigm, in: Kihara, J., Fatondji, D., Jones, J.W., Hoogenboom, G., Tabo, R., Bationo, A. (Eds.), Improving Soil Fertility Recommendations in Africa Using the Decision Support System for Agrotechnology Transfer (DSSAT),. Springer Netherlands, Dordrecht, pp. 169–184. https://doi.org/http://dx.doi.org/10.1007/978-94-007-2960-5

Behling, A., Sanquetta, C.R., Corte, A.P.D., Caron, B., Simon, A.A., Behling, M., Schmidt, D., 2015. Conversion efficiency of photosynthetically active radiation intercepted in biomass in stands of black wattle in Brazil. Bosque 36, 61–69. https://doi.org/10.4067/S0717-92002015000100007

Beiragi, M.A., Khorasani, S.K., Shojaei, S.H., Dadresan, M., Mostafavi, K., 2011. A Study on Effects of Planting Dates on Growth and Yield of 18 Corn Hybrids (Zea mays L.). Am. J. Exp. Agric. 1, 110–120.

Boberg, F., Berg, P., Thejll, P., Gutowski, W.J., Christensen, J.H., 2009. Improved confidence in climate change projections of precipitation evaluated using daily statistics from the PRUDENCE ensemble. Clim. Dyn. 32, 1097–1106. https://doi.org/10.1007/s00382-008-0446-y

Boote, K.J., Jones, J.W., Batchelor, W.D., Nafziger, E.D., Myers, O., 2003. Genetic coefficients in the CROPGRO-soybean model: Links to field performance and

genomics. Agron. J. 95, 32–51. https://doi.org/10.2134/agronj2003.0032
Boote, K.J., Sau, F., Hoogenboom, G., Jones, J.W., 2008. Experience with water balance, evapotranspiration, and predictions of water stress effects in the CROPGRO model. Response Crop. to Ltd. water Underst. Model. water Stress Eff. plant growth Process. 59–103. https://doi.org/10.2134/advagricsystmodel1.c3
Brown, H.E., Huth, N.I., Holzworth, D.P., Teixeira, E.I., Zyskowski, R.F., Hargreaves, J.N.G., Moot, D.J., 2014. Plant Modelling Framework: Software for building and running crop models on the APSIM platform. Environ. Model. Softw. 62, 385–398. https://doi.org/10.1016/j.envsoft.2014.09.005
Butler, E.E., Mueller, N.D., Huybers, P., 2018. Peculiarly pleasant weather for US maize. Proc. Natl. Acad. Sci. U. S. A. 115, 11935–11940. https://doi.org/10.1073/pnas.1808035115
Butler, K., 2015. Mann-Kendall for autocorrelated data.
Cairns, J.E., Hellin, J., Sonder, K., Araus, J.L., MacRobert, J.F., Thierfelder, C., Prasanna, B.M., 2013. Adapting maize production to climate change in sub-Saharan Africa. Food Secur. 5, 345–360. https://doi.org/10.1007/s12571-013-0256-x
Carberry, P.S., Abrecht, D.G., 1991. Tailoring crop models to the semiarid tropics, in: Muchow, R.C., Bellamy, J.A. (Eds.), Climatic Risk in Crop Production: Models and Management for the Semi-Arid Tropics and Subtropics. CAB International, Wallingford, UK, pp. 157–82.
Challinor, A.J., Koehler, A.K., Ramirez-Villegas, J., Whitfield, S., Das, B., 2016. Current warming will reduce yields unless maize breeding and seed systems adapt immediately. Nat. Clim. Chang. 6, 954–958. https://doi.org/10.1038/nclimate3061
Chen, J., Brissette, F.P., Leconte, R., 2012. WeaGETS – a Matlab-based daily scale weather generator for generating precipitation and temperature. Procedia Environ. Sci. 13, 2222–2235. https://doi.org/10.1016/j.proenv.2012.01.211
Chen, P., Liu, Y., 2014. The impact of climate change on summer maize phenology in the northwest plain of Shandong province under the IPCC SRES A1B scenario, in: IOP Conference Series: Earth and Environmental Science. IOP Publishing, pp. 1–6. https://doi.org/10.1088/1755-1315/17/1/012053
Chinene, V.R.N., 1985. Generation of field data for validation of crop models in Zambia, in: Woode, P.R. (Ed.), XI International Forum on Soil Taxonomy and Agrotechnology Transfer, Zambia, July 15 - August 1, 1985. Lusaka, Zambia, pp. 181–186.
Chisanga, C.B., Phiri, E., Chinene, V.R.N., 2017. Statistical Downscaling of Precipitation and Temperature Using Long Ashton Research Station Weather Generator in Zambia: A Case of Mount Makulu Agriculture Research Station. Am. J. Clim. Chang. 6, 487–512. https://doi.org/10.4236/ajcc.2017.63025
Chisanga, C.B., Phiri, E., Chizumba, S., Sichingabula, H., 2015. Evaluating CERES-Maize Model Using Planting Dates and Nitrogen Fertilizer in Zambia. J. Agric. Sci. 7, 1–20.
Costa, A.C., Soares, A., 2009. Homogenization of climate data: Review and new perspectives using geostatistics. Math. Geosci. 41, 291–305. https://doi.org/10.1007/s11004-008-9203-3
Crafts-Brandner, S.J., Salvucci, M.E., 2002. Sensitivity of Photosynthesis Heat Stress in a C4 Plant , Maize , to Heat Stress. Plant Physiol. 129, 1773–1780. https://doi.org/10.1104/pp.002170.or

CSIRO, BOM, 2015. Climate Change in Australia Information for Australia's Natural Resource Management Regions: Technical Report.
Dahmardeh, M., 2012. Effects of sowing date on the growth and yield of maize cultivars (Zea mays L.) and the growth temperature requirements. African J. Biotechnol. 11, 12450–12453. https://doi.org/10.5897/AJB12.201
Dalgliesh, N., Hochman, Z., Huth, N., Holzworth, D., 2016. A protocol for the development of APSoil parameter values for use in APSIM.
Das, H.P., Adamenko, T.I., Anaman, K.A., Gommes, R.G., Johnson, G., 2003. Agrometeorology related to extreme events (No. 201), Technical Note. Geneva, Switzerland.
Daur, I., Ozalkan, C., Sen, O.F., Sepetoglu, H.T., 2010. Relationship between some plant growth parameters and grain yield of chickpea (Cicer arietinum L.) during different growth stages. Turkish J. F. Crop. 15, 79–83.
de Mendiburu, F., 2016. agricolae: Statistical Procedures for Agricultural Research. R package version 1.2-4.
Deb, P., Kiem, A.S., Babel, M.S., Chu, S.T., Chakma, B., 2015a. Evaluation of climate change impacts and adaptation strategies for maize cultivation in the Himalayan foothills of India. J. Water Clim. Chang. 6, 596–614. https://doi.org/10.2166/wcc.2015.070
Deb, P., Shrestha, S., Babel, M.S., 2015b. Forecasting climate change impacts and evaluation of adaptation options for maize cropping in the hilly terrain of Himalayas: Sikkim, India. Theor. Appl. Climatol. 121. https://doi.org/10.1007/s00704-014-1262-4
Devak, M., Dhanya, C.T., 2014. Downscaling of Precipitation in Mahanadi Basin, India. Int. J. Civ. Eng. Res. 5, 111–120.
Dokoohaki, H., Gheysari, M., Mousavi, S.-F., Hoogenboom, G., 2017. Effects of different irrigation regimes on soil moisture availability evaluated by CSM-CERES-Maize model under semi-arid condition. Ecohydrol. Hydrobiol. 17, 207–216. https://doi.org/10.1016/j.ecohyd.2017.06.001
Dokoohaki, H., Gheysari, M., Mousavi, S.-F., Zand-Parsa, S., Miguez, F.E., Archontoulis, S. V., Hoogenboom, G., 2016. Coupling and testing a new soil water module in DSSAT CERES-Maize model for maize production under semi-arid condition. Agric. Water Manag. 163, 90–99. https://doi.org/10.1016/j.agwat.2015.09.002
Dos Santos, C.A.C., Dantas, L.G., De Brito, J.I.B., Rao, T.V.R., 2011. Trends in indices for extremes in daily temperature and precipitation over Utah, USA. Int. J. Climatol. 28.
du Plessis, J., 2003. Maize production. Resour. Cent. Dir. Agric. Inf. Serv. 1–38.
Famba, I.S., 2011. The Challenges of Conservation Agriculture to Increase Maize Yield in Vulnerable Production Systems in Central Mozambique. University of Natural Resources and Applied Life Sciences, Vienna.
Fetahu, S., Aliu, S., Rusinovci, I., Elezi, F., Bislimi, K., Behiluli, A., Shabani, Q., 2014. Variation of physiological growth indices, biomass and dry matter yield in some maize hybrids. Albanian J. Agric. Sci. 69–73.
Fodor, N., Challinor, A., Droutsas, I., Ramirez-Villegas, J., Zabel, F., Koehler, A.-K., Foyer, C.H., 2017. Integrating Plant Science and Crop Modeling: Assessment of the Impact of Climate Change on Soybean and Maize Production. Plant Cell Physiol. 58, 1833–1847. https://doi.org/10.1093/pcp/pcx141
Fonseca, D., Carvalho, M.J., Marta-Almeida, M., Melo-Goncalves, P., Rocha, A.,

2016. Recent trends of extreme temperature indices for the Iberian Peninsula. Phys. Chem. Earth 94, 66–76. https://doi.org/10.1016/j.pce.2015.12.005
Fosu-mensah, B.Y., 2012. Modelling maize (Zea mays L.) productivity and impact of climate change on yield and nutrient utilization in sub-humid Ghana, Ecology and Development Series.
Fowler, H.J., Blenkinsop, S., Tebaldi, C., 2007. Linking climate change modelling to impacts studies: Recent advances in downscaling techniques for hydrological modelling. Int. J. Climatol. 27, 1547–1578.
Fumpa-Makano, R., 2011. Forests and Climate Change Integrating Climate Change Issues into National Forest Programmes and Policy Frameworks, Background Paper for the National Workshop. Lusaka.
Garrison, M.V. V, Batchelor, W.D.D., Kanwar, R.S.S., Ritchie, J.T.T., Kanwar, R.S.S., Batchelor, W.D.D., Garrison, M.V. V, Batchelor, W.D.D., Kanwar, R.S.S., Ritchie, J.T.T., 1999. Evaluation of the CERES-Maize water and nitrogen balances under tile-drained conditions. Agric. Syst. 62, 189–200. https://doi.org/10.1016/S0308-521X(99)00064-5
GIZ, 2014. Integrating Climate Change into Financial Planning: Climate Proofing Manual for Zambia.
Gomez, K.A., Gomez, A.A., 1984. Statistical Procedures for Agriculture Research, Second Edi. ed. John Wiley & Sons, New York.
GRZ, UNDP, 2007. Enabling activities for the preparation of Zambia's second national communication to the United Nations Framework Convention on Climate Change (UNFCCC) Project.
Guan, K., Sultan, B., Biasutti, M., Baron, C., Lobell, D.B., 2017. Assessing climate adaptation options and uncertainties for cereal systems in West Africa. Agric. For. Meteorol. 291–305. https://doi.org/10.1016/j.agrformet.2016.07.021
Guenang, G.M., Kamga, F.M., 2014. Computation of the Standardized Precipitation Index (SPI) and Its Use to Assess Drought Occurrences in Cameroon over Recent Decades. J. Appl. Meteorol. Climatol. Vol. 2310–2324. https://doi.org/10.1175/JAMC-D-14-0032.1
Hao, Z., Ju, Q., Jiang, W., Zhu, C., 2013. Characteristics and scenarios projection of climate change on the tibetan plateau. Sci. World J. 9. https://doi.org/https://doi.org/10.1155/2013/129793
Harris, G.R., Collins, M., Sexton, D.M.H., Murphy, J.M., Booth, B.B.B., 2010. Probabilistic projections for 21st century European climate. Nat. Hazards Earth Syst. Sci. 10, 2009–2020. https://doi.org/10.5194/nhess-10-2009-2010
Harrison, S.R., 1990. Regression of a model on real-system output: An invalid test of model validity. Agric. Syst. 34, 183–190. https://doi.org/10.1016/0308-521X(90)90083-3
Hashmi, M.Z., Shamseldin, A.Y., Melville, B.W., 2009. Downscaling of future rainfall extreme events : a weather generator based approach. 18th World IMACS Congr. MODSIM09 Int. Congr. Model. Simul. Model. Simul. Soc. Aust. New Zeal. Int. Assoc. Math. Comput. Simul. July 2009 3928–3934.
Hassan, Z., 2014. Impact of climate change on rainfall over Kerian , Malaysia with Long Ashton Research Station Weather Generator.
Hassan, Z., Harun, S., 2013. Impact of Climate Change on Rainfall Over Kerian, Malaysia With Long Ashton Research Station Weather Generator (LARS-WG). Malaysian J. Civ. Eng. 25, 33–44.
Hassan, Z., Shamsudin, S., Harun, S., 2014. Application of SDSM and LARS-WG for simulating and downscaling of rainfall and temperature. Theor. Appl.

Climatol. 116, 243–257. https://doi.org/10.1007/s00704-013-0951-8
Hatfield, J.L., Prueger, J.H., 2015. Temperature extremes: Effect on plant growth and development. Weather Clim. Extrem. 10. https://doi.org/10.1016/j.wace.2015.08.001
He, L., Asseng, S., Zhao, G., Wu, D., Yang, X., Zhuang, W., 2015. Agricultural and Forest Meteorology Impacts of recent climate warming , cultivar changes , and crop management on winter wheat phenology across the Loess Plateau of China. Agric. For. Meteorol. 200, 135–143. https://doi.org/10.1016/j.agrformet.2014.09.011
Hoogenboom, G., Jones, J.W., Porter, C.H., Wilkens, P.W., Boote, K.J., Hunt, L. a., Tsuji, G.Y., 2010. Decision Support System for Agrotechnology Transfer Version 4.5. Volume 1: Overview. University of Hawaii, Honolulu, HI., Agricultural Systems.
Hoogenboom, G., Wilkens, P.W., Tsuji, G.Y., 1999. DSSAT v3, volume 4. University of Hawaii, Honolulu, Hawaii.
Huang, J., Zhang, J., Zhang, Z., Sun, S., Yao, J., 2011. Simulation of extreme precipitation indices in the Yangtze River basin by using statistical downscaling method (SDSM). Theor. Appl. Climatol. 1–19. https://doi.org/10.1007/s00704-011-0536-3
Hudson, N.I., Ruane, A.C., 2015. Appendix 2. Guide for Running AgMIP Climate Scenario Generation Tools with R in Windows, Version 2.3, in: Rosenzweig, C., Hillel, D. (Eds.), Handbook of Climate Change and Agroecosystems: The Agricultural Model Intercomparison and Improvement Project (AgMIP) Integrated Crop and Economic Assessments, Part 1. Imperial College Press, pp. 387–440.
Hussain, J., Khaliq, T., Ahmad, A., Akhtar, J., 2018. Performance of four crop model for simulations of wheat phenology, leaf growth , biomass and yield across planting dates. PLoS One 13, 1–14.
Inamullah, R.N., Shah, N.H., Arif, M., Siddiq, M., Mian, I.A., 2011. Correlations among grain yield and yield attributes in maize hybrids at various nitrogen levels. Sarhad J. Agric. 27, 531–538.
IPCC-TGCIA, 2007. General Guidelines on the Use of Scenario Data for Climate Impact and Adaptation Assessment. Version 2. Task Group on Scenarios for Climate Impact Assessment Intergovernmental Panel on Climate Change. https://doi.org/10.1144/SP312.4
IPCC, 2013a. Climate Change 2013: The Physical Science Basis. Contribution of Working Group I to the Fifth Assessment Report of the Intergovern- mental Panel on Climate Change, Intergovernmental Panel on Climate Change, Working Group I Contribution to the IPCC Fifth Assessment Report (AR5). Cambridge University Press, Cambridge, United Kingdom and New York, NY, USA, Geneva, Switzerland. https://doi.org/10.1029/2000JD000115
IPCC, 2013b. Summary for Policymakers, in: Stocker, T.F., D. Qin, G.-K. Plattner, M. Tignor, S.K. Allen, J. Boschung, A. Nauels, Y. Xia, V.B. and P.M.M. (Eds.), Climate Change 2013: The Physical Science Basis. Contribution of Working Group I to the Fifth Assessment Report of the Intergovernmental Panel on Climate Change. Cambridge University Press, Cambridge, UK, and New York, NY, USA, New York, NY, USA, p. 28. https://doi.org/10.1017/CBO9781107415324.004
IPCC, 2007. The Physical Science Basis. Contribution of Working Group I to the Fourth Assessment Report of the Intergovernmental Panel on Climate Change,

New York Cambridge University Press. Cambridge University Press, Cambridge, United Kingdom and New York, NY, USA. https://doi.org/10.1038/446727a
Jaggard, K.W., Qi, A., Ober, E.S., 2010. Possible changes to arable crop yields by 2050. Philos. Trans. R. Soc. Lond. B. Biol. Sci. 365, 2835–51. https://doi.org/10.1098/rstb.2010.0153
JAICAF, 2008. Agriculture and forestry in Zambia: present situation and issues for development. Lusaka.
Jamieson, P.D., Brooking, I.R., Porter, J.R., Wilson, D.R., 1995. Prediction of leaf appearance in wheat: a question of temperature. F. Crop. Res. 41, 35–44. https://doi.org/10.1016/0378-4290(94)00102-I
Jin, Z., Prasad, R., Shriver, J., 2016. Crop model- and satellite imagery-based recommendation tool for variable rate N fertilizer application for the US Corn system. Precis. Agric. 1–22. https://doi.org/10.1007/s11119-016-9488-z
Jing, Q., Shang, J., Huffman, T., Qian, B., Pattey, E., Liu, J., Dong, T., Drury, C.F., 2017. Using the CSM – CERES – Maize model to assess the gap between actual and potential yields of grain maize. J. Agric. Sci. 155, 239–260. https://doi.org/10.1017/S0021859616000290
Jones, C.A., Kiniry, J.R. (James R., Dyke, P.T., 1986. CERES-Maize: A simulation model of maize growth and development. Texas A & M University Press, Texas, USA.
Jones, J.W., Hoogenboom, G., Porter, C.H., Boote, K.J., Batchelor, W.D., Hunt, L.A., Wilkens, P.W., Singh, U., Gijsman, A.J., Ritchie, J.T., 2003. The DSSAT cropping system model. Eur. J. Agron. 18, 235–265. https://doi.org/10.1016/S1161-0301(02)00107-7
Jones, J.W., Hoogenboom, G., Wilkens, P.W., Porter, C.H., Tsuji, G.Y., 2010. Decision Support System for Agrotechnology Transfer Version 4.5. Volume 3. DSSAT v4.5: ICASA Tools. University of Hawaii, Honolulu, HI.
Jones, P.G., Thornton, P.K., 2013. Generating downscaled weather data from a suite of climate models for agricultural modelling applications. Agric. Syst. 114, 1–5. https://doi.org/10.1016/j.agsy.2012.08.002
Jones, P.G., Thornton, P.K., 2003. The potential impacts of climate change on maize production in Africa and Latin America in 2055. Glob. Environ. Chang. 13, 51–59. https://doi.org/10.1016/S0959-3780(02)00090-0
Kandil, E.E.E., 2013. Response of Some Maize Hybrids (Zea mays L.) to Different Levels of Nitrogenous Fertilization. J. Appl. Sci. Res. 9, 1902–1908.
Karmakar, R., Das, I., Dutta, D., Rakshit, A., 2016. Potential Effects of Climate Change on Soil Properties: A Review. Sci. Int. 4, 51–73. https://doi.org/10.17311/sciintl.2016.51.73
Karuma, A.N., Gachene, C.K.K., Gicheru, P.T., Mtakwa, P.W., Amuri, N., 2016. Effects of tillage and cropping systems on maize and beans yield and selected yield components in a semi-arid area of Kenya. Trop. Subtrop. Agroecosystems 19, 167–179.
Kassie, B.T., Van Ittersum, M.K., Hengsdijk, H., Asseng, S., Wolf, J., Rötter, R.P., 2014. Climate-induced yield variability and yield gaps of maize (Zea mays L.) in the Central Rift Valley of Ethiopia. F. Crop. Res. 160, 41–53. https://doi.org/10.1016/j.fcr.2014.02.010
Keating, B.A., Carberry, P.S., Hammer, G.L., Probert, M.E., Robertson, M.J., Holzworth, D., Huth, N.I., Hargreaves, J.N.G., Meinke, H., Hochman, Z., McLean, G., Verburg, K., Snow, V., Dimes, J.P., Silburn, M., Wang, E.,

Browna, S., Bristow, K.L., Asseng, S., Chapman, S., McCown, R.L., Freebairn, D.M., Smith, C.J., 2003. An overview of APSIM, a model designed for farming systems simulation. Eur. J. Agron. 18, 267–288. https://doi.org/10.1016/S1161-0301(02)00108-9

Keating, B.A., McCown, R.L., 2001. Advances in farming systems analysis and intervention. Agric. Syst. 70, 555–579. https://doi.org/10.1016/S0308-521X(01)00059-2

Kiniry, J.R., Williams, J.R., Vanderlip, R.L., Atwood, J.D., Reicosky, D.C., Mulliken, J., Cox, W.J., Mascagni, H.J.J., Hollinger, S.E., Wiebold, W.J., 1997. Evaluation of Two Maize Models for Nine U. S. Locations. Agron. J. 89, 421–426.

Kisaka, M.O., Mucheru-Muna, M., Ngetich, F.K., Mugwe, J.N., Mugendi, D.N., Mairura, F., Muriuki, J., 2015. Using Apsim-Model As a Decision-Support-Tool for Long-Term Integrated-Nitrogen-Management and Maize Productivity Under Semi-Arid Conditions in Kenya. Exp. Agric. 1–21.

Kisaka, O.M., Mucheru-Muna, M., Ngetich, F.K., Mugwe, J.N., Mugendi, D.N., Mairura, F., Muriuki, J., 2016. Using APSIM-model as a decision support tool for long-termin integrated nitrogen management and maize productivity under semi-arid conditions in Kenya. Exp. Agric. 52, 279–299. https://doi.org/10.1017/S0014479715000095

Knörzer, H., Lawes, R., Robertson, M., Graeff-Hönninger, S., Claupein, W., 2011. Evaluation and Performance of the APSIM Crop Growth Model for German Winter Wheat, Maize and Fieldpea Varieties in Monocropping and Intercropping Systems. J. Agric. Sci. Technol. B J. Agric. Sci. Technol. 1, 698–717.

Kucharik, C.J., 2008. Contribution of Planting Date Trends to Increased Maize Yields in the Central United States. Agron. J. https://doi.org/10.2134/agrojnl2007.0145

Lafitte, H.R., Edmeades, G.O., Johnson, E.C., 1997. Temperature responses of tropical maize cultivars selected for broad adaptation. F. Crop. Res. 49, 215–229. https://doi.org/10.1016/S0378-4290(96)01006-4

Lapp, S., Sauchyn, D., Wheaton, E., 2008. Institutional Adaptations to Climate Change Project: Future Climate Change Scenarios for the South Saskatchewan River Basin.

Lewis, S.C., King, A.D., 2017. Evolution of mean , variance and extremes in 21st century temperatures. Weather Clim. Extrem. 15, 10. https://doi.org/10.1016/j.wace.2016.11.002

Liaqat, W., Akmal, M., Ali, J., 2018. Sowing Dates Effect on Production of High Yielding Maize Varieties. Sarhad J. Agric. 34, 102–113. https://doi.org/10.17582/journal.sja/2018/34.1.102.113

Lin, Y., Feng, Z., Wu, W., Yang, Y., Zhou, Y., ABSTR, C.X., 2017. Potential Impacts of Climate Change and Adaptation on Maize in Northeast China. Crop Econ. Prod. Manag. 109, 1476–1490. https://doi.org/10.2134/agronj2016.05.0275

Lin, Y., Wu, W., Ge, Q., 2015. CERES-Maize model-based simulation of climate change impacts on maize yields and potential adaptive measures in Heilongjiang Province, China. J. Sci. Food Agric. 95, 2838–2849. https://doi.org/10.1002/jsfa.7024

Liu, L., Zhu, Y., Tang, L., Cao, W., Wang, E., 2013. Impacts of climate changes, soil nutrients, variety types and management practices on rice yield in East China: a

case study in the Taihu region. F. Crop. Res. 149, 40–48. https://doi.org/10.1016/j.fcr.2013.04.022
Liu, Y., Yang, S.J., Li, S.Q., Chen, F., 2012. Application of the Hybrid-Maize model for limits to maize productivity analysis in a semiarid environment. Sci. Agric. 69, 300–307. https://doi.org/10.1590/S0103-90162012000500003
Liu, Z., Hubbard, K.G., Lin, X., Yang, X., 2013. Negative effects of climate warming on maize yield are reversed by the changing of sowing date and cultivar selection in Northeast China. Glob. Chang. Biol. 19, 3481–3492.
Lizaso, J.I., Boote, K.J., Jones, J.W., Porter, C.H., Echarte, L., Westgate, M.E., Sonohat, G., 2011. CSM-IXIM: A New Maize simulation model for DSSAT version 4.5. Agron. J. 103, 766–779. https://doi.org/10.2134/agronj2010.0423
Lobell, D.B., Bänziger, M., Magorokosho, C., Vivek, B., 2011. Nonlinear heat effects on African maize as evidenced by historical yield trials. Nat. Clim. Chang. 1, 42–45. https://doi.org/10.1038/nclimate1043
Lukeba, J.-C.L., Vumilia, R.K., Nkongolo, K.C.K., Mwabila, M.L., Tsumbu, M., 2013. Growth and Leaf Area Index Simulation in Maize (Zea mays L.) under Small-Scale Farm Conditions in a Sub-Saharan African Region. Am. J. Plant Sci. 4, 575–583. https://doi.org/10.4236/ajps.2013.43075
Ma, L., Ahuja, L.R., Saseendran, S.A., Malone, R.W., Green, T.R., Nolan, B.T., Bartling, P.N.S., Flerchinger, G.N., Boote, K.J., Hoogenboom, G., 2011. Chapter 1 A Protocol for Parameterization and Calibration of RZWQM2 in Field Research, in: Ahuja, L.R., Ma, L. (Eds.), Methods of Introducing System Models into Agricultural Research. ASA, CSSA, SSSA, 5585 Guilford Rd., Madison, WI 53711-5801, USA, p. 64. https://doi.org/10.2134/advagricsystmodel2.c1
MacCarthy, D.S., Kihara, J., Adiku, S.G.K., 2017. Decision support tools for site-specific fertilizer recommendations and agricultural planning in selected countries in sub-Sahara Africa. Nutr. Cycl. Agroecosystems 1–16. https://doi.org/10.1007/s10705-017-9877-3
MacCarthy, D.S., Sommer, R., Vlek, P.L.G., 2009. Modeling the impacts of contrasting nutrient and residue management practices on grain yield of sorghum (Sorghum bicolor (L.) Moench) in a semi-arid region of Ghana using APSIM. F. Crop. Res. 113, 105–115. https://doi.org/10.1016/j.fcr.2009.04.006
Mahlstein, I., Spirig, C., Liniger, M.A., Appenzeller, C., 2015. Estimating daily climatologies for climate indices derived from climate model data and observations. J. Geophys. Res. Atmos. 120, 2808–2818. https://doi.org/10.1002/2014JD022327
Malekabadi, S.R., Pazoki, A., Mehrvar, M.R., 2014. Evaluating the effects Planting date on some Quantitative and Qualitative Characteristics of new Maize Varieties in the Region. Bull. Environ. Pharmacol. Life Sci. 3, 189–192.
Martre, P., Wallach, D., Asseng, S., Ewert, F., Jones, J.W., Rötter, R.P., Boote, K.J., Ruane, A.C., Thorburn, P.J., Cammarano, D., Hatfield, J.L., Rosenzweig, C., Aggarwal, P.K., Angulo, C., Basso, B., Bertuzzi, P., Biernath, C., Brisson, N., Challinor, A.J., Doltra, J., Gayler, S., Goldberg, R., Grant, R.F., Heng, L., Hooker, J., Hunt, L.A., Ingwersen, J., Izaurralde, R.C., Kersebaum, K.C., Müller, C., Kumar, S.N., Nendel, C., O'leary, G., Olesen, J.E., Osborne, T.M., Palosuo, T., Priesack, E., Ripoche, D., Semenov, M.A., Shcherbak, I., Steduto, P., Stöckle, C.O., Stratonovitch, P., Streck, T., Supit, I., Tao, F., Travasso, M., Waha, K., J, J.W.W., Wolf, O., 2015. Multimodel ensembles of wheat growth: Many models are better than one. Glob. Chang. Biol. 21, 911–925.

https://doi.org/10.1111/gcb.12768
Masanganise, J., Chipindu, B., Mhizha, T., Mashonjowa, E., 2012. MODEL PREDICTION OF MAIZE YIELD RESPONSES TO CLIMATE CHANGE IN NORTH-EASTERN ZIMBABWE. African Crop Sci. J. 20, 505–515.
Masanganise, J., Magodora, M., Mapuwei, T., Basira, K., 2014. An assessment of CMIP5 global climate model performance using probability density functions and a match metric method. Sci. Insights An Int. J. 4, 1–8.
Masoud, H., Philippe, G., Taha, B.M.J.O., André, H., 2005. Automated Statistical Downscaling (ASD) User's Guide For use with MATLAB.
Mburu, M.W.K., Maobe, S.N., Akundabweni, L.S.M., Ndufa, J.K., Mureithi, J.G., Gachene, C.K.K., Makini, F.W., Okello, J.J., 2010. Effect of Mucuna green manure and inforganic fertilizer urea nitrogen sources and application rates on harvest index of maize (Zea mays L.). World J. Agriculutral Sci.
McCown, R.L., Hammer, G.L., Hargreaves, J.N.G., Holzworth, D., Huth, N.I., 1995. APSIM: an agricultural production system simulation model for operational research. Math. Comput. Simul. 39, 225–231. https://doi.org/10.1016/0378-4754(95)00063-2
McCown, R.L.L., Hammer, G.L.L., Hargreaves, J.N.G.N.G., Holzworth, D.P.P., Freebairn, D.M.M., 1996. APSIM: a novel software system for model development, model testing and simulation in agricultural systems research. Agric. Syst. 50, 255–271. https://doi.org/10.1016/0308-521X(94)00055-V
Mckague, K., Rudra, R., Ogilvie, J., Ahmed, I., Gharabaghi, B., 2005. Evaluation of Weather Generator ClimGen for Southern Ontario. Can. Water Resour. J. 30, 315–330.
McKee, G.W., 1964. A Coefficient for Computing Leaf Area in Hybrid Corn. Agron. J. 56, 240. https://doi.org/10.2134/agronj1964.00021962005600020038x
Mcleod, A.I., 2011. Kendall: Kendall rank correlation and Mann-Kendall trend test. R package version 2.2.
McMaster, G.S., Wilhelm, W., 1997. Growing degree-days : one equation , two interpretations. Agric. For. Meteorol. 87, 291–300.
McSweeney, C.F., Jones, R.G., Booth, B.B.B., Lee, R.W., Rowell, D.P., Jones, C.F.M.R.G., Rowell, R.W.L.D.P., 2012. Selecting ensemble members to provide regional climate change information. J. Clim. 25, 7100–7121. https://doi.org/10.1175/JCLI-D-11-00526.1
Mesfin, T., Moeller, C., Parsons, D., Meinke, H., 2015. Maize (Zea mays L.) productivity as influenced by sowing date and nitrogen fertiliser rate at Melkassa, Ethiopia: parameterisation and evaluation of APSIM-Maize 20–24.
Meza, F.J., 2013. Recent trends and ENSO influence on droughts in Northern Chile: An application of the Standardized Precipitation Evapotranspiration Index. Weather Clim. Extrem. 1, 51–58. https://doi.org/10.1016/j.wace.2013.07.002
Mohamed, E., Lahcen, B., 2015. Using Statistical Downscaling of GCM Simulations to Assess Climate Change Impacts on Drought Conditions in the Northwest of Morocco. Mod. Appl. Sci. 9, 11. https://doi.org/10.5539/mas.v9n2p1
Monsi, M., Saeki, T., 2004. On the Factor Light in Plant Communities and its Importance for Matter Production. Ann. Bot. 95, 549–567. https://doi.org/10.1093/aob/mci052
Mourice, S.K., Rweyemamu, C.L., Tumbo, S.D., Amuri, N., 2014. Maize Cultivar Specific Parameters for Decision Support System for Agrotechnology Transfer (DSSAT) Application in Tanzania. Am. J. Plant Sci. 5, 821–833. https://doi.org/10.4236/ajps.2014.56096

Mousavi, R., Aboutalebian, M.A., Sepehri, A., 2012. The effects of on-farm seed priming and planting date on emergence characteristics , yield and yield components of a corn cultivar (SC 260) in Hamedan. Ann. Biol. Res. 3, 4427–4434.

Msongaleli, B.M., Rwehumbiza, F., Tumbo, S.D., Kihupi, N., 2015. Impacts of Climate Variability and Change on Rainfed Sorghum and Maize: Implications for Food Security Policy in Tanzania. J. Agric. Sci. 7, 124–142. https://doi.org/10.5539/jas.v7n5p124

MTENR, 2010. National Climate Change Response Strategy (NCCRS) Ministry of Tourism, Environment and Natural Resources. Government of the Republic of Zambia. Lusaka, Zambia.

MTENR, GEF, UNDP, 2007. Formulation of the National Adaptation Programme of Action on Climate Change. Ministry of Tourism, Environmental and Natural Resources, Lusaka, Zambia.

Mthandi, J., Kahimba, F.C., Tarimo, A.K.P.R., Salim, B.A., Lowole, M.W., 2014. Modification, calibration and validation of APSIM to suit maize (Zea mays L.) production system: A case of Nkango Irrigation Scheme in Malawi. Am. J. Agric. For. 2, 1–11. https://doi.org/10.11648/j.ajaf.s.2014020601.11

Muchanga, M., 2012. A Survey of Public Particpation in Planning for Climate Change Adaptation among Selected Areas of Zambia's Lusaka Province. Am. Int. J. Contemp. Res. 2, 81–90.

Muchow, R.C., Sinclair, T.R., Bennett, J.M., 1990. Temperature and Solar Radiation Effects on Potential Maize Yield across Locations. Agron. J. 82, 338–343.

Mulenga, B.P., Wineman, A., 2014. Climate Trends and Farmers' Perceptions of Climate Change in Zambia.

Mwansa, F.B., 2016. Assessing the potential of conservation agriculture to off-set the effects of climate change on crop productivity using APSIM. University of Zambia.

Myoung, B., Hee Kim, S., Kim, J., Kafatos, M., 2016. Regional Variations of Optimal Sowing Dates of Maize for the Southwestern. Trans. ASABE 59, 1759–1769. https://doi.org/10.13031/trans.59.11583

Nairn, J., Fawcett, R., 2014. The Excess Heat Factor: A Metric for Heatwave Intensity and Its Use in Classifying Heatwave Severity. Int. J. Environ. Res. Public Health 12, 227–253. https://doi.org/10.3390/ijerph120100227

Nairn, J., Fawcett, R., 2013. Defining heatwaves: heatwave defined as a heat-impact event servicing all communiy and business sectors in Australia, CAWCR technical report. Kent Town, Australia. https://doi.org/551.5250994

Nakicenovic, N., Alcamo, J., Davis, G., Vries, B. de, Fenhann, J., Gaffin, S., Gregory, K., Grübler, A., Jung, T.Y., Kram, T., Rovere, E.L. La, Michaelis, L., Mori, S., Morita, T., Pepper, W., Pitcher, H., Price, L., Riahi, K., Roehrl, A., Rogner, H.-H., Sankovski, A., Schlesinger, M., Shukla, P., Smith, S., Swart, R., Rooijen, S. van, Victor, N., Dadi, Z., 2000. Special Report on Emissions Scenarios: A Special Report of Working Group III of the Intergovernmental Panel on Climate Change. Cambridge University Press, Cambridge, Geneva, Switzerland.

Nangia, V., Ahmad, M. ud D., Jiantao, D., Changrong, Y., Hoogenboom, G., Xurong, M., Wenqing, H., Shuang, L., Qin, L., 2010. Modeling the field-scale effects of conservation agriculture on land and water productivity of rainfed maize in the Yellow River Basin, China. Int. J. Agric. Biol. Eng. 3, 5–17. https://doi.org/10.3965/j.issn.1934-6344.2010.02.005-017

Nape, K.M., 2011. Using Seasonal Rainfall with APSIM to Improve Maize Production in the Modder River Catchment. University of the Free State.
NCA, 2014. Highlights of Climate Change Impacts in the United States: The Third National Climate Assessment. U.S. Global Change Research Program. U.S. Government Printing Office.
NCA, 2010. Scenarios for Research and Assessment of Our Climate Future: Issues and Methodological Perspectives for the U.S., NCA Report Series, Volume 6. Workshop held at Arlington, Virginia on December 6-8, 2010. Arlingtone, Virginia.
Neild, R.E., Seeley, M.W., Richman, N.H., 1978. The computation of agriculturally oriented normals from monthly climatic summaries. Agric. Meteorol. 19, 181–187. https://doi.org/10.1016/0002-1571(78)90010-9
Nemati, A.R., Sharifi, R.S., 2012. Effects of rates and nitrogen application timing on yield, agronomic characterstics and nitrogen use efficiency in corn. Int. J. Agric. Crop Sci. 4, 534–539.
NSW, 2009. Maize growth and development. NSW Department of Primary Industries, State of New South Wales.
Osman, Y., Al-Ansari, N., Abdellatif, M., Aljawad, S.B., Knutsson, S., 2014. Expected Future Precipitation in Central Iraq Using LARS-WG Stochastic Weather Generator. Engineering 3, 948–959. https://doi.org/10.4236/eng.2014.613086
Otterå, O.H., Bentsen, M., Bethke, I., Kvamstø, N.G., 2009. Geoscientific Model Development Simulated pre-industrial climate in Bergen Climate Model (version 2): model description and large-scale circulation features. Geosci. Model Dev 2, 197–212.
Palijah, S., 2015. The implications of climate variability and change on rural household food security in Zambia: experiences from Choma District, Southern Province. University of Nairobi, Kenya.
Panda, D.K., Panigrahi, P., Mohanty, S., Mohanty, R.K., Sethi, R.R., 2016. The 20th century transitions in basic and extreme monsoon rainfall indices in India: Comparison of the ETCCDI indices. Atmos. Res. 181, 220–235. https://doi.org/10.1016/j.atmosres.2016.07.002
Pang, X.P., Letey, J., Wu, L., 1997. Yield and Nitrogen Uptake Prediction by CERES-Maize Model under Semiarid Conditions. Soil Sci Soc Am J 61, 254–256.
Perkins, S.E., Alexander, L. V., 2013. On the Measurement of Heat Waves. J. Clim. 26, 4500–4517.
Peterson, T.C., 2005. Climate change indices. World Meteorol. Organ. Bull. 54, 83–86.
Peykarestan, B., Seify, M., 2012. Impact of sowing date on growth and yield attributes of Pop Corn grown under different densities 3, 85–91.
Phiri, J.S., Moonga, E., Mwangase, O., Chipeta, G., 2013. Adaptation of zambian agriculture to climate change: a comprehensive review of the utilisation of the agro-ecological regions. Lusaka.
Qian, B., Gameda, S., Hayhoe, H., Jong, R. De, Bootsma, A., 2004. Comparison of LARS-WG and AAFC-WG stochastic weather generators for diverse Canadian climates. Most 26, 175–191. https://doi.org/10.3354/cr00755
Qian, B., Hayhoe, H., Gameda, S., 2005. Evaluation of the stochastic weather generators LARS-WG and AAFC-WG for climate change impact studies. Clim. Res. 29, 3–21.

Ritchie, J.T., Porter, C.H., Suleiman, A.A., Judge, J., Jones, J.W., 2009. Extension of an Existing Model for Soil Water Evaporation and Redistribution under High Water Content Conditions. Soil Sci. Soc. Am. J. https://doi.org/10.2136/sssaj2007.0325

Rodríguez, A., Ruiz-Ramos, M., Palosuo, T., Carter, T.R., Fronzek, S., Lorite, I.J., Ferrise, R., Pirttioja, N., Bindi, M., Baranowski, P., Buis, S., Cammarano, D., Chen, Y., Dumont, B., Ewert, F., Gaiser, T., Hlavinka, P., Hoffmann, H., Höhn, J.G., Jurecka, F., Kersebaum, K.C., Krzyszczak, J., Lana, M., Mechiche-Alami, A., Minet, J., Montesino, M., Nendel, C., Porter, J.R., Ruget, F., Semenov, M.A., Steinmetz, Z., Stratonovitch, P., Supit, I., Tao, F., Trnka, M., de Wit, A., Rötter, R.P., 2019. Implications of crop model ensemble size and composition for estimates of adaptation effects and agreement of recommendations. Agric. For. Meteorol. 264, 351–362. https://doi.org/10.1016/J.AGRFORMET.2018.09.018

Rosenzweig, C., Jones, J., Antle, J., Hatfield, J., 2015. Protocols for AgMIP Regional Integrated Assessments Version 6.0.

Rosenzweig, Cynthia, Jones, J.W., Hatfield, J.L., Antle, J.M., Ruane, A.C., Mutter, C.Z., 2014. The Agricultural Model Intercomparison and Improvement Project.

Rosenzweig, C., Jones, J.W., Hatfield, J.L., Ruane, A.C., Boote, K.J., Thorburn, P., Antle, J.M., Nelson, G.C., Porter, C., Janssen, S., Asseng, S., Basso, B., Ewert, F., Wallach, D., Baigorria, G., Winter, J.M., 2013. The Agricultural Model Intercomparison and Improvement Project (AgMIP): Protocols and pilot studies. Agric. For. Meteorol. 170, 166–182. https://doi.org/10.1016/J.AGRFORMET.2012.09.011

Rosenzweig, C., Jones, J.W., Hatfield, J.R., Antle, J.M., Ruane, A.C., Boote, K.J., Thorburn, P.J., Valdivia, R.O., Porter, C.H., Janssen, S., Wiebe, K., Mutter, C.Z., Lifson, S., Contreras, E.M., Athanasiadis, I., Baigorria, G., Cammarano, D., Descheemaeker, K., Hoogenboom, G., Lizaso, J., McDermid, S., Wallach, D., Adiku, S.D.K., Ahmad, A., Beletse, Y., Dileepkumar, G., Kihara, J., Masikati, P., Ponnusamy, P., Subash, N., Rao, K.P.C., Zubair, L., 2014. Regional Integrated Assessments of Farming Systems in Sub-Saharan Africa and South Asia. Summary Report: Phase 1.

Ruane, A.C., Cecil, L.D., Horton, R.M., Gordón, R., McCollum, R., Brown, D., Killough, B., Goldberg, R., Greeley, A.P., Rosenzweig, C., 2013. Climate change impact uncertainties for maize in Panama: Farm information, climate projections, and yield sensitivities. Agric. For. Meteorol. 170, 132–145. https://doi.org/10.1016/j.agrformet.2011.10.015

Ruane, A.C., Goldberg, R., Chryssanthacopoulos, J., 2015. Climate forcing datasets for agricultural modeling: Merged products for gap-filling and historical climate series estimation. Agric. For. Meteorol. 200, 233–248. https://doi.org/10.1016/j.agrformet.2014.09.016

Rudnick, D.R., Irmak, S., 2013. Impact of Water and Nitrogen Management Strategies on Maize Yield and Water Productivity Indices Under Linear-Move Sprinkler Irrigation. Trans. Asabe 56, 1769–1783. https://doi.org/10.13031/trans.56.10215

Ruiter, A., 2012. Delta-change approach for CMIP5 GCMs. Internship Report version 3. De Bilt.

Saberi, A.R., Aishah, H.S., 2013. Growth Analysis of Forage Sorghum (Sorghum Bicolor L) Varieties Under Influenced of Salinity and Irrigation Frequency. Int. J. Biotechnol. 2, 130–140.

Salo, T.J., Palosuo, T., Kersebaum, K.C., Nendel, C., Ewert, F., Bindi, M., Calanca, P., Klein, T., Salo, T.J., Palosuo, T., Kersebaum, K.C., Nendel, C., Angulo, C., 2016. Comparing the performance of 11 crop simulation models in predicting yield response to nitrogen fertilization. J. Agric. Sci. 154, 1218–1240. https://doi.org/10.1017/S0021859615001124

Sánchez, B., Rasmussen, A., Porter, J.R., 2014. Temperatures and the growth and development of maize and rice: A review. Glob. Chang. Biol. 20. https://doi.org/10.1111/gcb.12389

Sangoi, L., 2001. Understanding plant density effects on maize growth and development: an important issue to maximize grain yield. Ciência Rural. St. Maria 31, 159–168. https://doi.org/10.1590/S0103-84782001000100027

Saxton, K.E., Rawls, W.J., 2006. Soil Water Characteristic Estimates by Texture and Organic Matter for Hydrologic Solutions. Soil Sci. Soc. Am. J. 70, 1569–1578. https://doi.org/10.2136/sssaj2005.0117

Saxton, K.E., Willey, P.H.P., 2006. The SPAW model for agricultural field and pond hydrologic simulation, in: SPAW Model. pp. 1–37. https://doi.org/10.1201/9781420037432.ch17

Schauberger, B., Archontoulis, S., Arneth, A., Balkovic, J., Ciais, P., Deryng, D., Elliott, J., Folberth, C., Khabarov, N., Müller, C., Pugh, T.A.M., Rolinski, S., Schaphoff, S., Schmid, E., Wang, X., Schlenker, W., Frieler, K., 2017. Consistent negative response of US crops to high temperatures in observations and crop models. Nat. Commun. 8, 1–9. https://doi.org/10.1038/ncomms13931

Semenov, M.A., Barrow, E.M., 2002. LARS-WG: A Stochastic Weather Generator for Use in Climate Impact Studies version 3. User Manual. User Manual, Hertfordshire, UK.

Semenov, M.A., Barrow, E.M., 1997. Use of a stochastic weather generator in the development of climate change scenarios. Clim. Change 35, 397–414. https://doi.org/10.1023/A:1005342632279

Semenov, M.A., Brooks, R.J., 1999. Spatial interpolation of the LARS-WG stochastic weather generator in Great Britain. Clim. Res. 11, 137–148. https://doi.org/10.3354/cr011137

Semenov, M.A., Brooks, R.J., Barrow, E.M., Richardson, C.W., 1998. Comparison of the WGEN and LARS-WG stochastic weather generators for diverse climates. Clim. Res. 10, 95–107. https://doi.org/10.3354/cr010095

Semenov, M.A., Stratonovitch, P., 2015. Adapting wheat ideotypes for climate change : accounting for uncertainties in CMIP5 climate projections. Clim. Res. 65, 123–139. https://doi.org/10.3354/cr01297

Semenov, M.A., Stratonovitch, P., 2010. Use of multi-model ensembles from global climate models for assessment of climate change impacts. Clim. Res. 41, 1–14. https://doi.org/10.3354/cr00836

Shamsnia, S.A., Pirmoradian, N., 2013. Evaluation of different GCM models and climate change scenarios using LARS_WG model in simulating meteorological data (Case study: Shiraz synoptic station, Fars Province, Iran). IOSR J. Eng. 3, 2250–3021.

Sharifi, R.S., Namvar, A., 2016. Effects of time and rate of nitrogen application on phenology and some agronomical traits of maize (Zea mays L.). Biologija 62, 35–45.

Sichingabula, H.M., 1998. Rainfall variability, drought and implications of its impacts on Zambia, 1886-1996. IAHS-AISH Publ. 125–134.

Sinclair, T.R., Seligman, N.G., 1995. Crop Modeling: From Infancy to Maturity.

Agron. J. 88, 698–704. https://doi.org/doi:10.2134/agronj1996.00021962008800050004x
Singh, J., Hadda, M.S., 2014. Phenology and thermal indices of maize (Zea mays L.) influenced by subsoil compaction and nitrogen fertilization under semi-arid irrigated conditions. J. Appl. Nat. Sci. 6, 349–355.
Soil Survey Staff, 2014. Keys to Soil Taxonomy, Tenth Edition, 12th Edition, Natural Resources Conservation Service. Washington, DC.
Soler, C.M.., Sentelhas, P.C., Hoogenboom, G., 2005. Thermal time for phenological development of four maize hybrids grown off-season in a subtropical environment. J. Agric. Sci. https://doi.org/10.1017/S0021859605005198
Soltani, M., Laux, P., Kunstmann, H., Stan, K., Sohrabi, M.M., Molanejad, M., Sabziparvar, A.A., Ranjbar SaadatAbadi, A., Ranjbar, F., Rousta, I., Zawar-Reza, P., Khoshakhlagh, F., Soltanzadeh, I., Babu, C.A., Azizi, G.H., Martin, M. V., 2016. Assessment of climate variations in temperature and precipitation extreme events over Iran. Theor. Appl. Climatol. 126, 775–795. https://doi.org/10.1007/s00704-015-1609-5
Spitters, C.J.T., Toussaint, H.A.J.M., Goudriaan, J., 1986. Separating the diffuse and direct component of global radiation and its implications for modeling canopy photosynthesis Part I. Components of incoming radiation. Agric. For. Meteorol. 38, 217–229. https://doi.org/10.1016/0168-1923(86)90060-2
Stagge, J.H., Tallaksen, L.M., Xu, C.-Y., Van Lanen, H.A.J., 2014. Standardized precipitation-evapotranspiration index (SPEI): Sensitivity to potential evapotranspiration model and parameters, in: Hydrology in a Changing World: Environmental and Human Dimensions Proceedings of FRIEND-Water. IAHS Publ, Montpellier, France, pp. 1–8.
Steffen, W., Hughes, L., Perkins, S., 2014. Heatwaves: Hotter, Longer, More Often. Climate Council of Australian Ltd.
Stockle, C.O., Donatelli, M., Nelson, R., 2003. CropSyst, a cropping systems simulation model. Eur. J. Agron. 18, 289–307. https://doi.org/Pii S1161-0301(02)00109-0
Suman, J., 2007. An Empirical Economic Assessment of Impacts of Climate Change on Agriculture in Zambia.
Thorp, K.R., Youssef, M.A., Jaynes, D.B., Malone, R.W., Ma, L., 2009. DRAINMOD-N II: Evaluated for an agricultural system in Iowa and compared to RZWQM-DSSAT. Trans. ASABE 52, 1557–1573.
Trzaska, S., Schnarr, E., 2014. A Review of Downscaling Methods for Climate Change Projections. African and Latin American Resilience to Climate Change (ARCC).
Tsimba, R., Edmeades, G.O., Millner, J.P., Kemp, P.D., 2013. The effect of planting date on maize grain yields and yield components. F. Crop. Res. 150, 145–155. https://doi.org/10.1016/j.fcr.2013.05.028
UN, 2012. Climate Change: Barrier to Attaining Food Security. UN Policy Brief. Lusaka, Zambia.
UNDP, 2010. Adaptation to the effects of drought and climate change in Agro-ecological Regions I and II in Zambia. Lusaka, Zambia.
UNFCCC, 2012. Agriculture, in: CGE Training Materials for Vulnerability and Adaptation Assessment. p. 67.
Valadabadi, S.A., Farahani, H.A., 2010. Effects of planting density and pattern on physiological growth indices in maize (Zea mays L.) under nitrogenous fertilizer application. J. Agric. Ext. Rural Dev. 2, 40–47.

Valeriano, A., Ines, M., Droogers, P., Makin, I.W., Das Gupta, A., Loof, R., Clemente, R.S., Kyoshi, H., 1993. Crop Growth and Soil Water Balance Modeling to Explore Water Management Option (No. 22), IWMI Working Paper 22. Colombo, Sri Lanka.

Veldkamp, W.J., Muchinda, M., Delmotte, A.P., 1984. Agro-climatic Zones in Zambia. Soil Survey Unit, Land Use Branch, Department of Agriculture, Republic of Zambia, Lusaka.

Vicente-Serrano, S.M., Begueria, S., Lopez-Moreno, J.I., 2010. A multiscalar drought index sensitive to global warming: The standardized precipitation evapotranspiration index. J. Clim. 23, 1696–1718. https://doi.org/10.1175/2009JCLI2909.1

Waha, K., Huth, N., Carberry, P., Wang, E., 2015. How model and input uncertainty impact maize yield simulations in West Africa. Environ. Res. Lett. 10, 1–11. https://doi.org/10.1088/1748-9326/10/2/024017

Wallach, D., Mearns, L.O., Ruane, A.C., Rötter, R.P., Asseng, S., 2016. Lessons from climate modeling on the design and use of ensembles for crop modeling. Clim. Change 139, 551–564. https://doi.org/10.1007/s10584-016-1803-1

Wang, E., Chen, C., Yu, Q., 2009. Modeling the response of wheat and maize productivity to climate variability and irrigation in the North China Plain, in: 18th World IMACS / MODSIM Congress, Cairns, Australia 13-17 July 2009. Cairns, Australia, pp. 13–17.

Wang, Q., 2015. Linking APCC Seasonal Climate Forecasts to a Rice-Yield Model for South Korea, Research Report 2015-20. APEC Climate Center, South Korea.

Wang, X.L., 2008. Penalized Maximal F Test for Detecting Undocumented Mean Shift without Trend Change. J. Atmos. Ocean. Technol. 25, 368–384. https://doi.org/10.1175/2007JTECHA982.1

Wang, X.L., Chen, H., Wu, Y., Feng, Y., Pu, Q., 2010. New techniques for detection and adjustment of shifts in daily precipitation data series. Appl. Meteor. Clim. 49, 2416–2436. https://doi.org/http://dx.doi.org/10.1175/2010JAMC2376.1

Wang, X.L., Feng, Y., 2015. Overview of the RHtests_dlyPrcp software package for homogenization of daily precipitation: New techniques for detection and adjustment of shifts in daily precipitation data series. J. Appl. Meteor. Clim. 12, 2015–76. https://doi.org/10.1175/2007/JTECHA982.1

Wang, X.L., Feng, Y., 2013a. RHtests_dlyPrcp User Manual. Climate Research Division Atmospheric Science and Technology Directorate Science and Technology Branch, Environment Canada Toronto, Ontario, Canada.

Wang, X.L., Feng, Y., 2013b. RHtestsV4 User Manual. Climate Research Division Atmospheric Science and Technology Directorate Science and Technology Branch, Environment Canada Toronto, Ontario, Canada.

Wang, Z., Chen, J., Li, Y., Li, C., Zhang, L., Chen, F., 2016. Effects of climate change and cultivar on summer maize phenology. Int. J. Plant Prod. 10, 509–526.

White, J.W., Grace, P.R., 1999. Modeling Extremes of Wheat and Maize Crop Performance in the Tropics, in: White, J.W., Grace, P.R. (Eds.), Modeling Extremes of Wheat and Maize Crop Performance in the Tropics. El Batan, Mexico, pp. 1–75.

Wilby, R.L. and, Dawson, C.W., 2004. Using SDSM Version 3.1- A decision support tool for the assessment of regional climate change impacts User Manual. Environment 1–67.

Wilby, R.L., Charles, S.P., Zorita, E., Timbal, B., Whetton, P., Mearns, L.O., 2004. Guidelines for Use of Climate Scenarios Developed from Statistical Downscaling Methods. https://doi.org/citeulike-article-id:8861447
Wilby, R.L., Dawson, C.W., 2007. SDSM 4.2-A decision support tool for the assessment of regional climate change impacts, Version 4.2 User Manual. Lancaster Univ. Lancaster/Environment Agency Engl. Wales 1–94.
Willmott, C.J., 1984. On the Evaluation of Model Performance in Physical Geography, in: Spatial Statistics and Models. Springer Netherlands, Dordrecht, pp. 443–460. https://doi.org/10.1007/978-94-017-3048-8_23
Willmott, C.J., 1982. Some Comments on the Evaluation of Model Performance. Bull. Am. Meteorol. Soc. 63, 1309–1313. https://doi.org/10.1175/1520-0477
Willmott, C.J., Ackleson, S.G., Davis, R.E., Feddema, J.J., Klink, K.M., Legates, D.R., O'Donnell, J., Rowe, C.M., 1985. Statistics for the Evaluation and Comparison of Models. J. Geophys. Res. 90, 8995–9005. https://doi.org/10.1029/JC090iC05p08995
Wolday, K., Hruy, G., 2015. A Review on: Performance Evaluation of Crop Simulation Model (APSIM) in Prediction Crop Growth, Development and Yield in Semi Arid Tropics. J. Nat. Sci. Res. 5, 34–39.
WRB, 2015. World Reference Base for Soil Resources 2014, update 2015 International soil classification system for naming soils and creating legends for soil maps. World Soil Resources Reports No. 106. FAO, Rome, Italy.
Xiong, W., Matthews, R., Holman, I., Lin, E., Xu, Y., 2007. Modelling China's potential maize production at regional scale under climate change. Clim. Change 85, 433–451.
Xu, H., Twine, T.E., Girvetz, E., 2016. Climate Change and Maize Yield in Iowa. https://doi.org/10.1371/journal.pone.0156083
Yang, H.S., Dobermann, A., Lindquist, J.L., Walters, D.T., Arkebauer, T.J., Cassman, K.G., 2004. Hybrid-maize - A maize simulation model that combines two crop modeling approaches. F. Crop. Res. 87, 131–154. https://doi.org/https://doi.org/10.1016/j.fcr.2003.10.003
Yin, C., Li, Y., Urich, P., 2014. SimCLIM 2013 FAQ 1.
Zanchetta, S., Zanchi, a., Villa, I., Poli, S., Muttoni, G., 2009. The Shanderman eclogites: a Late Carboniferous high-pressure event in the NW Talesh Mountains (NW Iran). Geol. Soc. London, Spec. Publ. 312, 57–78. https://doi.org/10.1144/SP312.4
Zare, H., Fallah, M.H., Asadi, S., Mojab, A., Bannayan, M., 2016. Assessment of DSSAT and WOFOST sensitivity to temperature derived from AgMERRA, in: International Crop Modelling Symposium, ICROPM, 15-17 March 2016. Berlin, pp. 434–435.
Zeidan, M.S., Amany, A., Bahr El-Kramany, M.F., 2006. Effect of N fertilizer and plant density on yield and quality of maize in sandy soil. Res. J. Agric. Biol. Sci. 2, 156–161.
Zhang, Q., Xiao, M., Singh, V.P., Chen, Y.D., 2014. Max-stable based evaluation of impacts of climate indices on extreme precipitation processes across the Poyang Lake basin, China. Glob. Planet. Change 122, 271–281. https://doi.org/10.1016/j.gloplacha.2014.09.005
Zhang, X., Alexander, L., Heger, G.C., Jones, P., Tank, A.K., Peterson, T.C., Trewin, B., Zwiers, F.W., 2011. Indices for monitoring changes in extremes based on daily temperature and precipitation data. WIREs Clim. Chang. 1–20. https://doi.org/10.1002/wcc.147

Zhang, Y., Feng, L., Wang, E., Wang, J., Li, B., 2012. Evaluation of the APSIM-Wheat model in terms of different cultivars, management regimes and environmental conditions. Can. J. Plant Sci. 92, 937–949. https://doi.org/10.4141/cjps2011-266

Zhang, Y., Zhao, Y., Chen, S., Guo, J., Wang, E., 2015. Prediction of Maize Yield Response to Climate Change with Climate and Crop Model Uncertainties. J. Appl. Meteorol. Climatol. 785–794. https://doi.org/10.1175/JAMC-D-14-0147.1

Zinyengere, N., Crespo, O., Hachigonta, S., Tadross, M., 2014. Local impacts of climate change and agronomic practices on dry land crops in Southern Africa. Agric. Ecosyst. Environ. 197, 1–10. https://doi.org/https://doi.org/10.1016/j.agee.2014.07.002

APPENDICES

Appendix 1: Chemical and physical analysis of soil samples

VOLUMETRIC WATER CONTENT

The following procedure should be used to determine volumetric soil water content.

1. Collect a core sample or auger sample from each soil layer two weeks before planting.
2. Thoroughly mix and composite the auger samples in one bag for each layer.
3. Take a duplicate set of subsamples from the composite. Weigh (Wi) both sets of samples in soil moisture cans.
4. Oven dry the samples at 105°C for 24 hours or until a constant weight (Wd) is obtained.
5. Calculate the **gravimetric moisture content** (qg) as follows:

$$q_g = (W_i - W_d)/W_d$$

6. Determine the bulk density separately and convert gravimetric moisture content into volumetric moisture content (qv), as follows:

qv = (rb/rw) x qg

where rb is the bulk density and rw is the density of water equal to 1.

Pre-plant soil sampling

1. For each experimental plot, a representative number of samples from the surface layer (0–15 cm) and at least one set of subsurface samples from each layer should be taken. These samples should be taken from a cross-section of the experimental plot at least two weeks before planting. For example, for a 4 m x 8 m plot, eight surface samples should be collected, mixed thoroughly, and a representative subsample should be retained for analysis. Use an auger to collect the subsurface samples at depths of 0-20, 20-40, 40-60, 60-80, 80-100 cm.
2. Samples from each layer should be mixed thoroughly and sub-sampled (200 g) for soil chemical analysis.
3. Field moist soil samples for NO_3-N and NH_4-N determinations were stored in a cooler and refrigerated. Samples were analyzed within a week.

SOIL MOISTURE FACTOR DETERMINATION PROCEDURE

All soil data are reported on oven-dry basis; consequently, the moisture factor should be determined.

Procedure

1. Weigh 10 g soil into a weighed Aluminum (Al) dish.
2. Place in an oven at 105°C for 24 hours.
3. Weigh dried sample and Aluminum dish.

Calculation:

Sample + Al dish - Al dish = weight of dry sample.

Moisture Factor = moist sample weight dry sample weight

Repeat the above for air-dried soil samples as well.

SOIL pH DETERMINATION

1:1 Soil to H_2O and 1:1 Soil to 1N Potassium Chloride (KCl) Slurry

Apparatus

pH meter; 50-ml beakers.

Procedure

1. Weigh 20 g of air-dried composite soil sample into each of two 50-ml beakers.
2. Add 20 ml distilled water to one beaker, stir vigorously, let stand one hour, then read pH with a pH meter. Record this as pH in a 1:1 soil:water.
3. Add 20 ml 1N KCl to the remaining beaker, stir vigorously, let stand one hour, then read pH with a pH meter. Record this as pH in 1:1 soil:1N KCl.

KCL-EXTRACTABLE NITRATE AND AMMONIUM NITROGEN

Apparatus

Kemmerer Hallet nitrogen distillation unit; 100-ml sample flask with side arm; 50-ml Erlenmeyer flasks; 50-ml plastic tube; Whatman No. 5 filter paper.

Reagents

1. Potassium Chloride (KCl), 2N.
2. Magnesium Oxide (MgO-Heavy) - ignited at 650°C for one hour.
3. Devarda alloy-ground to a fine powder.
4. Mineral oil.

5. 2% boric acid (H_2BO_3).
6. Sulfamic acid (NH_2SO_3H) - dissolve 2 g in 100 ml water. Store the solution in a refrigerator or at 7°C.
7. Mixed indicator - 3 ml of 0.1% methyl red and 15 ml of 0.1% brom cresol green diluted to 1 liter with ethanol.
8. Standard sulfuric acid (H_2SO_4), 0.005N.

Preparation
1. Weigh 3 g of soil sample into 50-ml plastic tube.
2. Add 30 ml of 2N KCl.
3. Cap and shake for one hour.
4. Filter with Whatman No. 5 filter paper.
5. Pipette 25 ml aliquot into sample flask.

DETERMINATION OF NITROGEN (PAGE *ET AL.*, 1982)
1. Add 1 ml NH_2SO_3H into the aliquot and swirl a few seconds to destroy nitrite in extract.
2. Add 1 ml mineral oil to sample to prevent foaming during distillation.
3. Add 0.2 g of MgO to sample.
4. Place 50-ml Erlenmeyer flask, which contains 5 ml of 2% H_2BO_3 and 3 drops of mixed indicator, at the end of distillation unit.
5. Cap sample flask with side arm with ground glass cover.
6. Attach sample flask to distillation unit.
7. Distill 30 ml into boric acid solution. Set aside for NH_4-N determination. Titrate NH_4-N with standardized 0.005N H_2SO_4.
8. Stop distillation by removing side arm clamp of unit (do not turn off heating unit).
9. Remove ground glass cover of sample flask.
10. Add 0.2 g Devarda alloy.
11. Immediately replace ground glass cover and distill 30 ml into 50 ml flask containing 2% boric acid with 3 drops of mixed indicator. Set aside for NO_3-N determination. Titrate with 0.005N H_2SO_4.
12. Correct for blank.

Calculations
mg N = 1 ml of 0.005N H_2SO_4 x 70

EXTRACTABLE POTASSIUM ANALYSIS (SCS, USDA. 1972)
The following procedure applies not only for the determination of ammonium acetate extractable K but also for ammonium acetate extractable Ca, Mg, and Na.

Apparatus
Atomic Absorption 7 or flame photometer; Buchner funnel (Coors No.1); 250-ml suction flask; 100-ml volumetric flask; 125-ml Erlenmeyer flask; 500-ml volumetric flask; Whatman No. 42 filter paper.

Reagents
1. Ammonium acetate (CH_3COONH_4), 1N, pH 7.0.
Mix 68 ml ammonium hydroxide (NH_4OH), specific gravity 0.90, and 57 ml 99.5% acetic acid (CH_3COOH) per liter of solution desired.
Cool, dilute to volume with water, and adjust to pH 7.0 with CH_3COOH or NH_4OH. Optionally, prepare from CCH_3COONH_4 reagent salt and adjust pH.
2. Standards
Stock standard = 100 ppm
Working standard = 10, 20, 30 ppm.

Procedure
1. Weigh 10 g air-dried <2-mm soil into a 125-ml Erlenmeyer flask and add 15 ml CH_3COONH_4 solution.
2. Cover with stopper, shake the flask for several minutes, and allow to stand 18 hours or more.
3. Transfer contents of the flask to a Buchner funnel attached to suction flask (Coors No.1) fitted with moist Whatman No. 42 filter paper.
4. Filter, using suction.
5. Leach with additional 75 ml CH_3COONH_4, adding small amounts. Minimize leaching time to less than one hour.
6. Transfer leachate to a 100-ml volumetric flask and dilute volume with distilled water.
7. Retain CH_3COONH_4 extract for analysis of exchangeable cations - Ca, Mg, Na, K.

DETERMINATION OF K
- Flame Photometer
- Atomic Absorption

8. Compare absorption of samples at 766.5 nm on flame photometer, or atomic absorption at 383 (visual), with that of the standard solution to determine the amount of exchangable K.

PHOSPHORUS DETERMINATION (AYRES AND HAGIHARA, 1952)
P EXTRACTION: MODIFIED TRUOG
Apparatus
Spectrophotometer; 4-liter volumetric flask; 2-liter volumetric flask; 1-liter volumetric flask; 200-ml volumetric flask; 25-ml volumetric flask; dark pyrex bottle; 125-ml plastic bottle; 50-ml graduated test tubes; Whatman No. 42 filter paper.

Reagents
- Extracting solution, 0.02N sulfuric acid (H_2SO_4) and 0.03% ammonium sulfate $(NH_4)_2SO_4$. Mix 2.22 ml concentrated H_2SO_4 and 12 g $(NH_4)_2SO_4$. Dilute to 4 liters.
- Ascorbic acid reagent (see following page, Murphy and Riley, Reagent B, for method of preparation).
- Standard should be made with Extraction solution.

Procedure
1. Weigh 1 g soil sample (oven-dried) into 125-ml plastic bottle.
2. Add 100 ml of extracting solution.
3. Shake for 1/2 hour.
4. Filter with Whatman's No. 42 filter paper.
5. Save leachate for P determination. Prepare a blank with extracting solution.

P DETERMINATION
Proceed as in Murphy and Riley (see below for procedure).

P Determination: Murphy and Riley (Murphy and Riley, 1962)
Reagents
1. Standard P solution: 5 to 10 ppm solution in extracting solution.
2. Reagent A:
- Dissolve 12 g of ammonium molybdate $[(HN_4)_6Mo_7O_{21}: 4H_2O]$ in 250 ml of distilled water.
- In 100 ml distilled water dissolve 0.2908 g of antimony potassium tartrate.
- Pour both of the dissolved reagents into a 2000-liter volumetric flask, then add 1000 ml of 5N sulfuric acid (H_2SO_4), mix throughly, and fill to volume. Store in a dark pyrex bottle in a cool and dark compartment.

3. Reagent B:
Dissolve 1.056 g ascorbic acid in 200 ml of Reagent A and mix.
NOTE: Reagent B should be prepared daily.

Procedure
1. Pipette suitable aliquot into 25-ml or 50-ml volumetric flask.
2. Dilute to 20 ml with H_2O.
3. Add 4 ml of Reagent B to develop color.
4. Fill to volume and mix thoroughly.
5. After 20 minutes read optical density. Use any suitable spectrophotometer and read at 850-nm wavelength.

Preparation of Standard Curve
1. Pipette aliquots of P solution containing from 5-40 mg of P into 50-ml graduated tubes.
2. Add 4 ml of Reagent B, dilute to 50 ml, and read absorbance as stated above.

Calculations

$$ppm\ P = \frac{microgram\ of\ std}{absrobance\ of\ std}\ X\ \frac{total\ volume\ of\ extractant}{wt\ of\ sample\ X\ \ Aliquot\ of\ extract}\ X\ \frac{moisture}{factor}$$

KCL-EXTRACTABLE ACIDITY AND ALUMINUM (SCS, USDA. 1984)
For soils with pH <5.5, aluminum saturation is reported on Form I as a percent of effective cation exchange capacity.

Apparatus
7-1/2 cm. Buchner funnels; 250-ml suction flask; 125-ml Erlenmeyer flasks; Whatman No. 42 filter paper.

Reagent
1. Potassium chloride (KCl), 1N

- Standard Sodium hydroxide (NaOH): 0.05 N NaOH
- Standard Sulfuric acid (H_2SO_4) 0.05N

2. Potassium fluoride (KF), 1N

Procedure

- Weigh 10 g soil samples into 125-ml Erlenmeyer flasks.
- Add 50 ml 1N KCl to each flask, mix several times, and let stand for 30 minutes.
- Filter through moistened Whatman No. 42 filter paper in Buchner funnel, with suction flask.
- Leach each sample as rapidly as possible with about five 9 ml portions of KCl, using the first to help transfer the remaining soil in the Erlenmeyer flasks to the Buchner funnels.
- Add 3 drops phenolphthalein to the leachate in the suction flask.
- Titrate with standard NaOH to a pink color that persists for 30 seconds or more.
- Correct for a KCl blank to obtain KCl-extractable acidity.
- To obtain KCl extractable aluminum, add 10 ml KF to filtrate and titrate with standard H_2SO_4 until the pink color disappears.
- Set aside while other samples are titrated and then complete to a lasting colorless end point.
- Correct for blank.

Calculations

$$Acidity\ (meq/100g) = \frac{ml\ NaOH}{g\ sample} * N\ of\ \ NaOH\ \ * 100\ * \ moisture\ factor$$

$$Al\ (meq/100g) = \frac{ml\ H_2SO_4}{g\ sample}\ \ * \ \ N\ of\ H_2SO_4\ \ * 100\ * \ moisture\ factor$$

ORGANIC CARBON DETERMINATION USING THE WALKLEY AND BLACK METHOD

Determination of soil organic matter in soil using Potassium Dichromate ($K_2Cr_2O_7$), Ferrous Sulphate ($FeSO_4.7H_2O$) 1N. Making Potassium Dichromate: take 98.9 g per 2 liter of distilled water. The Walkley-Black Method has been estimated to recover about 76% of carbon but can be considerable variability.

Procedure:

- Weigh 1 g of soil
- Add 10 ml Potassium Dichromate
- Add 20 ml concentrated H_2SO_4, wait for 30 minutes
- Add 200 ml of distilled water
- Add phosphoric acid (H_3SO_4) 10 ml plus 30 ml
- Add 2-3 drops of Diphrenylamin indicator solution
- Fill to mark with distilled water.
- Titrate with $FeSO_4$

$$\% \text{ carbon} = \left(\frac{B-V}{W} \times 0.003 \times 100 \times 1.32\right) \times f$$

$$= \left(\frac{B-V}{W} \times 0.39\right) \times f$$

B is the volume of $FeSO_4$ solution used in the standardization procedure
V is the volume of Ferrous Sulphate used in the titration of the sample
W is the mass of sample
R is the volume of Potassium dichromate solution added to the sample
The correction factor (f) is B/R

References

Cheatle R. and Van't Klooster R. (1984). Methods of Soil Analysis. Technical Guide No. 16. Soil Survey Unit, Land Use Branch. Department of Agriculture. Republic of Zambia.

Van Ranst E., M. Verloo, A. Demeyer, and J.M. Pauwels. 1999. Manual for the soil chemistry and fertility laboratory. Analytical methods for soil and plants. Gent. Belgium

EXCHANGEABLE CATIONS CONCENTRATION

The exchangeable bases Ca^{2+}, Mg^{2+}, K^{+} and Na^{+} were extracted with 1.0 *M* neutral NH_4OAc extract (Black *et al.*, 1965). The exchangeable acidity cations (Al^{3+} and H^{+}) were extracted with 1.0 *M* KCl solution as described by Page *et al.* (1982).

After the extraction, the Ca^{2+} and Mg^{2+} were determined using a Perkin-Elmer atomic absoption spectrophotometer at wavelength of 422.7 nm and 285 nm respectively and K^{+} and Na^{+} by an Eppendorf flame photometer at wavelengths of 766.5 nm and 589 nm, respectively.

The exchangeable acidity was determined by titration using 0.10 *M* NaOH and phenolphthalein indicator from a colourless solution to a permanent pink end point.

Calculation

$$Exchangeable\ acidity\ (cmol(+)/kg\ soil = \frac{(vs - vb)\ *\ M}{g}$$

where

vb = ml of NaOH used to titrate blank
vs = ml of NaOH used to titrate the sample extract
g = weight of air-dried soil
M = molarity of NaOH used for the titration
The effective CEC was calculated by the summation of the basic and acidic cations.

DETERMINATION OF BASES (CA, MG, NA, K) AND CEC

Ammonium acetate (77.08 g/litre). Leave it overnight and measure pH, it should be buffered to pH 7. If pH is above 7 used acetic acid to lower it to 7.

Procedure:

Weigh 2.5 g of soil and add to leaching tubes. Add 25 ml of EDT [Ammonium acetate (NH_4Ac)] and collect leacheate. The leacheate is used to determine the bases using the AAS machine.

Strontium chloride is made by dissolving 1g/liter. It is also used in the extracting bases. 5.0 ml reagent and 0.5 ml sample. Dilution factor is 10x10=100. 4.5 ml reagent + 0.5 ml sample = 5 ml.

Determining bases and micronutrients the AAS machine was used to read the absorbency and calculate the amounts of bases. The soil sample is washed with ethanol to remove excess ammonium acetate. To determine the CEC add 10 ml of NaCl to leaching tubes and collect leacheate. Taking readings of absorbency using the AAS machine and determine the CEC.

CEC Calculation

CEC (meq/100 g soil) = $[N_{HCl}$ X $(V_{sample} - V_{blk})$ X 100 X 2]/mass of soil

Atomic absorption Spectroscopy – determination of cations (Ca, Mg, Na, K), trace elements (Zn, Cu, Fe and Mn)

Spectrophotometric determination of Phosphorus and Boron – theory and principles, coloured solutions, UV-VIS spectrophotometry, determination of phosphorus using Bray I, Beer Lambert Law, concentration, Absorbance and Transmittance calculations. Interpretation of phosphorus results. Determination of Boron in soils using the Azomethine-H indicator – extraction with hydrochloric acid.

TOTAL N CONCENTRATION

The total nitrogen content of the soil was determined by the modified Kjeldahl method which involves mineral nitrates in the soil by the use of salicylic acid to convert all the nitrates into ammonium salts (Tel and Hagarty, 1984). A 10 g soil was weighed into a 250 ml Kjeldahl digestion flask and 10 mls of distilled water added to it. Ten millilitres of concentrated H_2SO_4 were added followed by one tablet of selenium and potassium sulphate mixture and 0.10 g salicylic acid. The mixture was made to stand for 30 minutes and heated medley to convert any nitrates and nitrites into ammonium compounds. The mixture was then heated more strongly (300 – 350^{o}C) to digest the soil to a permanent clear colour. The digest was cooled and transferred to a 100 ml volumetric flask and made up to the mark with distilled water. A 20 ml aliquot of the solution was transferred into a tecator distillation flask and 10 mls of 40 % NaOH solution were added and steam from the tecator apparatus allowed to flow

into flask. The ammonium distilled was collected into 10 mls boric acid/ bromocresol green and methyl red solution. The distillate was titrated with 0.01 *M* HCl solution. A blank digestion, distillation and titration were also carried out as a check against traces of nitrogen in the reagents and water used.

Calculation %N = (a – b) x 1.4 *M* x Vs x t

$$\%N = \frac{(a-b)\ x\ 1.4\ M\ x\ V}{s\ x\ t}$$

where

a = ml HCl used for sample titration
b = ml HCl used for blank titration
s = weight of soil taken for digestion in grams
M = molarity of HCl
1.4 = 1.4 10^{-3} × 100% (14 = atomic weight of N)
V = total volume of digest
t = volume of aliquot taken for distillation

References

Cheatle R. and Van't Klooster R. (1984). Methods of Soil Analysis. Technical Guide No. 16. Soil Survey Unit, Land Use Branch. Department of Agriculture. Republic of Zambia.

Van Ranst E., M. Verloo, A. Demeyer, and J.M. Pauwels. 1999. Manual for the soil chemistry and fertility laboratory. Analytical methods for soil and plants. Gent. Belgium

PARTICLE SIZE DISTRIBUTION

The soil texture was determined by the hydrometer method of Bouyoucos (1962). The method relies on the effects of settling differential velocities of sand, clay and silt particles within a water column. Once the sand, silt and clay distribution were measured, the soil may be assigned to a texture class based on the soil texture triangle. Fifty grams of air – dried soil sample were weighed into a one – litre screw lid shaking bottle (W_T). Distilled water of 100 ml was added and the mixture was swirled to wet the soil thoroughly.

Fifty millilitres of 5 % sodium hexametaphosphate solution was added to each soil sample to complex Ca^{2+}, Al^{3+}, Fe^{3+} and other cations that bind clay and silt particles into aggregates. It was shaken using a stirrer 5 minutes and transferred into 1000 ml sedimentation cylinder. Distilled water was added to make up to the 1000 ml mark. The first hydrometer and temperature reading was recorded after 40 seconds. It was then allowed to stand for 2 hours for the second hydrometer and temperature reading to be recorded. The density of the soil suspension was determined with a hydrometer calibrated to read in grams of solids per liter after the sand settles out and again after the silt settles. Corrections were made for the density and temperature of the dispersing solution.

Calculation

% Sand = 100 – [H_1 + 0.2 (T_1 - 20) - 2] x 2
% Clay = [H_2 + 0. 2 (T_2 – 20) – 2] x 2
% Silt = 100 – (% Sand + % clay)

Where:

W_T = Total Weight of air-dried soil
H_1 = 1st Hydrometer reading at 40 seconds
T_1 = 1st Temperature reading at 40 seconds
H_2 = 2nd Hydrometer reading at 3 hours
T_2 = 2nd Temperature reading at 3 hours
-2 = Salt correction to be added to hydrometer reading
0.2 (T – 20) = Temperature correction to be added to hydrometer reading, and T = degrees Celsius.

Reference

Bouyoucos, G.J. 1962. Hydrometer method improved for making particle size analysis of soils. Agron. J. 54:464-465.

Appendix 2: Analysis of variance for irrigated field experiment

Net Assimilation Ration from V6 to R1 (silking)

```
ANALYSIS SPLIT PLOT:  nar_r4_v6
Class level information

variety  :  ZMS606 P30G19 P30B50
Nrate :  N1 N2 N3
rep  :  1 2 3

Number of observations:  27

Analysis of Variance Table

Response: nar_r4_v6
Df     Sum Sq    Mean Sq F value  Pr(>F)
rep            2 1.9444e-06 9.7218e-07  5.0403 0.08070 .
variety        2 6.6150e-08 3.3080e-08  0.1715 0.84829
Ea             4 7.7152e-07 1.9288e-07
Nrate          2 1.4520e-06 7.2599e-07  4.1797 0.04193 *
variety:Nrate  4 2.2506e-06 5.6264e-07  3.2392 0.05085 .
Eb            12 2.0844e-06 1.7370e-07
---
Signif. codes:  0 ‘***’ 0.001 ‘**’ 0.01 ‘*’ 0.05 ‘.’ 0.1 ‘ ’ 1

cv(a) = 21.7 %, cv(b) = 20.5 %, Mean = 0.002028278
```

Relative Growth Rate from V6 to R1 (silking)

```
ANALYSIS SPLIT PLOT:  rgr_r1_v6
Class level information

variety  :  ZMS606 P30G19 P30B50
Nrate :  N1 N2 N3
rep  :  1 2 3

Number of observations:  27

Analysis of Variance Table

Response: rgr_r1_v6
Df  Sum Sq Mean Sq F value  Pr(>F)
rep            2 0.12709 0.06355  1.0845 0.42044
variety        2 0.82251 0.41126  7.0183 0.04918 *
Ea             4 0.23439 0.05860
Nrate          2 0.12501 0.06251  1.2919 0.31035
variety:Nrate  4 0.61429 0.15357  3.1742 0.05375 .
Eb            12 0.58057 0.04838
---
Signif. codes:  0 ‘***’ 0.001 ‘**’ 0.01 ‘*’ 0.05 ‘.’ 0.1 ‘ ’ 1

cv(a) = 4.8 %, cv(b) = 4.4 %, Mean = 5.031222
```

Relative Growth Rate from R1 (silking) to dough stage (R1)

```
ANALYSIS SPLIT PLOT:  rgr_r4_r1
Class level information

variety  :  ZMS606 P30G19 P30B50
Nrate :  N1 N2 N3
rep  :  1 2 3

Number of observations:  27
```

```
Analysis of Variance Table

Response: rgr_r4_r1
Df  Sum Sq  Mean Sq F value Pr(>F)
rep            2 0.10994 0.054968  2.3684 0.2096
variety        2 0.09233 0.046165  1.9891 0.2514
Ea             4 0.09284 0.023210
Nrate          2 0.09660 0.048298  1.1248 0.3567
variety:Nrate  4 0.16290 0.040724  0.9484 0.4697
Eb            12 0.51527 0.042939

cv(a) = 2.9 %, cv(b) = 3.9 %, Mean = 5.269037
```

Relative Growth Rate from R4 (dough stage) to maturity

```
ANALYSIS SPLIT PLOT:  rgr_r6_r4
Class level information

variety  :  ZMS606 P30G19 P30B50
Nrate :  N1 N2 N3
rep  :  1 2 3

Number of observations:  27

Analysis of Variance Table

Response: rgr_r6_r4
Df  Sum Sq  Mean Sq F value  Pr(>F)
rep            2 0.24574 0.122870  2.2389 0.22261
variety        2 0.10073 0.050365  0.9178 0.46985
Ea             4 0.21951 0.054879
Nrate          2 0.25798 0.128988  4.5373 0.03408 *
variety:Nrate  4 0.18408 0.046019  1.6188 0.23299
Eb            12 0.34114 0.028429
---
Signif. codes:  0 ‘***’ 0.001 ‘**’ 0.01 ‘*’ 0.05 ‘.’ 0.1 ‘ ’ 1

cv(a) = 5.2 %, cv(b) = 3.7 %, Mean = 4.524778
```

Leaf area ratio from V6 to dough stage (R4)

```
ANALYSIS SPLIT PLOT:  lar_v6_r4
Class level information

variety  :  ZMS606 P30G19 P30B50
Nrate :  N1 N2 N3
rep  :  1 2 3

Number of observations:  27

Analysis of Variance Table

Response: lar_v6_r4
Df  Sum Sq Mean Sq F value Pr(>F)
rep            2  120.98   60.49  1.1514 0.4028
variety        2  929.54  464.77  8.8465 0.0340 *
Ea             4  210.15   52.54
Nrate          2  236.51  118.25  0.6773 0.5264
variety:Nrate  4 1493.70  373.43  2.1389 0.1384
Eb            12 2095.07  174.59
---
Signif. codes:  0 ‘***’ 0.001 ‘**’ 0.01 ‘*’ 0.05 ‘.’ 0.1 ‘ ’ 1

cv(a) = 18.2 %, cv(b) = 33.2 %, Mean = 39.84593
```

Crop Growth Rate from V6 to R1 (silking)

```
ANALYSIS SPLIT PLOT:  cgr_r1_v6
Class level information

variety  :  ZMS606 P30G19 P30B50
Nrate :  N1 N2 N3
rep  :  1 2 3

Number of observations:  27

Analysis of Variance Table

Response: cgr_r1_v6
Df Sum Sq Mean Sq F value  Pr(>F)
rep            2 1.0989 0.54946  1.0033 0.44347
variety        2 5.5807 2.79033  5.0950 0.07946 .
Ea             4 2.1906 0.54766
Nrate          2 0.6341 0.31703  0.6573 0.53595
variety:Nrate  4 4.8408 1.21021  2.5091 0.09733 .
Eb            12 5.7879 0.48233
---
Signif. codes:  0 ‘***’ 0.001 ‘**’ 0.01 ‘*’ 0.05 ‘.’ 0.1 ‘ ’ 1

cv(a) = 25.7 %, cv(b) = 24.1 %, Mean = 2.88037
```

Crop Growth Rate from R1 (silking) to dough stage (R4)

```
ANALYSIS SPLIT PLOT:  cgr_r4_r1
Class level information

variety  :  ZMS606 P30G19 P30B50
Nrate :  N1 N2 N3
rep  :  1 2 3

Number of observations:  27

Analysis of Variance Table

Response: cgr_r4_r1
Df Sum Sq Mean Sq F value   Pr(>F)
rep            2 34.770 17.3850 22.1530 0.006857 **
variety        2  9.363  4.6816  5.9656 0.063041 .
Ea             4  3.139  0.7848
Nrate          2  1.618  0.8088  0.1563 0.857048
variety:Nrate  4 11.068  2.7670  0.5346 0.713089
Eb            12 62.108  5.1757
---
Signif. codes:  0 ‘***’ 0.001 ‘**’ 0.01 ‘*’ 0.05 ‘.’ 0.1 ‘ ’ 1

cv(a) = 24.3 %, cv(b) = 62.5 %, Mean = 3.638333
```

Crop Growth Rate from R4 (dough stage) to maturity

```
ANALYSIS SPLIT PLOT:  cgr_r6_r4
Class level information

variety  :  ZMS606 P30G19 P30B50
Nrate :  N1 N2 N3
rep  :  1 2 3

Number of observations:  27

Analysis of Variance Table
```

```
Response: cgr_r6_r4
Df Sum Sq Mean Sq F value Pr(>F)
rep            2 15.000  7.4999  3.8181 0.1182
variety        2 14.656  7.3278  3.7304 0.1218
Ea             4  7.857  1.9643
Nrate          2 22.231 11.1157  2.6117 0.1144
variety:Nrate  4 21.882  5.4705  1.2853 0.3296
Eb            12 51.074  4.2561

cv(a) = -28.3 %, cv(b) = -41.7 %, Mean = -4.948185
```

Grain weight

```
ANALYSIS SPLIT PLOT:  grain.wt
Class level information

variety  :  ZMS606 P30G19 P30B50
Nrate :  N1 N2 N3
rep  :  1 2 3

Number of observations:  27

Analysis of Variance Table

Response: grain.wt
Df   Sum Sq Mean Sq F value  Pr(>F)
rep            2 11028202 5514101  2.2508 0.22137
variety        2  5007960 2503980  1.0221 0.43796
Ea             4  9799215 2449804
Nrate          2 12950430 6475215  6.2689 0.01368 *
variety:Nrate  4  9673094 2418274  2.3412 0.11397
Eb            12 12394927 1032911
---
Signif. codes:  0 ‘***’ 0.001 ‘**’ 0.01 ‘*’ 0.05 ‘.’ 0.1 ‘ ’ 1

cv(a) = 23.6 %, cv(b) = 15.3 %, Mean = 6636.223
```

Above-ground biomass

```
ANALYSIS SPLIT PLOT:  biomass.wt
Class level information

variety  :  ZMS606 P30G19 P30B50
Nrate :  N1 N2 N3
rep  :  1 2 3

Number of observations:  27

Analysis of Variance Table

Response: biomass.wt
Df   Sum Sq Mean Sq F value  Pr(>F)
rep            2 18685893 9342946  2.2714 0.21924
variety        2  5798832 2899416  0.7049 0.54671
Ea             4 16452996 4113249
Nrate          2 17253030 8626515  5.5726 0.01942 *
variety:Nrate  4 15985723 3996431  2.5816 0.09101 .
Eb            12 18576184 1548015
---
Signif. codes:  0 ‘***’ 0.001 ‘**’ 0.01 ‘*’ 0.05 ‘.’ 0.1 ‘ ’ 1

cv(a) = 21.8 %, cv(b) = 13.4 %, Mean = 9297.109
```

Stover weight

```
ANALYSIS SPLIT PLOT:  stover.wt
```

```
Class level information

variety  :  ZMS606 P30G19 P30B50
Nrate :  N1 N2 N3
rep  :  1 2 3

Number of observations:  27

Analysis of Variance Table

Response: stover.wt
Df  Sum Sq Mean Sq F value Pr(>F)
rep            2 1023746  511873  2.0677 0.2417
variety        2   80798   40399  0.1632 0.8548
Ea             4  990218  247555
Nrate          2  308623  154312  0.9145 0.4269
variety:Nrate  4  903529  225882  1.3387 0.3116
Eb            12 2024838  168737

cv(a) = 18.7 %, cv(b) = 15.4 %, Mean = 2660.885
```

100-seed weight

```
ANALYSIS SPLIT PLOT:  X100_seed_wt
Class level information

variety  :  ZMS606 P30G19 P30B50
Nrate :  N1 N2 N3
rep  :  1 2 3

Number of observations:  27

Analysis of Variance Table

Response: X100_seed_wt
Df  Sum Sq Mean Sq F value   Pr(>F)
rep            2  87.427  43.714 25.2626 0.005382 **
variety        2  66.992  33.496 19.3577 0.008769 **
Ea             4   6.921   1.730
Nrate          2   9.494   4.747  0.3659 0.701052
variety:Nrate  4  32.381   8.095  0.6240 0.654285
Eb            12 155.684  12.974
---
Signif. codes:  0 ‘***’ 0.001 ‘**’ 0.01 ‘*’ 0.05 ‘.’ 0.1 ‘ ’ 1

cv(a) = 4.5 %, cv(b) = 12.2 %, Mean = 29.41852
```

Grain number per square meters

```
ANALYSIS SPLIT PLOT:  seednosqm
Class level information

variety  :  ZMS606 P30G19 P30B50
Nrate :  N1 N2 N3
rep  :  1 2 3

Number of observations:  27

Analysis of Variance Table

Response: seednosqm
Df  Sum Sq Mean Sq F value   Pr(>F)
rep            2  501961  250980  0.7811 0.517150
variety        2 1537285  768643  2.3923 0.207340
Ea             4 1285213  321303
```

```
Nrate          2 1575091  787546  7.1299 0.009106 **
variety:Nrate  4 1154055  288514  2.6120 0.088504 .
Eb            12 1325490  110458
---
Signif. codes:  0 ‘***’ 0.001 ‘**’ 0.01 ‘*’ 0.05 ‘.’ 0.1 ‘ ’ 1

cv(a) = 23 %, cv(b) = 13.5 %, Mean = 2464.903
```

Appendix 3: Analysis of variance for rainfed field experiment

Grain yield

```
ANALYSIS SPLIT-SPLIT PLOT:  grain
Class level information

pd :  1 2 3
nrate :  112 56 168
variety  :  P30G19 P30B50 ZMS606
block  :  1 2 3

Number of observations:  81

Analysis of Variance Table

Response: grain
Df  Sum Sq Mean Sq F value  Pr(>F)
block             2   73570   36785  0.7953 0.51191
pd                2 1173409  586705 12.6851 0.01855 *
Ea                4  185006   46252
nrate             2   23712   11856  0.4378 0.65537
pd:nrate          4   53368   13342  0.4927 0.74148
Eb               12  324983   27082
variety           2   31808   15904  1.2697 0.29320
variety:pd        4   73894   18473  1.4748 0.23016
variety:nrate     4  128938   32234  2.5734 0.05410 .
variety:pd:nrate  8  154320   19290  1.5400 0.17808
Ec               36  450932   12526
---
Signif. codes:  0 ‘***’ 0.001 ‘**’ 0.01 ‘*’ 0.05 ‘.’ 0.1 ‘ ’ 1

cv(a) = 28.8 %, cv(b) = 22 %, cv(c) = 15 %, Mean = 747.229
```

Above-ground biomass

```
ANALYSIS SPLIT-SPLIT PLOT:  biomass_wt
Class level information

pd :  1 2 3
nrate :  112 56 168
variety  :  P30G19 P30B50 ZMS606
block  :  1 2 3

Number of observations:  81

Analysis of Variance Table

Response: biomass_wt
Df Sum Sq Mean Sq F value  Pr(>F)
block             2 111867   55933  0.8296 0.49959
pd                2 992163  496082  7.3577 0.04568 *
Ea                4 269695   67424
nrate             2  65816   32908  0.7458 0.49512
pd:nrate          4  84293   21073  0.4776 0.75177
Eb               12 529494   44125
variety           2 168958   84479  4.0210 0.02654 *
variety:pd        4 197524   49381  2.3504 0.07257 .
variety:nrate     4 242017   60504  2.8799 0.03624 *
variety:pd:nrate  8 222714   27839  1.3251 0.26275
Ec               36 756341   21009
---
Signif. codes:  0 ‘***’ 0.001 ‘**’ 0.01 ‘*’ 0.05 ‘.’ 0.1 ‘ ’ 1
```

```
cv(a) = 25.2 %, cv(b) = 20.4 %, cv(c) = 14.1 %, Mean = 1030.557
```

Stover

```
ANALYSIS SPLIT-SPLIT PLOT:  stover_wt
Class level information

pd :  1 2 3
nrate :  112 56 168
variety  :  P30G19 P30B50 ZMS606
block  :  1 2 3

Number of observations:  81

Analysis of Variance Table

Response: stover_wt
Df Sum Sq Mean Sq F value    Pr(>F)
block             2   4865    2432  0.6826  0.555843
pd                2  44421   22211  6.2328  0.059015 .
Ea                4  14254    3563
nrate             2  10608    5304  1.8353  0.201646
pd:nrate          4   4793    1198  0.4146  0.794982
Eb               12  34682    2890
variety           2 102204   51102 26.5906 8.101e-08 ***
variety:pd        4  33148    8287  4.3120  0.005949 **
variety:nrate     4  22000    5500  2.8619  0.037100 *
variety:pd:nrate  8  12042    1505  0.7832  0.620241
Ec               36  69185    1922
---
Signif. codes:  0 ‘***’ 0.001 ‘**’ 0.01 ‘*’ 0.05 ‘.’ 0.1 ‘ ’ 1

cv(a) = 21.1 %, cv(b) = 19 %, cv(c) = 15.5 %, Mean = 283.3272
```

100-seed weight

```
ANALYSIS SPLIT-SPLIT PLOT:  x_100_grain_wt
Class level information

pd :  1 2 3
nrate :  112 56 168
variety  :  P30G19 P30B50 ZMS606
block  :  1 2 3

Number of observations:  81

Analysis of Variance Table

Response: x_100_grain_wt
Df  Sum Sq Mean Sq  F value    Pr(>F)
block             2   68.54   34.27  12.4497  0.019158 *
pd                2 1630.40  815.20 296.1619 4.499e-05 ***
Ea                4   11.01    2.75
nrate             2   11.75    5.88   0.1752  0.841373
pd:nrate          4   43.63   10.91   0.3253  0.855640
Eb               12  402.34   33.53
variety           2  718.49  359.24  13.9822 3.210e-05 ***
variety:pd        4  456.04  114.01   4.4374  0.005108 **
variety:nrate     4  106.57   26.64   1.0370  0.401638
variety:pd:nrate  8  102.99   12.87   0.5011  0.847258
Ec               36  924.95   25.69
---
Signif. codes:  0 ‘***’ 0.001 ‘**’ 0.01 ‘*’ 0.05 ‘.’ 0.1 ‘ ’ 1
```

```
cv(a) = 4.6 %, cv(b) = 16 %, cv(c) = 14 %, Mean = 36.16086
```

seed number per square meter

```
ANALYSIS SPLIT-SPLIT PLOT:  seedno
Class level information

pd :  1 2 3
nrate :  112 56 168
variety  :  P30G19 P30B50 ZMS606
block  :  1 2 3

Number of observations:  81

Analysis of Variance Table

Response: seedno
Df  Sum Sq Mean Sq F value    Pr(>F)
block             2  265177  132589  0.9907    0.4472
pd                2  269774  134887  1.0079    0.4421
Ea                4  535334  133833
nrate             2   60964   30482  0.2458    0.7859
pd:nrate          4  273250   68312  0.5509    0.7022
Eb               12 1488104  124009
variety           2 4031189 2015595 21.8566 6.108e-07 ***
variety:pd        4  420529  105132  1.1400    0.3533
variety:nrate     4  733592  183398  1.9887    0.1171
variety:pd:nrate  8  505841   63230  0.6857    0.7012
Ec               36 3319888   92219
---
Signif. codes:  0 ‘***’ 0.001 ‘**’ 0.01 ‘*’ 0.05 ‘.’ 0.1 ‘ ’ 1

cv(a) = 17.6 %, cv(b) = 17 %, cv(c) = 14.6 %, Mean = 2077.002
```

Cob width

```
ANALYSIS SPLIT-SPLIT PLOT:  cob_w
Class level information

pd :  1 2 3
variety  :  P30G19 P30B50 ZMS606
nrate :  112 56 168
block  :  1 2 3

Number of observations:  81

Analysis of Variance Table

Response: cob_w
Df  Sum Sq Mean Sq F value    Pr(>F)
block             2 0.01298 0.00649  0.0901   0.91560
pd                2 2.74082 1.37041 19.0351   0.00904 **
Ea                4 0.28798 0.07199
variety           2 2.34945 1.17473 38.5250 5.988e-06 ***
pd:variety        4 0.37363 0.09341  3.0633   0.05914 .
Eb               12 0.36591 0.03049
nrate             2 0.06422 0.03211  0.3722   0.69184
nrate:pd          4 0.24002 0.06000  0.6955   0.60003
nrate:variety     4 0.29080 0.07270  0.8426   0.50741
nrate:pd:variety  8 0.38335 0.04792  0.5554   0.80663
Ec               36 3.10600 0.08628
---
Signif. codes:  0 ‘***’ 0.001 ‘**’ 0.01 ‘*’ 0.05 ‘.’ 0.1 ‘ ’ 1

cv(a) = 5.1 %, cv(b) = 3.3 %, cv(c) = 5.6 %, Mean = 5.274198
```

Cob length

```
ANALYSIS SPLIT-SPLIT PLOT:  cob_l
Class level information

pd :  1 2 3
variety  :  P30G19 P30B50 ZMS606
nrate :  112 56 168
block  :  1 2 3

Number of observations:  81

Analysis of Variance Table

Response: cob_l
Df Sum Sq Mean Sq F value    Pr(>F)
block             2   9.51   4.756  0.9346 0.4644900
pd                2 155.46  77.728 15.2739 0.0134054 *
Ea                4  20.36   5.089
variety           2  33.89  16.947  6.7752 0.0107326 *
pd:variety        4  97.31  24.326  9.7254 0.0009589 ***
Eb               12  30.02   2.501
nrate             2   0.57   0.285  0.0253 0.9750765
nrate:pd          4  11.84   2.959  0.2622 0.9002370
nrate:variety     4  34.53   8.633  0.7650 0.5550133
nrate:pd:variety  8  62.35   7.794  0.6906 0.6970771
Ec               36 406.28  11.285
---
Signif. codes:  0 ‘***’ 0.001 ‘**’ 0.01 ‘*’ 0.05 ‘.’ 0.1 ‘ ’ 1

cv(a) = 11.1 %, cv(b) = 7.8 %, cv(c) = 16.5 %, Mean = 20.38951
```

Cob weight

```
ANALYSIS SPLIT-SPLIT PLOT:  cob_wt
Class level information

pd :  1 2 3
nrate :  112 56 168
variety  :  P30G19 P30B50 ZMS606
block  :  1 2 3

Number of observations:  81

Analysis of Variance Table

Response: cob_wt
Df Sum Sq Mean Sq F value    Pr(>F)
block             2   1107   553.3  0.5076   0.63614
pd                2  11956  5977.8  5.4838   0.07142 .
Ea                4   4360  1090.1
nrate             2   3795  1897.5  2.5495   0.11947
pd:nrate          4   2561   640.1  0.8601   0.51499
Eb               12   8932   744.3
variety           2  44990 22495.2 48.5515 5.999e-11 ***
variety:pd        4  18206  4551.6  9.8237 1.772e-05 ***
variety:nrate     4   5041  1260.2  2.7199   0.04465 *
variety:pd:nrate  8   5803   725.4  1.5657   0.16983
Ec               36  16680   463.3
---
Signif. codes:  0 ‘***’ 0.001 ‘**’ 0.01 ‘*’ 0.05 ‘.’ 0.1 ‘ ’ 1

cv(a) = 23.2 %, cv(b) = 19.2 %, cv(c) = 15.1 %, Mean = 142.394
```

Maximum LAI

```
ANALYSIS SPLIT-SPLIT PLOT:  max_LAI
Class level information

pd :  1 2 3
nrate :  112 56 168
variety  :  P30G19 P30B50 ZMS606
block  :  1 2 3

Number of observations:  81

Analysis of Variance Table

Response: max_LAI
Df Sum Sq Mean Sq F value    Pr(>F)
block              2 3.4619 1.73093  1.9100 0.2616396
pd                 2 3.2581 1.62906  1.7976 0.2773575
Ea                 4 3.6250 0.90624
nrate              2 0.8017 0.40085  0.8420 0.4547958
pd:nrate           4 0.8774 0.21935  0.4607 0.7633013
Eb                12 5.7129 0.47608
variety            2 5.6682 2.83410 10.3781 0.0002762 ***
variety:pd         4 2.6845 0.67112  2.4575 0.0630133 .
variety:nrate      4 1.4482 0.36204  1.3257 0.2790947
variety:pd:nrate   8 2.1600 0.27000  0.9887 0.4609496
Ec                36 9.8310 0.27308
---
Signif. codes:  0 ‘***’ 0.001 ‘**’ 0.01 ‘*’ 0.05 ‘.’ 0.1 ‘ ’ 1

cv(a) = 25.7 %, cv(b) = 18.6 %, cv(c) = 14.1 %, Mean = 3.710864
```

Appendix 4: Expert Team on Sector Specific Indices

(i) Percentile-based indices: The percentile-based indices are defined as days over the warmest/coldest long-term percentiles. The temperature percentile-based indices included the occurrence of hot days (TX90p), warm nights (TN90p), cold days (TX10p), very warm day (TX95t), cold nights (TN10p) and a fraction of days with above average temperature (TXGT50p). The temperature percentile-based indices sample the coldest and warmest deciles for both maximum and minimum temperatures which enables evaluating the extent to which extremes are changing (Alexander et al., 2006). Precipitation percentile-based indices were: very wet days (R95pTOT) and extremely wet days (R99pTOT) and these indices represent the amount of rainfall falling above the 95th (R95pTOT) and 99th (R99pTOT) percentiles;
(ii) Absolute indices: represented maximum and minimum values of weather parameters within a season or year. The temperature absolute indices included: maximum warmest daily temperature (TXx), minimum coldest daily temperature (TNn), maximum daily minimum temperature (TNx), minimum daily maximum temperature (TXn), Number of days when TX >= 30 °C (TXGE30) and Number of days when TX >= 35 °C (TXGE35). The absolute precipitation indices are maximum 1-day precipitation amount (RX1day), maximum 5-day precipitation amount (RX5day). Extreme precipitation regimes are defined as monthly maximum 1-day precipitation amount (Rx1day) and monthly maximum consecutive 5-day precipitation amount (Rx5day) (Zhang et al., 2014);
(iii) Threshold indices: these are defined as the number of days (annual count of days) on which temperature or precipitation value falls above or below a fixed threshold, including annual occurrence of frost days (FD), annual occurrence of ice days (ID), summer days (SU), annual occurrence of tropical nights (TR) and number of very heavy precipitation days > 20 mm (R20mm [annual count of days when PRCPshold in
(iv) Duration indices: Duration indices define periods of excessive warmth, cold, wetness or dryness or in the case of growing season length - periods of mildness. Temperature duration indices include: excessive warmth (WSDI), cold spell duration indicator (CSDI), Growing Degree Days (GDDgrow), warm spell duration indicator (WSDI), diurnal temperature range (DTR) and extreme temperature range (ETR). The DTR and ETR indices were computed from TXx and TNn (Fonseca et al., 2016). Precipitation duration indices are GSL, consecutive dry days (CDD) and consecutive wet days (CWD). The CDD index is the length of the longest dry spell in a year while the CWD index is defined as the longest wet spell in a year; and
(v) Other indices: annual precipitation total (PRCPTOT), Standardized Precipitation Index (SPI), Standardized Precipitation Evapotranspiration Index (SPEI) and simple daily intensity index (SDII).

Appendix 5: Evaluation of CERES-Maize model

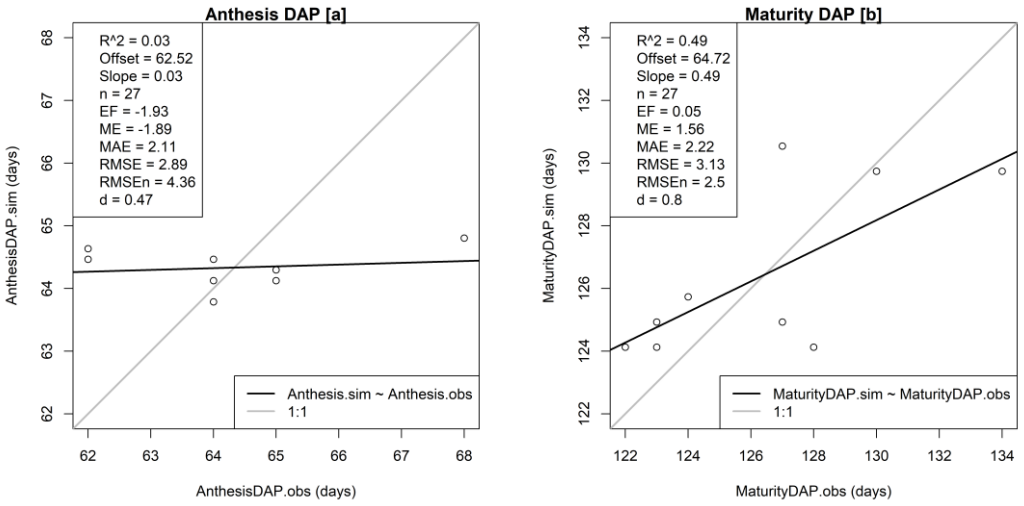

Comparison of simulated and measured DAP to anthesis (a) and maturity (b) using CERES-Maize

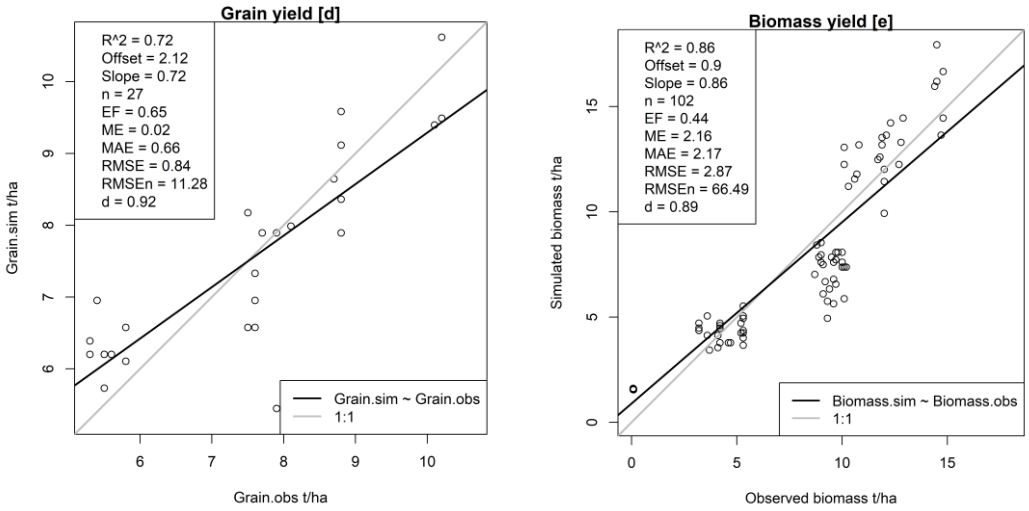

Comparison of simulated and measured grain yield (d) and biomass yield (e) (CERES-Maize)

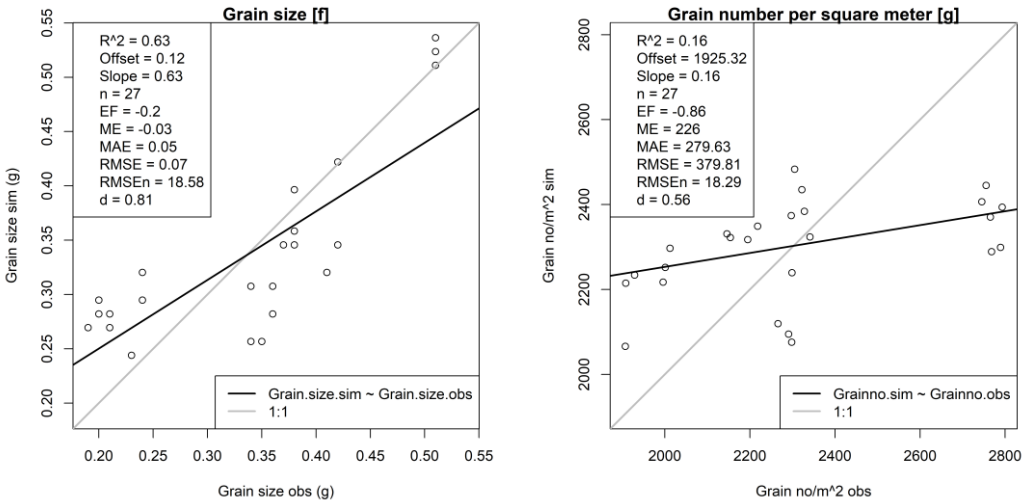

Comparison of simulated and measured grain size (f) and grain number m^{-2} (CERES-Maize)

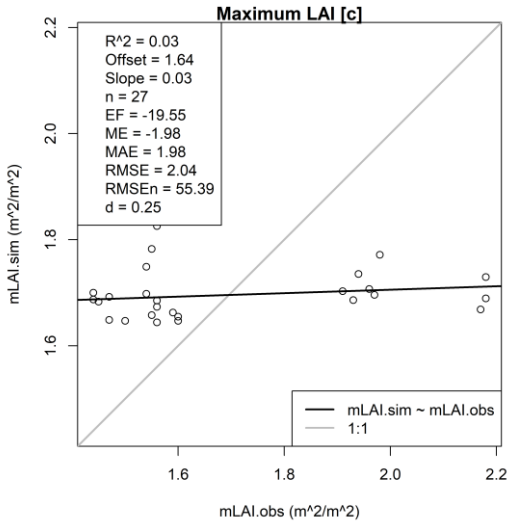

Comparison of simulated and measured mLAI (c) (CERES-Maize

Appendix 6: Evaluation of APSIM-Maize model

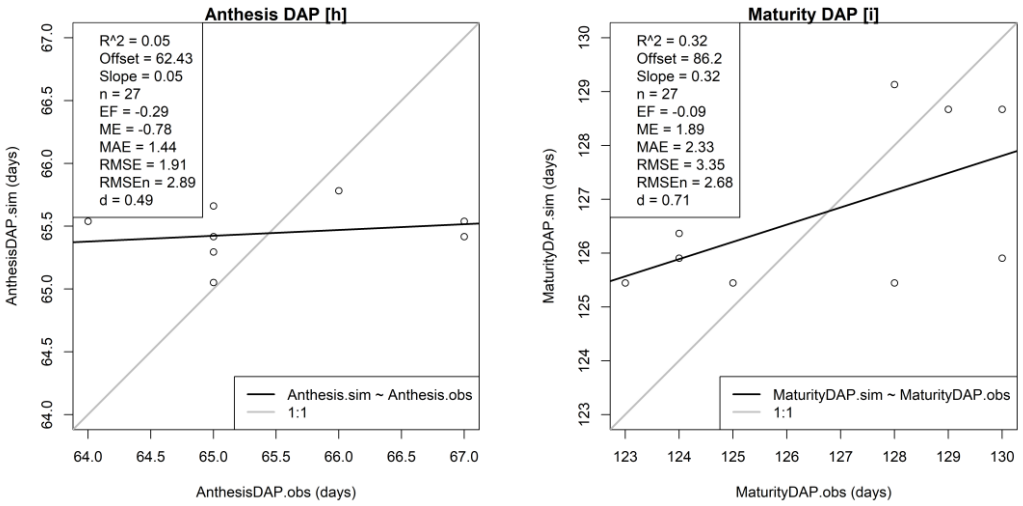

Comparison of simulated and measured DAP to anthesis (a) and maturity (b) using APSIM-Maize

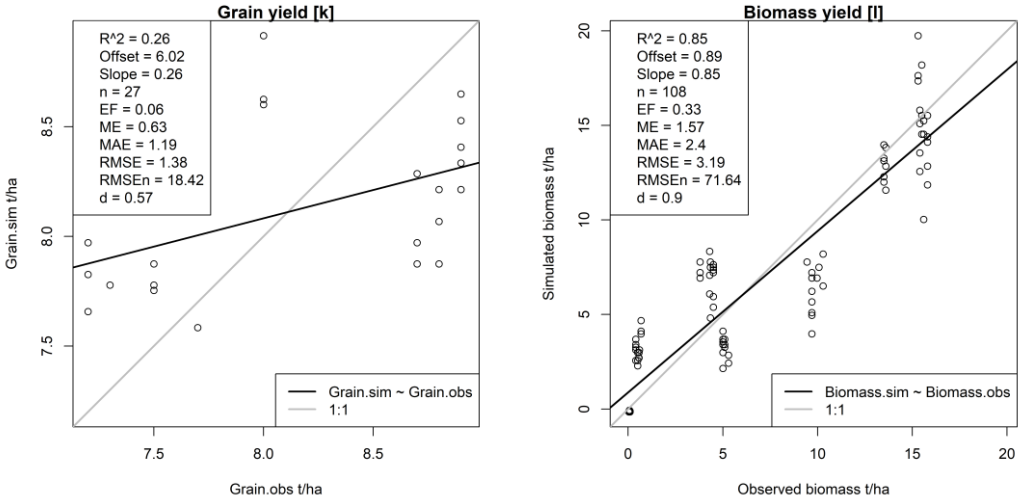

Comparison of simulated and measured grain yield (d) and biomass yield (e) (APSIM-Maize)

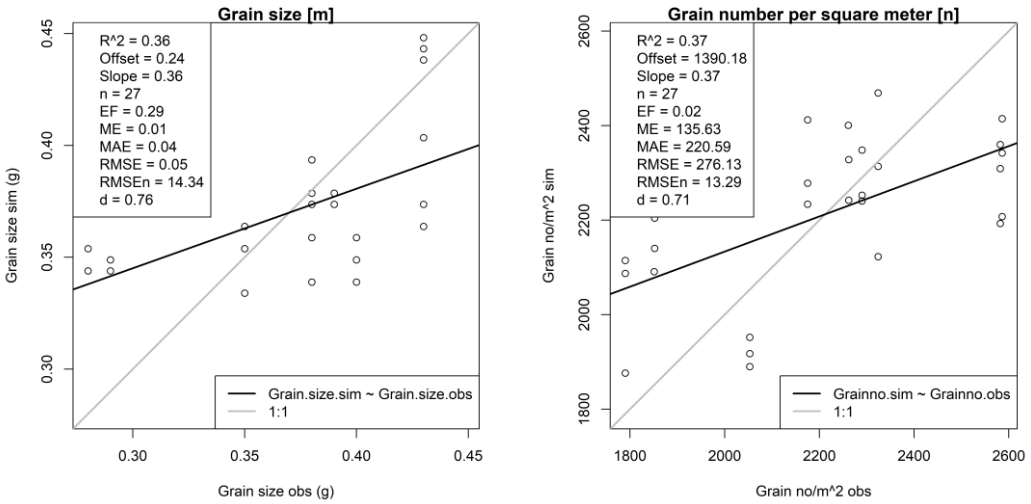

Comparison of simulated and measured grain size (f) and grain number m^{-2} (APSIM-Maize)

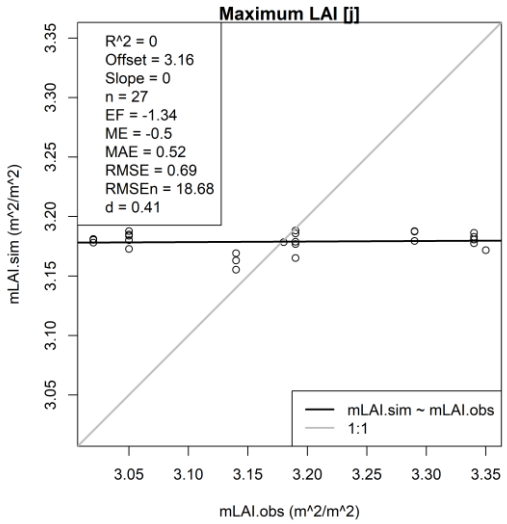

Comparison of simulated and measured mLAI (j) (APSIM-Maize)

Appendix 7: Projected % change in anthesis (DAP) over the 2050s using APSIM-Maize and CERES-Maize models under RCP4.5 and RCP8.5 scenarios

	APSIM-Maize			CERES-Maize		
	Baseline anthesis	% Δ based on 5 GCMs		Baseline anthesis	% Δ based on 5 GCMs	
Treatment	(DAP)	RCP4.5	RCP8.5	(DAP)	RCP4.5	RCP8.5
pd1_v1n1	65.60	-8.30	-11.31	43.83	-11.43	-15.00
pd1_v1n2	65.70	-8.44	-11.45	43.83	-11.43	-15.00
pd1_v1n3	65.77	-8.49	-11.44	43.83	-11.43	-15.00
pd2_v1n1	65.50	-7.64	-10.39	43.83	-11.43	-15.00
pd2_v1n2	65.50	-7.64	-10.39	43.83	-11.43	-15.00
pd2_v1n3	65.50	-7.64	-10.39	43.83	-11.43	-15.00
pd3_v1n1	65.30	-7.35	-10.29	43.83	-11.43	-15.00
pd3_v1n2	65.30	-7.35	-10.29	43.83	-11.43	-15.00
pd3_v1n3	65.30	-7.35	-10.29	43.83	-11.43	-15.00
pd1_v2n1	64.97	-7.92	-10.79	46.87	-14.43	-17.60
pd1_v2n2	65.07	-8.06	-10.93	46.87	-14.43	-17.60
pd1_v2n3	65.13	-8.13	-10.95	46.87	-14.43	-17.60
pd2_v2n1	65.27	-7.70	-10.46	46.87	-14.43	-17.60
pd2_v2n2	65.27	-7.70	-10.46	46.87	-14.43	-17.60
pd2_v2n3	65.27	-7.70	-10.46	46.87	-14.43	-17.60
pd3_v2n1	65.03	-7.67	-10.33	46.87	-14.43	-17.60
pd3_v2n2	65.03	-7.67	-10.33	46.87	-14.43	-17.60
pd3_v2n3	65.03	-7.67	-10.33	46.87	-14.43	-17.60
pd1_v3n1	63.83	-8.26	-11.11	44.33	-13.30	-16.16
pd1_v3n2	63.93	-8.40	-11.25	44.33	-13.30	-16.16
pd1_v3n3	63.97	-8.46	-11.26	44.33	-13.30	-16.16
pd2_v3n1	63.90	-8.25	-11.21	44.33	-13.30	-16.16
pd2_v3n2	63.90	-8.25	-11.21	44.33	-13.30	-16.16
pd2_v3n3	63.90	-8.25	-11.21	44.33	-13.30	-16.16
pd3_v3n1	63.57	-7.99	-11.02	44.33	-13.30	-16.16
pd3_v3n2	63.57	-7.99	-11.02	44.33	-13.30	-16.16
pd3_v3n3	63.57	-7.99	-11.02	44.33	-13.30	-16.16

Note: pd1: first planting date; pd2: second planting date; pd3: third planting date; v1: ZMS 606; v2: PHB30G19; v3: PHB30B50; n1: 67.20 kg N ha^{-1}; n2: 134.40 kg N ha^{-1}; n3: 201.60 kg N ha^{-1}

Appendix 8: Projected % change in maturity over the 2050s using APSIM-Maize and CERES-Maize models under RCP4.5 and RCP8.5 scenarios

	APSIM-Maize			CERES-Maize		
	Baseline maturity	% Δ based on 5 GCMs		Baseline maturity	% Δ based on 5 GCMs	
Treatment	(DAP)	RCP4.5	RCP8.5	(DAP)	RCP4.5	RCP8.5
pd1_v1n1	120.97	-8.53	-11.68	100.7	-10.60	-14.28
pd1_v1n2	121.07	-8.61	-11.75	100.7	-10.60	-14.28
pd1_v1n3	121.13	-8.66	-11.74	100.7	-10.60	-14.28
pd2_v1n1	121.37	-8.27	-11.34	100.7	-10.60	-14.28
pd2_v1n2	121.37	-8.27	-11.34	100.7	-10.60	-14.28
pd2_v1n3	121.37	-8.27	-11.34	100.7	-10.60	-14.28
pd3_v1n1	122.73	-8.99	-12.17	100.7	-10.60	-14.28
pd3_v1n2	122.73	-8.99	-12.17	100.7	-10.60	-14.28
pd3_v1n3	122.73	-8.99	-12.17	100.7	-10.60	-14.28
pd1_v2n1	119.47	-8.22	-11.45	104.5	-12.11	-15.99
pd1_v2n2	119.63	-8.35	-11.57	104.5	-12.11	-15.99
pd1_v2n3	119.63	-8.33	-11.55	104.5	-12.11	-15.99
pd2_v2n1	120.30	-8.32	-11.27	104.5	-12.11	-15.99
pd2_v2n2	120.30	-8.32	-11.27	104.5	-12.11	-15.99
pd2_v2n3	120.30	-8.32	-11.27	104.5	-12.11	-15.99
pd3_v2n1	121.43	-8.92	-12.12	104.5	-12.11	-15.99
pd3_v2n2	121.43	-8.92	-12.12	104.5	-12.11	-15.99
pd3_v2n3	121.43	-8.92	-12.12	104.5	-12.11	-15.99
pd1_v3n1	118.13	-8.45	-11.48	99.17	-10.41	-14.02
pd1_v3n2	118.23	-8.53	-11.56	99.17	-10.41	-14.02
pd1_v3n3	118.30	-8.58	-11.58	99.17	-10.41	-14.02
pd2_v3n1	118.73	-8.62	-11.98	99.17	-10.41	-14.02
pd2_v3n2	118.73	-8.62	-11.98	99.17	-10.41	-14.02
pd2_v3n3	118.73	-8.62	-11.98	99.17	-10.41	-14.02
pd3_v3n1	119.60	-9.14	-12.35	99.17	-10.41	-14.02
pd3_v3n2	119.60	-9.14	-12.35	99.17	-10.41	-14.02
pd3_v3n3	119.60	-9.14	-12.35	99.17	-10.41	-14.02

Note: pd1: first planting date; pd2: second planting date; pd3: third planting date; v1: ZMS 606; v2: PHB30G19; v3: PHB30B50; n1: 67.20 kg N ha^{-1}; n2: 134.40 kg N ha^{-1}; n3: 201.60 kg N ha^{-1}

Appendix 9: Mean, median, sd and cv of grain yield for baseline, RCP4.5 and RCP8.5 at N1

	CERES-Maize				APSIM-Maize			
variable	mean	median	sd	cv	mean	median	sd	cv
pd1_v1n1_bs	5.40	5.41	0.52	9.71	5.69	5.68	0.91	16.03
pd2_v1n1_bs	5.38	5.41	0.51	9.43	5.22	5.22	1.32	25.23
pd3_v1n1_bs	5.38	5.41	0.51	9.43	4.61	4.61	1.61	34.99
pd1_v2n1_bs	5.62	5.55	0.41	7.38	5.61	5.70	0.90	16.04
pd2_v2n1_bs	5.62	5.55	0.41	7.38	5.10	5.09	1.34	26.29
pd3_v2n1_bs	5.62	5.55	0.41	7.38	4.46	4.39	1.58	35.33
pd1_v3n1_bs	5.19	5.12	0.29	5.66	5.57	5.40	0.93	16.62
pd2_v3n1_bs	5.19	5.12	0.29	5.66	5.07	5.02	1.41	27.79
pd3_v3n1_bs	5.19	5.12	0.29	5.66	4.47	4.53	1.58	35.27
pd1_v1n1_rcp45	6.00	6.07	0.42	7.03	5.92	6.12	0.93	15.72
pd2_v1n1_rcp45	6.00	6.07	0.42	7.03	5.26	5.16	1.53	29.10
pd3_v1n1_rcp45	6.00	6.07	0.42	7.03	4.54	4.70	1.70	37.47
pd1_v2n1_rcp45	5.98	6.04	0.52	8.68	5.78	5.99	0.96	16.57
pd2_v2n1_rcp45	5.98	6.04	0.52	8.68	5.10	5.01	1.54	30.14
pd3_v2n1_rcp45	5.98	6.04	0.52	8.68	4.38	4.41	1.68	38.23
pd1_v3n1_rcp45	6.41	6.43	0.28	4.32	5.76	5.80	0.93	16.08
pd2_v3n1_rcp45	6.41	6.43	0.28	4.32	5.11	4.99	1.54	30.24
pd3_v3n1_rcp45	6.41	6.43	0.28	4.32	4.42	4.47	1.65	37.39
pd1_v1n1_rcp85	5.63	5.68	0.50	8.87	5.98	6.22	0.97	16.18
pd2_v1n1_rcp85	5.63	5.68	0.50	8.88	5.28	5.13	1.52	28.83
pd3_v1n1_rcp85	5.63	5.68	0.50	8.88	4.55	4.91	1.72	37.91
pd1_v2n1_rcp85	5.73	5.70	0.45	7.84	5.84	6.10	0.97	16.58
pd2_v2n1_rcp85	5.73	5.70	0.45	7.84	5.13	4.99	1.54	30.03
pd3_v2n1_rcp85	5.73	5.70	0.45	7.84	4.38	4.62	1.70	38.72
pd1_v3n1_rcp85	6.06	6.04	0.32	5.31	5.77	6.01	0.95	16.49
pd2_v3n1_rcp85	6.06	6.04	0.32	5.31	5.03	4.94	1.49	29.55
pd3_v3n1_rcp85	6.06	6.04	0.32	5.31	4.36	4.63	1.66	38.14

Note: sd: standard deviation; cv: coefficient of variation

Appendix 10: Mean, median, sd and cv of grain yield for baseline, RCP4.5 and RCP8.5 at N2

	CERES-Maize				APSIM-Maize			
variable	mean	median	sd	cv	mean	median	sd	cv
pd1_v1n2_bs	5.69	5.61	1.01	17.72	7.56	7.74	1.52	20.10
pd2_v1n2_bs	5.69	5.61	1.01	17.72	6.38	7.22	2.22	34.80
pd3_v1n2_bs	5.69	5.61	1.01	17.72	4.66	4.51	1.94	41.65
pd1_v2n2_bs	5.49	5.47	1.01	18.44	7.36	7.81	1.50	20.36
pd2_v2n2_bs	5.49	5.47	1.01	18.44	6.08	7.02	2.14	35.15
pd3_v2n2_bs	5.49	5.47	1.01	18.44	4.44	4.21	1.88	42.38
pd1_v3n2_bs	6.95	6.84	0.73	10.57	7.06	7.35	1.35	19.11
pd2_v3n2_bs	6.95	6.84	0.73	10.57	5.84	6.61	1.98	33.83
pd3_v3n2_bs	6.95	6.84	0.73	10.57	4.40	4.28	1.80	41.01
pd1_v1n2_rcp45	5.90	5.90	0.51	8.61	7.23	7.49	1.35	18.69
pd2_v1n2_rcp45	5.90	5.90	0.51	8.61	6.12	6.46	2.03	33.21
pd3_v1n2_rcp45	5.90	5.90	0.51	8.61	4.66	4.93	2.01	43.14
pd1_v2n2_rcp45	5.43	5.42	0.61	11.20	6.93	7.18	1.32	19.11
pd2_v2n2_rcp45	5.43	5.42	0.61	11.20	5.85	6.49	1.99	34.02
pd3_v2n2_rcp45	5.43	5.42	0.61	11.20	4.43	4.52	1.91	43.08
pd1_v3n2_rcp45	7.27	7.28	0.44	6.06	6.62	6.89	1.25	18.94
pd2_v3n2_rcp45	7.27	7.28	0.44	6.06	5.69	5.99	1.84	32.26
pd3_v3n2_rcp45	7.27	7.28	0.44	6.06	4.43	4.67	1.84	41.51
pd1_v1n2_rcp85	5.37	5.51	0.56	10.37	6.96	7.19	1.40	20.15
pd2_v1n2_rcp85	5.37	5.51	0.56	10.37	5.99	6.68	1.94	32.39
pd3_v1n2_rcp85	5.37	5.51	0.56	10.37	4.66	5.04	2.01	43.07
pd1_v2n2_rcp85	5.11	5.08	0.59	11.60	6.68	6.92	1.32	19.73
pd2_v2n2_rcp85	5.11	5.08	0.59	11.60	5.72	6.50	1.91	33.44
pd3_v2n2_rcp85	5.11	5.08	0.59	11.60	4.44	4.71	1.92	43.27
pd1_v3n2_rcp85	6.81	6.73	0.60	8.79	6.38	6.63	1.25	19.57
pd2_v3n2_rcp85	6.81	6.73	0.60	8.79	5.55	5.93	1.78	32.10
pd3_v3n2_rcp85	6.81	6.73	0.60	8.79	4.44	4.95	1.87	42.05

Note: sd: standard deviation; cv: coefficient of variation

Appendix 11: Mean, median, sd and cv of grain yield for baseline, RCP4.5 and RCP8.5 at N3

	CERES-Maize				APSIM-Maize			
variable	mean	median	sd	cv	mean	median	sd	cv
pd1_v1n3_bs	5.97	5.89	0.94	15.70	7.77	7.88	1.74	22.38
pd2_v1n3_bs	5.97	5.89	0.94	15.70	6.35	7.27	2.31	36.35
pd3_v1n3_bs	5.97	5.89	0.94	15.70	4.64	4.51	1.97	42.55
pd1_v2n3_bs	4.80	4.69	0.70	14.54	7.50	7.84	1.66	22.18
pd2_v2n3_bs	4.80	4.69	0.70	14.54	6.06	7.05	2.21	36.54
pd3_v2n3_bs	4.80	4.69	0.70	14.54	4.42	4.20	1.91	43.19
pd1_v3n3_bs	7.07	7.02	0.84	11.86	7.09	7.24	1.46	20.58
pd2_v3n3_bs	7.07	7.02	0.84	11.86	5.83	6.62	2.03	34.83
pd3_v3n3_bs	7.07	7.02	0.84	11.86	4.38	4.28	1.83	41.86
pd1_v1n3_rcp45	6.25	6.21	0.54	8.67	7.30	7.51	1.48	20.30
pd2_v1n3_rcp45	6.25	6.21	0.54	8.67	6.13	6.62	2.07	33.76
pd3_v1n3_rcp45	6.25	6.21	0.54	8.67	4.63	4.93	2.04	44.04
pd1_v2n3_rcp45	6.03	5.96	0.68	11.35	6.98	7.19	1.42	20.41
pd2_v2n3_rcp45	6.03	5.96	0.68	11.35	5.87	6.65	2.02	34.47
pd3_v2n3_rcp45	6.03	5.96	0.68	11.35	4.40	4.52	1.94	44.01
pd1_v3n3_rcp45	7.19	7.28	0.46	6.45	6.64	6.90	1.34	20.16
pd2_v3n3_rcp45	7.19	7.28	0.46	6.45	5.70	6.08	1.86	32.59
pd3_v3n3_rcp45	7.19	7.28	0.46	6.45	4.42	4.67	1.86	42.07
pd1_v1n3_rcp85	5.83	5.93	0.55	9.39	6.97	7.23	1.51	21.70
pd2_v1n3_rcp85	5.83	5.93	0.55	9.39	6.01	6.79	1.97	32.73
pd3_v1n3_rcp85	5.83	5.93	0.55	9.39	4.65	5.04	2.02	43.58
pd1_v2n3_rcp85	5.77	5.68	0.55	9.52	6.69	6.94	1.39	20.80
pd2_v2n3_rcp85	5.77	5.68	0.55	9.52	5.73	6.57	1.93	33.73
pd3_v2n3_rcp85	5.77	5.68	0.55	9.52	4.43	4.71	1.93	43.71
pd1_v3n3_rcp85	6.66	6.62	0.56	8.39	6.38	6.64	1.30	20.31
pd2_v3n3_rcp85	6.66	6.62	0.56	8.39	5.57	5.97	1.80	32.35
pd3_v3n3_rcp85	6.66	6.62	0.56	8.39	4.43	4.95	1.88	42.46

Note: sd: standard deviation; cv: coefficient of variation

Appendix 12: Simulated baseline grain and above-ground biomass using APSIM-Maize and CERES-Maize models

Treatment	APSIM-Maize		CERES-Maize	
	Grain (t ha^{-1})	Biomass (t ha^{-1})	Grain (t ha^{-1})	Biomass (t ha^{-1})
pd1_v1n1	5.69	11.06	5.38	9.43
pd1_v1n2	7.56	13.87	5.66	9.63
pd1_v1n3	7.77	14.40	5.97	10.27
pd2_v1n1	5.22	10.10	5.36	9.39
pd2_v1n2	6.38	12.58	5.66	9.63
pd2_v1n3	6.35	12.80	5.97	10.27
pd3_v1n1	4.61	9.65	5.36	9.39
pd3_v1n2	4.66	10.71	5.66	9.63
pd3_v1n3	4.63	10.75	5.97	10.27
pd1_v2n1	5.61	11.27	5.61	10.21
pd1_v2n2	7.36	13.97	5.46	9.91
pd1_v2n3	7.50	14.36	4.80	9.64
pd2_v2n1	5.10	10.29	5.61	10.21
pd2_v2n2	6.08	12.61	5.46	9.91
pd2_v2n3	6.06	12.80	4.80	9.64
pd3_v2n1	4.46	9.76	5.61	10.21
pd3_v2n2	4.44	10.73	5.46	9.91
pd3_v2n3	4.42	10.77	4.80	9.64
pd1_v3n1	5.57	11.30	5.19	9.18
pd1_v3n2	7.06	13.92	6.91	10.38
pd1_v3n3	7.09	14.28	7.05	10.76
pd2_v3n1	5.07	10.31	5.19	9.18
pd2_v3n2	5.84	12.57	6.91	10.38
pd2_v3n3	5.83	12.79	7.05	10.76
pd3_v3n1	4.47	9.80	5.19	9.18
pd3_v3n2	4.40	10.78	6.91	10.38
pd3_v3n3	4.38	10.81	7.05	10.76

Appendix 13: Percent change in grain yield under RCP4.5 and RCP8.5 at N1, N2 and N3

	CERES-Maize			APSIM-Maize		
	N1	N2	N3	N1	N2	N3
pd1_v1_rcp45	12.35	6.96	6.97	4.37	-3.57	-5.11
pd2_v1_rcp45	12.61	6.96	6.97	0.35	-2.86	-1.80
pd3_v1_rcp45	12.61	6.96	6.97	-2.68	-1.08	-1.09
pd1_v2_rcp45	6.85	2.00	27.96	3.37	-5.33	-6.21
pd2_v2_rcp45	6.85	2.00	27.96	-0.23	-2.58	-1.65
pd3_v2_rcp45	6.85	2.00	27.96	-2.88	-1.05	-1.17
pd1_v3_rcp45	23.86	5.96	2.99	3.67	-5.83	-5.93
pd2_v3_rcp45	23.86	5.96	2.99	0.26	-1.48	-0.77
pd3_v3_rcp45	23.86	5.96	2.99	-2.34	0.20	0.58
pd1_v1_rcp85	5.41	-2.32	-0.20	5.42	-7.24	-9.46
pd2_v1_rcp85	5.65	-2.32	-0.20	1.05	-4.29	-2.89
pd3_v1_rcp85	5.65	-2.32	-0.20	-2.71	-1.12	-0.60
pd1_v2_rcp85	2.55	-3.99	22.80	4.52	-8.51	-9.99
pd2_v2_rcp85	2.55	-3.99	22.80	0.52	-4.31	-3.17
pd3_v2_rcp85	2.55	-3.99	22.80	-2.94	-0.69	-0.19
pd1_v3_rcp85	17.04	-0.83	-4.61	4.15	-9.10	-9.35
pd2_v3_rcp85	17.04	-0.83	-4.61	-0.75	-3.32	-2.42
pd3_v3_rcp85	17.04	-0.83	-4.61	-3.86	0.03	0.69

Appendix 14: Simulated percent change of grain yield using APSIM-Maize model under RCP4.5 and RCP8.5

Trt	ccsm4_rcp45	gdfl_esm2g_rcp45	hadgem2_es_rcp45	miroc5_rcp45	mpi_esm_mr_rcp45	ens_rcp45	ccsm4_rcp85	gdfl_esm2g_rcp85	hadgem2_es_rcp85	miroc5_rcp85	mpi_esm_mr_rcp85	ens_rcp85
pd1_v1n1	4.07	4.49	2.56	4.09	5.10	4.06	5.38	6.69	2.12	4.96	5.86	5.00
pd1_v1n2	-6.04	-1.51	-4.90	-4.27	-4.85	-4.31	-8.98	-4.38	-10.24	-6.98	-9.16	-7.95
pd1_v1n3	-8.19	-2.57	-6.50	-5.94	-7.11	-6.06	-11.78	-6.13	-12.21	-9.40	-12.07	-10.32
pd2_v1n1	0.80	0.86	0.23	1.08	0.79	0.75	0.26	2.73	-1.29	0.97	2.70	1.07
pd2_v1n2	-6.34	0.71	-5.31	-2.86	-6.59	-4.08	-9.73	0.62	-5.74	-7.37	-8.47	-6.14
pd2_v1n3	-5.95	1.29	-4.63	-2.32	-6.05	-3.53	-9.18	1.55	-4.78	-6.69	-7.92	-5.41
pd3_v1n1	-3.50	1.16	-3.13	0.40	-3.15	-1.64	-3.56	3.06	-3.67	-2.04	-1.73	-1.59
pd3_v1n2	-3.05	5.03	-3.38	4.04	-2.75	-0.02	-4.12	8.73	-0.42	-3.30	-2.20	-0.26
pd3_v1n3	-3.14	5.13	-3.12	3.67	-2.84	-0.06	-3.79	8.87	-0.01	-2.96	-1.81	0.06
pd1_v2n1	2.86	3.71	1.92	3.16	4.23	3.18	4.40	6.03	1.25	3.58	5.58	4.17
pd1_v2n2	-7.57	-3.12	-6.22	-5.86	-6.63	-5.88	-10.59	-5.41	-10.88	-8.48	-10.44	-9.16
pd1_v2n3	-9.10	-3.64	-7.06	-6.62	-8.10	-6.90	-12.54	-6.43	-12.31	-10.19	-12.51	-10.80
pd2_v2n1	-0.62	0.69	-0.27	0.33	0.22	0.07	0.60	2.53	-1.54	-0.19	1.68	0.61
pd2_v2n2	-6.88	0.80	-4.08	-2.60	-5.74	-3.70	-8.80	0.69	-5.82	-7.34	-8.53	-5.96
pd2_v2n3	-6.42	1.19	-3.46	-2.18	-5.14	-3.20	-8.39	1.47	-5.11	-6.78	-8.06	-5.37
pd3_v2n1	-3.74	1.75	-3.81	0.29	-3.27	-1.76	-3.96	2.83	-2.62	-2.80	-1.94	-1.70
pd3_v2n2	-3.02	5.74	-4.48	3.26	-2.80	-0.26	-4.13	8.07	0.61	-3.25	-1.94	-0.13
pd3_v2n3	-3.10	5.82	-4.17	2.82	-2.97	-0.32	-3.80	8.29	1.03	-2.89	-1.51	0.22
pd1_v3n1	3.21	4.47	2.27	3.05	3.89	3.38	3.67	6.21	0.65	3.23	4.72	3.70
pd1_v3n2	-7.27	-3.65	-6.73	-6.64	-6.88	-6.23	-10.78	-5.31	-11.69	-9.28	-10.85	-9.58
pd1_v3n3	-7.86	-3.24	-6.56	-6.63	-7.53	-6.36	-11.30	-5.45	-11.74	-9.67	-11.45	-9.92
pd2_v3n1	0.25	1.39	-0.47	1.25	0.78	0.64	-0.68	0.27	-4.85	-0.21	0.87	-0.92
pd2_v3n2	-5.58	1.30	-1.88	-1.67	-4.93	-2.55	-7.31	-1.49	-4.17	-5.06	-6.78	-4.96
pd2_v3n3	-5.28	1.63	-1.45	-1.42	-4.57	-2.22	-7.00	-0.98	-3.38	-4.63	-6.48	-4.49
pd3_v3n1	-3.27	1.62	-3.58	1.33	-2.34	-1.25	-4.58	2.88	-4.46	-3.29	-3.40	-2.57
pd3_v3n2	-2.26	5.88	-2.43	4.39	-1.72	0.77	-2.57	9.01	1.59	-2.17	-1.45	0.88
pd3_v3n3	-2.17	6.22	-2.18	4.28	-1.63	0.91	-2.23	9.40	2.01	-1.84	-1.07	1.25

Note: pd1: first planting date; pd2: second planting date; pd3: third planting date; v1: ZMS 606; v2: PHB30G19; v3: PHB30B50

Appendix 15: Simulated percent change of grain yield using CERES-Maize model under RCP4.5 and RCP8.5

Trt	ccsm4_rcp45	gdfl_esm2g_rcp45	hadgem2_es_rcp45	miroc5_rcp45	mpi_esm_mr_rcp45	ens_rcp45	ccsm4_rcp85	gdfl_esm2g_rcp85	hadgem2_es_rcp85	miroc5_rcp85	mpi_esm_mr_rcp85	ens_rcp85
pd1_v1n1	15.00	12.06	8.64	11.76	10.69	11.63	10.06	6.63	-10.51	9.03	8.35	4.71
pd1_v1n2	6.27	4.62	7.55	1.05	1.39	4.18	1.36	5.53	-31.70	-0.60	-0.23	-5.13
pd1_v1n3	9.12	6.01	0.10	4.03	4.47	4.75	4.46	-0.65	-19.05	2.06	1.31	-2.37
pd2_v1n1	15.28	12.33	8.90	12.03	10.96	11.90	10.33	6.88	-10.41	9.29	8.61	4.94
pd2_v1n2	6.27	4.62	7.55	1.05	1.39	4.18	1.36	5.53	-31.70	-0.60	-0.23	-5.13
pd2_v1n3	9.12	6.01	0.10	4.03	4.47	4.75	4.46	-0.65	-19.05	2.06	1.31	-2.37
pd3_v1n1	15.28	12.33	8.90	12.03	10.96	11.90	10.33	6.88	-10.41	9.29	8.61	4.94
pd3_v1n2	6.27	4.62	7.55	1.05	1.39	4.18	1.36	5.53	-31.70	-0.60	-0.23	-5.13
pd3_v1n3	9.12	6.01	0.10	4.03	4.47	4.75	4.46	-0.65	-19.05	2.06	1.31	-2.37
pd1_v2n1	6.27	7.92	3.49	8.40	7.18	6.65	6.22	12.53	-14.57	2.79	3.74	2.14
pd1_v2n2	-1.11	2.45	-3.94	2.28	-2.64	-0.59	-1.29	10.25	-33.93	-5.63	-2.03	-6.52
pd1_v2n3	25.52	26.52	24.18	28.74	23.89	25.77	24.78	39.59	-4.58	18.36	22.91	20.21
pd2_v2n1	6.27	7.92	3.49	8.40	7.18	6.65	6.22	12.53	-14.57	2.79	3.74	2.14
pd2_v2n2	-1.11	2.45	-3.94	2.28	-2.64	-0.59	-1.29	10.25	-33.93	-5.63	-2.03	-6.52
pd2_v2n3	25.52	26.52	24.18	28.74	23.89	25.77	24.78	39.59	-4.58	18.36	22.91	20.21
pd3_v2n1	6.27	7.92	3.49	8.40	7.18	6.65	6.22	12.53	-14.57	2.79	3.74	2.14
pd3_v2n2	-1.11	2.45	-3.94	2.28	-2.64	-0.59	-1.29	10.25	-33.93	-5.63	-2.03	-6.52
pd3_v2n3	25.52	26.52	24.18	28.74	23.89	25.77	24.78	39.59	-4.58	18.36	22.91	20.21
pd1_v3n1	23.61	23.30	20.72	26.84	23.25	23.54	21.85	20.86	-2.15	24.06	19.11	16.75
pd1_v3n2	8.22	5.66	0.19	8.06	4.17	5.26	5.02	0.11	-16.33	5.06	-1.04	-1.43
pd1_v3n3	5.51	4.30	-9.87	7.63	2.37	1.99	1.13	-9.66	-17.77	2.28	-3.21	-5.45
pd2_v3n1	23.61	23.30	20.72	26.84	23.25	23.54	21.85	20.86	-2.15	24.06	19.11	16.75
pd2_v3n2	8.22	5.66	0.19	8.06	4.17	5.26	5.02	0.11	-16.33	5.06	-1.04	-1.43
pd2_v3n3	5.51	4.30	-9.87	7.63	2.37	1.99	1.13	-9.66	-17.77	2.28	-3.21	-5.45
pd3_v3n1	23.61	23.30	20.72	26.84	23.25	23.54	21.85	20.86	-2.15	24.06	19.11	16.75
pd3_v3n2	8.22	5.66	0.19	8.06	4.17	5.26	5.02	0.11	-16.33	5.06	-1.04	-1.43
pd3_v3n3	5.51	4.30	-9.87	7.63	2.37	1.99	1.13	-9.66	-17.77	2.28	-3.21	-5.45

Note: pd1: first planting date; pd2: second planting date; pd3: third planting date; v1: ZMS 606; v2: PHB30G19; v3: PHB30B50

Appendix 16: Simulated percent change of biomass using APSIM-Maize model under RCP4.5 and RCP8.5

Trt	ccsm4_rcp45	gdfl_esm2g_rcp45	hadgem2_es_rcp45	miroc5_rcp45	mpi_esm_mr_rcp45	ens_rcp45	ccsm4_rcp85	gdfl_esm2g_rcp85	hadgem2_es_rcp85	miroc5_rcp85	mpi_esm_mr_rcp85	ens_rcp85
pd1_v1n1	0.00	0.22	-3.75	-46.41	0.26	-9.94	-0.45	0.42	-5.79	-1.35	0.06	-1.42
pd1_v1n2	-7.11	-4.58	-7.80	-47.85	-6.73	-14.81	-9.72	-6.55	-12.10	-8.62	-9.80	-9.36
pd1_v1n3	-9.34	-5.58	-9.29	-49.24	-8.90	-16.47	-12.65	-8.41	-14.21	-10.99	-12.89	-11.83
pd2_v1n1	-1.77	-0.58	-4.02	-47.75	-1.55	-11.14	-2.08	-1.08	-6.03	-2.43	-1.29	-2.58
pd2_v1n2	-7.62	-3.03	-7.45	-50.73	-7.54	-15.27	-10.24	-3.75	-9.64	-8.61	-10.13	-8.47
pd2_v1n3	-8.13	-2.91	-7.75	-51.54	-8.06	-15.68	-10.94	-3.81	-9.77	-9.11	-11.01	-8.93
pd3_v1n1	-3.59	-2.75	-5.82	-51.98	-3.62	-13.55	-4.99	-1.84	-6.16	-5.09	-4.45	-4.51
pd3_v1n2	-6.33	-1.75	-7.94	-54.69	-6.23	-15.39	-8.60	-0.78	-7.19	-8.11	-8.09	-6.56
pd3_v1n3	-6.34	-1.49	-7.87	-55.30	-6.26	-15.45	-8.61	-0.56	-7.07	-8.10	-8.11	-6.49
pd1_v2n1	-0.69	-0.23	-3.76	-48.68	-0.14	-10.70	-0.57	0.00	-6.07	-1.58	-0.14	-1.67
pd1_v2n2	-7.89	-5.21	-8.43	-50.41	-7.50	-15.89	-10.62	-7.32	-12.56	-9.36	-10.74	-10.12
pd1_v2n3	-9.52	-5.67	-9.32	-51.26	-9.16	-16.99	-12.94	-8.55	-14.22	-11.24	-13.11	-12.01
pd2_v2n1	-2.19	-1.13	-4.65	-50.28	-2.05	-12.06	-2.06	-1.30	-6.72	-2.83	-1.50	-2.88
pd2_v2n2	-7.98	-3.16	-7.53	-53.05	-7.56	-15.86	-10.38	-4.04	-9.75	-8.77	-10.37	-8.66
pd2_v2n3	-8.36	-3.06	-7.62	-53.68	-7.87	-16.12	-11.01	-4.01	-9.77	-9.13	-11.07	-9.00
pd3_v2n1	-3.94	-2.69	-5.94	-54.19	-3.48	-14.05	-5.29	-1.94	-6.46	-5.27	-4.69	-4.73
pd3_v2n2	-6.54	-1.71	-8.29	-57.27	-6.24	-16.01	-8.79	-1.08	-7.33	-8.37	-8.33	-6.78
pd3_v2n3	-6.53	-1.42	-8.23	-57.85	-6.26	-16.06	-8.78	-0.87	-7.20	-8.34	-8.34	-6.71
pd1_v3n1	-0.46	0.36	-3.54	-49.20	-0.13	-10.59	-0.37	0.20	-6.11	-1.33	-0.13	-1.55
pd1_v3n2	-7.81	-5.18	-8.56	-52.64	-7.55	-16.35	-10.61	-7.28	-12.86	-9.74	-11.00	-10.30
pd1_v3n3	-9.51	-5.74	-9.56	-53.67	-9.24	-17.54	-12.62	-8.68	-14.29	-11.50	-13.03	-12.03
pd2_v3n1	-1.89	-0.71	-4.55	-50.16	-1.55	-11.77	-2.17	-1.52	-6.58	-3.02	-1.48	-2.95
pd2_v3n2	-7.74	-3.01	-7.39	-54.31	-7.48	-15.99	-10.39	-5.54	-10.18	-8.82	-10.24	-9.03
pd2_v3n3	-8.35	-3.19	-7.70	-55.08	-8.12	-16.49	-11.20	-5.75	-10.55	-9.36	-11.15	-9.60
pd3_v3n1	-3.77	-2.61	-5.79	-53.77	-3.39	-13.87	-5.42	-1.90	-6.47	-5.36	-5.13	-4.86
pd3_v3n2	-6.75	-1.90	-8.10	-57.38	-6.53	-16.13	-9.04	-1.12	-7.25	-8.45	-8.70	-6.91
pd3_v3n3	-6.72	-1.59	-8.03	-57.80	-6.52	-16.13	-9.00	-0.89	-7.11	-8.42	-8.68	-6.82

Note: pd1: first planting date; pd2: second planting date; pd3: third planting date; v1: ZMS 606; v2: PHB30G19; v3: PHB30B50

Appendix 17: Simulated percent change of biomass yield using CERES-Maize model under RCP4.5 and RCP8.5

Trt	ccsm4_rcp45	gdfl_esm2g_rcp45	hadgem2_es_rcp45	miroc5_rcp45	mpi_esm_mr_rcp45	ens_rcp45	ccsm4_rcp85	gdfl_esm2g_rcp85	hadgem2_es_rcp85	miroc5_rcp85	mpi_esm_mr_rcp85	ens_rcp85
pd1_v1n1	11.41	8.79	1.16	9.93	9.40	8.14	8.26	-0.77	-9.43	8.55	7.87	2.90
pd1_v1n2	8.86	7.17	4.57	6.17	5.93	6.54	5.56	2.29	-17.94	5.24	5.71	0.17
pd1_v1n3	9.12	6.28	-3.40	6.07	6.09	4.83	5.80	-4.60	-11.63	5.85	5.07	0.10
pd2_v1n1	11.87	9.23	1.57	10.37	9.84	8.58	8.70	-0.36	-9.32	8.99	8.31	3.26
pd2_v1n2	8.86	7.17	4.57	6.17	5.93	6.54	5.56	2.29	-17.94	5.24	5.71	0.17
pd2_v1n3	9.12	6.28	-3.40	6.07	6.09	4.83	5.80	-4.60	-11.63	5.85	5.07	0.10
pd3_v1n1	11.87	9.23	1.57	10.37	9.84	8.58	8.70	-0.36	-9.32	8.99	8.31	3.26
pd3_v1n2	8.86	7.17	4.57	6.17	5.93	6.54	5.56	2.29	-17.94	5.24	5.71	0.17
pd3_v1n3	9.12	6.28	-3.40	6.07	6.09	4.83	5.80	-4.60	-11.63	5.85	5.07	0.10
pd1_v2n1	5.53	5.11	1.38	6.68	6.02	4.95	5.54	6.63	-13.67	3.58	4.94	1.40
pd1_v2n2	3.56	4.80	2.01	5.57	3.50	3.89	4.24	10.43	-20.51	1.53	4.18	-0.03
pd1_v2n3	16.08	15.83	15.82	18.03	16.26	16.41	16.85	22.58	-3.95	13.42	16.35	13.05
pd2_v2n1	5.53	5.11	1.38	6.68	6.02	4.95	5.54	6.63	-13.67	3.58	4.94	1.40
pd2_v2n2	3.56	4.80	2.01	5.57	3.50	3.89	4.24	10.43	-20.51	1.53	4.18	-0.03
pd2_v2n3	16.08	15.83	15.82	18.03	16.26	16.41	16.85	22.58	-3.95	13.42	16.35	13.05
pd3_v2n1	5.53	5.11	1.38	6.68	6.02	4.95	5.54	6.63	-13.67	3.58	4.94	1.40
pd3_v2n2	3.56	4.80	2.01	5.57	3.50	3.89	4.24	10.43	-20.51	1.53	4.18	-0.03
pd3_v2n3	16.08	15.83	15.82	18.03	16.26	16.41	16.85	22.58	-3.95	13.42	16.35	13.05
pd1_v3n1	15.46	11.86	4.67	14.03	13.04	11.81	11.61	4.88	-7.12	12.69	9.92	6.39
pd1_v3n2	9.61	6.17	0.17	8.38	6.57	6.18	6.02	-0.21	-12.11	6.97	2.25	0.58
pd1_v3n3	8.59	4.69	-8.30	7.62	4.99	3.52	3.82	-8.25	-12.25	5.26	1.14	-2.05
pd2_v3n1	15.46	11.86	4.67	14.03	13.04	11.81	11.61	4.88	-7.12	12.69	9.92	6.39
pd2_v3n2	9.61	6.17	0.17	8.38	6.57	6.18	6.02	-0.21	-12.11	6.97	2.25	0.58
pd2_v3n3	8.59	4.69	-8.30	7.62	4.99	3.52	3.82	-8.25	-12.25	5.26	1.14	-2.05
pd3_v3n1	15.46	11.86	4.67	14.03	13.04	11.81	11.61	4.88	-7.12	12.69	9.92	6.39
pd3_v3n2	9.61	6.17	0.17	8.38	6.57	6.18	6.02	-0.21	-12.11	6.97	2.25	0.58
pd3_v3n3	8.59	4.69	-8.30	7.62	4.99	3.52	3.82	-8.25	-12.25	5.26	1.14	-2.05

Note: pd1: first planting date; pd2: second planting date; pd3: third planting date; v1: ZMS 606; v2: PHB30G19; v3: PHB30B50